The role of trace metal micronutrients in the growth and niche separation of marine ammonia-oxidising microorganisms



Roxana T. Shafiee

Department of Earth Sciences

University of Oxford

A thesis submitted for the degree of

Doctor of Philosophy

Supervised by Prof. Rosalind E.M Rickaby & Dr Joseph T. Snow

THE ROLE OF TRACE METAL MICRONUTRIENTS IN THE GROWTH AND NICHE SEPARATION OF MARINE AMMONIA-OXIDISING MICROORGANISMS

Roxana T. Shafiee – *Department of Earth Sciences and Oriel College, Oxford*

Trinity term 2021

ABSTRACT

Nitrogen is essential to life on Earth. In the oceans, the availability and chemical speciation of nitrogen constrains how effectively CO_2 is removed from the atmosphere by phytoplankton and delivered to the deep ocean — with implications for global climate. Nitrogen availability and speciation are controlled by marine microorganisms, with ammonia-oxidising archaea and bacteria (AOA and AOB) mediating the first step in the oxidative nitrogen cycle. A scarcity of trace metals (such as iron (Fe) and copper (Cu)) has been repeatedly shown to limit other components of microbial nitrogen cycling in oceans. Yet, the role of trace metals in AOA and AOB growth remains largely underexplored. The research presented here brings together microbial physiology, metallomics, proteomics and comparative genomics to ask whether there is physiological precedent for iron and copper availability to govern the growth, distribution and niche separation of AOA and AOB in the oceans. We found that growth rate of the marine AOA isolate, *Nitrosopumilus maritimus*, in culture is determined by Fe availability. *N. maritimus* displays an unchelated iron (Fe′) half-saturation constant 1–2 orders of magnitude greater for growth than numerous marine phytoplankton and heterotrophic bacterial species — driven by a reduced uptake affinity for Fe′. When growth is limited by Fe′, proteomic analysis revealed that *N. maritimus* primarily minimises Fe demand by reducing Fe-dense ferredoxins which putatively interact with Complex I to generate the reduced co-factor NAD(P)H — potentially functionally substituting these ferredoxins for Fe-free alternatives. In doing so, Fe-binding proteins which play a more central role in electron transfer and ammonia oxidation can be preferentially retained, allowing *N. maritimus* to continue in supporting key energy-yielding pathways under Fe limitation. Marine AOA and AOB isolates were found to display contrasting requirements and uptake strategies for Fe and Cu at the genetic, proteomic, and physiological level. We found that the AOB isolate, *Nitrosococcus oceani* displays a greater affinity for Fe′ but requires greater cupric Cu (Cu^{2+}) for growth compared with the marine AOA isolate, *N. maritimus*. We predict that this may allow AOB to inhabit shallower, euphotic waters

where NH_4^+ supply is high, but competition for Fe is rife. In contrast to AOB, AOA isolates have a greater affinity and toxicity threshold for Cu^{2+} providing an additional explanation to the greater success of AOA in the marine environment where Cu^{2+} availability can be highly variable. These data are used to develop the testable hypothesis, with support from comparative genomics and biogeochemical datasets, that Cu^{2+} widely limits AOA and AOB growth in the oceans, particularly in the Pacific Ocean where Cu^{2+} concentrations are often below that needed by AOA and AOB isolates for growth. Further, Fe and Cu ecophysiologies are hypothesised to contribute to the observed depth distribution of AOA and AOB in the oceans —— with contrasting trophic strategies for Fe and Cu acquisition potentially allowing AOA and AOB to occupy distinct trace metal niches in the oceans. This may explain the chemical niche that allows AOB to persist in the oceans, despite being uncompetitive for NH_4^+ compared with AOA. The research presented here develops an improved understanding of the physicochemical factors that govern ammonia oxidation in the marine environment — with far-reaching implications for the current, past and future biogeochemical nitrogen and carbon cycles.

THE ROLE OF TRACE METAL MICRONUTRIENTS IN THE GROWTH AND NICHE SEPARATION OF MARINE AMMONIA-OXIDISING MICROORGANISMS

Roxana T. Shafiee – *Department of Earth Sciences and Oriel College, Oxford*

EXTENDED ABSTRACT

Ammonia oxidation sits at the heart of the biogeochemical nitrogen (N) cycle as the first step in nitrification — the sequential oxidation of ammonium (NH_4^+) to nitrite (NO_2^-) and nitrate (NO_3^-). In the oceans, ammonia oxidation is carried out by chemolithoautotrophic archaea (AOA) and bacteria (AOB) with AOA typically outnumbering AOB due to their greater uptake affinity for ammonium (NH_4^+). Levels of irradiance and NH_4^+ supply are conventionally considered to be the primary determinants of AOA growth and distribution in the ocean. Yet, widespread observations of AOA in sunlit surface waters and NH_4^+ saturation of AOA growth in some regions indicate that additional factors may govern marine AOA growth. Further, the dominance of AOA in oceanic regimes wherein NH_4^+ supply is theoretically sufficient to support high AOB abundances questions the chemical niche that allows AOB to persist (albeit at low concentrations) in the marine environment. Throughout the open ocean, the scarcity of trace metal micronutrients (such as iron (Fe) and copper (Cu)) governs the growth and ecology of marine N-cycling microorganisms. Yet, the role of trace metals in controlling the growth, distribution and niche separation of AOA and AOB remains uncertain. The research presented here brings together microbial physiology, proteomics and comparative genomics to ask if there is physiological precedent for Fe and Cu availability in the oceans to govern the growth, distribution and niche separation of AOA and AOB in the oceans.

(1) In chapter two, the Fe requirements and uptake strategies of the marine ammonia-oxidising archaeal isolate, *Nitrosopumilus maritimus,* are examined in order to understand the potential for Fe to shape the distribution of AOA in the oceans. The marine AOA isolate, *Nitrosopumilus maritimus*, displays the highest Fe′ half-saturation constant for growth of any marine microorganism studied to date, driven by a low affinity for unchelated Fe′ rather than an intrinsically high cellular Fe demand. While *N. maritimus* can utilise organically-complexed Fe — likely through a reductive uptake strategy — *N. maritimus* is unable to synthesise its own siderophores. These physiological characteristics, underpinned by a genetic absence of Fe-specific transporters, suggest the evolution of AOA into an oceanic niche wherein there is high Fe availability and, therefore, little selection pressure to evolve efficient Fe-uptake strategies. The observed AOA physiology aligns with documented AOA maxima at the base of the euphotic zone where competition for Fe′ is removed, and Fe supply is high due to the remineralisation of organic matter.

(2) Chapter three examines the proteomic response of *N. maritimus* when limited for Fe, shedding light on the potential molecular strategies adopted by AOA to survive Fe scarcity. When Fe limited, there are significant changes to the intensity of proteins involved in key cellular processes, including ammonia oxidation, the tricarboxylic acid cycle, and biosynthesis — indicating that Fe plays an essential role in the biochemistry of marine AOA. Changes in protein intensities under Fe limitation reveal that *N. maritimus* employs numerous potential compensatory strategies to minimise Fe demand and increase Fe uptake. *N. maritimus* primarily reduces Fe demand by reducing the abundance of Fe-dense ferredoxins, potentially substituting these ferredoxins for Fe-free alternatives. Proteomic results reveal a link between Fe limitation and phosphonate uptake, which is unrelated to its nutritional phosphorus (P) requirement, suggesting an as of yet undetermined link between Fe and P cycling in marine AOA.

(3) In chapter four, the Fe and Cu requirements of the marine AOB *Nitrosococcus oceani* are examined at the physiological, metallomic and genomic level. These data are compared with those of AOA from chapter two (Fe requirements) and previously published work on AOA Cu requirements (Amin et al. 2013**) to gain insight into the role of trace metals in the niche separation of AOA and AOB.** AOA and AOB isolates display contrasting physiologies in response to Fe and Cu, and harbour distinct intracellular metal quotas and uptake strategies. The analyses show that *N. oceani* is able to grow at lower concentrations of unchelated Fe (Fe′) compared with *N. maritimus*, demonstrating a greater uptake affinity for Fe′. These data challenge the assertion that the Cu-centric biochemistry of AOA provides a physiological advantage to AOA over AOB in an ocean wherein Fe is scarce — by showing that an AOB isolate can survive at lower Fe′ compared with an AOA isolate. In contrast, *N. oceani* is more susceptible to growth limitation and toxicity by cupric ion (Cu^{2+}) availability compared to *N. maritimus* which is able to grow over a broader range of Cu^{2+} concentrations (Amin et al. 2013). The analyses show that unlike *N. maritimus*, *N. oceani* is not able to utilise exogenous chelated Fe and does not use a reductive uptake strategy during Fe acquisition. Using comparative genomics, the biochemical basis (i.e., the Fe- and Cu-binding proteome and trace metal transport proteins) that likely gives rise to the contrasting physiologies in isolates is observed to be widespread among taxonomically diverse marine AOA and AOB. Based on the physiological data presented in this study, the following hypotheses are presented regarding the role of Fe and Cu in the growth and niche separation of AOA and AOB in the oceans:

(a) As Cu^{2+} requirements for *N. oceani* and *N. maritimus* growth exceed Cu^{2+} concentrations widely documented in the marine environment, there is a physiological precedent for Cu^{2+} to limit overall ammonia oxidation in large tracts of the open ocean –

– particularly the northeast Pacific where Cu^{2+} is chronically scarce. This warrants further investigation.

(b) *N. maritimus*' ability to grow over a broader range of Cu^{2+} concentrations and capacity to use organically-complexed Fe through a 'generalist' reductive uptake strategy may further contribute to the success of AOA over AOB in the oceans — wherein Cu^{2+} concentrations vary by 5 orders of magnitude between ocean basins and with depth, and where organically-complexed Fe is chemically heterogenous.

(c) Contrasting Cu and Fe trophic strategies in AOA and AOB provide physiological support for the role of trace metals in the niche separation of AOA and AOB. A greater affinity for Fe′ may allow AOB to inhabit shallower, euphotic waters where NH_4^+ supply is high, but competition for Fe′ is rife. In contrast, the higher affinity for NH_4^+ allows AOA to sit deeper in the water column, where access to Fe (especially chelated Fe) is greater, as other microorganisms become limited by light or dissolved organic carbon.

(d) The greater Fe demand of AOB at μ_{max} compared with AOA suggests the relatively earlier emergence of AOB than AOA when considered in the context of evolving trace metal availabilities over geologic time.

ACKNOWLEDGEMENTS

My utmost gratitude goes to my supervisors Ros Rickaby and Joe Snow who despite having no prior experience working with the fastidious ammonia oxidisers, embraced the challenge with enthusiasm. Their support and generosity with their time and expertise, buoyed my motivation following endless rounds of punishing reviewers' comments and allowed me to develop the verve necessary to continue my scientific career. For this, I am very grateful.

I have been fortunate to be part of a vibrant research group and department; my particular thanks go to Joan Zhang, Phil Holdship and all the past and current members of the OceanBug group for making my time at Oxford a positive and memorable one. Outside of Oxford, I am deeply appreciative of the time and expertise donated by all the scientists who I have pestered over the years. In particular, I am very grateful to Heather Richmond and the Jim Prosser's group at the University of Aberdeen for showing me the ropes of ammonia oxidisers and providing cultures on demand. I am also indebted to Chris Dupont for providing continued support and guidance – this generosity is deeply appreciated. My thanks also go to Dianne Newman and Jared Leadbetter for affording me the opportunity to partake in the transformative Microbial Diversity course. The experience bolstered my interest in microbiology and has invariably shaped the career trajectory that I am on now.

My foremost thanks go to my family, who treat their support and encouragement of my work like an Olympic sport. My successes are also their successes and I hope that my siblings – Natasha, Rebecca, Laila and Keyan – appreciate the vital role that they played in facilitating this research. Last but not least, I want to thank my father, who has always been my number one cheerleader, and to whom I dedicate this thesis.

CONTENTS

1 INTRODUCTION 12
1.1 Nitrogen and carbon cycling are inextricably linked ... 12
1.2 The marine nitrogen cycle ... 16
1.3 Nitrification ... 20
1.4 Microbial ammonia oxidation ... 21
1.5 Factors controlling ammonia oxidation and niche separation of ammonia oxidisers ... 39
1.6 Trace metals and the nitrogen cycle ... 51
1.7 Trace metals and ammonia oxidation ... 56
1.8 Aims and approach ... 65

2 IRON REQUIREMENTS AND UPTAKE STRATEGIES OF THE GLOBALLY ABUNDANT MARINE AMMONIA-OXIDISING ARCHAEON, *NITROSOPUMILUS MARITIMUS* STRAIN SCM1 74
2.1 Abstract ... 74
2.2 Introduction ... 76
2.3 Materials & methods ... 78
2.4 Results ... 83
2.5 Discussion ... 90
2.6 Conclusion ... 100
2.7 Statement of authorship ... 102

3 PROTEOMIC RESPONSE OF THE MARINE AMMONIA-OXIDISING THAUMARCHAEON, *NITROSOPUMILUS MARITIMUS* TO IRON LIMITATION REVEALS STRATEGIES TO COMPENSATE FOR NUTRIENT SCARCITY 103
3.1 Abstract ... 103
3.2 Introduction ... 104
3.3 Experimental procedures ... 107
3.4 Results & discussion ... 113
3.5 Conclusion ... 131
3.6 Statement of authorship ... 132

4 MARINE AMMONIA-OXIDISING ARCHAEA AND BACTERIA OCCUPY DISTINCT IRON AND COPPER NICHES 133
4.1 Abstract ... 133
4.2 Introduction ... 135
4.3 Materials & methods ... 137
4.4 Results and discussion ... 143
4.5 Implications for marine ammonia oxidation, niche separation and evolution ... 158
4.6 Conclusion ... 167
4.7 Statement of authorship ... 168

5 CONCLUDING REMARKS AND OUTLOOK 169
5.1 Key findings ... 169
5.2 Trace metals within the context of other physicochemical factors ... 173
5.3 Contribution and wider Significance ... 177
5.4 Future research ... 178
5.5 Closing remarks ... 184

6 REFERENCES 185
APPENDIX I 225
APPENDIX II 246
APPENDIX III 269

LIST OF FIGURES

Figure 1.1 Patterns of nutrient limitation 13
Figure 1.2 Role of dissolved NO_3^-: NH_4^+ availability on phytoplankton community composition 16
Figure 1.3 Microbial pathways in the marine nitrogen cycle 18
Figure 1.4 Depth distribution of inorganic nitrogen in the oceans 19
Figure 1.5 Microbially-mediated nitrification pathways 21
Figure 1.6 SEM images of marine ammonia-oxidising archaea and bacteria 22
Figure 1.7 Ammonia-oxidising bacteria and archaea on the tree of life 25
Figure 1.8 Phylogeny of ammonia-oxidising bacteria 26
Figure 1.9 Phylogeny of ammonia-oxidising archaea 27
Figure 1.10 Proposed pathways for bacterial and archaeal ammonia oxidation 28
Figure 1.11 Measured marine archaeal and bacterial *amoA* and ammonia oxidation rates 36
Figure 1.12 Archaeal and bacterial ammonia oxidation kinetics 41
Figure 1.13 Trace metals required by microbial nitrogen cycling in the oceans 53
Figure 1.14 Cu requirements of different components of microbial nitrogen cycling 57
Figure 1.15 Evolution of trace metal bioavailability in the oceans over geologic time 64
Figure 1.16 Outline of experimental approach to research aims and questions 69
Figure 1.17 Contrasting microbial growth responses of two microorganisms with similar Fe:C quotas 72
Figure 1.18 The role of 'omics in understanding microbial trace metal requirements 73
Figure 2.1 Effect of Fe′ on NO_2^- production and specific growth rate (μ) of *N. maritimus* 87
Figure 2.2 Absorbance spectra of *N. maritimus* supernatant after treatment with Chrome Azurol S solution 88
Figure 2.3 *N. maritimus* growth with Fe′ and organically-complexed Fe, FeDFB 89
Figure 2.4 *N. maritimus* Fe requirements compared with cosmopolitan marine microorganisms 93
Figure 3.1 *N. maritimus* growth rate and intracellular Fe quota under Fe replete and deplete treatments 119
Figure 3.2 Significant intensity changes to proteins involved in ammonia oxidation under Fe limitation 120
Figure 3.3 Significant intensity changes to proteins involved in the TCA cycle under Fe limitation 123
Figure 3.4 Significant intensity changes to proteins involved in transmembrane uptake 130
Figure 4.1 Cu and Fe requirements of *N. oceani* compared with AOA and other marine microorganisms 148
Figure 4.2 AOA and AOB Cu and Fe requirements based on genome-predicted proteomes 149
Figure 4.3 Abundance of metal transport systems in marine AOA and AOB 156
Figure 4.4 Predicted effect of oceanic [Cu^{2+}] on AOA and AOB growth rates based on laboratory growth cultures 160
Figure 4.5 Schematic showing hypothesised spatial niches of AOB and AOA 164
Figure A1.1 Effect of EDTA concentration on NO_2^- production by *N. maritimus* 229
Figure A1.2 Correlation between cell counts and NO_2^- concentrations in *N. maritimus* 230
Figure A1.3 SEM images of *N. maritimus* 231
Figure A1.4 Effect of Fe re-addition on *N. maritimus* nitrite production 232
Figure A1.5 Relationship between Fe quota and growth rate in marine microorganisms 233

Figure A1.6 Reads homologous to *N. maritimus* transporter genes detected in *Tara* oceans database 234
Figure A1.7 Archaeal hits from *Tara* oceans database homologous to metal uptake genes 235
Figure A1.8 FeDFB uptake of *N. maritimus* and phytoplankton as a function of cell surface area 236
Figure A2.1 Effect of protein extraction buffer on *N. maritimus*' protein yield 248
Figure A2.2 Production of NO_2^- by Fe-limited and Fe-replete *N. maritimus* cultures 249
Figure A2.3 Log-log scatter plots of raw and LFQ protein intensities 250
Figure A2.4 Spectral counts of AMO subunits generated using the Ocean Protein Portal 251
Figure A2.5 Comparison of Fe and Cu limitation on protein and gene expression 252
Figure A2.6 Proteins showing a significant LFQ intensity change under Fe limitation 253
Figure A2.7 Hypothetical pathways linking increased Phn intensity under Fe limitation with Mpn production 254
Figure A2.8 Oceanic dissolved Fe from GEOTRACES Intermediate Data Product 2017 256
Figure A2.9 Analysis of *phnD* biogeography from *Tara* Oceans Gene Atlas 257
Figure A3.1 *N. oceani* Fe and Cu dose response curves and cellular trace metal quotas 280
Figure A3.2 Effect of Fe′ and Cu′ on NO_2^- production in the marine AOB, *N. oceani* 281
Figure A3.3 SEM images of *N. oceani* under Fe-limited and Fe-replete conditions 282
Figure A3.4 Fe and Cu binding proteome of marine open ocean and coastal AOA and AOB 283
Figure A3.5 Fe affinities of marine AOA and AOB compared to cosmopolitan marine microorganisms 284
Figure A3.6 Extended bioinformatic analysis of transporter families in AOA and AOB genomes 286
Figure A3.7 *N. oceani* growth rates under different Fe substrates and concentrations 287
Figure A3.8 Cu requirements of different components of microbial N cycle 288
Figure A3.9 Mean AOA and AOB *amoA* gene abundances with depth 289
Figure A3.10 Relationship between genome-predicted proteome Cu/Fe demand expressed proteome demand 290
Figure A3.11 Expressed proteome trace metal demand of AOA and AOB 291
Figure A3.12 AOB detoxification genes in *Tara* oceans database 292
Figure A3.13 AOB detoxification transcripts in *Tara* oceans database 293

LIST OF TABLES

Table 1.1 Physicochemical factors governing growth and niche separation of ammonia oxidisers 48
Table 1.2 Trace metal-containing enzymes required in nitrogen cycling processes 52
Table 2.1 Effect of Fe on growth rate and cellular quotas of *N. maritimus* 86
Table 3.1 Top 10 proteins based on LFQ spectral counts in Fe-replete and Fe-limited treatments 116
Table 4.1 *N. oceani* growth and intracellular quota in response to changing Fe and Cu 146
Table A1.1 Fe requirements of marine phytoplankton and heterotrophs 238
Table A1.2 Steady-state Fe′ and FeDFB uptake rates of marine phytoplankton and heterotrophic bacteria 240
Table A1.3 Metal transport systems encoded in marine AOA genomes 241
Table A1.4 Ferric chelate reductases used in BLASTp analysis 244
Table A1.5 Candidate ferric reductases in *N. maritimus* 245
Table A2.1 Proteins which change significantly in LFQ intensity between Fe treatments 260
Table A2.2 Putative Fe-containing proteins and their corresponding LFQ intensity in *N. maritimus* 262
Table A2.3 Comparison of Cu, NH_4^+ and Fe limitation on protein abundances and gene expression 265
Table A2.4 Analysis of *phnD* gene biogeography from *Tara* Oceans Gene Atlas 268
Table A3.1 Cu requirements of marine microorganisms compiled from published literature. 296
Table A3.2 Fe requirements of marine microorganism compiled from published literature 297
Table A3.3 Analysis of Fe and Cu binding sites in AOB and AOB genome expressed proteomes 298
Table A3.4 Percentage of AOA and AOB Fe/Cu-binding expressed proteomes 299
Table A3.5 Known microbial trace metal transport systems 300
Table A3.6 Oceanic dissolved Cu^{2+} measurements compiled from published literature 303
Table A3.7 Marine archaeal and bacterial *amoA* gene abundances compiled from published literature 308
Table A3.8 Biogeography of AOB Cu efflux genes and transcripts 308

1 INTRODUCTION

The following introduction gives an overview of the cycling of nitrogen (N) — the seventh element in the periodic table — by microorganisms in the oceans. This introduction specifically provides a primer on marine ammonia oxidation, the first oxidative step in the marine N cycle — outlining the current understanding of the physicochemical factors thought to govern the growth and niche separation of the microorganisms that drive this process. Finally, the current knowledge of the role of trace metal micronutrients in microbial N cycling and ammonia oxidation is introduced, followed by an explanation of the key aims and objectives of this thesis.

1.1 NITROGEN AND CARBON CYCLING ARE INEXTRICABLY LINKED

Nitrogen (N) is essential for life on Earth, forming an integral component of DNA, RNA and proteins — the building blocks of life. Following hydrogen (H), carbon (C) and oxygen (O), N is the most abundant element in biomass, representing 7% of the cellular mass in marine microbes (Geider & La Roche, 2002; Moore et al. 2013). In the oceans, N is required by photosynthetic microorganisms (phytoplankton) that inhabit the sunlit surface layer (the euphotic zone). The nutritional N requirement of phytoplankton, which fix CO_2 from the atmosphere, creates an inextricable link between marine biogeochemical C and N cycling. In the following sections, the role of overall N availability and N chemical speciation in regulating marine primary productivity and C cycling are discussed. This is followed by a discussion of the microbial processes responsible for cycling N in the oceans, which determine N availability and speciation.

1.1.1 Nitrogen availability

The availability of N is considered to control biological productivity in both the modern and ancient ocean, with implications for the evolution of the biosphere over geologic time (Gruber, 2008; Moore et al. 2013; Zerkle & Mikhail, 2017). In ~75% of the surface open ocean, phytoplankton growth is either limited solely or co-limited with phosphorus (P) by the availability of inorganic forms of N (Figure 1.1 – Moore et al. 2008; Graziano et al. 1996; Moore et al. 2013), particularly throughout the low-latitude ocean where the resupply of nutrients from the subsurface is slow. By hindering the growth of primary producers, N availability in turn exerts control over the so-called biological pump — the mechanism by which C, principally in the form of particulate material, is vertically transported into the ocean interior and prevented from ventilating back to the atmosphere over centennial timescales (Sabine et al. 2004).

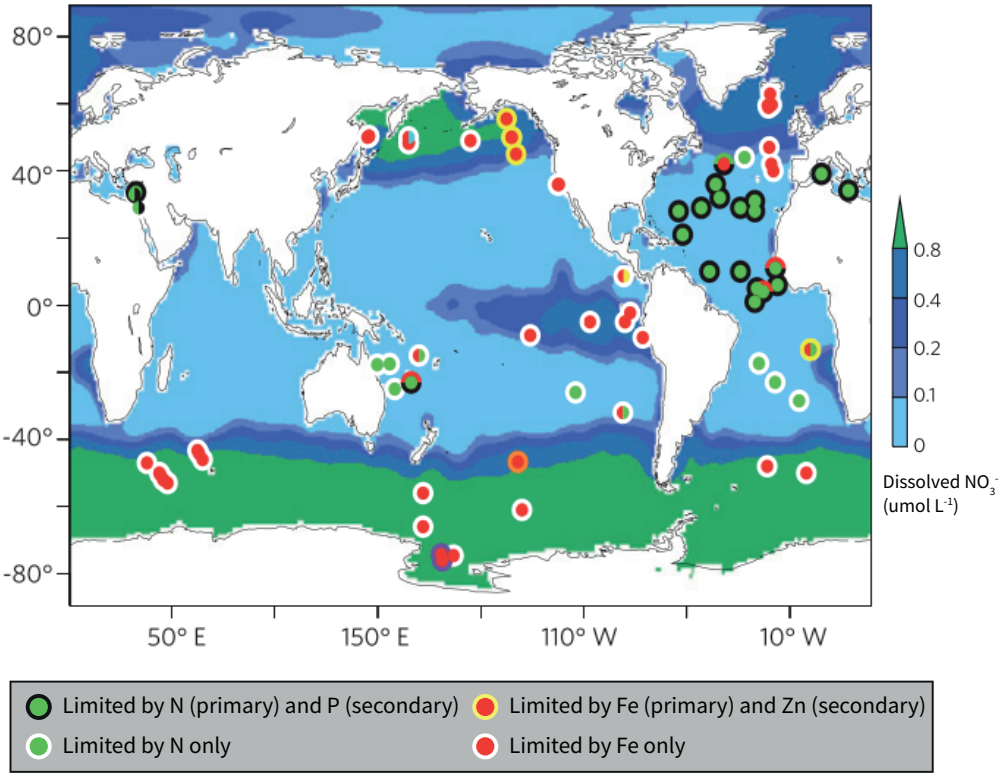


Figure 1.1 Patterns of nutrient limitation

Map modified from Moore et al. (2013) showing the primary and secondary limiting nutrients, with background colour indicating the dissolved NO_3^-. Copyright © 2013, Reprinted with

permission from Nature Publishing Group, a division of Macmillan Publishers Limited. All Rights Reserved (License number: 5178840109258)

1.1.2 Nitrogen speciation

The total N inventory of the modern, oxygenated oceans is determined by the balance of microbial processes that supply N into the oceans through N_2 fixation and remove N through denitrification (discussed in greater detail in Section 1.2). In addition to the quantity of N, the chemical speciation (or oxidation state) of N available to primary producers has an important role in determining phytoplankton community structure in the marine environment. Although abundant (in the μM range, constituting ~70% of the total marine dissolved N pool), most organic N in the oceans, except urea, amino acids, and nucleotides (Bronk et al. 2007), is not readily bioavailable to phytoplankton. Instead, it is inorganic forms of N that typically control phytoplankton growth (Aluwihare & Meador, 2008; Mulholland & Lomas, 2008). Specifically, inorganic N in its most chemically reduced form, ammonium (NH_4^+), is classically viewed as the favoured N species for uptake by phytoplankton (Glibert et al. 2016) as it is in the same oxidation state as the amino acids that build proteins. However, the nutritional preference for NH_4^+ is not universal. Larger phytoplankton, such as diatoms, are considered nitrate (NO_3^-) opportunists (Glibert et al. 2016); high NO_3^-: NH_4^+ availability favours the growth of eukaryotic phytoplankton such as diatoms and coccolithophores, whereas low NO_3^-:NH_4^+ availability favours the growth of mixotrophic dinoflagellates, cyanobacteria and heterotrophic bacteria (Figure 1.2 – Van Oostende et al. 2017; Lomas & Glibert, 1999; Fawcett et al. 2011). Eukaryotic phytoplankton are more mechanically resistant to grazing (Hamm et al. 2003) and form heavier aggregates that sink more effectively through the water column than prokaryotic phytoplankton communities (Fawcett et al. 2011; Fontanez et al. 2015). The result is greater export of C into the ocean interior and a

stronger biological pump in high NO_3^-: NH_4^+ regions; diatoms alone account for ~40% of particulate organic C export from surface waters (Jin et al. 2006). Therefore, through its control on phytoplankton community composition, NO_3^- availability plays an indirect role in the strength of the biological pump, which modulates global climate.

The microbial process responsible for NO_3^- production in the oceans — thereby influencing phytoplankton community composition and the biological pump as described above — is nitrification. In upwelling regions or regions with intense mixing, NO_3^- is primarily supplied from nitrification at depth (Fawcett et al. 2015; Fernández et al. 2009), with euphotic zone nitrification providing a small proportion (typically less than 10%) of the NO_3^- assimilated by phytoplankton (Peng et al. 2018; Shiozaki et al. 2016). In oligotrophic regions with little upwelling, nitrification in the euphotic zone (or in the mixed layer (ML) if the euphotic zone is shallower than the ML) is the primary source of NO_3^- (Clark et al. 2008) and thereby contributes more significantly to NO_3^- uptake by primary producers. For instance, in the North Pacific Tropical Gyre Province, nitrification is estimated to account for up to 87% of NO_3^- assimilation by primary producers (Shiozaki et al. 2016).

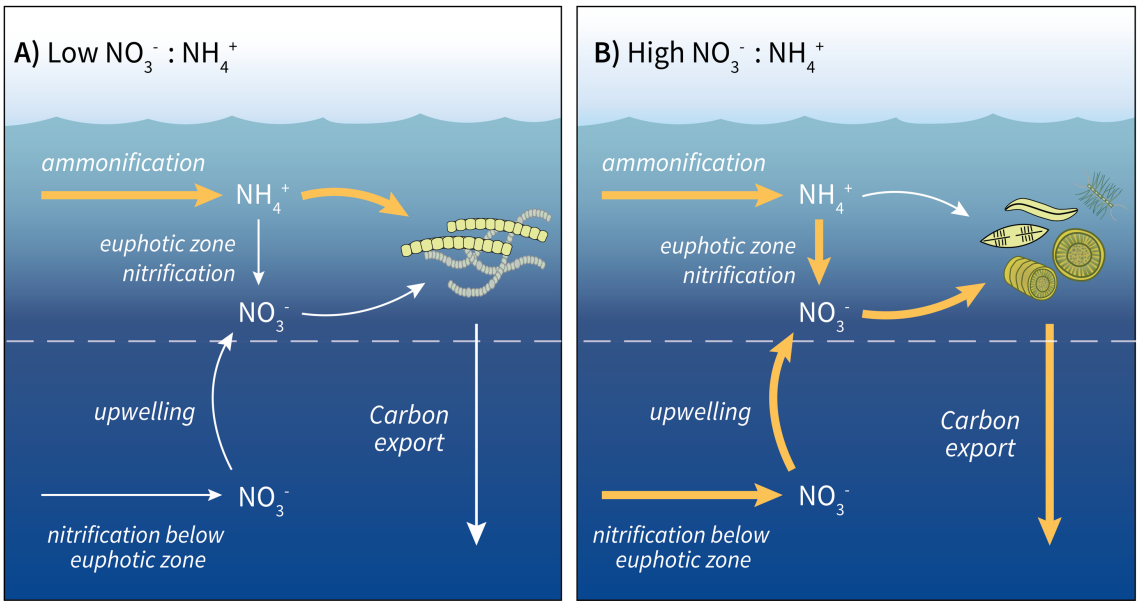


Figure 1.2 Role of dissolved NO_3^-: NH_4^+ availability on phytoplankton community composition

The effect of **A)** low NO_3^-: NH_4^+ availability versus **B)** high low NO_3^-: NH_4^+ availability on phytoplankton community composition and carbon export to depth. Surface NO_3^-: NH_4^+ is determined by the rates of euphotic zone nitrification and the upwelling of NO_3^- formed through nitrification below the euphotic zone (or the mixed layer depth).

1.2 THE MARINE NITROGEN CYCLE

In the oceans, N exists in both organic (particulate and dissolved organic N, PON and DON respectively) and dissolved inorganic forms (ammonium (NH_4^+), nitrite (NO_2^-) and nitrate (NO_3^-)). Unlike other key macronutrients (such as silicon and P), the cycling of N is dominated by microorganisms that transform N between its oxidation states, ranging from –III to +V (Figure 1.3). DIN supports both assimilatory organic biomass production and dissimilatory energy-yielding processes, thereby acting as a nutrient, electron donor, and electron acceptor — supporting a wealth of different marine microbial metabolisms in the oceans.

1.2.1 Aerobic nitrogen cycling

Around half of the N on Earth is in the atmosphere, in the form of gaseous N_2 (Canfield et al. 2010). Specialist prokaryotic microorganisms (called diazotrophs) can reduce N_2

dissolved in seawater into NH_4^+, thereby 'fixing' N into their organic biomass. Following cell death, heterotrophic bacteria and zooplankton break down particulate and dissolved organic N (PON and DON), releasing fixed N back into the oceanic milieu as NH_4^+ and urea (CH_4N_2O) through the process of ammonification. NH_4^+ regenerated through ammonification is rapidly assimilated as a nutrient, particularly by microbial groups unable to perform N_2 fixation. In some oceanic regions where there is little new N input through N_2 fixation (Needoba et al. 2007; Dugdale & Goering, 1967), notably in open ocean sub-tropical regions, primary productivity relies solely on the supply of regenerated N (Sohm et al. 2011; Moore et al. 2009; Grabowski et al. 2008). NH_4^+ is also used by chemolithotrophic microorganisms that yield energy through the stepwise or complete oxidation of NH_4^+ to NO_3^- in the process of nitrification (discussed in Section 1.3). As such, NH_4^+ and NO_2^- rarely accumulate to significant concentrations in the oxygenated open ocean (~0.4 μmol L^{-1}, Figure 1.4) before being rapidly depleted through assimilatory or dissimilatory processes. In the oligotrophic Atlantic Ocean, these processes completely turn over the regenerated DIN pool within one day (Clark et al. 2008). The result is that most of the DIN in the oceans is in an oxidised form as NO_3^-, which accumulates to μM levels in the oceans, especially in the deep ocean where there is little to no consumption of NO_3^- (Figure 1.4, Levitus et al. 1993). Maximum concentrations of NH_4^+ and NO_2^- typically occur shallower in the water column, reflecting an imbalance towards processes that produce rather than consume these species. NH_4^+ and NO_2^- maxima are formed when their supply (either through PON/DON regeneration, ammonia oxidation or impartial nitrate reduction – Figure 1.3) outstrips demand by phytoplankton, ammonia- and nitrite-oxidising microorganisms — particularly when these microorganisms are limited by other physicochemical factors such as light or micronutrients (Saino et al. 1983; Lomas & Lipschultz, 2006; Santoro et al. 2013; Jacquot et al. 2013).

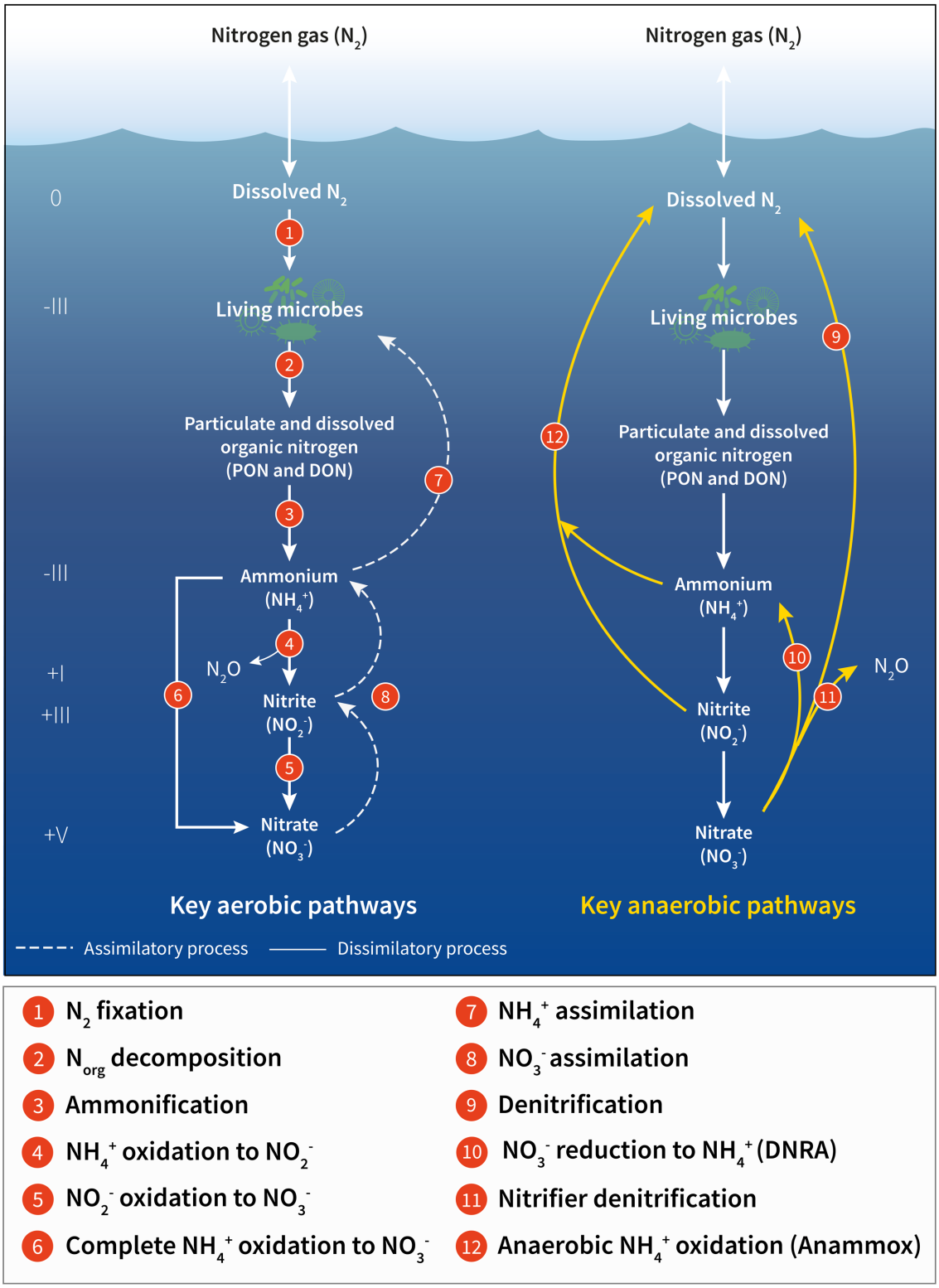


Figure 1.3 Microbial pathways in the marine nitrogen cycle

Key aerobic (white arrows) and anaerobic pathways (yellow arrows) in the marine N cycle. The oxidation state of N in inorganic and organic forms is indicated on the left-hand side of the figure. Solid arrows indicate dissimilatory processes, and dashed arrows indicate assimilatory processes.

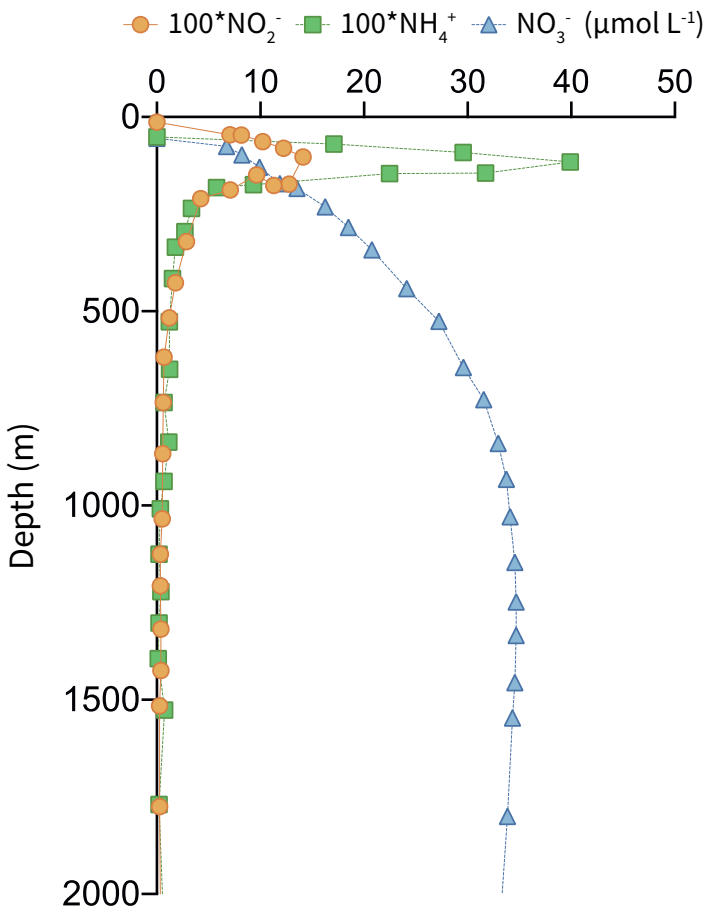


Figure 1.4 Depth distribution of inorganic nitrogen in the oceans

Data replotted from Gruber (2008).

1.2.2 Anaerobic nitrogen cycling

Oxidised forms of N (NO_2^- and NO_3^-) produced through nitrification support a range of dissimilatory metabolisms in low O_2 regimes, which ultimately return N to the atmosphere as N_2 (Figure 1.3; Lam & Kuypers, 2011). Oxidised forms of N are reduced back to N_2, nitrous oxide (N_2O) or NH_4^+ through heterotrophic denitrification, anaerobic ammonium oxidation (anammox) (Van de Graaf et al. 1995; Dalsgaard et al. 2005) or dissimilatory nitrate or nitrite reduction to ammonium (DNRA; Kartal et al. 2007). In these processes, microorganisms use NO_3^- or NO_2^- as a terminal electron acceptor when O_2 is low (Figure 1.3). Up to 40% of total N loss from the oceans occurs in oxygen minimum zones (OMZs), which collectively cover only ~1% of ocean volume worldwide

(Gruber, 2008; Lam & Kuypers, 2011). Anaerobic N cycling in OMZs results in inorganic N depth profiles distinct from those found in oxygenated regimes. For instance, NO_3^- accumulates at shallower depths than NO_2^- in OMZs (Peng et al. 2015; Ganesh et al. 2018; Bertagnolli & Stewart, 2018). Although O_2 concentrations in OMZs fall within the low nM to pM range, oxidative processes — such as nitrification — are not totally absent and make important contributions to biogeochemical N cycling in OMZs (See Box 1).

1.3 NITRIFICATION

Nitrification links the oxidative and reduced arms of the biogeochemical N cycle and is the last step in the remineralisation of organic N in the marine environment (Figure 1.3). Nitrification is primarily a two-step process mediated by distinct sets of microorganisms that carry out each step (Figure 1.5), however, a third group of microorganisms have recently been discovered that are capable of performing complete ammonia oxidation to nitrate (comammox; Daims et al. 2015; van Kessel et al. 2015). It is the first step of nitrification, aerobic ammonia (NH_3) oxidation to nitrite (NO_2^-), which is considered to be the rate-limiting component of nitrification (Kowalchuk & Stephen, 2001), except to some extent in the primary NO_2^- maximum in the oceans (Lomas and Lipschultz, 2006). Ammonia oxidation to nitrite (hereafter referred to simply as 'ammonia oxidation') is carried out by chemolithoautotrophic ammonia-oxidising archaea (AOA) and bacteria (AOB). Ammonia (NH_3), rather than ammonium (NH_4^+), is the substrate for ammonia oxidation by AOB (Suzuki et al. 1974; Burton & Prosser, 2001) and is assumed to be the substrate for AOA (Martens-Habbena et al. 2009; Beman et al. 2011). Hereafter, ammonia or NH_3 is used in reference to the microbial process of ammonia oxidation, and ammonium or NH_4^+ is used to refer to the combined pool of the species at equilibrium in seawater — i.e., NH_3 and NH_4^+. Written forms rather than chemical forms of these species are used when it aids in readability. The following

sections take a closer look at the biochemistry, physiology, and taxonomy of bacterial and archaeal ammonia oxidisers.

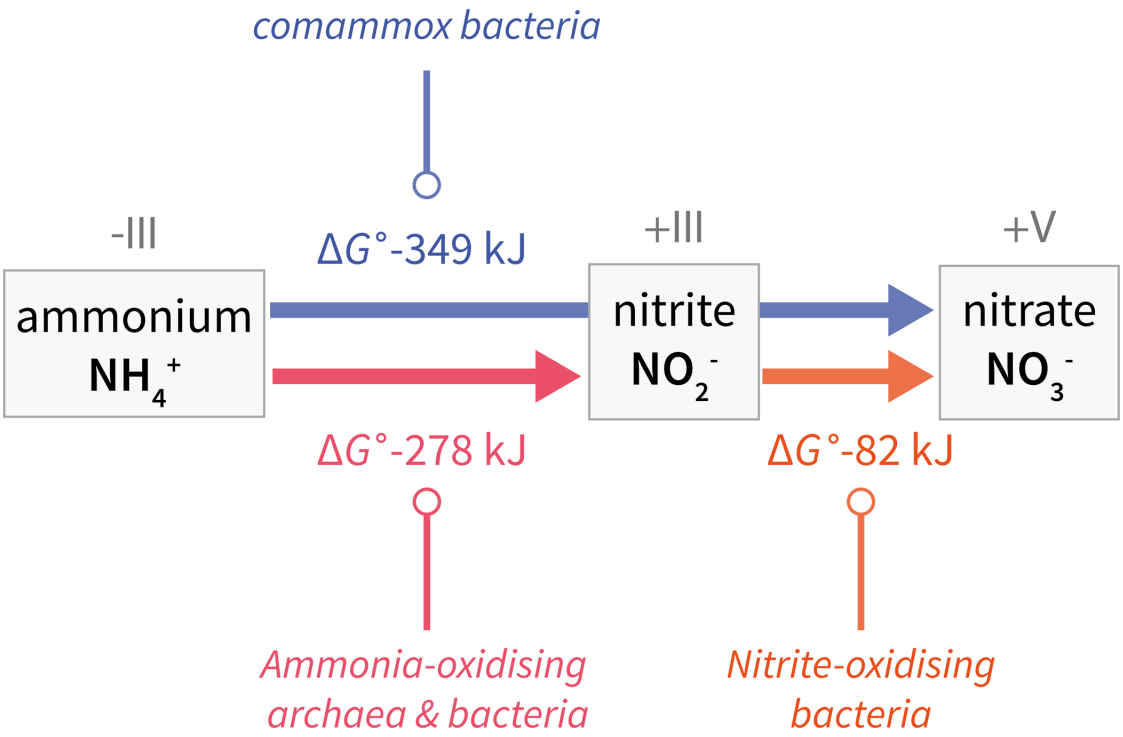


Figure 1.5 Microbially-mediated nitrification pathways

Key microbially-mediated pathways in marine nitrification. The standard Gibbs free energy (ΔG◦) of each respiratory pathway is indicated. The oxidation state of N in each chemical form is also shown.

1.4 MICROBIAL AMMONIA OXIDATION

1.4.1 Two cohorts of ammonia oxidisers

For over 100 years after the discovery of AOB at the end of the 19th century (Winogradsky, 1890), only Proteobacteria were considered capable of performing aerobic ammonia oxidation (Purkhold et al. 2003). In 2004, *amoA* genes encoding the alpha subunit of ammonia monooxygenase (AMO) — the hallmark enzyme of ammonia oxidation — were discovered in association with metagenomic archaeal scaffolds in marine surface waters (Venter et al. 2004) and soils (Schleper et al. 2005; Treusch et al.

2005). Archaeal ammonia oxidation was verified in 2005 through isolation and physiological characterisation of *Nitrosopumilus maritimus* strain SCM1 from a marine aquarium (Figure 1.6 – Könneke et al. 2005; Francis et al. 2005).

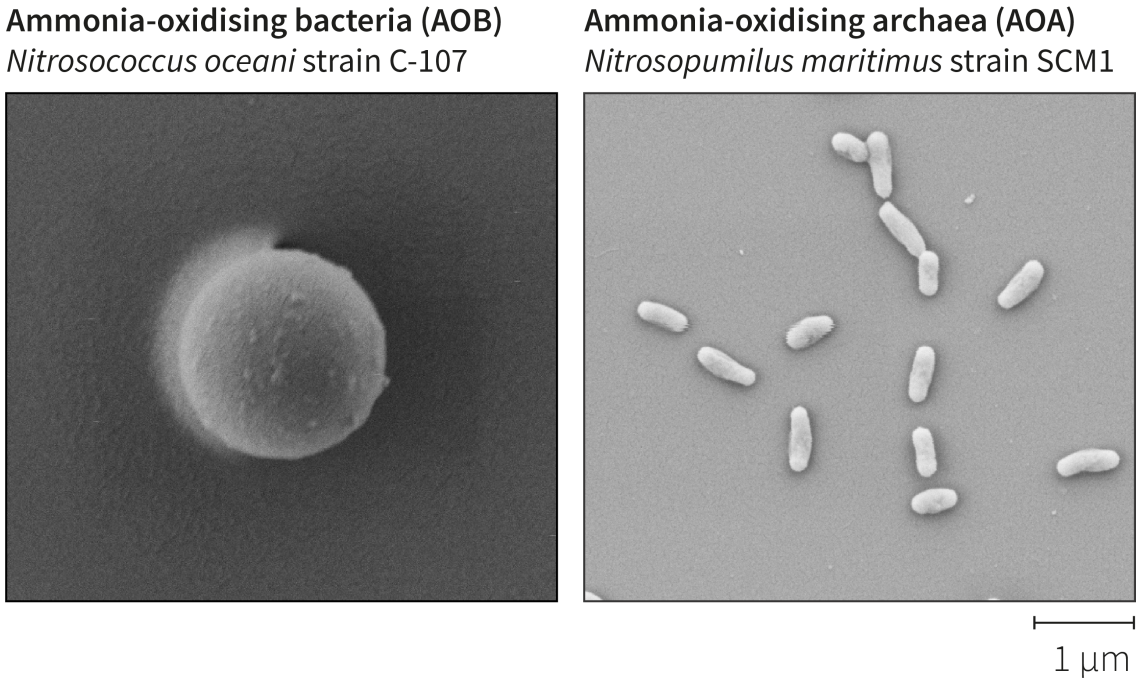


Figure 1.6 SEM images of marine ammonia-oxidising archaea and bacteria

Scanning Electron Micrographs of the marine AOB, *Nitrosococcus oceani*, and the ammonia-oxidising archaeon, *Nitrosopumilus maritimus* (images from Shafiee et al. 2019, 2021a — Chapters two and four).

The low growth rates and biomass yields of both marine AOA and AOB make their isolation into pure laboratory cultures extremely challenging. To date, there are only a handful of marine AOA and AOB that have been successfully isolated into pure culture (Könneke et al. 2005; Kim et al. 2016; Qin et al. 2017b; Klotz et al. 2006). Nevertheless, there has been great progress in physiological and biochemical characterisation of ammonia oxidisers using available pure and enrichment cultures (Ahlgren et al. 2017, Bayer et al. 2016, Berg et al. 2015, Mosier & Francis, 2011; Santoro & Casciotti, 2011; Merbt et al. 2011; Martens-Habbena et al. 2009) and molecular DNA-based methods — particularly of the *amoA* gene (Francis et al. 2005; Alves et al. 2018). A principal finding

of the research to date is that AOA widely outnumber AOB in the marine environment (Mincer et al. 2007; Wuchter et al. 2006; Santoro et al. 2010; Santoro et al. 2013; Horak et al. 2013; Newell et al. 2013; Peng et al. 2016). The dominance of AOA is purportedly underpinned by physiological traits that make AOA ostensibly well adapted to the nutrient-poor marine environment (discussed in greater detail in Section 1.5).

1.4.2 Differences between ammonia-oxidising archaea and bacteria

1.4.2.1 Taxonomy and phylogeny

Most evidently, AOA and AOB are taxonomically distinct microorganisms, belonging to different domains of life and possessing different evolutionary histories (Figure 1.7 – Ren et al. 2019; Ward et al. 2021). AOB are polyphyletic, with the ability to oxidise ammonia apparently arising multiple times (Ward, 2008). All discovered AOB fall into the Betaproteobacteriales and the Nitrosococcales orders, within the Gamma (γ-) proteobacteria. Recent reclassifications based on whole genome phylogenies, now place what was previously the Betaproteobacteria class into a new order Betaproteobacteriales within the class of Gammaproteobacteria (Parks et al. 2018). AOB within the Betaproteobacteriales are divided into the *Nitrosomonas* and *Nitrosospira* genera and *Nitrosomonas* are further subdivided into six clusters based on either 16S rRNA or *amoA* gene phylogeny. Three *Nitrosomonas* clusters – cluster 6b (containing the *Nitrosomonas marina* lineage), cluster 9 (*Nitrosomonas* sp. Nm143 lineage), and the *Nitrosomonas cyrotolerans* lineage AOB – are commonly detected in marine or other saline environments (Prosser et al. 2014). Recent work indicates that the genetic clustering of *Nitrosomonas* correlates with the physiological adaptations to ammonium availability (Sedlacek et al. 2019). AOB within the Nitrosococcales order fall into one family (Nitrosococcaceae) and genus (*Nitrosococcus*) of which there are four known species (*Nitrosoccocus halophilus*, *Nitrosococcus oceani*, *Nitrosococcus wardiae* and

Nitrosococcus watsonii). While *Nitrosococcus*-like sequences are only found in marine or saline environments, *Nitrosospira* and *Nitrosomonas*-like sequences have been retrieved from both marine and terrestrial environments (Ward, 2008). *Nitrosospira*-like sequences often dominate in gene sequences retrieved from the oceanic environments (Bano & Hollibaugh, 2000; O'Mullan & Ward, 2005; Bernhard et al. 2010; Rotthauwe et al. 1997). *Nitrosococcus*-like sequences, principally of the species *Nitrosococcus oceani*, have also been detected in the marine environment (Ward & O'Mullan, 2002; Wang et al. 2020; Lam et al. 2009), but their contributions to the AOB populations remains unclear due to the historical bias towards the use of *Nitrosospira* primers (see Box 2). However, global metagenomic and metatranscriptomic databases, such as the *Tara* Oceans Gene Atlas, show that genes and transcripts ascribed to the *Nitrosococcus* genus are widespread and abundant (see Appendix III) relative to their *Nitrosospira* and *Nitrosomonas* counterparts, suggesting their contribution to the AOB community activity may be high. However, it cannot be ruled out that this is due to differential abundance of gene copy numbers between different AOB species (See Box 2), which requires further investigation.

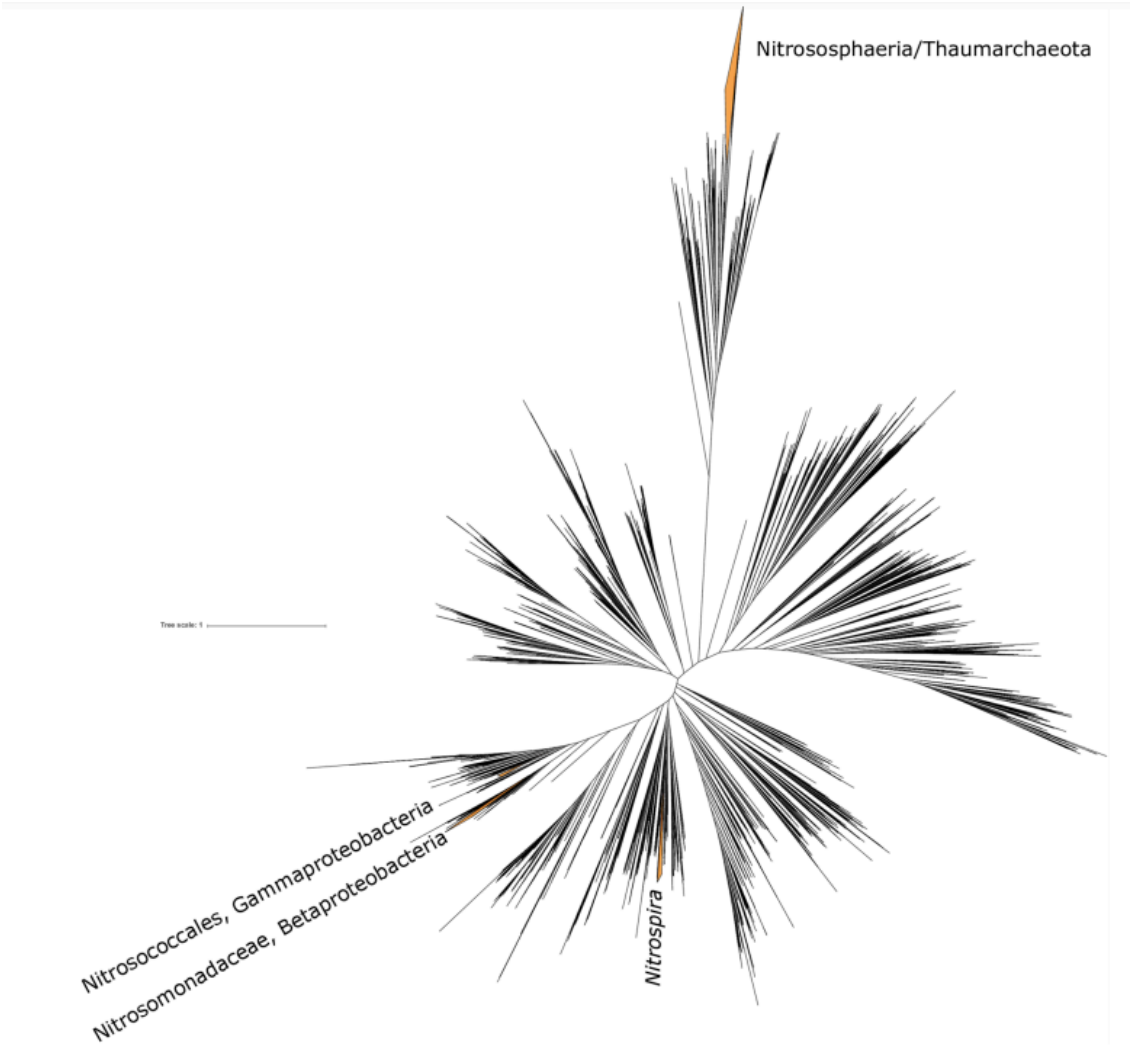


Figure 1.7 Ammonia-oxidising bacteria and archaea on the tree of life

Figure from Ward et al. (2021) showing the tree of life built with concatenated ribosomal proteins. Clades of ammonia-oxidising organisms highlighted in orange and labelled. The distribution of ammonia oxidation is polyphyletic, spread across one lineage within the Archaea (*Nitrososphaeria*) and three within the Bacteria (*Nitrosococcales*, *Nitrosomonadaceae* and *Nitrospira*). Note that this tree of life is based on previous AOB classifications, with recent reclassifications based on whole genome phylogenies, now place what was previously the Betaproteobacteria class into a new order Betaproteobacteriales within the class of Gammaproteobacteria (Parks et al. 2018) – see Section 1.4.2.1. Copyright © Ward et al. (2021)

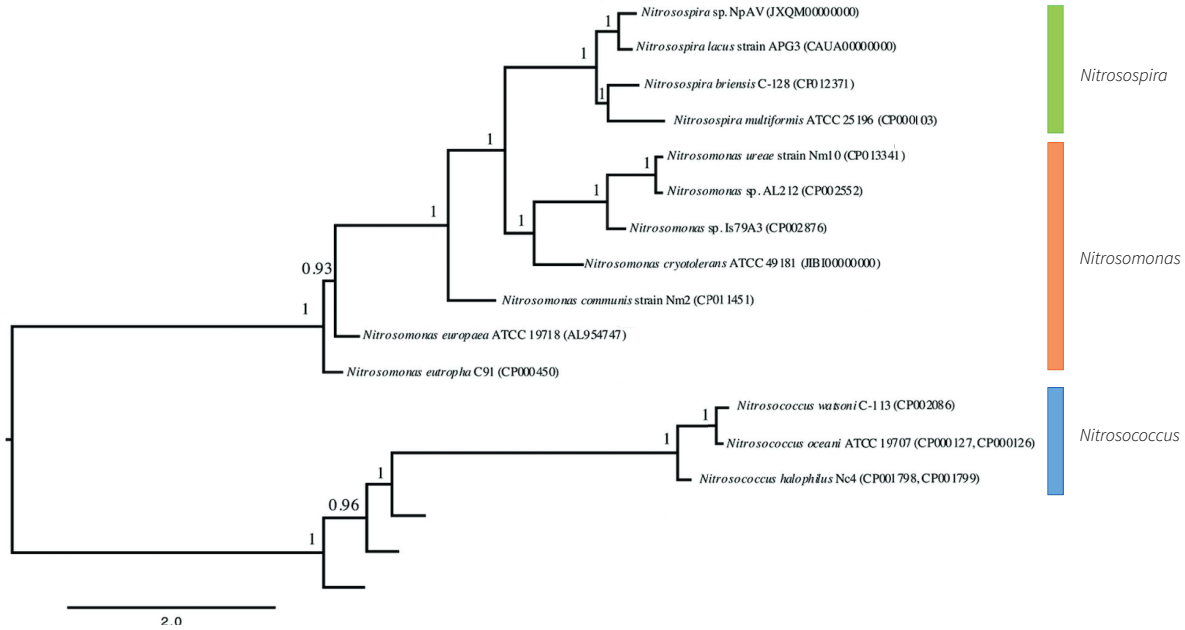


Figure 1.8 Phylogeny of ammonia-oxidising bacteria

Rooted maximum likelihood phylogeny of ammonia-oxidising bacteria based on conserved amino-acid sequences, modified from Kozlowski et al. (2016). AOB genera *Nitrosospira*, *Nitrosomonas* and *Nitrosococcus* shown. Copyright © Kozlowski et al. (2016)

Based on 16S rRNA and *amoA* sequences, AOA are diverse and highly abundant in marine and terrestrial environments (Figure 1.9 – Francis et al. 2005; Leininger et al. 2006). Marine AOA belong to the Marine Group I Archaea — one of the four groups of planktonic marine archaea (Delong 1992, Fuhrman et al. 1992; Fuhrman & Davis, 1997; Lopez-Garcia et al. 2001). Marine AOA, together with terrestrial AOA, were originally classified into the *Crenarchaeota* phylum but later classified into the *Thaumarchaeota* (Brochier-Armanet et al. 2008). However, a recently updated archaeal taxonomy (available at https://gtdb.ecogenomic.org/), based on more 16S rRNA sequences, now places all cultivated AOA — both marine and terrestrial — into the class of *Nitrososphaeria* within the phylum *Thermoproteota* (Parks et al. 2020; Rinke et al. 2020).

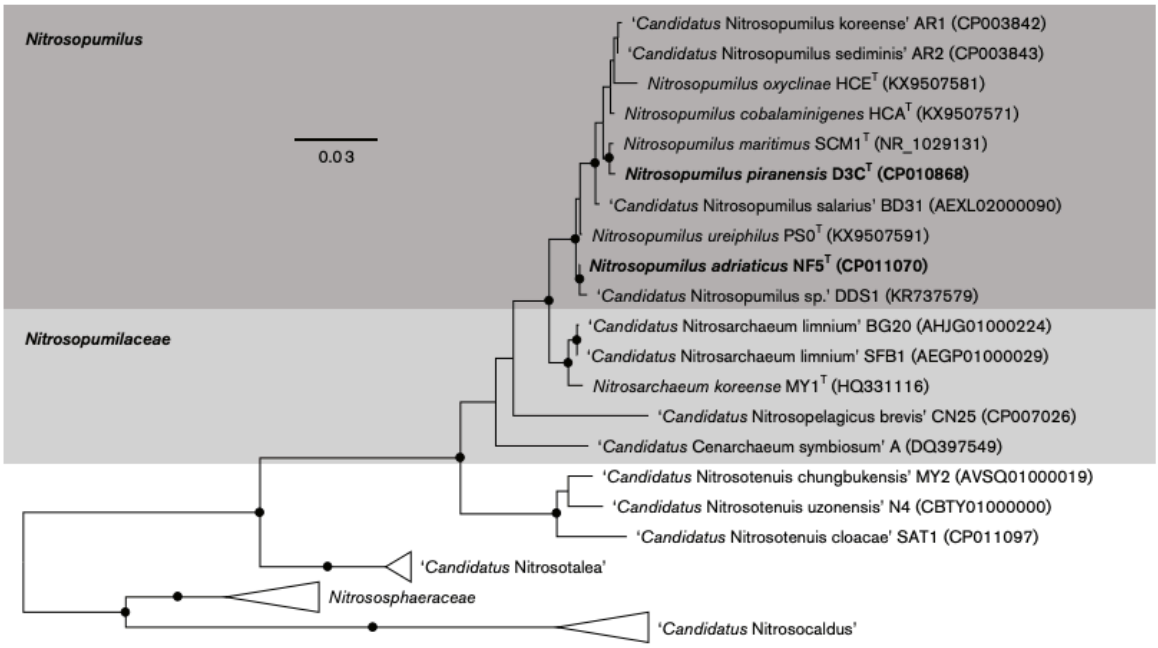


Figure 1.9 Phylogeny of ammonia-oxidising archaea

Phylogenetic maximum-likelihood tree of full-length 16S rRNA gene sequences from cultivated members of the class *Nitrososphaeria*. Figure from Bayer et al. (2019). Copyright © Bayer et al. 2019

1.4.2.2 Ammonia oxidation

AOA and AOB are chemolithoautotrophic, deriving energy through the oxidation of an inorganic electron donor (ammonia), using O_2 as an electron acceptor and producing hydrogen ions and NO_2^-. In both AOA and AOB, the first step of ammonia oxidation is catalysed by membrane-associated ammonia monooxygenase (AMO), which consumes molecular O_2. AMO has never been completely purified and characterised *in vitro*, with most of its structural and mechanistic features deduced from its primary sequence homology with methane monooxygenase of methanotrophs (Arp et al. 2002). In its active form, AMO is a metalloprotein that putatively contains 2–3 atoms of copper (Cu), 1–2 atoms of iron (Fe), with some evidence that it also contains zinc (Zn) (Sazinsky & Lippard, 2015; Woodland & Dalton, 1984).

A three-step pathway for bacterial ammonia oxidation was recently proposed (Lehtovirta-Morley, 2018; Figure 1.10), whereby ammonia is firstly oxidised to

hydroxylamine (NH_2OH) by AMO, then to NO by hydroxylamine dehydrogenase (previously termed hydroxylamine oxidoreductase — HAO, Hooper & Terry, 1978), and finally to NO_2^- by a nitrite reductase — although this has yet to be demonstrated experimentally (Caranto & Lancaster, 2017). Pure or enrichment AOA cultures do not possess the hydroxylamine dehydrogenase genes found in AOB (Walker et al. 2010; Kim et al. 2016), and therefore the network of electron carriers that link the oxidation of NH_2OH to NO_2^- in AOA remains unresolved. However, it is hypothesised that this system involves several Cu-containing plastocyanins encoded in AOA genomes (Walker et al. 2010; Kerou et al. 2016; Kozlowski et al. 2016) although this has yet to be confirmed empirically. The recent discovery that bacterial ammonia oxidation is a three-step process raises the possibility that archaeal ammonia oxidation is also a three-step process (Carini et al. 2018).

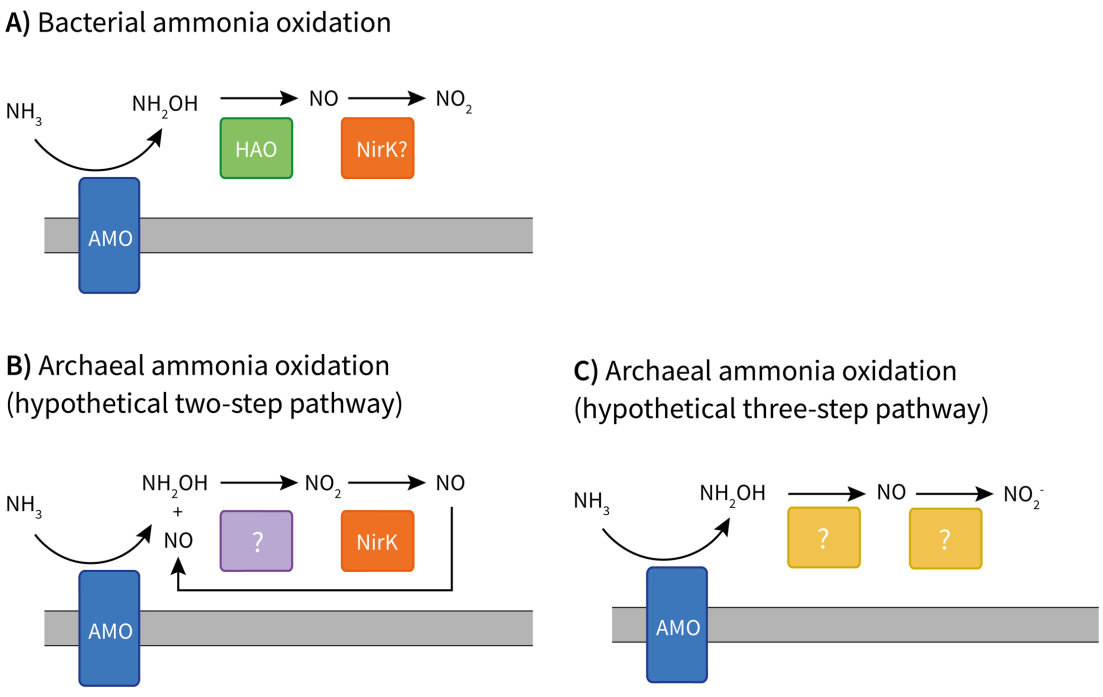


Figure 1.10 Proposed pathways for bacterial and archaeal ammonia oxidation

A) Proposed model for bacterial ammonia oxidation **B)** Proposed two-step model for archaeal ammonia oxidation (Kozlowski et al. 2016) and **C)** Proposed three-step model for archaeal ammonia oxidation (Lehtovirta-Morley, 2018).

BOX 1 – AMMONIA OXIDATION UNDER LOW OXYGEN AND NITROUS OXIDE PRODUCTION

Although an oxidative process, ammonia oxidation and the activity of AOA and AOB is not confined to oxygenated environments, with low O_2 environments permitting the co-occurrence of oxidative and reductive processes. Significant rates of ammonia oxidation have been detected in low O_2 environments, such as oxygen minimum zones (OMZs), which typically show the highest ammonia oxidation rates at the upper boundaries of the OMZs (Lipschultz et al. 1990; Ward et al. 1989; Lam et al. 2009). AOA isolates appear adapted to both high and low O_2 (Peng et al. 2016; Qin et al. 2017a), performing ammonia oxidation even under the nM to pM O_2 levels characteristic of OMZs. Indeed, AOA are considered to contribute more significantly to ammonia oxidation in OMZs (Lam et al. 2009; Peng et al. 2016).

The growth of both AOA and AOB is associated with the production of nitrous oxide, N_2O, a potent greenhouse gas and stratospheric ozone-depleting agent. N_2O is produced as a by-product of NH_4^+ oxidation in AOA (Stieglmeier et al. 2014; Kozlowski et al. 2016; Santoro & Casciotti, 2011), with greater N_2O yields under lower O_2 (Goreau et al. 1980; Löscher et al. 2012; Qin et al. 2017a). AOA have been suggested to be largely responsible for oceanic N_2O emissions (Santoro & Casciotti, 2011). AOB are also able to produce N_2O as a by-product of ammonia oxidation (Caranto & Lancaster, 2017; Caranto et al. 2016) and in the process of "nitrifier denitrification" (Stein, 2011; Wrage et al. 2001; Shaw et al. 2006; Casciotti & Ward, 2001; Casciotti & Ward, 2005; Stieglmeier et al. 2014). While AOB N_2O production through nitrifier denitrification increases under O_2 limitation (Goreau et al. 1980; Wrage et al. 2001; Zhu et al. 2013; Stieglmeier et al. 2014) there are observations of

N_2O production through nitrifier denitrification in oxygenated water columns (Wilson et al. 2014).

This thesis primarily focuses on ammonia oxidation in the oxygenated oceans but acknowledges the growing body of evidence demonstrating the significant role played by AOA/AOB in regions of low O_2, especially in the production of N_2O (e.g. Santoro & Casciotti, 2011). As OMZs continue to expand, characterising the growth of AOA and AOB in these regions will grow in importance. The priorities for future research into ammonia oxidation under low O_2 is discussed in greater detail in Section 5.4.3.

1.4.2.3 Carbon fixation

Although there is an emerging body of evidence pointing to the potential for a mixotrophic lifestyle (Qin et al. 2014; Bayer et al. 2016, Prosser & Nicol, 2012), AOA and AOB are primarily autotrophic, fixing their own C. Therefore, AOA and AOB contribute to marine primary productivity both directly and indirectly by influencing phytoplankton community composition, as outlined in Section 1.1. It is estimated that C fixation by AOA in meso– and bathypelagic waters of the North Atlantic could account for 15–53% of phytoplankton export production from surface water (Reinthaler et al. 2010), assuming ~30% export production leaves the euphotic zone. On a global scale, seawater AOA are estimated to fix approximately 400 Tg C y^{-1} (Hügler & Sievert, 2011). Yet, this still represents only a fraction of total marine primary productivity, with phytoplankton fixing ~30,000–50,000 Tg C y^{-1} (Falkowski, 1994).

In contrast to the mechanisms of ammonia oxidation, which are still not fully resolved, the pathways for the autotrophic assimilation of C have been identified in both cohorts of ammonia oxidisers (Arp et al. 2007; Könneke et al. 2014). In AOB, C is fixed via the Calvin-Benson-Bassham (shortened to Calvin) cycle (Arp et al. 2007), whereas all AOA

characterised thus far use a modified version of the 3-hydroxypropionate/4-hydroxybutyrate (3-HP/4-HB) cycle (Berg et al. 2007; Könneke et al. 2014). The archaeal 3-HP/4-HB cycle represents the most energy-efficient aerobic autotrophic pathway yet characterised (Könneke et al. 2014) in terms of the amount of cell biomass generated per mole of ATP.

1.4.3 Distribution and abundance of marine ammonia-oxidising archaea and bacteria and marine ammonia-oxidation rates

In the oceans, archaeal and bacterial *amoA* genes are quantified as an indication of the relative cell abundances of AOA and AOB. However, there are known caveats to using *amoA* genes as an indication of cell abundances (discussed in Box 2). While AOA and AOB *amoA* measurements made in the marine environment continue to increase, there is still a shortage of data surrounding the abundance and distribution of marine ammonia oxidisers — particularly in the open ocean where sampling is more logistically challenging. Figure 1.11 is not intended to provide an exhaustive compilation of marine archaeal and bacterial *amoA* measurements and ammonia oxidation rates (particularly in coastal regions where there are a greater number of observations), but highlights that there are key open ocean regions in which data are lacking. As shown in Figure 1.11, quantification of *amoA* abundances and ammonia oxidation rates have largely focused on the Atlantic and Pacific Oceans, with fewer studies in the Indian Ocean. Further still, the number of studies quantifying bacterial *amoA* abundances (particularly of AOB belonging to the Nitrosococcales order) are lower than those investigating archaeal *amoA* abundances. The finding that AOA usually make a greater contribution to marine ammonia oxidation than AOB (Martens-Habbena et al. 2009; discussed in greater detail in the following sections) has likely shifted research efforts to characterising AOA distribution, specifically in relation to AOA ecotypes (see Box 3).

Archaeal *amoA* genes are typically detected at abundances ~ three orders of magnitude greater than those of AOB in the marine environment (Mincer et al. 2007; Wuchter et al. 2006; Santoro et al. 2010; Santoro et al. 2013; Horak et al. 2013; Newell et al. 2013; Peng et al. 2016—Figure 1.11). Assuming that the number of *amoA* copies per cell are similar (see Box 2 for further discussion), the preponderance of archaeal *amoA* genes suggests that AOA largely outnumber AOB throughout the marine environment, with the dominance of AOA additionally supported by 16S rRNA quantification (Wuchter et al. 2006). The dominance of AOA over AOB in the oceans means that marine ammonia oxidation rates (measured in nmol L^{-1} of NH_4^+ oxidised to NO_2^-, NO_3^- or both these species per day) typically co-vary with AOA abundances (Horak et al. 2018; Santoro et al. 2013; Mincer et al. 2007; Beman et al. 2008; Church et al. 2010; Hollibaugh et al. 2010; Newell et al. 2013; Santoro et al. 2013), specifically of the Water Column A AOA ecotype (Box 3; Shiozaki et al. 2016; Santoro et al. 2017). However, exceptions have been documented, for instance in OMZs (Newell et al. 2011; Lam et al. 2009), where the activity of AOB (gene expression – mRNA ml^{-1}) has been seen to correlate with NH_4^+ oxidation rates (Lam et al. 2009).

AOA *amoA* copies and ammonia oxidation rates in the marine environment range between undetectable using currently available methods (Olson, 1981a; Lipschultz et al. 1990, Ward & Kilpatrick, 1991; Raimbault et al. 1999; Clark et al. 2008) up to a maximum of 5×10^7 *amoA* copies ml^{-1} and ~10^3 nmol NH_4^+ oxidised L^{-1} d^{-1}. The current understanding of the abundance and distribution of AOB in the marine environment (as shown in Figure 1.11) is largely based on the detection of Betaproteobacteriales *amoA* sequences, rather than those of the Nitrosococcales order (previously referred to as simply γ -AOB). The historical bias towards detection of Betaproteobacteriales AOB over Nitrosococcales is discussed further in Box 2, and the following sections describe those

trends observed primary from studies of Betaproteobacteriales-AOB. AOB *amoA* in the marine environment is more frequently undetected relative to archaeal *amoA* (Mincer et al. 2007; Shiozaki et al. 2016; Newell et al. 2013; Santoro et al. 2013) and reaches lower maximum abundances (~8×10^5 copies ml^{-1} detected in the Puget Sound Estuary — Horak et al. 2013; Figure 1.11A). Unlike AOA, bacterial *amoA* does not typically mirror overall ammonia oxidation rates (Horak et al. 2013; Santoro et al. 2015) —— but as previously stated, rare exceptions do exist (Lam et al. 2009). Maximum *amoA* gene copies (of both AOA and AOB) and NH_4^+ oxidation rates are typically observed in coastal regions compared with open ocean regimes (Sutka et al. 2004; Martens-Habbena et al. 2015; Ward & Zafiriou, 1988). This trend is considered to be the result of a greater NH_4^+ supply, which as the energy substrate for ammonia oxidation, is considered to act as a first-order control on AOA/AOB growth (Ward, 2008).

In addition to showing lateral variation, AOA and AOB *amoA* copies and ammonia oxidation rates also vary with depth in the water column, with ammonia oxidation detected as deep as 3000m (Ward & Zafiriou, 1988). Maximum AOA *amoA* abundances (~10^6 *amoA* copies ml^{-1}) and ammonia oxidation rates are typically observed at the base of the euphotic zone, with lower rates in both the overlying sunlit surface waters and the underlying mesopelagic waters (Santoro et al. 2013; Newell et al. 2013 – Figure 1.11). In contrast, maximum AOB *amoA* copies are documented at < 100 m (averaging ~10^4 copies per ml^{-1}) and continue to decline with depth to a minimum at ~300 m (1.5×10^2 copies ml^{-1}), remaining constant with increasing depth (Figure 1.11). However, it should be noted that the fewer number of bacterial *amoA* datasets introduces a greater degree of uncertainty in relation to the trends of AOB distribution relative to those of AOA.

Low AOA abundances and ammonia oxidation rates in the euphotic zone have historically been attributed to photoinhibition of AOA/AOB growth (Merbt et al. 2011),

and more recently to competition with fast-growing phytoplankton for NH_4^+ (Ward, 2008; Smith et al. 2014) — especially under NH_4^+-poor regimes (Wan et al. 2018). At the base of the euphotic zone where light levels are reduced, photoinhibition of ammonia oxidisers is thought to be alleviated while phytoplankton become light limited, thereby reducing their NH_4^+ uptake. Combined with the increased NH_4^+ supply through organic material remineralisation (ammonification) this enhances NH_4^+ supply to ammonia oxidisers (Ward 2008; Bouskill et al. 2012). Low nitrification rates below the euphotic zone in the mesopelagic are similarly thought to be associated with a reduction in the NH_4^+ flux due to the decreasing supply of NH_4^+ from organic matter decomposition with increasing depth (Kalvelage et al. 2013; Ward, 2008). The accumulation of NO_3^- in the deep ocean (Figure 1.4) therefore represents persistent but low nitrification rates coupled with the absence of a significant consumption of NO_3^-.

While these explanations are generally supported by co-varying depth profiles of NH_4^+ supply, irradiance and AOA abundances/NH_4^+ oxidation rates (Santoro et al. 2015), a growing body of literature shows that NH_4^+ oxidation rates are significantly variable in surface waters (Figure 1.11B) and do not always correspond to NH_4^+ availability (Shiozaki et al. 2016; Jacquot et al. 2013; Horak et al. 2013; Smith et al. 2014) or light levels (Lomas et al. 2009; Newell et al. 2013; Lipschultz, 2001; Beman et al. 2011). This suggests additional factors may exert control over ammonia oxidation rates in the marine environment.

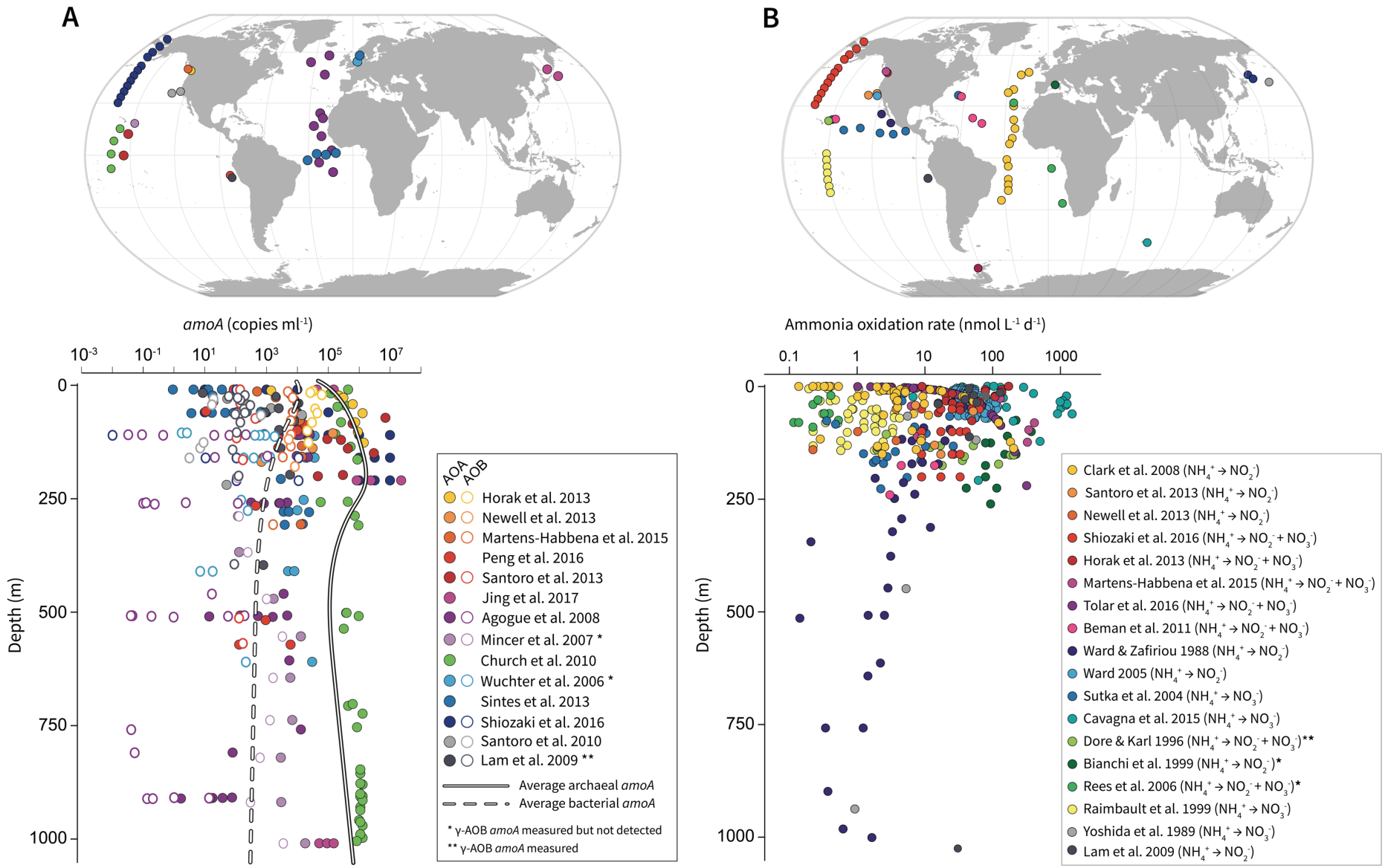

A
B
amoA (copies ml-1)
10-3
10-1
101
103
105
107
0
250
500
750
1000
Depth (m)
AOA
AOB
Horak et al. 2013
Newell et al. 2013
Martens-Habbena et al. 2015
Peng et al. 2016
Santoro et al. 2013
Jing et al. 2017
Agogue et al. 2008
Mincer et al. 2007 *
Church et al. 2010
Wuchter et al. 2006 *
Sintes et al. 2013
Shiozaki et al. 2016
Santoro et al. 2010
Lam et al. 2009 **
Average archaeal amoA
Average bacterial amoA
* γ-AOB amoA measured but not detected
** γ-AOB amoA measured
Ammonia oxidation rate (nmol L-1 d-1)
0.1
1
10
100
1000
Clark et al. 2008 (NH4+ → NO2-)
Santoro et al. 2013 (NH4+ → NO2-)
Newell et al. 2013 (NH4+ → NO2-)
Shiozaki et al. 2016 (NH4+ → NO2- + NO3-)
Horak et al. 2013 (NH4+ → NO2- + NO3-)
Martens-Habbena et al. 2015 (NH4+ → NO2- + NO3-)
Tolar et al. 2016 (NH4+ → NO2- + NO3-)
Beman et al. 2011 (NH4+ → NO2- + NO3-)
Ward & Zafiriou 1988 (NH4+ → NO2-)
Ward 2005 (NH4+ → NO2-)
Sutka et al. 2004 (NH4+ → NO3-)
Cavagna et al. 2015 (NH4+ → NO3-)
Dore & Karl 1996 (NH4+ → NO2- + NO3-)**
Bianchi et al. 1999 (NH4+ → NO2-)*
Rees et al. 2006 (NH4+ → NO2- + NO3-)*
Raimbault et al. 1999 (NH4+ → NO3-)
Yoshida et al. 1989 (NH4+ → NO3-)
Lam et al. 2009 (NH4+ → NO2-)

Figure 1.11 Measured marine archaeal and bacterial *amoA* and ammonia oxidation rates

A) Compiled data of archaeal and bacterial *amoA* genes (copies ml^{-1}) and **B)** ammonia oxidation rates (in units nmol NH_4^+ oxidised L^{-1} d^{-1}) as a function of depth in the marine environment, with location of samples shown on the above maps. Archaeal *amoA* shown is based on general archaeal primers rather than those specifically designed to detect WCA and WCB ecotypes (see Box 3 for description of ecotypes). Unless otherwise denoted, AOB abundances are those based on Betaproteobacteriales primers (typically using marine *Nitrosospira*-like amoA primers, e.g., Rotthauwe et al. 1997). Some studies (Wuchter et al. 2006; Mincer et al. 2007) do attempt to quantify Nitrosococcales-AOB but were unable to detect them (denoted by *). Average abundances with depth denoted by dashed (AOB) and solid (AOA) lines were calculated in this thesis. Ammonia oxidation rates include NH_4^+ oxidised to either NO_2^-, NO_3^- or both. As NH_4^+ oxidation to NO_2^- is the rate-limiting step of nitrification, the assumption has been made that NH_4^+ oxidation rates presented here will be largely determined by this first step — and therefore measurements of $NH_4^+ \rightarrow NO_3^-$ and $NH_4^+ \rightarrow NO_2^- + NO_3^-$ will be largely comparable. In the majority of studies ammonia oxidation rates are measured using a radio-labelled NH_4^+ spike ($^{15}NH_4^+$) and tracking its incorporation into oxidised N forms. Instances where ammonia oxidation rates have been measured using other methods e.g. by inhibiting NO_2^- oxidation and measuring the change in NO_2^- over time (Bianchi et al. 1999; Rees et al. 2006) are outlined. This figure does not provide an exhaustive compilation of marine ammonia oxidation rates but aims to capture the trends in *amoA* copies and ammonia oxidation rates. All data references are outlined in the reference list.

BOX 2 – *AMOA* GENE BIOGEOGRAPHY

Research into the diversity and ecology of ammonia oxidisers has relied heavily on the quantification and analysis of *amoA*, the gene encoding the alpha subunit of the hallmark enzyme of ammonia oxidation — ammonia monooxygenase (AMO). Consequently, the *amoA* gene has become the second most frequently sequenced marker gene in microbial ecology following the 16S ribosomal RNA (rRNA) gene. While the abundance of archaeal or bacterial *amoA* is typically used as a relative proxy of cell numbers, it should be noted that there is potential for *amoA* gene copies per cell to vary between species. For instance, Lam et al. (2007) found that *amoA*:16S rRNA gene ratios varied in different oxygen regimes in the Black Sea, showing ratios of 0.3–

0.7 in oxic waters, 1.2–2.8 in sub-oxic zones and 0.01–0.04 in the anoxic zone. This indicates that using *amoA* abundances alone to reflect the relative dominance of AOA and AOB communities should be considered with the caveat that there is potential for *amoA* gene copies to reflect species-specific variation, and ideally should be supported with additional cell enumeration analyses.

Understanding the genetic diversity of *amoA* sequences has enabled more specific primers to be developed, for instance, to detect the distinct ecotypes of AOA (See Box 3). It is now evident that there is enormous diversity in *amoA* sequences among ammonia oxidisers, particularly within the AOA (Alves et al. 2018). However, primer selection inherently imposes a degree of bias into how the distribution of ammonia oxidisers in the marine environment is understood — especially within efforts to understand AOB in the marine environment. The majority of studies enumerating open ocean AOB use solely Betaproteobacteriales (previously referred to as β-AOB) *amoA* primers (Agogué et al. 2008; Santoro et al. 2013; Horak et al. 2013; Newell et al. 2013; Peng et al. 2016). As a result, the current understanding of AOB distribution in the oceans is primarily based on the distribution of Betaproteobacteriales *amoA* sequences and therefore may not be capturing the true distribution and abundance patterns of the AOB. Studies which have used Nitrosococcales (previously referred to as γ-AOB) *amoA* primers either do not detect Nitrosococcales AOB (Wuchter et al. 2006) or find that PCR amplification produces unspecific bands, indicating that Nitrosococcales *amoA* amplification approaches require optimisation (Shiozaki et al. 2016). There are exceptions wherein Nitrosococcales *amoA* gene copies have been successfully detected and are equivalent or greater in abundance than Betaproteobacteriales *amoA* gene copies (Lam et al. 2009). Improving the understanding of the Nitrosococcales (i.e., the *Nitrosococcus* AOB) at the genetic level will allow for more effective

Nitrosococcales AOB primers to be developed, improving our understanding of the distribution and abundances of Nitrosococcales AOB in the marine environment.

The presence of *amoA* genes in DNA extracted from environmental samples gives an indication of the organisms capable of ammonia oxidation, while the presence of *amoA* transcripts indicates the presence of active ammonia-oxidising microorganisms. In the oxygenated marine environment, maxima of *amoA* gene copies and transcripts typically co-occur (Church et al. 2010; Jing et al. 2017; Horak et al. 2013) or co-vary such that when more cells are present, the number of actively transcribing cells can be assumed to be greater (Abell et al. 2010; Tolar et al. 2016; Duff et al. 2017; Leininger et al. 2006) although the ratio of gene copies to transcripts may vary depending on the environment and AOA/AOB community composition. In some oceanic regions, such as OMZs, gene expression and transcript abundance can become decoupled (Lam et al. 2009), with AOB showing a greater number of *amoA* transcripts per cell (Lam et al. 2007). Taken together, these factors demonstrate that there are many caveats that need to be considered when interpreting environmental molecular data.

1.5 FACTORS CONTROLLING AMMONIA OXIDATION AND NICHE SEPARATION OF AMMONIA OXIDISERS

As previously described, the distribution of AOA — and thereby ammonia oxidation rates in the oceans — has conventionally been attributed to the combined effects of NH_4^+ supply and irradiance. However, a growing body of evidence *in situ* indicates that these sole factors are insufficient to explain the distribution of AOA in the environment, most notably the high ammonia oxidation rates in sunlit surface waters and the dominance of AOA in high energy marine regimes. These discrepancies are discussed in greater detail in the following sections.

1.5.1 Ammonium

The Archaea, as a domain, thrive in areas of chronic energetic stress (Valentine, 2007). Multiple lines of evidence indicate that AOA are oligotrophic specialists or 'oligotrophs' that are well adapted to the nutrient-poor environment of the open ocean, compared with their bacterial counterparts. First and foremost, AOA have smaller cell sizes and therefore have higher surface area to volume ratios compared with AOB — a strategy known to be effective for nutrient uptake in oligotrophic regimes (Poindexter, 1981). AOA also have smaller genomes than AOB (~1.65 Mb for *N. maritimus*; 1.23 Mb for *Ca.* N. brevis, 3.6 Mb for *N. oceani*) with a high coding density postulated to reduce the energetic cost of cellular replication in nutrient-poor environments. In addition, AOA have the most energy-efficient aerobic autotrophic pathway characterised to date in terms of the amount of cell biomass generated per mole of ATP (Könneke et al. 2014). Taken together, these traits all point to a trophic lifestyle that makes AOA well adapted to the low energy, oligotrophic ocean.

One of the key factors considered to control the abundances, relative distribution and niche separation of AOA and AOB in the marine environment is the availability of their shared energy substrate, NH_4^+. The first isolated AOA demonstrated an NH_4^+ affinity not only exceeding that of cultivated marine and terrestrial AOB but of all cultivated marine microorganisms, including heterotrophic bacteria and phytoplankton (Figure 1.12; Martens-Habbena et al. 2009 and references therein). It has been suggested that the high affinity of AOA for NH_4^+ compared to other marine microorganisms may be due to the higher affinities and densities of the archaeal AMO or transporters for NH_3/NH_4^+ (Urakawa et al. 2011). In addition, recent research suggests that the chemical properties of the distinctive archaeal S-layer — common to all archaea — allow AOA to accumulate greater concentrations of NH_4^+ at their cell surface (Li et al. 2018). Most significantly, *N. maritimus*' NH_4^+ kinetics correlate well with the *in-situ* kinetics of the oligotrophic open ocean with large AOA populations, indicating that AOA are indeed the dominant ammonia oxidisers in the oligotrophic oceans (Martens-Habbena et al. 2009).

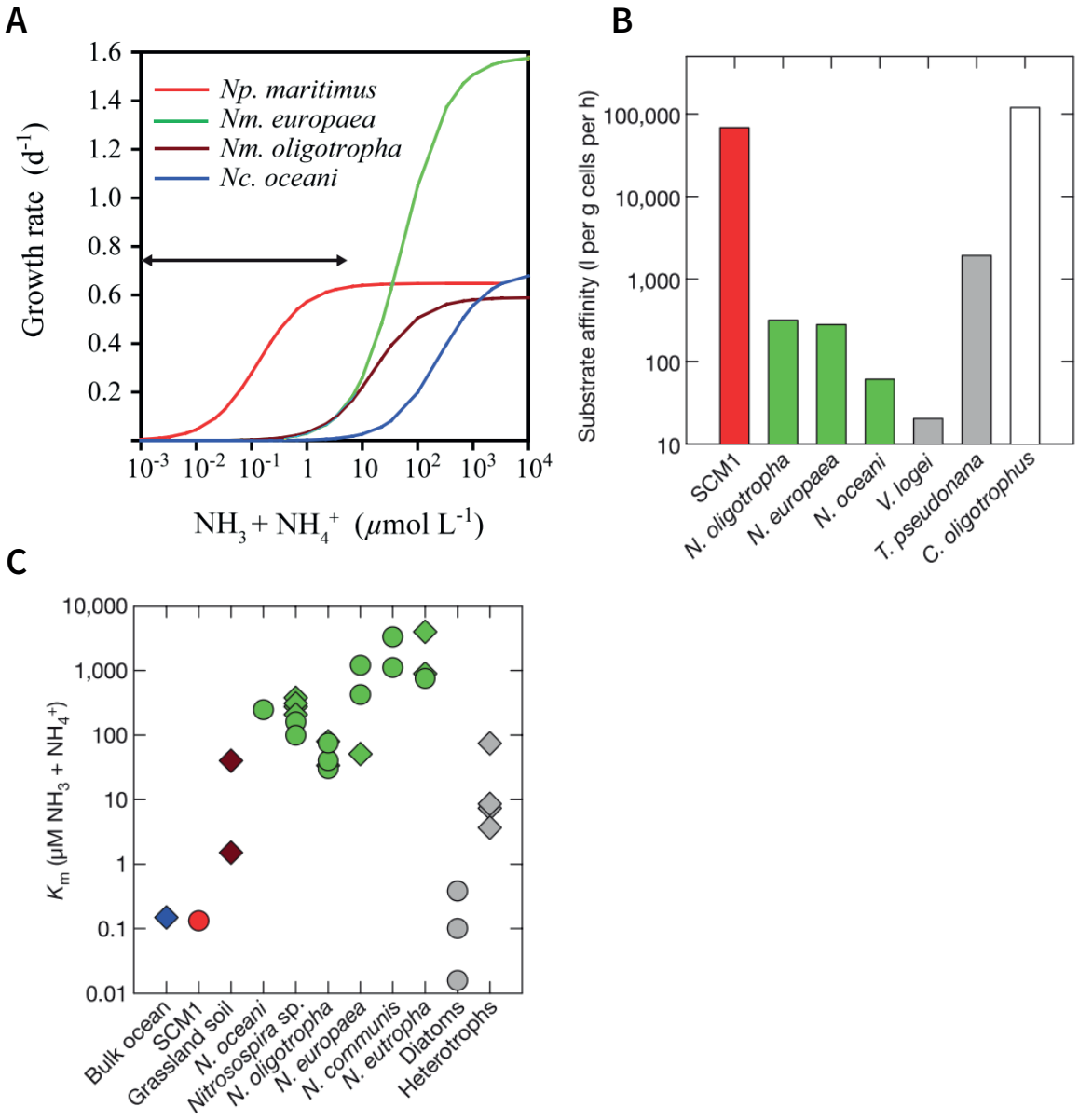


Figure 1.12 Archaeal and bacterial ammonia oxidation kinetics

A) Growth response of AOA (Np. maritimus – *N. maritimus*) and AOB (*Nm. europaea*, *Nm. oligotropha*, *Nc. oceani*) to increasing NH_4^+ /NH_3 concentration, from Urakawa et al. (2014) **B)** NH_4^+ substrate affinity of *N. maritimus* (in red) compared with AOB (in green), marine phytoplankton (grey) and the marine bacterium (*C. oligotrophus*) from Martens-Habbena et al. (2009) **C)** NH_4^+ half-saturation constant (K_m) of marine AOA, AOB and other marine microorganisms compared with *in situ* K_m measured in the oceans, from Martens-Habbena et al. (2009). Copyright © 2009, Springer Nature, reprinted with permission (license number: 5177530078224).

Their demonstrated high affinity for NH_4^+ — and therefore the low NH_4^+ threshold for growth (Figure 1.12) — makes AOA theoretically well adapted to the low energy

environment of the open ocean. A superior NH_4^+ affinity has been widely evoked to explain the dominance of AOA *amoA* genes over those of AOB in the open ocean, where NH_4^+ fluxes are extremely low (Martens-Habbena et al. 2009; Bayer et al. 2016; Horak et al. 2013), with NH_4^+ rarely accumulating to > ~0.4 μmol L^{-1}. However, NH_4^+ kinetics alone do not explain why AOA still dominate in coastal regimes where NH_4^+ supply is greater and ostensibly sufficient to support high AOB growth (Urakawa et al. 2011; Martens-Habbena et al. 2009; Reji et al. 2019). This contrasts with soil environments, wherein ammonia oxidiser communities are dominated by AOB in NH_4^+ fertilised soils relative to non-fertilised soils (Jia & Conrad, 2009; Leininger et al. 2006; Verhamme et al. 2011; Zhang et al. 2010; Di et al. 2009; Di et al. 2010).

Despite demonstrating a high NH_4^+ affinity, AOA are suggested to be outcompeted by phytoplankton for NH_4^+ in marine surface waters (Smith et al. 2014) due to their slow growth (Könneke et al. 2005) and their high N demand per mole of C fixed (Veuger et al. 2013) — particularly when phytoplankton communities do not have access to other forms of N (Wan et al. 2018). Yet, in numerous instances, marine AOA communities appear not to be NH_4^+ limited: incubation experiments indicate that AOA communities are often substrate replete (Smith et al. 2014; Horak et al. 2013; Shiozaki et al. 2016), becoming substrate saturated at < 100 nM NH_4^+ (Olson et al. 1981a; Newell et al. 2013) even in seemingly NH_4^+ oligotrophic regions. These discrepancies highlight the potential for other factors — besides the NH_4^+ kinetics and the supply of NH_4^+ — to influence both the preponderance of AOA over AOB in the marine environment and the low abundances of AOA in marine surface waters.

1.5.2 Irradiance and other physicochemical factors

Additional physicochemical factors have been proposed to control AOA abundances (and therefore ammonia oxidation rates) and contribute to AOA dominance over AOB in

the marine environment (Table 1.1). These include the effect of irradiance, the utilisation of other N substrates for growth, the potential for mixotrophy, O_2 affinity, and pH sensitivity. However, the precise role of these factors in controlling *in-situ* ammonia oxidation rates and niche separation remain poorly constrained due to contradictory results and are substantially less studied compared with the effect of NH_4^+. The most well-studied of other factors besides energy availability is the response of ammonia-oxidising communities (both *in situ* and in laboratory culture) to irradiance. Ammonia oxidation rates in both AOB and AOA typically scale with irradiance levels (Olson, 1981b; Ward, 1985; Horrigan & Springer, 1990; Qin et al. 2014). For instance, in the Southern Ocean, AOA populations decrease dramatically — especially in surface waters — as irradiance increases during the transition from winter to summer (Church et al. 2003). While initial work postulated that this was due to direct inhibition of AOA/AOB activities with increasing light exposure, recent work suggests AOA inhibition may in fact be a result of reactive oxygen species (ROS), such as hydrogen peroxide (H_2O_2), formed under high irradiation (Kim et al. 2016; Tolar et al. 2016) by abiotic and biotic processes. AOA are reported to be more sensitive to irradiance compared with AOB (Merbt et al. 2011), potentially due to the lack of catalases in AOA, which are responsible for ROS detoxification (Kim et al. 2016). However, the effect of light on AOA and AOB remains a poorly constrained variable due to mixed effects of light on AOA ecotypes (Horak et al. 2018; Qin et al. 2014) and does not explain widespread observations of significant surface nitrification in the sunlit euphotic zone (Lomas et al. 2009; Newell et al. 2013) and low nitrification rates in lowly lit euphotic zones (Beman et al. 2011; Lipschultz et al. 2001). The extent to which AOA are obligate autotrophs or able to use organic carbon compounds to supplement their biosynthetic carbon demand — and the role of organic carbon use in AOA and AOB niche separation — also remains highly

uncertain, particularly in the mesopelagic (~ 1000m). While pure isolates of AOA grow as strict autotrophs, their growth rates and cell yields are enhanced in the presence of the organic acid, α-ketoglutarate (Qin et al. 2014). However, the growth of AOA enrichment cultures and cultures grown in natural seawater often are not enhanced by the addition of organic compounds (Bayer et al. 2016; Santoro et al. 2015), and there is only limited evidence for organic carbon assimilation or respiration in cultures (Kim et al. 2016). This led to the hypothesis that organic compounds have a role in scavenging hydrogen peroxide or other radical oxygen species as AOA have few biochemical defences against these damaging species (Kim et al. 2016). However, a significant role for alternative metabolisms involving assimilation and respiration of organic carbon, have been proposed in the deep mesopelagic where ammonia oxidation rates are insufficient to maintain a high enough turnover of cells and explain AOA abundances at depth (Santoro et al. 2019). As there are no mesopelagic isolates on which to test these physiological traits (see further discussion below), current approaches aim to use stable-isotope-tracing experiments that track the fate of organic carbon into AOA biomolecules (Yakimov et al. 2014). AOB across a range of environments have also been shown to be able assimilate and oxidise organic compounds (Krummel & Harms, 1982; Koops et al. 1991; Hommes et al. 2003) but the significance of mixotrophy for the distribution of AOB in the marine environment remains an area of uncertainty. For both AOA and AOB, it also remains unclear what role organic carbon assimilation and respiration may play in promoting a particle-attached versus free living lifestyle in the water column, with implications for niche separation with and between these groups (discussed further in Section 1.5.3).

Much of the current physiological understanding of AOA and their potential role in niche separation between the AOA and AOB is based on pure isolate belonging to the

Nitrosopumilus genus, of which *Nitrosopumilus maritimus* strain SCM1 is the type strain. *N. maritimus* and other AOA have been isolated using relatively high ammonium concentrations (0.25–1 mmol L^{-1} NH_4^+) and high temperatures (25–30 °C) which likely underpin selection of AOA strains from the genus *Nitrosopumilus* in cultivation studies, which does not capture the true diversity of AOA identified in environmental surveys (Francis et al. 2005; Sintes et al. 2013). Therefore, the current physiological understanding of the AOA likely does not provide a true representation of the diversity in the physiological traits of AOA. There is particular uncertainty surrounding the physiological traits of AOA in the mesopelagic — which as mentioned above may possess novel organic carbon-based metabolisms — as all cultivated marine AOA originate from either surface waters or sediments.

1.5.3 Free-living versus particle-attached lifestyles

Microorganisms in the marine environment can be divided into free-living (0.2 –3 μm) and associated with particles (> 3 μm) which provide a nutrient-rich microenvironment (Turley & Mackie, 1994) — although a continuum between these two lifestyles does exist. Free-living or planktonic microorganisms are typically oligotrophic (or "background adapted") and succeed by utilising the persistent low background concentrations of nutrients, whereas particle-associated microorganisms are typically copiotrophs (or "patch adapted") relying on transient nutrient hotspots (Lauro et al. 2009). This is primarily understood in terms of the supply of organic carbon to heterotrophic bacteria (Smith et al. 1992; Delong et al. 1993) but there has been some investigation into how N supply may drive contrasting lifestyle preferences in AOA and AOB (Zhong et al. 2020; Santoro et al. 2019; Bayer et al. 2016; Phillips et al. 1999). Contrasting affinities for NH_4^+ may drive a particle vs planktonic lifestyle niche separation between the AOA and AOB — with AOB potentially showing a preference for particles to fulfil their higher

NH_4^+ demand. While this is generally supported by observations of AOA being largely planktonic (Zhong et al. 2020; Santoro et al. 2019) and particle associated AOB communities (Phillips et al. 1999), emerging evidence indicates that there are exceptions and the potential for further niche separation both within the AOA and AOB. For instance, genomic comparisons of coastal AOA strains '*Ca*. N. adriaticus' NF5 and '*Ca*. N. piranensis' D3C revealed that these strains may occupy different niches in marine coastal waters, corresponding to a more particle-associated life mode versus a free- living life mode, respectively (Bayer et al. 2016). Within the AOB, groups have been found to display different lifestyle preferences — with particle associated sequences predominately related to the *Nitrosomonas* and planktonic samples showing enrichment in the *Nitrosospira* (Phillips et al. 1999). It is not entirely clear whether these lifestyle preferences are driven solely by differing energy requirements, or whether other physiological differences are also important. For instance, it has been suggested that the association with particles may help mitigate photoinhibitory effects (Phillips et al. 1999), meaning that sensitivity of different groups to irradiance may be a contributing factor.

Characteristic /Variable	As applied to AOA vs AOB	References
Cell geometry	• **AOA have a greater surface area to volume ratio than AOB;** AOA are smaller compared with AOB; *N. maritimus* (AOA) is rod-shaped with a diameter of 0.17 – 0.22 μm/ length of 0.5-0.9 μm, *N. oceani* (AOB) is coccoid, with a diameter of 1.5 μm.	Könneke et al. 2005; Klotz et al. 2006
Genome size	• **AOA have smaller genomes than AOB;** (~1.65 Mb for *N. maritimus*; 1.23 Mb for *Ca*. N. brevis) with a high coding density relative to AOB (*N. oceani*: 3.6 Mb) postulated to reduce the energetic cost of cellular replication in nutrient-poor environments.	Walker et al. 2010; Santoro et al. 2015; Klotz et al. 2006
NH_4^+ affinity	• **AOA *N. maritimus* has elevated NH_4^+ affinity relative to AOB** (0.1μM for *N. maritimus*, ~500 μM for *N. oceani*); attributed to differences in affinity of transporters and chemical properties of archaeal S-layer.	Martens-Habbena et al. 2005; Martens-Habbena & Stahl, 2011; Urakawa et al. 2011; Horak et al. 2013; Newell et al. 2013; Li et al. 2018
N substrates	• **Both AOA and AOB have been shown to be able to gain energy through urea oxidation both in culture and in the field**; although this appears to be limited to particular species. The role of urea on niche partitioning is not clear.	Bayer et al. 2016; Qin et al. 2014; Burton & Prosser, 2001; Hallam et al. 2006; Palatinszky et al. 2015; Kitzinger et al. 2019; Stieglmeier et al. 2014; Alonso-Sáez et al. 2012; Carini et al. 2018; Tolar et al. 2017
O_2	• **Marine AOA appear better adapted to both high and low O_2 conditions than AOB in culture**; AOA appear to outnumber AOB in both oxygenated and low O_2 environments, with low O_2 environments linked to greater N_2O production by AOA.	Martens-Habbena et al. 2009; Park et al. 2010; Qin et al. 2017a; Bristow et al. 2016; Peng et al. 2016; Santoro et al. 2011

Light/ROS	• **Irradiance shown to decrease AO in both AOA and AOB** — but inconsistencies between levels of light and nitrification rates (e.g. low nitrification rates in lowly lit euphotic zones compared to highly lit zones). • **AOA are reported to be more sensitive to irradiance compared with AOB**; this may be because AOA do not have ROS detoxification mechanism.	Hooper & Terry, 1973; Olson, 1981b; Ward, 1985; Horrigan & Springer, 1990; Church et al. 2003; Qin et al. 2014; Merbt et al. 2011,2012; Beman et al. 2011; Lipschultz et al. 2001; Shiozaki et al. 2016; Lomas et al. 2009; Newell et al. 2013; Tolar et al. 2016; Kim et al. 2016.
Carbon substrates	• **Genomes indicate that some AOA and AOB have the potential for mixotrophic growth; s**ome coastal AOA strains are demonstrated obligate mixotrophs, requiring organics for growth, but this is not universal — the requirement for organics is potentially linked to a ROS detoxification mechanism, rather than as an energy source. The role of mixotrophy in niche differentiation is not clear but could provide an advantage in oligotrophic environments.	Walker et al. 2010; Qin et al. 2014; Lichtman, 2007
pH	• **AOB are more sensitive to changes in pH, with AOA known to generally thrive in low pH environments;** Marine AOA isolates have a lower typical growth optimum ~7 compared to AOB isolates ~pH 8.	Beman et al. 2008; Qin et al. 2014; Suzuki et al. 1974; Könneke et al. 2005; Qin et al. 2014; Hatzenpichler, 2012 (and references therein)
Temperature	• ***In situ* AOA and AOB growth deemed insensitive to temperature;** AOA/AOB have overlapping temperature optima (Q_{10} for marine cultivated AOB* ranges from 2.5 – 5; AOA Q_{10} = 2.5 – 2.9). Role of temperature in niche separation not clear.	Könneke et al. 2005; Qin et al. 2014; Hansen et al. 1981 (*sediment AOB)

Table 1.1 Physicochemical factors governing growth and niche separation of ammonia oxidisers

BOX 3 – AMMONIA-OXIDISING ARCHAEAL ECOTYPES

While this thesis primarily focuses on the niche separation between AOB and AOA, there is also evidence for niche separation within the AOA and AOB groups. For instance, analysis of *amoA* gene diversity in the marine environment (Francis et al. 2005) identified that AOA group into distinct 'ecotypes' — ecologically differentiated but phylogenetically similar populations (Cohan, 2001) — that are shaped by the physicochemical features of the surrounding environment. A well-known example of the ecotype model is that of the marine cyanobacteria *Prochlorococcus* spp. which groups into high light-adapted and low light-adapted ecotypes (Moore et al. 1998). As the dominant ammonia oxidisers in the ocean, research has focused on understanding the factors driving AOA ecotype distributions. Archaeal *amoA* sequences from the open ocean fall into surface and deep-water ecotypes (Francis et al. 2005; Hallam et al. 2006; Mincer et al. 2007; Beman et al. 2008; Santoro et al. 2010; Mosier & Francis, 2011; Sintes et al. 2013, 2016), which are predicted to be distinguished in response to high and low NH_4^+ supply. High NH_4^+ ecotypes — referred to as the Water Column A or WCA ecotype — generally dominate where total archaeal *amoA* is the most abundant in the water column (i.e. at the base of the euphotic zone) and typically correlate with overall ammonia oxidation rates (Beman et al. 2008; Shiozaki et al. 2016; Smith et al. 2014). In contrast, the low NH_4^+ ecotype (Water Column B or WCB) is typically dominant below 300 m depth. There is no cultured representative of the WCB ecotype, therefore it is not yet possible to test physiologically that NH_4^+ distinguishes the ecotypes. Dissolved inorganic C, pH, trace metals, light, and temperature are also suggested to underpin AOA ecotype separation (Sintes et al. 2013, 2015, 2016; Qin et al. 2014; Bayer et al. 2016), potentially explaining the distribution of AOA ecotypes throughout the oceans.

1.5.4 Outstanding questions

The previous sections demonstrate that there are clear inconsistencies between the physicochemical variables traditionally considered to control ammonia oxidation — such as irradiance and NH_4^+ supply — and the observed AOA abundances and ammonia oxidation rates. Taken together, these suggest that there are **additional factors that govern AOA distribution and ammonia oxidation rates in the oceans**. The increasing number of observations of ammonia oxidation in the marine euphotic zone over the last few decades (Figure 1.11) continue to challenge the prevailing paradigm that light and NH_4^+ supply are the only important controls on marine ammonia oxidation rates.

In addition, the growing body of evidence demonstrating physiological traits that make AOA well-suited to the oligotrophic oceans (outlined in Section 1.5) questions the **physicochemical niche occupied by AOB, which allows them to persist in the marine environment (albeit at low abundances).** AOA additionally prevail in marine environments which are theoretically suited to support high AOB growth (based on our current understanding of their physiology), indicating that there may **be additional unknown factors that further contribute to the success of AOA over AOB and that separate the chemical niches of these microorganisms** — especially in regions where AOB should be successful, such as environments with high NH_4^+.

BOX 4 – OUTSTANDING QUESTIONS

1. Are there additional physicochemical factors that govern AOA distribution and ammonia oxidation rates in the oceans?

2. What factors contribute to the ecological success of AOA over AOB?

3. What is the physicochemical niche occupied by AOB that allows AOB to persist in the marine environment?

1.6 TRACE METALS AND THE NITROGEN CYCLE

In order to transform N between its various redox states (Figure 1.3), microorganisms utilise enzymes containing trace metal co-factors (metalloproteins), creating a fundamental requirement for trace metals in N cycling (Figure 1.13). Trace metals are not only essential in the key proteins which transform N (e.g. nitrogenase, ammonia monooxygenase or nitrate reductase – Table 1.2) but are also widely used in other processes essential for microbial growth. Examples of these processes include photosynthesis, respiration and C fixation. A dozen or so elements with an atomic mass above 50 are known to have a biological role (Da Silva & Williams, 2001), of which manganese (Mn), iron (Fe), cobalt (Co), nickel (Ni), copper (Cu), zinc (Zn), and cadmium (Cd) have been best studied by oceanographers (Donat & Bruland, 1990).

Process	Key enzymes	Metal
N_2 fixation	Nitrogenase	**Fe**, **Mo**, **V**
NH_4^+ assimilation	Glutamine synthetase; Glutamate dehydrogenase	
NO_3^- assimilation	**1. $NO_3^- \rightarrow NO_2^-$** Assimilatory nitrate reductase (NAS) **2. $NO_2^- \rightarrow NH_3$** Assimilatory nitrite reductase (cNIR)	**Fe, Mo** **Fe**, **Mo**
NH_4^+ oxidation	**1. $NH_3 \rightarrow NH_2OH$** Ammonia monooxygenase (AMO) **2a. $NH_2OH \rightarrow NO$ (AOB)** Hydroxylamine dehydrogenase (HAO) **2b. $NH_2OH \rightarrow NO$ (AOA)** Unknown **3. $NO \rightarrow NO_2^-$** Cu-containing (Cu-NIR) nitrite reductases*	**Cu**, **Fe** (**Zn***) **Fe** **Cu***
NO_2^- oxidation	**1. $NO_2^- \rightarrow NO_3^-$** Nitrite oxidoreductase (NXR)	**Fe**, **Mo**
Denitrification	**1. $NO_3^- \rightarrow NO_2^-$** membrane-bound and periplasmic dissimilatory nitrate reductases (NAP, NAR); nitrite oxidoreductase (NXR) **2. $NO_2^- \rightarrow NO$** Nitrite reductase (Cu-NIR); Nitrite reductase (cd1-NIR) **3. $NO \rightarrow N_2O$** cytochrome c-dependent (cNOR), quinol-dependent (qNOR) and copper-containing quinol-dependent nitric oxide reductases (CuANOR); NADH-dependent cytochrome P450 nitric oxide reductase (P_{450}NOR) **4. $N_2O \rightarrow N_2$** nitrous oxide reductase (NOS)	**Fe**, **Mo** **Fe**, **Cu** **Fe**, **Cu** **Cu**
DNRA	**1. $NO_3^- \rightarrow NO_2^-$** membrane-bound (NAR) and periplasmic dissimilatory nitrate reductases (NAR,NAP); nitrite oxidoreductase (NXR) **2. $NO_2^- \rightarrow NH_3$** ε-hydroxylamine oxidoreductase (εHAO); octahaem nitrite reductase (ONR) (Fe)	**Fe**, **Mo**
ANAMMOX	**1. $NH_3 \rightarrow N_2H_4$** hydrazine synthase (HZS) **2. $NO \rightarrow N_2H_4$** nitric oxide dismutase (NO-D) **3. $N_2H_4 \rightarrow N_2$** hydrazine dehydrogenase (HDH)	**Fe**
COMMAMOX (putative pathway)	**1. $NH_3 \rightarrow NH_2OH$** Ammonia monooxygenase (AMO) **2. $NH_2OH \rightarrow NO$** (AOB) Hydroxylamine dehydrogenase (HAO) **3. $NO \rightarrow NO_2^-$** copper-containing (Cu-NIR) nitrite reductases **4. $NO_2^- \rightarrow NO_3^-$** Nitrite oxidoreductase (NXR)	**Cu**, **Fe**, **Mo**

Table 1.2 Trace metal-containing enzymes required in nitrogen cycling processes

Enzymes required in N cycling processes (including abbreviated names), and their demonstrated or predicted trace metal co-factors from Kuypers et al. (2018). Grey shading indicates assimilatory processes. Trace metals shown are the following: **Fe (iron)**; **Cu (copper)**; **Mo (molybdenum)**; **V (Vanadium)**; **Zn (Zinc)**. Most enzymatic metal requirements have not been experimentally demonstrated and are based on significant sequence homology to characterised

proteins * indicates prediction based on the high number of proteins homologous to Cu-proteins but with undetermined functions in AOA genomes (Walker et al. 2010; Santoro et al. 2015) **indicates non-essential trace metals, but can be substituted when other trace metals are limiting.

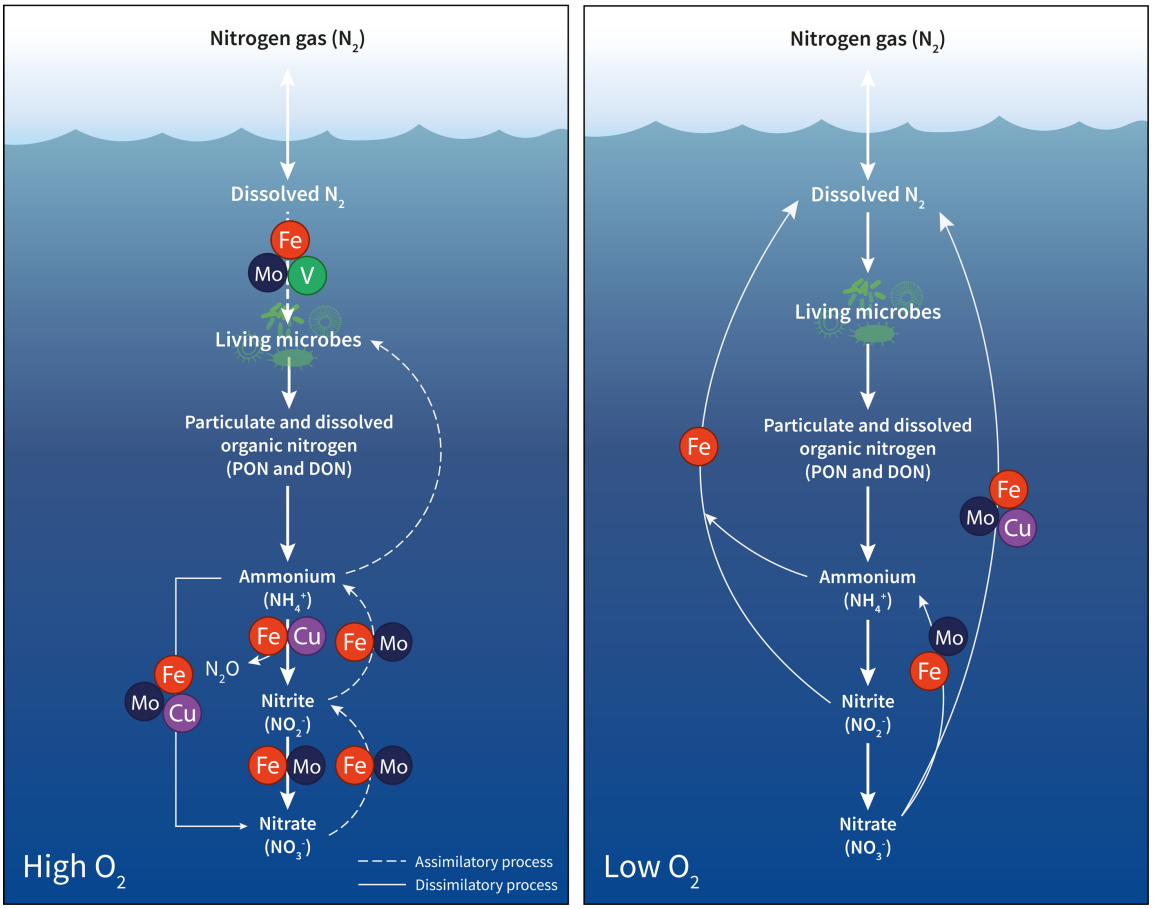


Figure 1.13 Trace metals required by microbial nitrogen cycling in the oceans

Trace metals utilised in the metalloenzymes mediating different components of the N cycle under high and low O_2.

1.6.1 Limitation of nitrogen cycling

The most well-studied metalloprotein in N cycling is nitrogenase, the Fe and molybdenum (Mo) (and in some instances vanadium (V) – Robson et al. 1986) containing enzyme which allows diazotrophs to fix N_2 from the atmosphere. The current understanding of nitrogenase forms part of the extensive research efforts over the last century to uncover how the availability of trace metals in the oceans shapes the growth and ecology of phytoplankton that drive the biological pump in both the modern and ancient oceans (Moore et al. 2013; Morel & Price, 2003). Most notably, it has been

repeatedly shown that low dissolved Fe concentrations, which are typically < 1 pmol L^{-1} Fe (Johnson et al. 1997), limit the growth and N_2 fixation rates of diazotrophs (Moore et al. 2008; Mills et al. 2004; Moore et al. 2009; Snow et al. 2015) and hinder the ability of phytoplankton to assimilate NO_3^- in marine surface waters (Timmermans et al. 1994). In as much as 40% of the oceans — notably the Southern Ocean, equatorial Pacific Ocean, and North Pacific Ocean — Fe is the primary control on N_2 fixation, limiting the supply of NH_4^+ to the marine biosphere (Moore et al. 2001; Moore et al. 2013).

1.6.2 Trace metal niche separation

In addition to controlling overall rates of primary productivity (Moore et al. 2013; Figure 1.1), trace metals also act as a selective pressure that encourages microorganisms to develop distinct trace metal ecophysiologies. In doing so, microorganisms may occupy distinct chemical trace metal niches allowing them to co-exist and persist even when competing for similar resources — analogous to physical niches for light (Brun et al. 2015) or temperature (Thomas et al. 2012) among phytoplankton taxa.

For instance, by reducing the Fe required for metabolic processes such as photosynthesis, coccolithophores are able to proliferate under oceanic regimes that are chronically deprived of Fe (Sunda & Huntsman, 2015; Sunda & Huntsman, 1995; Hutchins et al. 2002). In contrast, diatoms can rapidly bloom during episodic pulses of Fe and store excess Fe in ferritin proteins, allowing them to persist during periods of Fe scarcity (Marchetti et al. 2012; Cohen et al. 2018). Marine microorganisms have additionally carved separate Fe niches through the ability to utilise distinct forms of organically-complexed Fe — either through the production of Fe-chelating agents (siderophores) or reductive uptake strategies (Hutchins et al. 1999; Lis et al. 2015b; Hogle et al. 2016).

Heterotrophic bacterial niche separation based on trace metal acquisition strategies have also been linked to the preference of heterotrophs for a particle-attached or free-living lifestyles (Hogle et al. 2018 – see Section 1.5.3 for further discussion of particle versus attached trophic lifestyle). Particle associated heterotrophs are shown to have a preponderance of TonB-dependent transporters (TBDTs) allowing them to assimilate the high molecular weight organic complexes (including organically complexed Fe) associated with particles (Hogle et al. 2018; Manck et al. 2020). In contrast, planktonic (or background adapted) oligotrophic heterotrophs have more systems dedicated to inorganic Fe uptake — structurally simpler (and bioavailable) forms of Fe which are released through the hydrolysing activity of particle-associated bacteria on sinking organic matter. These patterns indicate the potential for a synergistic relationship between marine microorganisms based on their trace metal references, with copiotrophic microorganisms providing the more bioavailable forms of Fe needed by oligotrophic planktonic microorganisms. It has yet to be explored whether AOA and AOB show a similar relationship between attachment lifestyle — fundamentally driven by the need to fulfil energy requirements — and the prevailing trace metal acquisition strategy.

1.6.3 Trace metals in non-photosynthetic nitrogen transformations

The understanding of how trace metals shape the ecophysiology of non-photosynthetic N-cycling microorganisms remains critically under-developed compared with that of marine phytoplankton. This is despite initial evidence to suggest that low levels of the bio-essential metals, such as Cu, could limit other components of the N cycle, both in the modern and ancient oceans (see Box 6 for discussion on ancient oceans). For instance, low levels of dissolved bioavailable Cu (Cu^{2+}) in OMZs were initially suggested to impose Cu limitation in the final step of denitrification, resulting in the accumulation of the greenhouse gas N_2O (Granger & Price, 2003) — although this has since been shown

likely not to be the case (Ward et al. 2008). To date, there has been much less focus on the role of trace metals on the transformation of N between N-input and N-loss processes from the ocean — specifically the rate-limiting step of nitrification, ammonia oxidation to nitrite (introduced in Section 1.4). This is despite a basis for trace metals to play a key role in the growth and niche separation of AOA and AOB, which is discussed in the following sections.

1.7 TRACE METALS AND AMMONIA OXIDATION

1.7.1 Copper

The role of trace metals in ammonia oxidation has historically been focussed on the fact that AMO, the enzyme catalysing NH_3 oxidation to NH_2OH, is homologous to particulate methane monooxygenase (MMO) — a Cu-binding membrane enzyme composed of three subunits (Fisher et al. 2018; Holmes et al. 2005). Since this discovery, both AOA and AOB have been shown to have an obligate Cu requirement, with the growth of all known ammonia oxidisers inhibited by the Cu chelator allylthiourea (Hatzenpichler et al. 2008; Taylor et al. 2010; Lehtovirta-Morley et al. 2013; Shen et al. 2013). The first genome sequence of the marine AOA isolate, *N. maritimus* strain SCM1, additionally revealed the presence of numerous Cu-rich halocyanin and plastocyanin enzymes (Walker et al. 2010) in lieu of Fe-dense cytochromes typically found in the electron transport chain of AOB (Blainey et al. 2011; Zannoni, 2004); an observation now confirmed in all AOA sequences assessed to date (Santoro et al. 2015; Bayer et al. 2016; Qin et al. 2017b). The apparent preponderance of genes encoding Cu proteins was found to translate into a high physiological Cu demand in culture: Amin et al. (2013) found that the cupric ion (Cu^{2+}) requirement for optimal growth of *N. maritimus* (1 pmol L^{-1} Cu^{2+}) exceeded Cu^{2+} typically measured in the marine environment (~0.01–0.1 pmol L^{-1} Cu^{2+}) and those of other marine microorganisms (Figure 1.14). On this basis, it was suggested

that archaeal ammonia oxidation might be limited in oceanic regions where Cu^{2+} falls below the limiting threshold for AOA. Subsequent *in-situ* studies in coastal regions have suggested that low Cu availability may limit ammonia oxidation rates, based on correlations between Cu^{2+} and ammonia oxidation rates/*amoA* abundances (Jacquot et al. 2013; Shiozaki et al. 2016). Since this initial physiological characterisation, transcriptomic analyses have found that Cu limitation of terrestrial and marine AOA in laboratory cultures impairs nearly every biochemical pathway — most notably ammonia oxidation (Qin et al. 2018; Reyes et al. 2020).

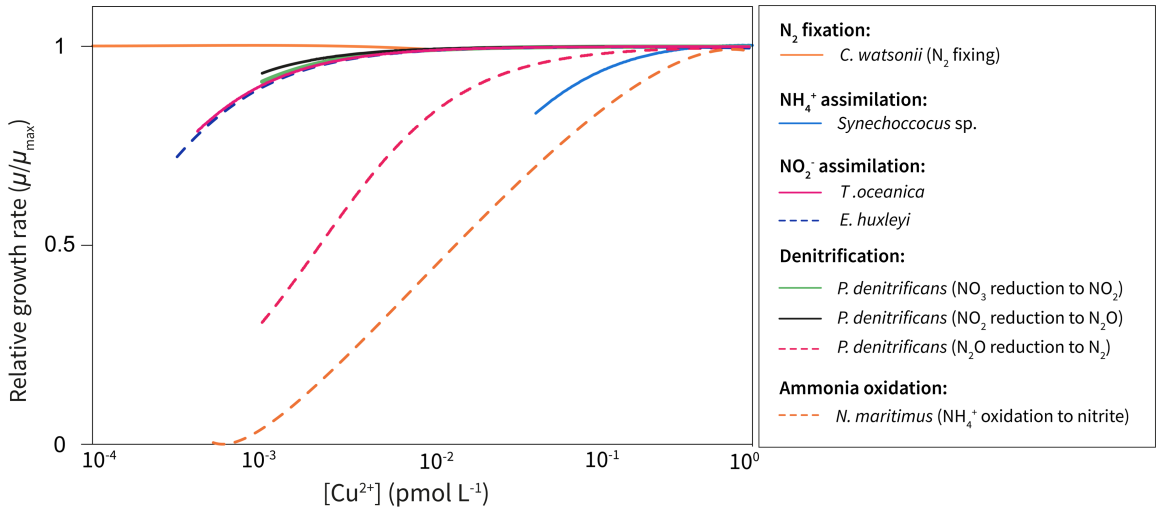


Figure 1.14 Cu requirements of different components of microbial nitrogen cycling

Relative growth rate of marine N-cycling microorganisms in response to increasing cupric ion concentration (Cu^{2+}). Full data available in Table A3.1.

BOX 5 – BIOGEOCHEMICAL TRACE METAL CYCLING

Iron (Fe)

The key role played by Fe in controlling productivity in around a third of the global oceans (De Baar et al. 2005; Moore et al. 2001), has driven a wealth of research into the biogeochemical Fe cycling in the oceans and as such, Fe is by far the most extensively studied trace element in the oceans. Despite being the fourth most abundant element in the Earth's crust, Fe is present at vanishingly low concentrations

throughout the oceans. This is because at the circumneutral pH and oxic conditions that characterises the ocean, Fe is poorly soluble and precipitates out of solution as ferric oxyhydroxide solids (Millero, 1998). As a result, concentrations of dissolved Fe (< 0.2 mm size fraction) are often in the nanomolar or sub nanomolar range (Johnson et al., 1997). Over 99% of this dissolved Fe pool, is complexed by organic ligands (Gledhill & van den Berg, 1994; Gledhill & Buck, 2012) with organic complexation playing a key role in modulating the bioavailability of Fe to marine microorganisms.

Fe shows a typical depth profile characterised by low surface concentrations, associated with biological uptake, and increased concentrations in deep waters as organic matter remineralisation releases Fe. However, this depth profile is not as pronounced as seen for the major nutrients (e.g. C and N), due to Fe scavenging into colloidal forms as water masses age (Wu et al. 2001; Bergquist et al. 2007). However, there is inter and intra basin variability in dissolved Fe concentrations with depth, with North Atlantic profiles showing greater dissolved Fe at depth relative to the Pacific and Southern Ocean (Boyd & Ellwood, 2010). These differences are thought to be driven by differing proximity to Fe sources and the influence of Fe removal from water masses as they age (Wu et al. 2001; Boyd & Ellwood, 2010). Ultimately, the concentrations of dissolved Fe in the oceans are determined by the balance between biotic and abiotic processes which remove Fe from the water column (principally biological uptake and scavenging) and those which supply Fe – both as new and recycled Fe discussed below.

Fe supply to marine microorganisms can be considered in terms of that which is new (i.e., adding to the ocean inventory) and that which is recycled from organic matter. In coastal waters, inputs of new Fe from sedimentary and riverine sources result in pronounced nearshore to offshore gradients in dissolved Fe concentrations

(Nishioka et al. 2007). Although riverine Fe is an important supply term at source, much of the Fe delivered to the oceans is rapidly scavenged in estuarine environments (Boyle et al. 1977). In the northeast subarctic Pacific, the west and east Pacific atmospheric dust is also key source of new Fe (Martin & Gordon, 1988) with aerosol Fe flux globally linked with the location of arid regions (Boyd & Ellwood, 2010). Hydrothermal activity (Klunder et al. 2011), iceberg melt (Smith et al. 2007), seasonal sea-ice retreat (Lannuzel et al. 2008) and volcanism (Gaiero et al. 2003) have also been identified in Fe supply, particularly in the Southern Ocean. Ocean biota play a pivotal role in recycling Fe, thereby making Fe available once more for biological uptake. Pelagic Fe recycling is mediated by a range of microzooplankton, microzooplankton viruses and heterotrophic bacteria which work to release Fe from organic matter, known as regenerated Fe supply. The contribution of new Fe supply to regenerated (recycled) Fe supply varies throughout the oceans, ranging from ~10% in high-nitrate low-chlorophyll waters (Boyd et al. 2005) to 50% in high-Fe waters (Sarthou et al. 2008).

Copper (Cu)

In a similar manner to Fe, the concentrations of dissolved Cu in the marine environment are driven by the balance between uptake processes (principally biological uptake) and supply patterns and processes. While the biogeochemical cycling of Cu and Fe are largely similar, there is a key difference in that the residence time of Cu in the upper ocean is 6 approximately 2 to 9 years (Semeniuk et al. 2016), relative to Fe (17 to 424 days, Bergquist & Boyle, 2006). As a biologically useful nutrient, Cu also displays a nutrient style depth profile, characterised by relatively lower surface concentrations due to biological uptake and elevated concentrations at depth associated with remineralisation. Most of the dissolved Cu pool is organically

complexed, rendering the most bioavailable forms of Cu (in particular the cupric ion, Cu^{2+}) to femto to picomolar levels. As Cu^{2+} is also a toxin at low concentrations, the biological complexation of Cu^{2+} in the oceans is also considered to play a role in mitigating potential ecotoxicological effects (Moffet & Brand, 1996).

Cu^{2+} concentrations range over five orders of magnitude between the surface and deep ocean (Figure 4.4 — 0.0001–10 pmol L^{-1} Cu^{2+}) and varies three orders of magnitude between ocean basins (0.0010 pmol L^{-1} Cu^{2+} in the Pacific (Coale & Bruland, 1988; Whitby et al. 2018) to 0.2 pmol L^{-1} Cu^{2+} in the North Atlantic (Heller & Croot, 2015). As with Fe, dissolved Cu concentrations are lower in regions with fewer aeolian and sedimentary continental sources, with older water masses in the Pacific showing Cu enrichment at depth relative to the Atlantic. Sources of Cu to the oceans are similar to those for Fe including riverine discharge (Bruland & Franks 1983; Jacquot & Moffett 2015), deep-sea marine sediments (Boyle et al. 1977), inputs from the continental shelves (Heggie et al. 1987) as well as hydrothermal vents (Sander & Koschinsky, 2011) and atmospheric deposition (Duce et al. 1991). Atmospheric deposition is particularly important in regions that are downwind of natural and anthropogenic aerosol sources such as the Mediterranean (e.g., Jordi et al. 2012), and the East China Sea (Hsu et al. 2010).

1.7.2 Trace metal requirements of AOA and AOB: a paucity of data

The finding that AOA ostensibly eschew Fe proteins in favour of Cu proteins — in contrast to their bacterial counterparts — has been widely suggested to contribute to their success in the modern oceans where Fe is chronically scarce and typically less abundant than Cu (Box 5). A similar trade-off between Fe and Cu requirements, although with a

different biochemical basis, has been demonstrated in open ocean diatoms, which have a greater Cu demand but lower Fe demand relative to coastal diatoms (Peers & Price, 2006).

However, to date, the corresponding physiological data required to test whether genome-level differences between AOA and AOB translate into contrasting metal trophic strategies are lacking. While genomic comparison provides an initial insight into the potential for differences in trace metal requirements and uptake strategies, it is the physiological response to trace metals that ultimately determines how the ecophysiological niches of AOA and AOB will be shaped by trace metal availability (explained further in Box 7), especially the strategies employed under trace metal scarcity. Specifically, there is a paucity of data examining the physiological Fe requirements and uptake strategies of AOA and both the Fe and Cu requirements of marine AOB. These data are required to test the hypothesis that AOA and AOB have contrasting Fe and Cu requirements (AOB have a high Fe, low Cu requirement; AOA have a low Fe, high Cu requirement) which provides an advantage to AOA in an ocean where Fe is scarce, contributing to their widespread success. These data also allow insight into how trace metals potentially govern the distribution and spatial niches of AOA and AOB in the oceans (and therefore ammonia oxidation rates) — specifically whether total ammonia oxidation (both by AOA and AOB) is Cu limited in some oceanic regions, as has been suggested based on AOA Cu requirements (Amin et al. 2013; Jacquot et al. 2013). This understanding is especially pertinent in light of the growing number of observations indicating that there are likely additional physicochemical controls governing ammonia oxidation rates in the marine environment (outlined in Section 1.5.3).

There is clear precedent for trace metals to govern AOA and AOB growth and distribution in the oceans — and potentially explain observed discrepancies — given that trace metals, particularly Fe, have been demonstrated to influence nearly every other

component of the global N cycle (Moore et al. 2008; Mills et al. 2004; Moore et al. 2009; Timmermans et al. 1994) and are chronically scarce in the oceans. In particular, Fe requirements and strategies to cope with Fe scarcity are widely considered to underpin the distribution and competitiveness of not only photoautotrophic N-cycling communities (Hutchins et al. 1999; Hutchins et al. 2002; Moore et al. 2013) but marine microbes more generally (Tortell et al. 1996; Fourquez et al. 2014) with key implications for biogeochemical nutrient cycling (Moore et al. 2013; Tagliabue et al. 2017). Therefore, examination of the Fe requirements and strategies to deal with Fe scarcity has the potential to provide important insights into both the distribution and success of AOA in the modern oceans. Comparison of AOA and AOB trace metal requirements further allows us to consider how trace metals shape the niche separation of AOA and AOB, working towards an explanation of how AOB persist in the modern oceans — despite numerous lines of physiological evidence indicating that they are poorly suited to the oceans compared with their archaeal counterparts. Finally, an examination of the trace metal requirements of AOA and AOB requirements provides an additional perspective to the long-standing question of the relative emergence and evolution of ammonia oxidation (Box 6).

BOX 6 – THE MARINE NITROGEN CYCLE AND TRACE METALS OVER GEOLOGIC TIME

As in the modern oceans, N cycling has been closely tied with C cycling and, therefore, the evolution of the biosphere over geologic time (Zerkle & Mikhail, 2017). Stable isotopes of N have been used to infer that the aerobic N cycle, including nitrification, commenced shortly after the Great Oxygenation Event (GOE) ~2.3 billion years ago (Ga) (Zerkle et al. 2017). The production of oxidised N in the oceans for the first time is suggested to have allowed for the diversification of eukaryotic phytoplankton (Stüeken et al. 2016) and the emergence of heterotrophic pathways

(such as denitrification and anammox), allowing N_2 to be returned to the atmosphere — creating the modern N cycle that we recognise today.

The redox sensitivity of trace metals means that the solubility and thus bioavailability of key trace metals has also evolved in tandem with the oxygenation of the oceans. The progressive oxygenation of the oceans over geologic time has driven changes in the bioavailability of essential trace metals, notably enhancing the availability of Cu, Zn and Mo due to metal-sulphide dissolution but drastically reducing the availability of Fe, Co and Mn, which are insoluble under oxic conditions (Figure 1.15, Anbar, 2008; Saito et al. 2003). The scarcity of Mo and Cu prior to oxygenation has been suggested to potentially have limited N cycling due to their requirement in nitrogenase, ammonia monooxygenase and nitrate reductase (Table 1.2; Anbar & Knoll, 2002; Granger & Ward, 2003; Glass et al. 2012; Zerkle et al. 2006)

Molecular clock analyses constrain the timing of marine AOA and AOB emergence to 1084–959 million years ago (Mya) and 1169–596 Mya, respectively (Ward et al. 2021; Ren et al. 2019). The overlapping error of such approaches demands additional tools to constrain the relative emergence times of archaeal and bacterial ammonia oxidisers. Consideration of evolving trace metal availabilities in the ocean over geologic time offers an approach that may complement molecular clock analyses, providing new insight into the relative timing of the emergence of AOA and AOB. This is because modern microbial trace metal requirements are suggested to be vestigial to the conditions under which the microorganism emerged and diversified. For instance, cyanobacteria are shown to have a greater Fe demand compared with eukaryotic phytoplankton, potentially reflecting their relatively earlier emergence in an ocean which was richer in Fe (Saito et al. 2003; da Silva & Williams, 2001).

Therefore, examination of Fe and Cu requirements of extant AOA and AOB may provide an insight into the relative emergence of these groups of microorganisms — shedding light on which of these groups of ammonia oxidisers were more prevalent in the early oceans.

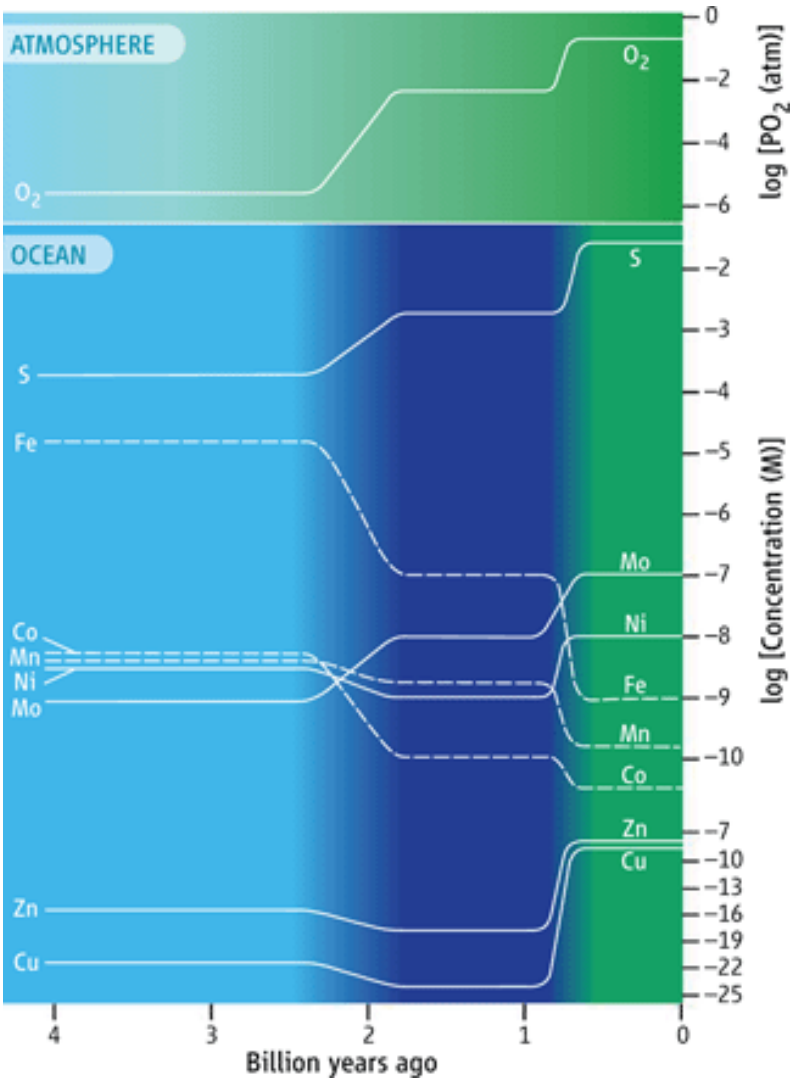


Figure 1.15 Evolution of trace metal bioavailability in the oceans over geologic time

Predicted trace metal bioavailabilities over time in response to evolving oxidative state of the oceans, from Anbar (2008). Copyright © 2008, The American Association for the Advancement of Science, reprinted with permission (license number: 5177521387028)

1.8 AIMS AND APPROACH

1.8.1 Aims and questions

The overarching objective of this thesis is to provide the outstanding physiological characterisations necessary to understand how the key bio-essential trace metals — iron (Fe) and copper (Cu) — contribute to the growth, distribution and niche separation of marine ammonia-oxidising archaea (AOA) and bacteria (AOB) in the oceans. In doing so, this thesis brings together approaches in trace metal biogeochemistry and microbial N cycling with the aim of understanding whether the Fe and Cu ecophysiology of marine AOA and AOB provides an explanation to the outstanding questions in marine nitrification (explained in greater detail in Section 1.5.3):

KEY QUESTIONS

1. What are the requirements and uptake strategies of AOA for the micronutrient (Fe) at the physiological and the metallomic level? (Chapter two)
2. How may the physiological Fe requirements and strategies for uptake of different chemical forms of AOA contribute to the observed vertical spatial niche occupied by AOA in the water column? (Chapter two)
3. How may Fe requirements and strategies for uptake explain the global success of the AOA in the oceans? (Chapter two)
4. What cellular compensatory strategies — at the proteomic level — are used by AOA during Fe limitation? (Chapter three)
5. How do the strategies to survive Fe limitation compare with transcriptomic and proteomic responses to other forms of stress — such as NH_4^+ limitation, Cu limitation and reactive oxygen species stress? (Chapter three)
6. How might potential biochemical level strategies to survive Fe scarcity explain the global success of the AOA? (Chapter three)

7. What are the Fe and Cu requirements of marine AOB at the physiological and metallomic level and how do these compare with those of marine AOA isolates? (Chapter four)
8. How may contrasting Fe and Cu physiological requirements and uptake strategies contribute to the niche separation of AOA over AOB in the marine environment, as suggested by initial comparative genomics? (Chapter four)
9. Is there a physiological basis for widespread Cu limitation of total ammonia oxidation in the oceans? (Chapter four)
10. Do contrasting trace metal requirements provide insight into the relative evolution of AOA and AOB? (Chapter four)

1.8.2 Approach and outline of thesis

To explore the questions outlined above, this thesis primarily adopts a culture-based approach to understanding the physiological trace metal requirements of marine AOA and AOB. In chapter three, the physiological results are complemented and expanded with analysis of the proteomic response to trace metals to glean the underpinning molecular basis giving rise to observed physiologies. Further, a comparative genomics approach is widely employed in chapter four to explore whether the genetic basis giving rise to distinct physiologies are likely widespread among marine AOA and AOB, which are not yet available in pure culture. Together with previously published data on the Cu requirements of marine AOA (Amin et al. 2013), these approaches are used to understand the potential for trace metals to govern the growth, distribution and niche separation of AOA and AOB in the oceans (Figure 1.16)

CHAPTER TWO examines the physiological Fe requirements and uptake strategies of the model marine AOA isolate, *Nitrosopumilus maritimus* strain SCM1 providing the first assessment of the role of Fe in marine ammonia oxidation to nitrite. Chapter two reports

on the results of growth experiments conducted under trace metal clean conditions to define the Fe concentrations optimal for growth, the Fe substrates available for growth, and the strategies for Fe uptake in *N. maritimus*. This chapter additionally draws a comparison with the Fe requirements and uptake strategies of cosmopolitan marine primary producers, which have been extensively characterised, to contextualise the results. The insights provided through culture-based experiments are used to examine AOA Fe ecophysiology, exploring how marine Fe availability shapes the spatial niche occupied by AOA and examining the potential for marine ammonia oxidation to be limited by Fe in the oceans.

CHAPTER THREE builds on the results of chapter two, in which a clear physiological growth response to Fe availability is demonstrated. Chapter three examines the proteomic response of *N. maritimus* to Fe limitation, shedding light on the underpinning molecular strategies adopted by AOA to survive Fe scarcity. Chapter three compares label-free quantitation (LFQ) intensities between Fe-limited and Fe-replete *N. maritimus* cultures, elucidating the proteomic strategies that underpin the physiological responses seen in chapter two. Further, chapter three compares the Fe-specific cellular response of AOA to previously published work that examines the response of AOA to Cu and reactive oxygen species (ROS) stress.

CHAPTER FOUR examines the physiological response of the marine AOB isolate, *Nitrosococcus oceani*, to Fe and Cu availability**,** contrasting results with those of AOA (*N. maritimus*) from results of Chapter two and previously published work (Amin et al. 2013). Chapter four uses comparative genomics to assess how widespread the proteomic and trace metal transport basis giving rise to contrasting physiologies is in phylogenetically diverse marine AOA and AOB that are not yet available in pure culture. Chapter four explores how contrasting requirements and uptake strategies for Fe and Cu

play out into: (1) the distinct metal niches occupied by AOA and AOB in the oceans; (2) the success of AOA over AOB; (3) the physicochemical niche occupied by AOB, despite being poor competitors for NH_4^+. Finally, this chapter discusses the contrasting trace metal requirements in the context of evolving trace metal requirements over time, providing insight into the potential for trace metals to indicate the relative emergence of these different groups of ammonia oxidisers.

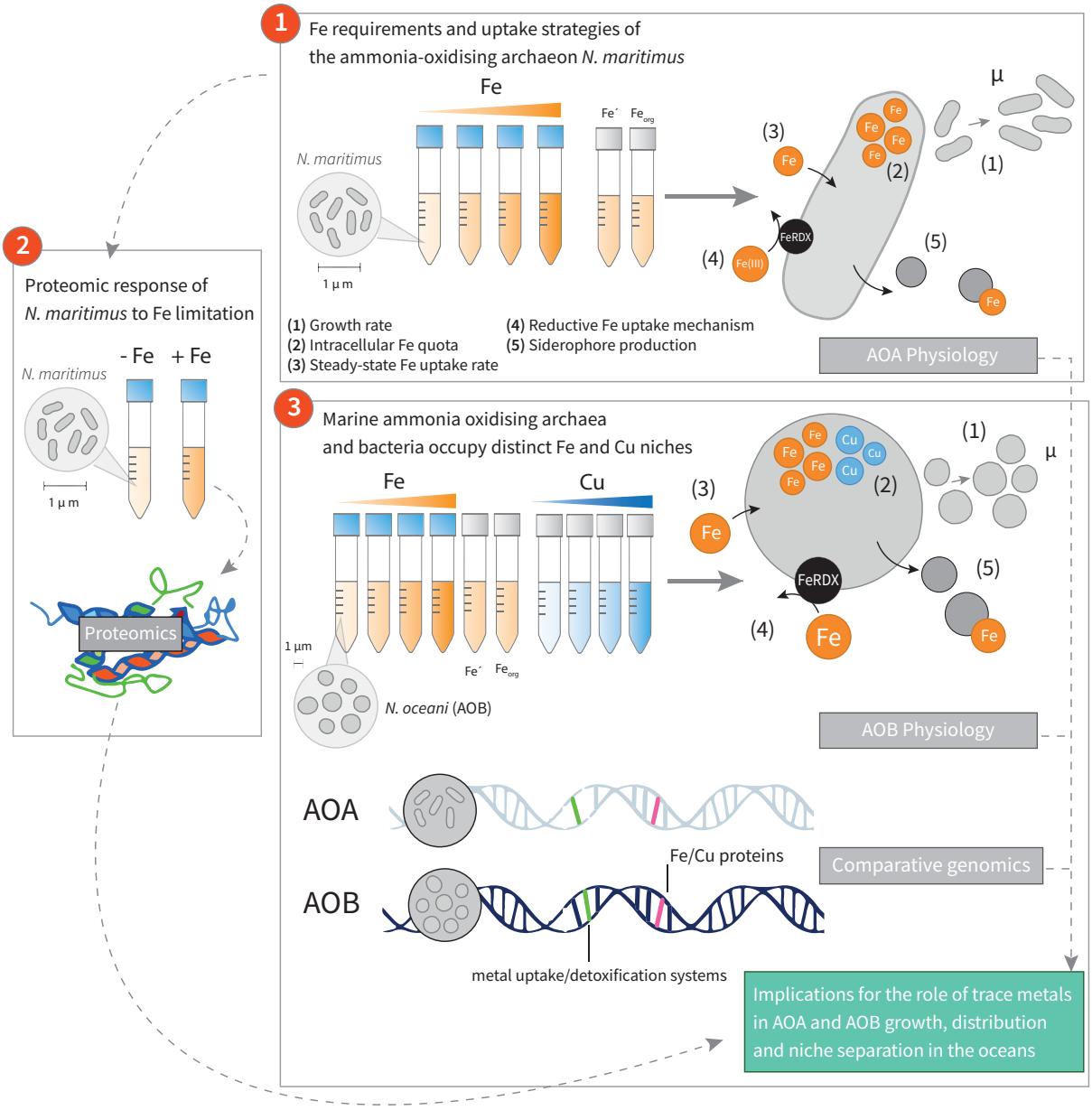


Figure 1.16 Outline of experimental approach to research aims and questions

Schematic outline of the experimental approach of each thesis chapter, showing how approaches (physiology, proteomics and comparative genomics) are used to understand the role of trace metals in AOA growth, distribution and niche separation in the oceans (green box). The specific aspects of the Fe and Cu physiological characterisation of AOA and AOB, in chapters two and four, are outlined (labelled numbers in the AOB schematic correspond to the key in the AOA schematic). Note that this thesis outlines the Fe physiology of the marine AOA isolate *N. maritimus*, and the Fe and Cu physiology of the AOB isolate *N. oceani*. The Cu physiology of *N. maritimus* – which is also used to inform interpretations for niche separation – was examined by a previous study (Amin et al. 2013).

BOX 7 – MICROBIAL TRACE METAL REQUIREMENTS: A FOCUS ON PHYSIOLOGY

Researchers employ a range of approaches to understand how trace metals shape the growth, distribution, and chemical niches of marine microorganisms. These approaches span from predicting trace metal requirements from microbial genomes (e.g., Dupont et al. 2006; 2010; Zerkle et al. 2005) to measuring the physiological responses of microorganisms to changing trace metal availabilities in the laboratory and field (e.g. Sunda & Huntsman, 1995; Moore et al. 2013). Understanding how trace metals impact microbial growth and ecology has benefitted enormously from developments in the 'omics fields. Metagenomic, –proteomic and –transcriptomic datasets can illuminate geographically widespread trace metal limitation of microbial growth through an understanding of the molecular-level microbial responses to trace metal scarcity (Saito et al. 2015). For instance, the identification of the phytoplankton Fe deficiency-induced protein A (IdiA) involved in cellular Fe scavenging has been used as a marker for Fe stress in open ocean field populations (Webb et al. 2001; Saito et al. 2014; Chappell et al. 2015 — Figure 1.18A).

The utility of meta-'omic datasets in diagnosing widespread trace metal limitation of phytoplankton has been enabled by decades of initial physiological characterisation of the effect of low trace metal concentrations on microbial growth in laboratory cultures (Brand et al. 1983; Rueter et al. 1990) facilitated by the development of trace metal ion buffers (Hutner et al. 1950; Price et al. 1989). Once a physiological response to changing trace metal availability has been established, interrogating the 'omics-based response provides the foundation for the design of valuable *in-situ* limitation biomarkers.

However, 'omic-level characterisations alone are insufficient to assess whether microbial communities will be limited by trace metals *in situ* and how trace metals

shape microbial community structure. First and foremost, genomic, transcriptomic and proteomic approaches assume that microbial genomes are accurately annotated. Often a high proportion of genome annotation is based on sequence homology, meaning that trace metal requirements inferred from these analyses are largely putative. Further still, it is estimated that around half of metalloproteins have not yet been characterised (Cvetkovic et al. 2010), making it near impossible to map an organisms metalloproteome with the genome alone. Even if the cellular metal quota is directly quantified (termed the 'metallome', usually measured as moles of metal per cell using inductively coupled plasma mass spectrometry, ICP-MS), this is not sufficient to determine how microbial growth rate (μ) will respond to trace metal availability. For instance, *Ostreococcus* sp. RCC789 (a coastal green algae) and *Emiliania huxleyi* (an open ocean coccolithophore) both have similar minimum intracellular Fe quotas required to begin growth (QFe_{min}) (Figure 1.17 – Sunda & Huntsman, 1995; Botebol et al. 2017). However, haptophytes can grow at an order of magnitude lower extracellular Fe′ compared with green algae, demonstrating efficient Fe-uptake kinetics, which are not revealed from measuring the metallome alone.

Although the presence of trace metal transport systems and uptake strategies can be inferred from examining the proteome or metabolome (e.g. ABC transporters or siderophores), there are still many unknowns that hold implications for trace metal uptake rates. For instance, what is the affinity of the transporter for the target trace metal? What trace metal substrates are available to an extracellular reductase? All of these factors contribute to the uptake rate of trace metals, which — in combination with the minimum cellular metal quota needed for growth (i.e., the metallome) — will ultimately determine the concentration of an extracellular trace metal required to reach a given μ (Figure 1.18).

In sum, understanding the physiological response to changing trace metal availability is the cornerstone of ecophysiology that dictates the distribution and spatial niche separation of microorganisms in the ocean. To this end, the approach of this thesis is to focus on the physiological response of key available marine AOA and AOB isolates, with support from 'omics' (metallomics, proteomics and comparative genomics) to provide context to the underpinning molecular basis which ultimately gives rise to the observed physiologies.

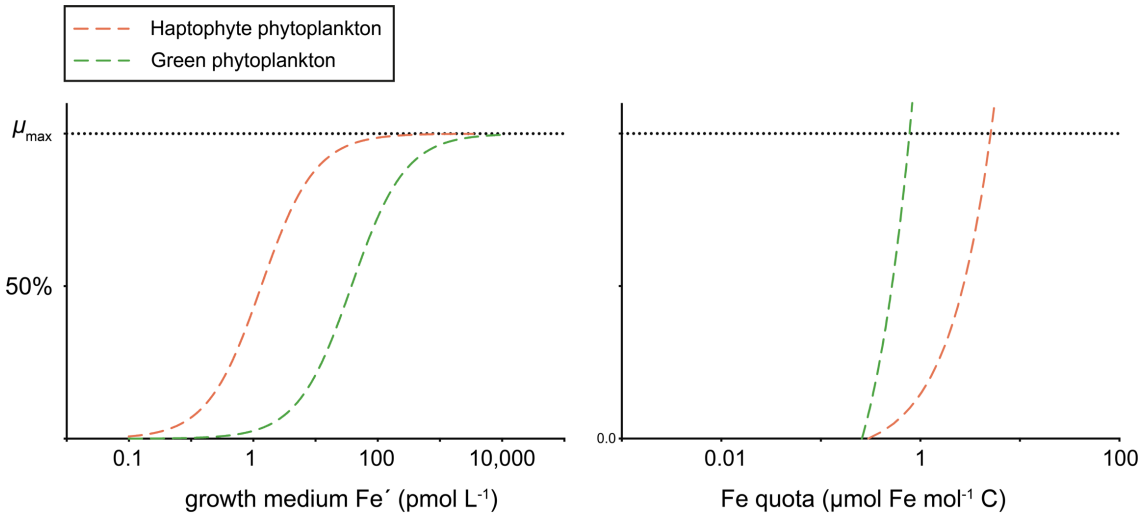


Figure 1.17 Contrasting microbial growth responses of two microorganisms with similar Fe:C quotas

Dose-response curve of *Ostreococcus* sp. (labelled green phytoplankton) and *Emiliania huxleyi* (labelled haptophyte phytoplankton) in response to unchelated Fe (Fe′) (left) and Fe quota (Fe:C µmol mol^{-1}) as a function of growth rate, μ (right) indicating that both species have similar minimum Fe quotas to begin growth but have different responses to extracellular Fe′ availability.

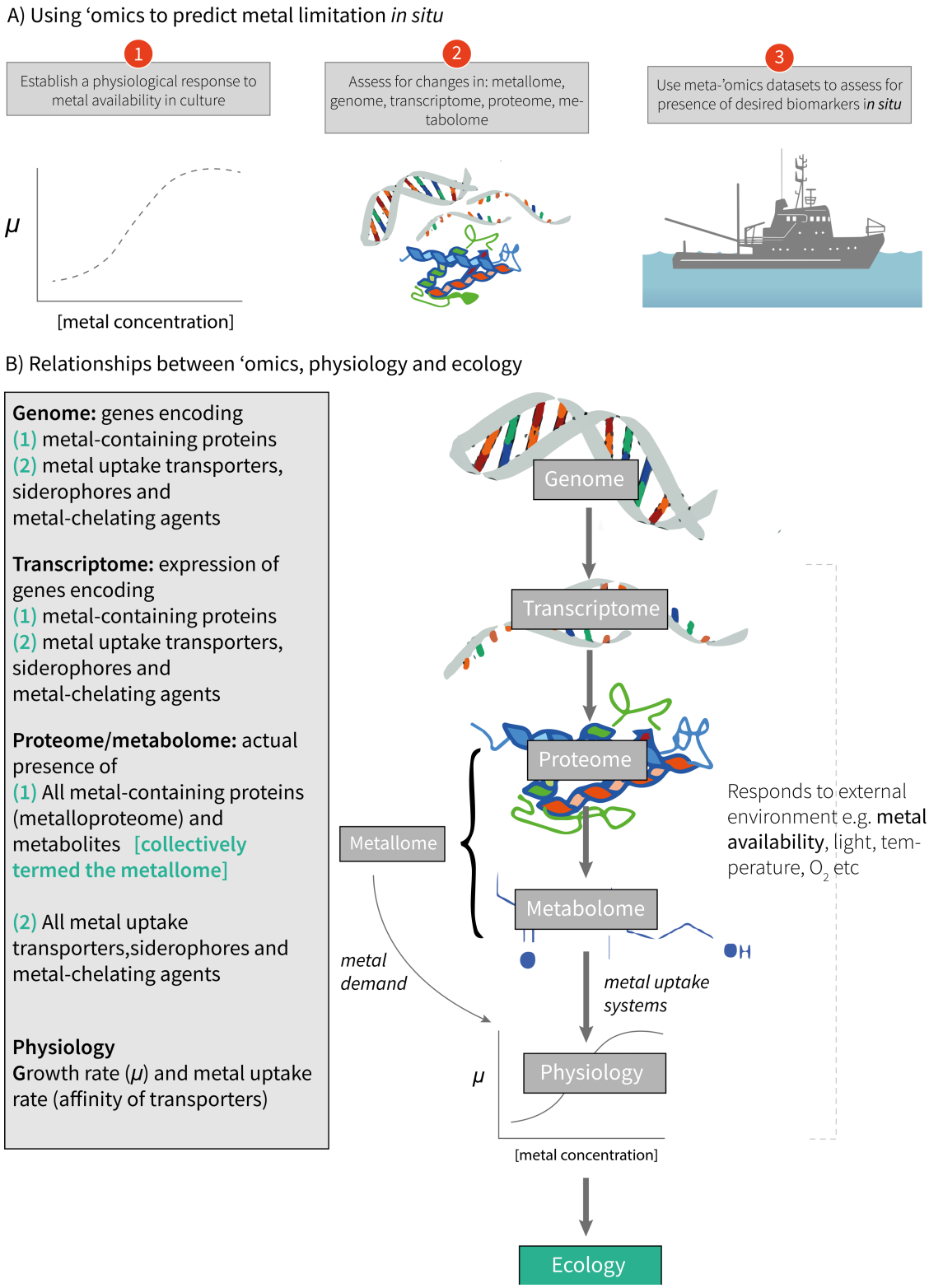


Figure 1.18 The role of 'omics in understanding microbial trace metal requirements

A) How 'omics datasets can be used to develop biomarkers to assess for trace metal limitation *in situ* **B)** The relationship between the genome, transcriptome, proteome and metabolome on microbial physiology and ecology, highlighting the impact of both the metallome and non metal-binding proteins mediating trace metal uptake on the physiology in response to trace metal availability.

2 IRON REQUIREMENTS AND UPTAKE STRATEGIES OF THE GLOBALLY ABUNDANT MARINE AMMONIA-OXIDISING ARCHAEON, *NITROSOPUMILUS MARITIMUS* STRAIN SCM1

This chapter provides the physiological and metallomic characterisation of the Fe requirements and uptake strategies of the marine AOA isolate, *Nitrosopumilus maritimus* strain SCM1. In doing so, this chapter provides the physiological Fe characterisation of AOA necessary to address the overarching thesis aim of examining how Fe and Cu contribute to the growth, distribution, and niche separation of marine ammonia-oxidising archaea (AOA) and bacteria (AOB) in the oceans — addressed in chapter four. This chapter aims to use physiological Fe requirements and uptake strategies to provide an explanation to the vertical niche occupied by AOA in the water column.

This chapter is a reprint of material as it appears in The ISME Journal (2019, doi.org/10.1038/s41396-019-0434-8), co-authored by Dr Joseph Snow, Dr Qiong Zhang and Professor Rosalind Rickaby. All material is identical to the published version, except for Figure 2.4 which has been amended for styling purposes. All supporting material is located in Appendix I.

2.1 ABSTRACT

Ammonia-oxidising archaea (AOA) mediate the rate-limiting step of nitrification, the central component of the marine nitrogen (N) cycle that converts ammonia to nitrite then nitrate. Competition with phytoplankton for ammonium and light inhibition are considered to restrict AOA activity to below the euphotic zone, but observations of surface nitrification now demand a further understanding of the factors driving AOA distribution and activity. Pico- to nanomolar concentrations of iron (Fe) limit the growth of microorganisms in a significant portion of the world's surface oceans, yet there is no

examination of the role of Fe in AOA growth despite the process of ammonia oxidation being considered to rely on the micronutrient. Here we investigate the Fe requirements and Fe-uptake strategies of *Nitrosopumilus maritimus* strain SCM1, a strain representative of globally abundant marine AOA. Using trace metal clean culturing techniques, we found that *N. maritimus* growth is determined by Fe availability, displaying a free inorganic Fe (Fe′) half-saturation constant 1–2 orders of magnitude greater for cell growth than numerous marine phytoplankton and heterotrophic bacterial species — driven by a reduced uptake affinity for Fe′. In addition, we discovered that whilst unable to produce siderophores to enhance access to Fe, *N. maritimus* is able to use the exogenous siderophore desferrioxamine B (DFB), likely through a reductive uptake pathway analogous to that demonstrated in phytoplankton. Our work suggests AOA growth in surface waters may be Fe limited and advances our understanding of AOA ecophysiology on cellular and mechanistic levels, holding implications for ecosystem dynamics and the biogeochemical N cycle.

2.2 INTRODUCTION

Ammonia oxidation is the first and rate-limiting step of nitrification, mediated by ammonia-oxidising bacteria and archaea (AOB and AOA, respectively). Nitrification links the reduced and oxidised components of the biogeochemical nitrogen (N) cycle through the conversion of ammonium (NH_4^+) to nitrite (NO_2^-) and then nitrate (NO_3^-). Greater ratios of NO_3^- to NH_4^+ in marine surface waters are shown to promote the growth of faster-sinking microphytoplankton (such as diatoms) relative to picophytoplankton, thereby driving increased carbon export to the deep ocean (Peterson et al. 2005; Guidi et al. 2008; Fawcett et al. 2011; Berg et al. 2003; Glibert et al. 2016). Nitrification rates also have an additional climatic impact through the release of the by-product nitrous oxide (N_2O) — a potent greenhouse gas (Freing et al. 2012; Löscher et al. 2012). In the oceans AOA, belonging to the phylum *Thaumarchaeota*, largely outnumber their bacterial counterparts (Mincer et al. 2007; Wuchter et al. 2006) and are among the most ubiquitous and abundant microbes, constituting ~20% of total marine prokaryotic cells (Karner et al. 2001). Due to their key role in biogeochemical N cycling, investigation has focused on understanding the factors that determine the distribution of *Thaumarchaeota* and nitrification rates throughout the water column. Photoinhibition of AOA growth (Merbt et al. 2012; Horak et al. 2013; Tolar et al. 2016; Horak et al. 2018) and competition with phytoplankton for NH_4^+ (Xu et al. 2019; Ward, 2008; Smith et al. 2014) have both been evoked to explain why peak nitrification rates typically occur at the base of the euphotic zone. However, observations of high nitrification rates in the euphotic zone indicate that this is not universally the case (Dore & Karl, 1996; Yool et al. 2007), suggesting that our understanding of the factors shaping the distribution of AOA is incomplete. No studies to date have directly examined the role of the trace metal micronutrient iron (Fe) in *Thaumarchaeota* growth, despite a vast body of evidence showing that Fe influences the

growth of a range of marine N-cycling microorganisms in a significant portion of the world's oceans (Moore et al. 2008; Mills et al. 2004; Moore et al. 2009). The only study to date to directly examine the role of trace metals in *Thaumarchaeota* growth, demonstrated that the marine model AOA species *Nitrosopumilus maritimus* (strain SCM1) has a high copper (Cu) requirement (Amin et al. 2013), driven by numerous multi-Cu oxidases and blue Cu proteins resembling sulpho- and plastocyanin enzymes (Walker et al. 2010). In contrast, AOB purportedly utilise a greater number of Fe-based enzymes and fewer Cu-proteins suggesting that AOB may possess a greater Fe requirement but lower Cu requirement (Blainey et al. 2011; Zannoni, 2004). Whether oceanic trace metal availability shapes the ecological niche separation of AOB vs. AOA, in a similar way to NH_4^+ (Urakawa et al. 2014; Martens-Habbena et al. 2009) in the oligotrophic oceans has yet to be explored. In addition, it remains unknown which Fe substrates are available for uptake by *N. maritimus*, the strategies *N. maritimus* employs to gain access to low levels of Fe in the oceans, and how together these traits influence the distribution of AOA throughout the water column. In order to aid in Fe acquisition, marine microorganisms may produce high-affinity Fe^{3+} binding ligands called siderophores, which increase the bioavailability of Fe to some microorganisms (Gledhill & Buck, 2012). The ability of microbes to utilise different classes of siderophores, taken up through either siderophore-specific transmembrane proteins or through extracellular reduction of Fe-chelates (Lis et al. 2015; Shaked & Lis, 2012), can provide microorganisms with a competitive advantage in Fe-poor niches of the ocean.

Here we use trace metal clean culturing techniques to examine the role of Fe in the growth of the model marine AOA, *N. maritimus* strain SCM1, with the aim of understanding how Fe in the oceans may drive the distribution of marine AOA species. We specifically examine the role of environmentally important Fe substrates in AOA

growth including unchelated inorganic Fe (Fe′) and organic siderophore-bound Fe. Our study is the first to shed light on the role of Fe in AOA growth, presenting implications for how Fe in the marine environment may shape the ecological niche that AOA occupy in the water column.

2.3 MATERIALS & METHODS

2.3.1 Archaeal cultures and growth media

Polycarbonate culture vessels and culturing apparatus were acid cleaned (10% HCl v/v, 24 hours) and UV-sterilised prior to use. Triplicate cultures of *Nitrosopumilus maritimus* strain SCM1 (herein referred to as *N. maritimus*) were grown in modified SCM medium (Könneke et al. 2005) and maintained at 28 °C in the dark. Macronutrients used in media preparation were treated with Chelex 100 resin (BioRad, Watford, UK) to remove trace metal contaminants (Price et al. 1989). Media pH was buffered with HEPES, to maintain pH at 7.5. To investigate the effect of unchelated inorganic Fe concentration ([Fe′]) on *N. maritimus* growth, ethylenediamine tetraacetic acid (EDTA; Merck, Darmstadt, Germany) was used to buffer Fe and other trace metals in culture; [Fe′] was controlled by varying the addition of $FeCl_3$ and maintaining a constant concentration of EDTA at 12 µmol L^{-1}. We did not observe a difference in growth rate in cultures with equivalent [Fe′] (7500 pmol L^{-1}) but with varying [EDTA]; cultures with 12 µmol L^{-1} EDTA, relative to regular SCM media with 7.5 µmol L^{-1} [EDTA] did not produce an inhibitory effect (Figure A1.1). [Fe′] in cultures was calculated using Visual Minteq software (Gustafsson, 2010), including background Fe contamination of 50 nmol L^{-1} from basal SCM medium with included macronutrients and vitamins but without added trace metals, determined using inductively coupled plasma mass spectrometry (Zhang et al. 2018). Cultures were acclimated to trace metal concentrations stated by transferring cultures consecutively into new media until growth rates did not vary with statistical significance (ANOVA, $p < 0.05$).

Growth was determined by measuring concentrations of nitrite ($[NO_2^-]$) spectrophotometrically (Griess, 1879), which was observed to correlate with cell counts at both high and low [Fe′] (Figure A1.2). Specific growth rate (d^{-1}) was calculated over the linear phase of semi-log plots of NO_2^- over time. *N. maritimus* and published marine microbial growth rate data in response to [Fe′] (Sunda & Huntsman, 1995; Sunda & Huntsman, 1997; Berman-Frank et al. 2001; Shi et al. 2012; Schulz et al. 2004; Boatman et al. 2018; Sunda & Huntsman, 2015) were fit to a Monod function:

$$\mu = \frac{\mu_{max} \cdot [Fe']}{K_s + [Fe']} \quad \text{(eq. 1)}$$

Whereby μ is specific growth rate (d^{-1}), μ_{max} is the maximum specific growth rate, [Fe′] is the concentration of unchelated inorganic Fe and K_s is the half-saturation constant for growth.

2.3.2 Calculation of steady-state uptake rate constant

In order to compare the Fe-uptake rates of *N. maritimus* with published uptake rates of other marine microorganisms compiled in our study (Lis et al. 2015a; Lis et al. 2015b; Sunda & Huntsman, 1997; Lane et al. 2009; Marchetti et al. 2006; Strzepek et al. 2011; Maldonado & Price, 2001; Shaked et al. 2004; Hassler & Schoemann, 2009 – Table A1.1), we calculated the steady-state uptake rate (ρ_{ss}) in mol Fe per cell h^{-1} and the steady-state uptake constant (k_{in}) in units L $cell^{-1}$ h^{-1} as defined by Shaked & Lis (2012). Cell numbers used in our calculations were obtained by using a conversion factor of 6.01×10^{10} cells per mole of NO_2^- produced — derived from measurements of cell counts with increasing $[NO_2^-]$ (Figure A1.2).

$$\rho_{ss} = Q \cdot \mu \quad \text{(eq. 2)}$$

$$k_{in} = \frac{\rho_{ss}}{[S]} \quad \text{(eq. 3)}$$

Whereby Q is equal to the cellular Fe quota (mol Fe $cell^{-1}$), μ is specific growth rate (h^{-1}) and S is the concentration of the Fe substrate (either Fe′ or FeDFB) (mol L^{-1}). Furthermore, we were able to normalise the uptake rate constant to cell surface area (k_{in} /S.A.) in order to obtain an uptake constant independent of cell surface area and therefore proportional to the affinity of the uptake system. *N. maritimus* surface area was calculated based on average dimensions of cells imaged using scanning electron microscopy (Figure A1.3). *N. maritimus* cells were rod-shaped with a diameter of 0.1–0.2 µm and length of 0.45–0.58 µm (Figure A1.3). Cell surface area was calculated using an average diameter of 0.15 µm and length of 0.52 µm. These dimensions agree with previous analyses of *N. maritimus* cell size (Könneke et al. 2005) which showed rod-shaped cells with a diameter of 0.17–0.22 µm and a length of 0.5–0.9 µm. All steady-state uptake rates and constants used in our comparison were compiled and calculated by Lis et al. (2015a) from published datasets (Table A1.2).

2.3.3 Siderophore production and Fe-complex uptake pathway

To examine whether *N. maritimus* is able to grow using siderophore-bound Fe, *N. maritimus* was cultured in media with the addition of desferrioxamine B mesylate (DFB; Merck), a fungal siderophore that has a greater stability constant (logK′FeL,Fe′ = 11.8) for Fe^{3+} compared with EDTA (logK′FeL,Fe′ = 8.6, pH 8) (Maldonado et al. 2005; Hudson et al. 1992). [Fe′] in DFB-buffered media was calculated using the equation [Fe′] = [FeDFB]/([DFB′] × [$K_{Fe'DFB}^{cond}$]). A 1.3-fold excess of DFB was added over Fe, resulting in [Fe′] of 5.2×10^{-9} pmol L^{-1}, considered to be negligible, thereby making Fe bound to DFB (FeDFB) the main Fe substrate in these experiments. EDTA concentrations were kept constant at 12 µmol L^{-1} EDTA to buffer other trace metals as done in previous studies (Strzepek et al. 2011; Maldonado & Price, 2001).

Siderophore secretion by *N. maritimus* was tested using a liquid Chrome Azurol S (CAS) assay (Schwyn & Neilands, 1987). Prior to this assay, potential siderophores were preconcentrated from the supernatant of 300 and 1050 pmol L^{-1} Fe′ cultures (grown in the absence of EDTA), using Solid Phase Extraction (SPE) cartridges (Isolute ENV+, 1g 25 ml, Biotage, Hengoed, UK). Cartridges were precleaned with 5 ml methanol and 5 ml 11.2 mmol L^{-1} ammonium carbonate (pH 7.5). 1 L of 0.1 µm-filtered culture supernatant was passed through the column at a flow rate of 8 ml min^{-1}, followed by 5 ml of 11.2 mmol L^{-1} ammonium carbonate to remove salts. Siderophores were eluted with 5 ml of 1:20:80 (v/v/v) formic acid/water/methanol. The SPE eluent from all samples was dried under high purity N_2 to 100 µL and then made up to 500 µL with 0.1% (v/v) formic acid (Sigma-Aldrich) prior to analysis. The sensitivity of this method was tested by preconcentrating 1 L of 1–100 pmol L^{-1} DFB solutions — which are typically undetectable by the CAS Assay — using the SPE columns. The lowest concentration detected using this method was 10 pmol L^{-1} DFB, which was used as a positive control. Uninoculated EDTA-free SCM media passed through the SPE column was used as a blank. Absorbance spectra were measured between 400 and 800 nm and siderophore production was observed as a decrease in the absorbance peak at 630 nm.

We used the ferrozine assay (Shaked & Lis, 2012) to identify whether *N. maritimus* adopts a reductive Fe-uptake pathway in Fe acquisition. *N. maritimus* cultures acclimated to total [Fe] of 1050 nmol L^{-1} [(both EDTA and DFB experiments) were treated with 200 µmol L^{-1} ferrozine (FZ; 5,6-Diphenyl-3-(2-pyridyl)-1,2,4-triazine) at the beginning of experiments. As Fe^{2+}-FZ_3 complexes are unavailable for uptake across the plasma membrane (Shaked et al. 2005), any reduction in growth rate suggests a reductive uptake pathway is present in Fe acquisition. FZ concentrations used in our experiments have been previously shown to be suitable in binding Fe^{2+} without inducing abiotic reduction of Fe^{3+}

species (Kranzler et al. 2011). All Fe-uptake experiments were performed in the dark to prevent the photoreduction of Fe^{3+}-chelates.

2.3.4 Cellular Fe and P content

All samples and reagents were processed using trace metal clean techniques and acid-washed plasticware (10% HCl v/v, 24 hours) in a clean laboratory prior to trace element analysis. *N. maritimus* cells cultured in 300, 550, and 1050 pmol L^{-1} Fe′ were harvested in late exponential phase by centrifugation at 5000 × g for 25 minutes and then rinsed with Chelex 100-treated SCM media to remove weakly-bound surface trace metals. Cells were digested in acid-cleaned Teflon as follows: refluxing at 100 °C with 16 N quartz distilled (q.d.) HNO_3 (produced in-house) and H_2O_2 (ROMIL UpA™, Cambridge, UK) in a ratio of 3:2 overnight. The liquid was then allowed to evaporate to dryness and 2% q.d. HNO_3 was added to reflux for an hour to resuspend the dried samples. ^{56}Fe and ^{31}P concentrations were determined using a Quadrupole ICP-MS Perkin Elmer NexION 350 with Elemental Scientific Flow Injection Auto-sampler (FIAS) in a method optimised for high salt matrixes (Zhang et al. 2018).

2.3.5 Fe rescue experiments

In order to confirm whether Fe limits *N. maritimus* growth in EDTA-buffered experiments, we performed an 'Fe rescue' of experiments which showed suppressed or no cell growth in the second subculture before cultures had become fully acclimated. We supplemented 50 and 150 pmol L^{-1} Fe treatments with additional $FeCl_3$ at 120 hours resulting in final [Fe′] of 1050 pmol L^{-1}. Control cultures received no additional $FeCl_3$.

2.3.6 Data analysis

All statistical analyses were performed using Minitab v.13.1. Data were examined for normality and equal variance prior to Student's *T* test and analysis of variance (ANOVA) statistical tests. Significant results are reported at the 95% confidence level ($p < 0.05$).

2.4 RESULTS

2.4.1 Effect of unchelated Fe (Fe′) on total nitrite production and specific growth rates

Cultures of *N. maritimus* were acclimated to a range of unchelated inorganic Fe concentrations ([Fe′]), as described above. Treatments at < 250 pmol L^{-1} Fe′ did not support *N. maritimus* growth as evidenced by a total lack of NO_2^- production (Figure 2.1). We observed *N. maritimus* growth in all tested conditions ≥ 250 pmol L^{-1} Fe′. Treatments at 250 and 300 pmol L^{-1} Fe′ showed suppressed growth curves, producing significantly lower final [NO_2^-] ($p < 0.05$), compared with 550–7550 pmol L^{-1} Fe′ treatments which produced indistinguishable growth curves and maximum [NO_2^-] reached.

To provide confirmation that growth inhibition was due to Fe limitation, we supplemented cultures showing little and no growth in the second experimental sub-culture (where cultures were experiencing Fe stress but before they had become acclimated) with $FeCl_3$ to reach a final [Fe′] of 1050 pmol L^{-1} (Figure A1.4). We observed enhanced NO_2^- production in all supplemented cultures, compared with non-supplemented controls; 150 pmol L^{-1} Fe′ treatments supplemented with additional Fe produced 900 µmol L^{-1} NO_2^- within 11 days and 50 pmol L^{-1} Fe′ cultures produced 900 µmol L^{-1} NO_2^- within 15 days.

Maximum specific growth rates, μ_{max}, were observed in 7550 pmol L^{-1} Fe′ treatments (Table 2.1). The half-saturation constant (K_s), based on a Monod curve fitted to our data

(eq. 1) was 361.5 pmol L^{-1} Fe′. Specific growth rate (μ) varied significantly between 250 and 1050 pmol L^{-1} Fe′ treatments ($p < 0.05$), ranging between 27–99% of μ_{max} (Table 2.1; Figure 2.1). Cultures treated with 250 pmol L^{-1} Fe′ grew at the lowest μ (27% of μ_{max}) followed by 300 pmol L^{-1} Fe′ treated cultures which grew at 81% of μ_{max}. We observed no significant increase in μ/μ_{max} when [Fe′] > 1050 pmol L^{-1} ($p > 0.05$), suggesting that these cultures were Fe replete.

2.4.2 Cellular Fe quotas

Cellular Fe and P concentrations were measured in response to increasing [Fe′], between 300–7500 pmol L^{-1} Fe′. We observed a scaling between *N. maritimus* cellular Fe and P concentrations, [Fe′] and μ (Table 2.1). Fe:P varied significantly between treatments growing at different μ ($p < 0.05$), ranging between 11.4 (± 4.7) and 39.3 (± 11.8) mmol Fe mol^{-1} P. We observed maximum cellular Fe:P in cultures growing at μ_{max}.

2.4.3 Steady-state uptake rate of Fe′ and FeDFB

A requirement of steady-state uptake rate (ρ_{ss}) calculations is for cellular Fe quota and specific growth rates to be used when [Fe′] is limiting to growth. We therefore calculated ρ_{ss} based on the cellular Fe quota (Q) of *N. maritimus* treatments at 300 and 550 pmol L^{-1} Fe′, that were growing at 81 and 93% of μ_{max}. The Fe′ steady-state uptake rate (ρ_{ss}) was 1.1×10^{-22} mol Fe $cell^{-1}$ hr^{-1} ($\pm 3.1 \times 10^{-23}$) and the Fe′ steady-state uptake rate constant ($k_{in} - \rho_{ss}$ /[Fe′]) was 4.5×10^{-13} L $cell^{-1}$ hr^{-1} ($\pm 1.2 \times 10^{-13}$). The steady-state uptake rate constant of FeDFB (k_{in}) was significantly lower than that of Fe′ ($p < 0.05$) at 2.8×10^{-15} L $cell^{-1}$ hr^{-1} ($\pm 1.6 \times 10^{-16}$).

2.4.4 *N. maritimus* siderophore production and FeDFB uptake

We conducted a CAS assay to determine whether *N. maritimus* produces siderophores. In this assay, there was no evidence for siderophore production in the medium of either

300 pmol L^{-1} or 1050 pmol L^{-1} Fe′ treatments, as the absorbance spectra of culture supernatants did not differ significantly from the blank (Figure 2.2). However, this result does not completely rule out the production of very low concentrations (< 10 pmol L^{-1} detection limit) of siderophores by *N. maritimus*. The ability of *N. maritimus* to grow using siderophore-bound Fe was examined using growth media wherein all Fe was bound to the hydroxamate siderophore, DFB (FeDFB), thereby reducing [Fe′] in the medium to negligible concentrations (see Section 2.3.3 for full details). We observed no *N. maritimus* growth at 150 nmol L^{-1} FeDFB. Only treatments with 1050 nmol L^{-1} FeDFB displayed growth, reaching μ of 0.44 d^{-1} (Figure 2.3). However, this μ is significantly lower than the μ in EDTA buffered treatments with 1050 pmol L^{-1} Fe′ ($p < 0.05$), which reached a μ of 0.50 d^{-1}.

2.4.5 The role of reduction in Fe uptake

In order to determine whether reduction of Fe^{3+} to Fe^{2+} is a component of *N. maritimus'* Fe acquisition strategy, we examined the effect of ferrozine (FZ) addition on *N. maritimus'* growth rate. FZ significantly reduced μ in both EDTA and DFB buffered cultures ($p < 0.05$), compared with the untreated controls (Figure 2.3). This suggests a requirement for Fe^{3+} reduction in *N. maritimus*' Fe-uptake strategy. In EDTA treatments, addition of FZ reduced μ by 30% compared to DFB treatments wherein FZ reduced μ by 100%.

[Fe] (nmol L^{-1})	**[Fe´]** (pmol L^{-1})	**Fe** (pmol $cell^{-1}$)	**P** (pmol $cell^{-1}$)	**Fe:P** (mmol mol^{-1})	μ (d^{-1})	μ/μ_{max}
200	200				0	0
250	250				0.13 (± 0.05)	0.27 (± 0.02)
300	300	5.0×10^{-6} ($\pm 4.3 \times 10^{-6}$)	5.5×10^{-4} ($\pm 1 \times 10^{-4}$)	11.4 (± 4.7)	0.41 (± 0.05)	0.81 (± 0.09)
550	550	6.5×10^{-6} ($\pm 1.3 \times 10^{-6}$)	3.3×10^{-4} ($\pm 5.4 \times 10^{-5}$)	18.8 (± 3.2)	0.47 (± 0.02)	0.93 (± 0.05)
1050	1050	1.1×10^{-4} ($\pm 4.2 \times 10^{-5}$)	2.6×10^{-3} ($\pm 1.2 \times 10^{-4}$)	39.3 (± 11.8)	0.50 (± 0.01)	0.99 (± 0.09)
7550	7550	0.78 (± 0.07)	3.93 (± 0.05)	199.95 (± 4.9)	0.51 (± 0.01)	1 (± 0.02)

Table 2.1 Effect of Fe on growth rate and cellular quotas of *N. maritimus*

Relationships between total [Fe], [Fe´], cellular Fe and P concentration, specific growth rate (μ) and relative growth rate (μ/μ_{max}) in *N. maritimus*. Values in parentheses represent standard deviation. For growth rate data $n = 20$, for cellular quota data $n = 3$.

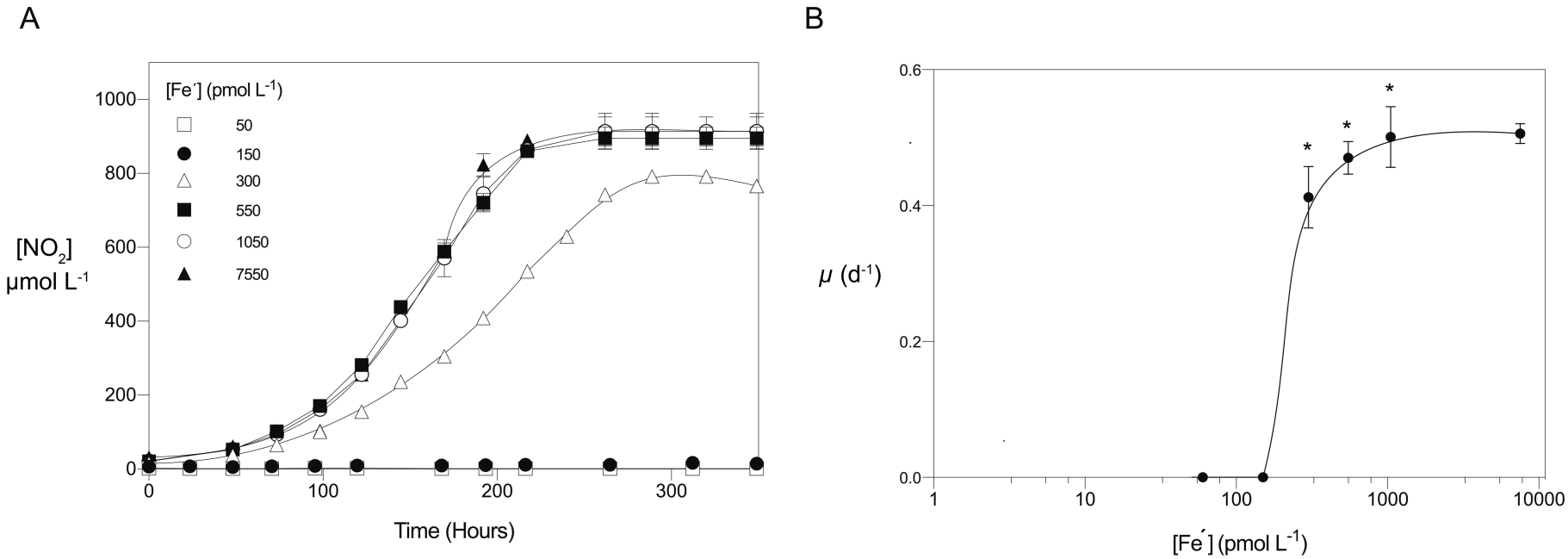


Figure 2.1 Effect of Fe′ on NO_2^- production and specific growth rate (μ) of *N. maritimus*

Effect of unchelated Fe (Fe′) on the production of nitrite (NO_2^-) and the acclimated, specific growth (μ) of *N. maritimus*. * denotes growth rates statistically different from each other. Error bars indicate standard deviation, $n = 20$. Copyright © 2019, Shafiee et al.

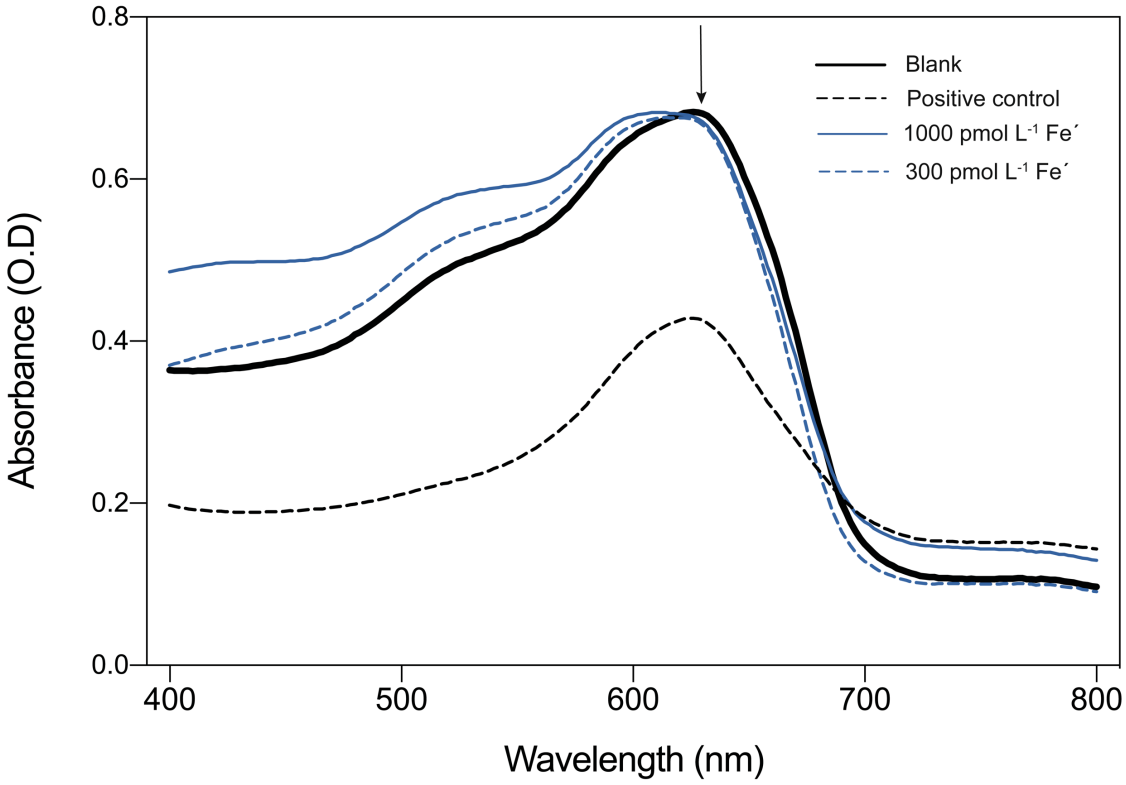


Figure 2.2 Absorbance spectra of *N. maritimus* supernatant after treatment with Chrome Azurol S solution

Absorbance spectra of *N. maritimus* culture supernatant with 300 (blue dashed line) and 1050 pmol L^{-1} Fe´ (blue solid line) measured between 400 – 800 nm following treatment with chrome azurol S (CAS) assay solution. Siderophore production was denoted as a decrease in absorbance from the blank (SCM medium without chelating agent – solid black line) at 630 nm, marked with an arrow. 10 pmol L^{-1} DFB solution was used as a positive control. n = 3. Copyright © 2019, Shafiee et al.

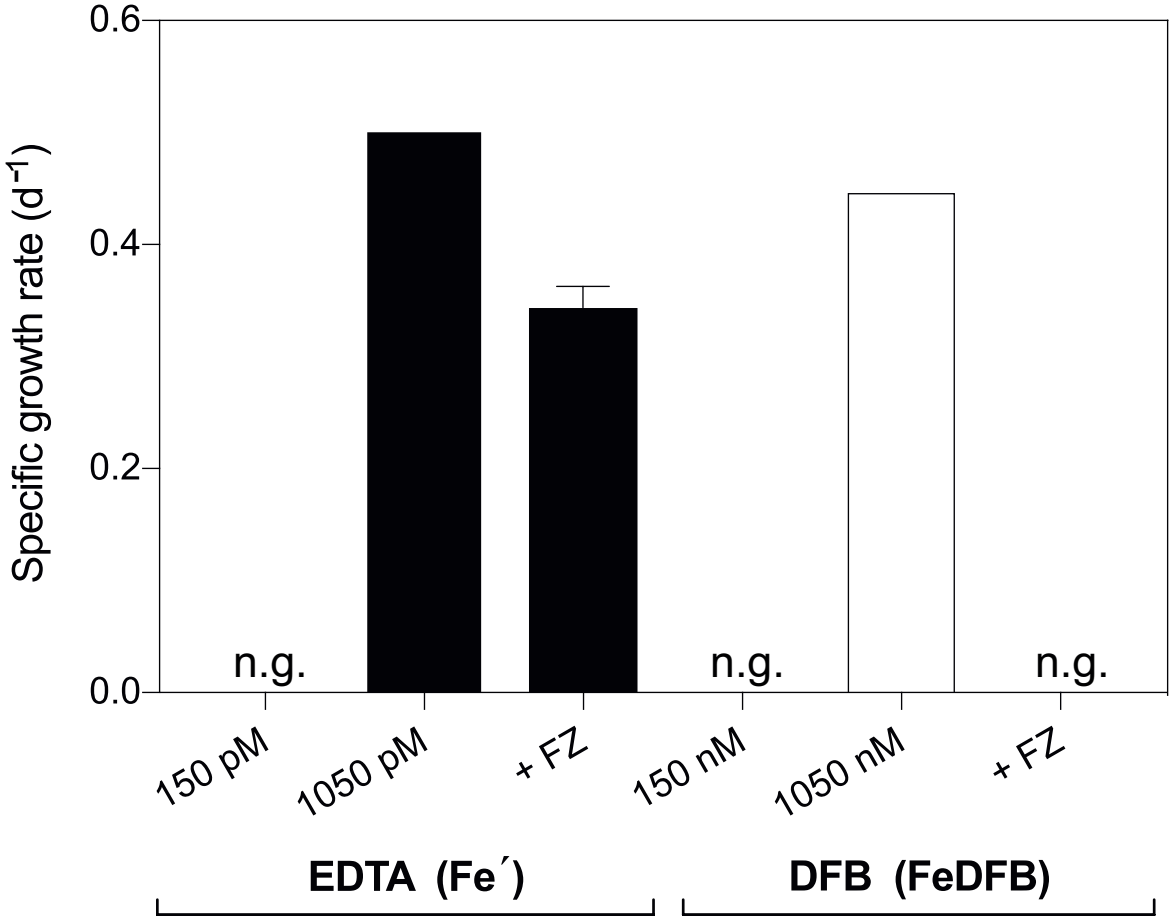


Figure 2.3 *N. maritimus* growth with Fe´ and organically-complexed Fe, FeDFB

Effect of Fe on *N. maritimus'* specific growth rate (μ) in EDTA-buffered experiments wherein the bioavailable substrate is Fe´ (solid bars) and DFB buffered experiments wherein there is negligible Fe´ and all Fe is bound to DFB (FeDFB – open bars); effect of Fe^{2+} specific chelator, ferrozine (FZ) on specific growth rates of *N. maritimus* in these cultures (+ FZ). n.g. indicates no *N. maritimus* growth. Concentrations on x-axis indicate the available substrate (i.e., Fe´ or FeDFB). Error bars indicate standard deviation, n = 11. Copyright © 2019, Shafiee et al.

2.5 DISCUSSION

2.5.1 *N. maritimus* has an elevated K_s compared with marine phytoplankton driven by a reduced affinity for Fe′

In order to place our results into the context of the microbial community, we compared the Fe requirements of *N. maritimus* with published datasets of a range of environmentally important marine microorganisms (Figure 2.4). There are a great wealth of data surrounding the role of Fe on marine phytoplankton growth, motivated by the finding that Fe limits primary productivity in ~30% of the world's surface ocean (Martin & Fitzwater, 1988; Boyd et al. 2007). We compared the effect of [Fe′] on growth rate (including the half-saturation constant, K_s), the steady-state Fe′ uptake rate and critical cellular Fe:P quota (explained in Appendix I) between published phytoplankton, marine heterotrophic bacterial datasets and *N. maritimus* data from this study.

We observed that *N. maritimus* displays the greatest half-saturation constant (K_s) for Fe′ amongst the organisms assessed, despite not showing the highest critical cellular Fe quota (Figure 2.4). In phytoplankton and marine bacteria, the critical cellular Fe quota (the minimum cellular Fe demand/quota required to reach μ_{max} – Figure A1.5) is an important determinant in K_s as surface area normalised Fe′ uptake rate is remarkably consistent (Lis et al. 2015a). The similarity in uptake rate constants (k_{in}) across a range of taxonomically diverse phytoplankton and marine bacteria reflects the selective pressure placed on marine microorganisms to evolve efficient Fe-uptake systems in environments wherein Fe is chronically low (Hudson & Morel, 1990). This is evident in the genomes of phytoplankton and heterotrophic bacteria, which commonly encode Fe-specific membrane transport proteins (e.g. FeoA/B/C, AfuA, FTR1) in addition to general metal cation transporters (Morrissey & Bowler, 2012; Hogle et al. 2016). However, *N. maritimus* does not follow the observed proportionality in steady-state uptake rate

constants that have emerged from phytoplankton and bacteria data, displaying a reduced affinity for Fe′ relative to cell surface area (Figure 2.4; $p < 0.05$). Perhaps unsurprisingly, genes encoding Fe-specific membrane transport proteins identified in eukaryotes and prokaryotes are absent from the genome of *N. maritimus* (Walker et al. 2010). Instead, it appears that *N. maritimus* only has genes encoding generalist divalent cation transporters belonging to the Tro and ZIP ABC transporter families (Table A1.3; Nmar_0328, Nmar_0330, Nmar_0331, Nmar_0329, Nmar_1130, Nmar_1662). We therefore hypothesise that the high K_s of *N. maritimus* is driven by a reduced affinity for Fe′ due to a lack of Fe-specific metal uptake proteins and not by a distinctly elevated critical cellular Fe quota. The only marine AOA documented to have genes for Fe-specific membrane uptake proteins is *Candidatus* Nitrosopelagicus brevis str. CN25 (herein *Ca.* N. brevis) (Table A1.3 Metal transport systems encoded in marine AOA genomes), encoded by T478_0963. However, an initial search of the *Tara* metagenomic database (Figure A1.6, Figure A1.7), returns a greater number of *Thaumarcheotal* hits for genes homologous to the non-specific metal transporters found in *N. maritimus* over the Fe^{2+} specific transporters found in *Ca.* N. brevis. This suggests that *N. maritimus'* Fe-uptake dynamics may be representative of Fe-uptake processes among *in-situ* marine AOA.

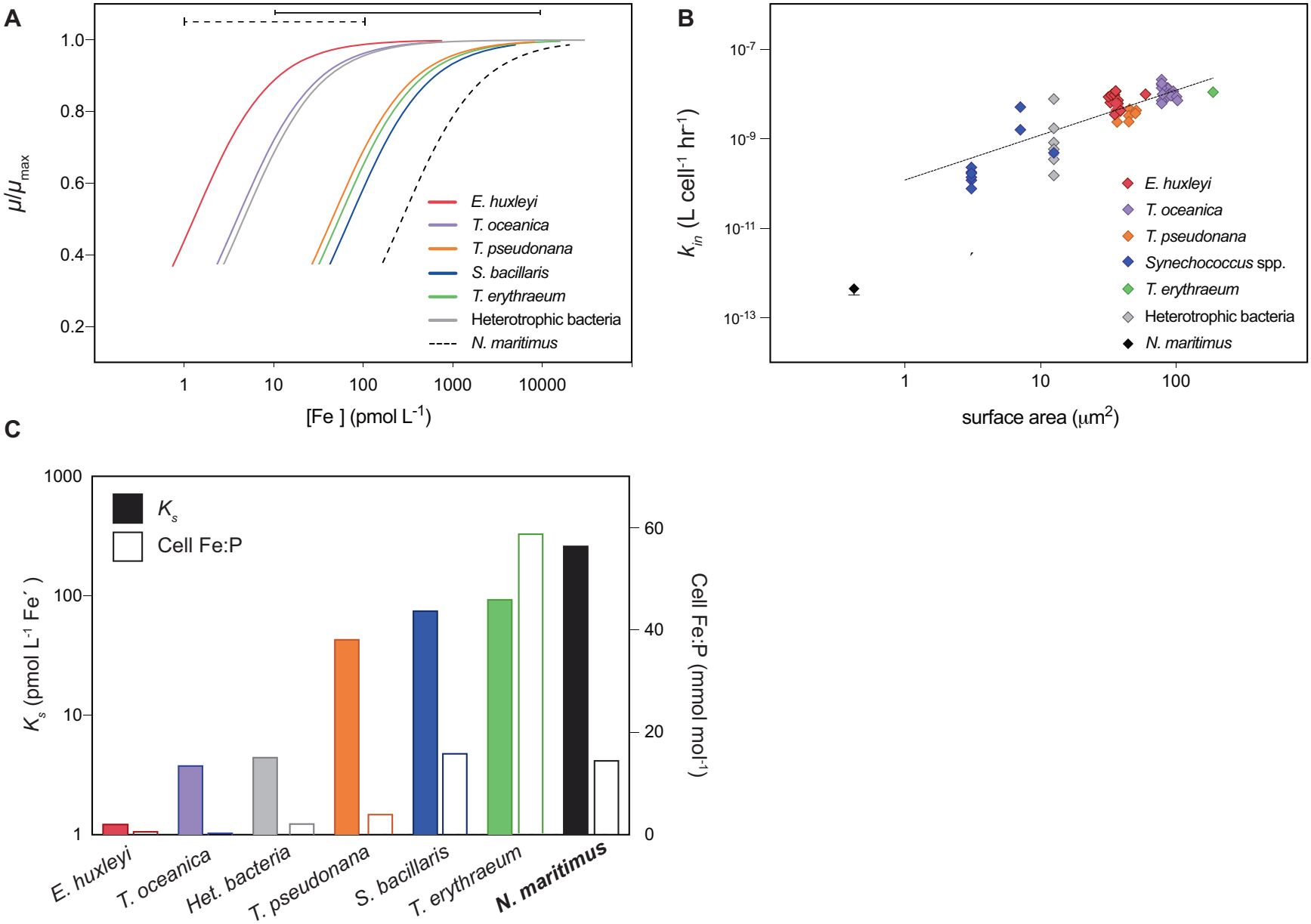

A
1.0
0.8
0.6
0.4
0.2
μ/μmax
1
10
100
1000
10000
[Fe] (pmol L-1)
E. huxleyi
T. oceanica
T. pseudonana
S. bacillaris
T. erythraeum
Heterotrophic bacteria
N. maritimus
B
10-7
10-9
10-11
10-13
kin (L cell-1 hr-1)
1
10
100
surface area (μm2)
E. huxleyi
T. oceanica
T. pseudonana
Synechococcus spp.
T. erythraeum
Heterotrophic bacteria
N. maritimus
C
1000
100
10
1
Ks (pmol L-1 Fe´)
Ks
Cell Fe:P
60
40
20
0
Cell Fe:P (mmol mol-1)
E. huxleyi
T. oceanica
Het. bacteria
T. pseudonana
S. bacillaris
T. erythraeum
N. maritimus

Figure 2.4 *N. maritimus* Fe requirements compared with cosmopolitan marine microorganisms

A) Monod curves fitted to compiled phytoplankton and heterotrophic bacteria (appreviated to het. bac in figure) data showing the effect of [Fe′] on relative growth rate (μ/μ_{max}) compared with data from this study (*N. maritimus*). The range of oceanic total [Fe] (solid line) and [Fe′] (dashed line) from the following studies are displayed on plot A: Cochlan, 2001; Pakulski et al. 1996; Johnson et al. 1997; Planquette et al. 2007; Klunder et al. 2012; Tagliabue et al. 2012; Fitzimmons et al. 2016; Rijkenberg et al. 2014 **B)** Fe′ steady-state uptake rate (k_{in} – L cell^{-1} hr^{-1}) of phytoplankton, heterotrophic bacteria and *N. maritimus* as a function of surface area. **C)** Half-saturation constants (K_s) based on Monod curves fitted to compiled data (solid bars) and critical cellular Fe:P as estimated from linear regression of relative growth rate (in Fe limited cells) against cellular Fe:P (open bars). Published datasets and references used can be found in Table A1.1 & Table A1.2. Copyright © 2019, Shafiee et al.

2.5.2 Fe requirement of *N. maritimus*

Our data compilation indicates that *Synechococcus bacillaris* and *Trichodesmium erythraeum*, have the greatest critical cellular Fe:P required to reach μ_{max} (Figure 2.4 and Figure A1.5). This is unsurprising in both cases: the N_2-fixation capacity of *T. erythraeum* drives a high Fe requirement due to the presence of Fe-rich nitrogenase proteins (Berman-Frank et al. 2007; Richier et al. 2012; Snow et al. 2015); the elevated Fe:P in *S. bacillaris* compared with eukaryotic diatoms and haptophytes can be explained by a higher proportion of Fe-rich photosystem I versus photosystem II (Melis, 1989; Strzepek & Harrison, 2004). Given that *N. maritimus* does not have photosynthetic or N_2 fixation capabilities, our observed Fe quota may be greater than initially expected. However, previously published proteomic analyses indicate that ferredoxin, an Fe-S protein encoded by the gene Nmar_0239, is the most highly expressed protein in exponentially growing *N. maritimus* cells (Qin et al. 2018). Analyses of *Ca.* N. brevis also revealed that Fe-S proteins were among the most highly expressed genes and proteins (Carini et al. 2018; Santoro et al. 2015). In both cases, Fe-S proteins are co-expressed with key ammonia monooxygenase modules implying that Fe-S proteins play a central role in the electron transport chain of *Thaumarchaeota* in addition to Cu as previously suggested (Walker et al. 2010; Amin et al. 2013). It is yet to be explored whether the presence of cytochromes in AOB, drives a similar, lower or greater Fe requirement in AOB — in doing so influencing the niche differentiation between AOB and AOA in the oceans, in addition to NH_4^+ affinity (Urakawa et al. 2014; Martens-Habbena, 2009).

2.5.3 Utilisation of siderophore-bound Fe through a reductive uptake pathway

In oceanic surface waters, > 99.9% of Fe is complexed by organic ligands (Gledhill & Buck, 2012), thereby rendering the concentration of the unchelated Fe ion (Fe′) to vanishingly low concentrations and creating a requirement for photochemical or redox mechanisms to maintain an adequate supply of Fe′ (Barbeau, 2006). The high [Fe′] required to see growth in our *N. maritimus* cultures (> 150 pmol L^{-1} Fe′), strongly suggests that *N. maritimus* is able to access another source of Fe in the oceans to fulfil its Fe requirements, or else AOA would unlikely be so widespread in the marine environment (Karner et al. 2001; Wuchter et al. 2006; Shiozaki et al. 2016; Santoro et al. 2017 — among many other studies which have quantified AOA abundances in the marine environment). We observed that while *N. maritimus* is not able to produce siderophores to enhance access to Fe under low [Fe′] (Figure 2.2), *N. maritimus* can grow using Fe bound to the strong hydroxamate siderophore, DFB, likely through a reductive uptake pathway as demonstrated in range of marine phytoplankton (Figure 2.3) (Lis et al. 2015b; Kranzler et al. 2011) or an alternative yet unknown uptake pathway. The use of a reductive Fe-uptake pathway (for both EDTA and DFB) agrees with bioinformatic evidence showing that *N. maritimus* only has metal uptake proteins capable of divalent cation transport across the inner membrane (Table A1.3), necessitating the reduction of ferric Fe-complexes before they can be imported into the cell. As our experiments were performed in the dark, we can exclude the possibility of abiotic photoreduction of organic chelates as a source of Fe^{2+} to divalent uptake pathways and can be confident that *N. maritimus* is actively reducing the Fe-organic complex.

Ferric reductases present in phytoplankton have been characterised (Lis et al. 2015b; Kranzler et al. 2011), however to date only one archaeal ferric reductase, from *Archaeoglobus fulgidus,* has been isolated and characterized (Vadas et al. 1999). The

ferric reductase responsible for reducing ferric chelates before uptake across the inner membrane has not yet been identified in *N. maritimus*. To identify candidate ferric-reductase proteins, we performed a BLASTp search of all known ferric-chelate reductases (prokaryotic and eukaryotic) against the *N. maritimus* genome (see Appendix I and Table A1.4**).** Our search highlighted one candidate gene, Nmar_0180, which returned a significant *E* value (*E* value threshold defined as 10^{-25}) and high bit score. Nmar_0180 encodes an NADP oxidoreductase F_{420}-dependent coenzyme (Table A1.5), which shows significant sequence homology with proteins that have ferric-chelate reductase (NADPH) capability identified from two archaea, *Halobacterium salinarum* and *Methanocaldococcus jannaschii* (GO: 0052851). Further work isolating and characterizing the activity of the protein encoded by Nmar_0180 is required in order to ascertain whether this protein is responsible for reducing Fe^{3+} before uptake by divalent metal transporters.

2.5.4 Surface water nitrification

Several studies have attributed the low nitrification rates in surface waters to competition with marine phytoplankton for NH_4^+ (Ward, 2008; Smith et al. 2014; Urakawa et al. 2014; Martens-Habbena et al. 2009) suggesting that it is only when phytoplankton become light limited below the euphotic zone that this competition is removed. Although this is generally supported by coupled depth profiles of organic matter remineralisation (which liberates NH_4^+) and nitrification rates (Santoro et al. 2013; Santoro et al. 2017; Shiozaki et al. 2016), rates of nitrification are significantly variable in surface waters (Yool et al. 2007) and do not always relate to NH_4^+ availability and AOA abundance. For example, Smith and colleagues (2014) showed that even when there is ample substrate and low phytoplankton abundance, only a small fraction of the NH_4^+ pool is oxidised, suggesting that an additional factor controls nitrification in surface waters.

The reduced affinity of *N. maritimus* for both DFB and unchelated Fe compared with marine phytoplankton and heterotrophic bacteria (Figure 2.4) suggests that AOA are also uncompetitive for Fe in the euphotic zone providing a plausible additional factor which limits AOA growth in surface waters. Enhanced nitrification rates have been observed in oceanic surface waters during natural Fe fertilisation events in the Southern Ocean (Cavagna et al. 2015; Fripiat et al. 2015). Whether this is driven by an increased supply of Fe remains an interesting avenue to be explored in light of our experimental results.

Although our siderophore uptake experiments were only performed with DFB, we hypothesise that the potential reductive uptake strategy of *N. maritimus* may confer *N. maritimus* with the ability to access other forms of chelated Fe. Fe reductases identified in other marine microorganisms (both prokaryotes and eukaryotes) have been shown to be 'generalist', being able to reduce a wide range of Fe-chelates (Kranzler et al. 2011; Lis et al. 2015b). As *N. maritimus* is able to reduce FeDFB, which is a hexadentate siderophore forming a very stable octahedral coordination, it is plausible that *N. maritimus* is also able to reduce weaker bound Fe-chelates with a greater reducing potential, such as exopolysaccharides and humic acids (Lis et al. 2015b). However, this remains to be experimentally explored as other factors — such as the ligand charge — are important determinants in the ability of a ferric reductase to reduce Fe-chelates (Lis et al. 2015b). The nature of the Fe reductase that *N. maritimus* utilises may also clarify why *N. maritimus* has a lower affinity for FeDFB compared to other marine microorganisms (Figure A1.8), ultimately shedding light on the fundamental driving factors behind the reduced competitiveness of *N. maritimus* in the euphotic zone.

2.5.5 Below the euphotic zone

Despite several observations of nitrification in surface waters (Yool et al. 2007), maximum rates of nitrification and abundances of AOA are repeatedly observed at the base of the euphotic zone (Karner et al. 2001; Santoro et al. 2013; Church et al. 2010). As described previously, this is often attributed to an enhanced supply of NH_4^+ in association with remineralising organic matter (Ward, 2008; Santoro et al. 2017) and the alleviation of phytoplankton competition. However, additions of the trace metal chelator TETA in the equatorial Pacific caused a reduction in nitrification rates by up to 23% between 150m – 300m depth (Santoro et al. 2017), implicating a key role for trace metals in shaping the distribution of AOA and nitrification rates below the euphotic zone. As phytoplankton become light-limited with increasing depth, AOA competition with phytoplankton for Fe would be alleviated in a similar way that has been suggested for NH_4^+ (Ward, 2008; Smith et al. 2014). Marine heterotrophic bacteria also decline in abundance at the base of the euphotic zone (Bundy et al. 2018; Karner et al. 2001; Campbell et al. 1997) likely driven by the reduction in dissolved organic carbon (DOC) at this depth which numerous studies have shown to be limiting to heterotrophic bacterial growth (Kirchman et al. 1990; Van Wambeke et al. 2008; Eiler et al. 2003; Kirchman, 1994). Fe additions alone have not been shown to enhance heterotrophic bacterial growth (Kirchman et al. 2000; Church et al. 2000) or have only been shown to enhance growth through an indirect effect on phytoplankton DOC production (Kirchman, 1994; Kirchman et al. 2000; Church et al. 2000; Cochlan, 2001; Pakulski et al. 1996). Taken together this suggests that it is unlikely that heterotrophic bacteria compete with AOA for Fe at the base of the euphotic zone. Reduction in Fe uptake by both phytoplankton and bacterial communities would enable AOA relatively uncontested access to Fe at the base of the euphotic zone. We speculate that such a niche may provide AOA with sufficient Fe to reach its metabolic demands despite having relatively low affinity Fe-uptake pathways. Moreover, the reduced

competition for Fe comes with a reduced evolutionary pressure to improve Fe-uptake pathways and so goes some way to explaining why *N. maritimus* appears to be a poor competitor for Fe at the biochemical level.

2.6 CONCLUSION

Our work is the first to examine the role of Fe in *Thaumarchaeota* growth, providing evidence that the marine ammonia-oxidising archaeon *Nitrosopumilus maritimus* has the highest half-saturation constant for Fe′ of any microorganism examined to date. We showed that whilst unable to synthesise siderophores, *N. maritimus* is able to access Fe bound to the organic siderophore DFB, and likely employs a reductive uptake pathway as part of its Fe acquisition strategy.

Our work presents an additional explanation as to why nitrification rates are often lowest in surface waters and greatest at the base of the euphotic zone (Ward, 2008; Santoro et al. 2013; Santoro et al. 2017). This provides greater depth to our current understanding of AOA distribution which currently focuses largely on NH_4^+ availability (Martens-Habbena et al. 2009). We suggest that AOA are potentially outcompeted for Fe in surface waters by phytoplankton and heterotrophic bacteria which have a greater affinity for important Fe substrates, supporting findings of previous work indicating that other factors besides NH_4^+ availability regulate nitrification rates in surface waters (Merbt et al. 2012; Tolar et al. 2016; Smith et al. 2014). We suggest that at the base of the euphotic zone, where phytoplankton and heterotrophic bacteria are limited by other factors (light and DOC), AOA are able to proliferate leading to the highest observed rates of nitrification. The curious lack of specificity in AOA Fe-uptake systems — in contrast with phytoplankton and marine bacteria (Morrissey & Bowler, 2012) — also agrees with the growth of AOA in an environment wherein there is reduced competition for Fe, such as the base of the euphotic zone.

Future research should focus on examining Fe-uptake dynamics in additional species of marine AOA, to develop a more encompassing view of marine AOA ecophysiology

which is not purely based on the cultivation results of one marine AOA isolate. Additionally, future work should identify the ferric reductase responsible for archaeal Fe uptake and determine the proteins driving the Fe demand of *N. maritimus* at the genomic and proteomic level. Furthermore, our laboratory experiments should be corroborated with ship-board incubation experiments to determine whether AOA are Fe limited, starting in regions of persistent Fe scarcity, such as the Southern Ocean.

2.7 STATEMENT OF AUTHORSHIP

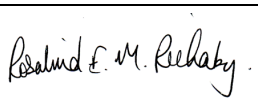
Title of Paper	Iron requirements and uptake strategies of the globally abundant marine ammonia-oxidising archaeon, *Nitrosopumilus maritimus* SCM1
Publication Status	✓ **Published** □ Accepted for Publication □ Submitted for Publication written in a manuscript style □ Unpublished and unsubmitted work
Publication Details	Shafiee, R. T., Snow, J. T., Zhang, Q., & Rickaby, R. E. (2019). Iron requirements and uptake strategies of the globally abundant marine ammonia-oxidising archaeon, Nitrosopumilus maritimus SCM1. *The ISME Journal*, *13*(9), 2295-2305.

Student Confirmation

Student Name:	Roxana T Shafiee	
Contribution to the Paper	• Conceived idea (in cooperation with RR, JS) • Made trace metal clean culture media and prepared all acid-cleaned culture apparatus. • Cultured AOA under a range of Fe concentrations, generating a dose-response curve • Performed iron rescue experiments, siderophore experiments (including preconcentration onto columns) and reduction experiments • Harvested cells for ICP-MS analysis, performed ICP-MS analysis (with QZ) and analysed ICP-MS data, calculated Fe:P quotas • Calculated steady-state uptake rates • Prepared cells for SEM analysis, performed SEM imaging • Prepared cells for flow cytometry, performed flow cytometry imaging and analysed data • Performed analysis of *Tara* oceans dataset • Performed blast analysis for potential ferric reductases • Compiled Fe physiology data from phytoplankton/heterotrophic bacteria studies • Performed statistical analyses • Made all paper figures/graphs • Discussed/interpretated broad scale implications of results (with JS and RR) • Wrote and revised manuscript in response to reviewers' comments.	
Signature:		**Date:** 21/05/2021

Supervisor Confirmation

By signing the Statement of Authorship, you are certifying that the candidate made a substantial contribution to the publication, and that the description described above is accurate.

Supervisor name:	Professor Rosalind Rickaby	
Signature:		**Date:** 21/05/2021

3 PROTEOMIC RESPONSE OF THE MARINE AMMONIA-OXIDISING THAUMARCHAEON, *NITROSOPUMILUS MARITIMUS* TO IRON LIMITATION REVEALS STRATEGIES TO COMPENSATE FOR NUTRIENT SCARCITY

This chapter examines the underpinning proteomic response to Fe limitation of the marine AOA isolate, *Nitrosopumilus maritimus* strain SCM1, following on from the physiological effect of Fe limitation demonstrated in Chapter 2. The objective of this chapter is to uncover the biochemical level strategies which allow AOA to survive Fe scarcity and how these compare to the transcriptomic and proteomic responses to other forms of stress and limitation. This fits into the overarching aim of the thesis to examine how trace metal availability plays into the niche separation of marine AOA and AOB, by outlining the potential mechanisms employed by AOA which contribute to their global success in the oceans and the vertical space they occupy in the water column.

This chapter is a reprint of material as it appears in Environmental Microbiology (2021, doi: 10.1111/1462-2920.15491), co-authored by Dr. Joseph Snow, Dr Qiong Zhang, Dr Svenja Hester and Professor Rosalind Rickaby. All supporting material is located in Appendix II.

3.1 ABSTRACT

Dissolved iron (Fe) is vanishingly low in the oceans, with ecological success conferred to microorganisms that can restructure their biochemistry to maintain high growth rates during Fe scarcity. Chemolithoautotrophic ammonia-oxidising archaea (AOA) are highly abundant in the oceans, constituting ~30% of cells below the euphotic zone. Here we examine the proteomic response of the AOA isolate *Nitrosopumilus maritimus* to growth-limiting Fe concentrations. Under Fe limitation, we observed a significant reduction in the intensity of Fe-dense ferredoxins associated with respiratory complex I whilst

complex III and IV proteins with more central roles in the electron transport chain remained unchanged. We concomitantly observed an increase in the intensity of Fe-free functional alternatives such as flavodoxin and plastocyanin, thioredoxin and alkyl hydroperoxide which are known to mediate electron transport and reactive oxygen species detoxification, respectively. Under Fe limitation, we found a marked increase in the intensity of the ABC phosphonate transport system (Phn), highlighting an intriguing link between Fe and P cycling in *N. maritimus*. We hypothesise that an elevated uptake of exogenous phosphonates under Fe limitation may either supplement *N. maritimus*' endogenous methylphosphonate biosynthesis pathway — which requires Fe — or enhance the production of phosphonate-containing exopolysaccharides known to efficiently bind environmental Fe.

3.2 INTRODUCTION

Ammonia-oxidising archaea (AOA) occupy a diverse array of ecosystems from hot springs to the oligotrophic open ocean. All cultivated AOA, recently placed into the updated class of *Nitrososphaeria* within the phylum *Thermoproteota* (Parks et al. 2020; Rinke et al. 2020) perform the first step of nitrification, the central component of the biogeochemical nitrogen (N) cycle, by oxidising ammonium (NH_4^+) to nitrite (NO_2^-). In the oceans, surface water nitrification can account for up to 30% of phytoplankton N nutrition (Yool et al. 2007) and provides an oxidised N niche for the large microphytoplankton (such as diatoms) that drive greater carbon export to the deep ocean relative to picophytoplankton such as cyanobacteria (Fawcett et al. 2011; Berg et al. 2003; Glibert et al. 2016). Marine AOA constitute up to 30% of total prokaryotic cells below the euphotic zone (Karner et al. 2001) and as such contribute a major fraction of gene copies and transcripts in marine metagenomes and metatranscriptomes (Hollibaugh et al. 2011). Marine AOA also play a role in major biogeochemical cycles through their

contribution to the production of nitrous oxide (N_2O, Freing et al. 2012; Santoro & Casciotti, 2011), methane (Metcalf et al. 2012), and cobalamin (Doxey et al. 2015; Heal et al. 2017).

The success of marine AOA is owed to adaptations which make these microorganisms well suited to the inhospitable open ocean wherein nutrient fluxes are low. Large surface area to volume ratios (Könneke et al. 2005), a high affinity for NH_4^+ (Martens-Habbena et al. 2009), an energy efficient C-fixation pathway (Könneke et al. 2014) and streamlined genomes with a low proportion of non-coding DNA (Walker et al. 2010; Santoro et al. 2015) make marine AOA oligotrophic specialists or 'oligotrophs'. In ~30% of surface oceans, low concentrations of dissolved iron (Fe) limit the growth of marine phytoplankton (Moore et al. 2013), but the role of Fe in modulating the growth of non-photosynthetic but environmentally important microbial groups has traditionally received much less attention. Recently we demonstrated that the model AOA isolate *Nitrosopumilus maritimus* strain SCM1, despite possessing a unique Cu-centric biochemistry compared to its ammonia-oxidising bacterial counterparts (Walker et al. 2010; Amin et al. 2013; Shafiee et al. 2021a — Chapter four), requires a greater concentration of unchelated Fe (Fe′) for growth than many cosmopolitan marine microorganisms (Shafiee et al. 2019 — Chapter two). A greater Fe requirement for growth relative to other marine microorganisms suggests that AOA must occupy an Fe-rich niche, and indeed aligns with observations of AOA maxima at the base of the euphotic zone (Santoro et al. 2013; Shiozaki et al. 2016). At this depth, Fe supply is great due to the combined effect of a decrease in competition for Fe (as phytoplankton become light limited) and Fe remineralisation from sinking organic matter. Fe fluxes from remineralisation can be episodic, depending heavily on levels of surface productivity and as such AOA may undergo prolonged periods of Fe starvation between nutrient pulses.

Marine microorganisms have evolved a number of strategies to survive Fe scarcity including: a reduction in Fe demand by downregulating the expression of Fe-binding proteins (retrenchment); replacing Fe-dense proteins with Fe-free substitutes (La Roche et al. 1996; Erdner et al. 1999; Snow et al. 2015); producing Fe-chelating compounds to enhance access to extracellular Fe (Boiteau et al. 2016) or increasing the transcription or affinity of membrane transporter proteins (Kustka et al. 2007; Allen et al. 2008; Cohen et al. 2018; Maldonado et al. 2006). The biochemical strategies implemented under Fe scarcity can be gleaned from the change in protein abundance (proteome) which acts as the basis of developing biomolecular tools to detect Fe limitation in vast expanses of mixed microbial communities *in situ*. For example, the phytoplankton Fe deficiency induced protein A (IdiA) involved in cellular Fe scavenging has been used as a marker for Fe stress in open ocean field populations (Webb et al. 2001; Saito et al. 2014; Chappell et al. 2015). The application of proteomic biomarkers provides a powerful alternative to traditional nutrient amendment experiments —which often alter community composition and do not necessarily capture the multi-complexed nature of stressors — which can be applied to wide geographic regions.

Here we examine the proteomic response of the model marine AOA isolate, *Nitrosopumilus maritimus* strain SCM1 (herein referred to as *N. maritimus*) to Fe limitation. We present the label-free quantitative intensity profiles of *N. maritimus* under Fe-limited and Fe-replete growth, thereby gaining important insight into the potential mechanisms adopted by AOA to navigate Fe scarcity.

3.3 EXPERIMENTAL PROCEDURES

3.3.1 *Nitrosopumilus maritimus* cultures and growth media

Polycarbonate culture vessels and culturing apparatus were acid cleaned (10 % HCl v/v, 24 hours) and UV sterilised prior to use. Triplicate cultures of *Nitrosopumilus maritimus* strain SCM1 (herein referred to as *N. maritimus*), were grown in modified SCM medium (Könneke et al. 2005) buffered with HEPES at pH 7.5 and maintained at 28 °C in the dark. Basal salt medium and macronutrients were treated with Chelex 100 chelating ion exchange resin (BioRad, Watford, UK) to remove trace metal contaminants (Price et al. 1989) and passed through an acid-washed (10% HCl as before) 0.1 µm polycarbonate filter to sterilise in a trace metal-free clean laboratory. *N. maritimus* was cultured at inorganic Fe concentrations ([Fe′]) previously shown to be limiting (250 pmol L^{-1} Fe′) and replete (1050 pmol L^{-1} Fe′) to growth (Shafiee et al. 2019 — Chapter two), but without promoting excess Fe storage. Ethylenediamine tetraacetic acid (EDTA; Merck, Darmstadt, Germany) (final concentration 12 µmol L^{-1}) was used to buffer Fe and other trace metals in cultures; [Fe′] was controlled by varying the addition of $FeCl_3$ from filter-sterilised concentrated stocks made using > 99.999% trace metal basis salts (Sigma-Aldrich, UK). [Fe′] in cultures was calculated using Visual Minteq software (Gustafsson et al. 2010), including background Fe contamination of 50 nmol L^{-1} from basal SCM medium with macronutrients and vitamins but without added trace metals — this was determined using inductively coupled plasma mass spectrometry (ICP-MS) as described by Zhang et al. (2018). Cultures were acclimated to limiting and replete [Fe′] by transferring cultures consecutively into new media until specific growth rates (μ) did not vary with statistical significance (ANOVA, $p < 0.05$). Growth was determined by measuring concentrations of nitrite ([NO_2^-]) spectrophotometrically over time (Griess, 1879), which correlates with cell counts even at low [Fe′] (Shafiee et al. 2019 — Chapter

two). Specific growth rate (d^{-1}) was calculated over the linear phase of semi-log plots of NO_2^- concentration over time. Differences in specific growth rate (μ) between 250 and 1050 pmol L^{-1} Fe′ treatments were tested for statistical significance using a two-tailed Student's *T* test in Minitab software (version 19.2020.2.0).

3.3.2 Cellular Fe and P quota

All samples and reagents were processed using trace metal clean techniques and in acid-washed plasticware (10% HCl v/v, 24 hours) in a clean laboratory prior to trace element analysis. *N. maritimus* cells cultured in two-litre triplicates at 250 and 1050 pmol L^{-1} Fe′, were harvested in mid-exponential phase by centrifugation at 5000 × g for 40 minutes at 4°C. Cell pellets of each replicate were divided into sub-samples for further trace metal analysis and proteomic analysis (cells for protein extraction were stored at -80 °C prior to protein extraction). For trace metal analysis, cell pellets were washed three times with Chelex-treated SCM basal salt medium, which has shown to be effective in removing weakly bound surface metals (Shafiee et al. 2019 — Chapter two; Zhang et al. 2018). Cells were digested in acid-cleaned Teflon as follows: refluxing at 100 °C with 16N quartz distilled (q.d.) HNO_3 (produced in-house) and H_2O_2 (ROMIL UpA™, Cambridge, UK) in a ratio of 3:2 overnight. The liquid was then allowed to evaporate to dryness and 2% q.d. HNO_3 was added to reflux for an hour to resuspend the dried samples. ^{56}Fe and ^{31}P concentrations were determined using a Quadrupole ICP-MS Perkin Elmer NexION 350 with Elemental Scientific Flow Injection Auto-sampler (FIAS) in a method optimised for high salt matrixes (Zhang et al. 2018). Per cell Fe quotas were calculated based on the relationship between NO_2^- and cell counts delineated in Shafiee et al. (2019)/Chapter two.

3.3.3 Protein extraction

Prior to protein analysis frozen cell pellets were thawed on ice, then lysed by sonication in 10 × 10 s bursts (Hielscher UP200S ultrasonic processor, 70% amplitude) in 1 ml of 0.5% SDS/0.5% Triton extraction buffer (on ice). A 0.5% SDS/0.5% Triton extraction buffer (in a base of 20 mM Tris-Cl, pH 8) was predetermined to be the most effective detergent ratio for protein extraction from a range of buffer combinations in preliminary extraction experiments using *N. maritimus* cells (Figure A2.1). A pierce BCA protein assay kit (Thermo Fisher Scientific, UK) was used to determine protein concentration following extraction, using the same matrix as the protein extraction buffer. Protein concentration in extracts ranged between 0.6 µg/µl in Fe-limited samples to 1.42 µg/µl in Fe-replete cells. Forty ug of protein digest from each biological replicate was used for subsequent proteolytic digestion and detergent removal.

3.3.4 SP3 protocol

Proteolytic digestion and detergent removal from the cell lysate were performed using a single-pot, solid-phase-enhanced sample preparation protocol (Hughes et al. 2019). Proteins in extraction buffer were denatured in 8 M urea (prepared in 100 mM ammonium bicarbonate buffer) at room temperature (RT) for 30 minutes. Disulphide bridges were reduced with Bond-Breaker™ TCEP Solution (Thermo Scientific) at a final concentration of 10 mM at RT for 30 minutes, followed by addition of freshly prepared 2-chloroacetamide (in 100 mM ammonium bicarbonate buffer – final concentration 50 mM) at RT for 30 minutes in the dark. Protein sample was added to 100 ug of prepared Sera-Mag™ SpeedBeads™ Carboxylate-Modified Magnetic Particles (Sigma-Aldrich). In brief, magnetic particles were prepared by forming a slurry with HPLC grade Milli-Q water (bead to Milli-Q ratio of 1:4), allowing particles to settle on the magnetic rack and removing supernatant. Rinsing was repeated three times. Acetonitrile (ACN, Sigma-Aldrich) was added to protein sample and prepared particles to 77% final ACN

concentration and incubated for 30 minutes at RT. Sample tubes were placed on a magnetic rack and incubated for a further 10 minutes at RT until the supernatant ran clear. To remove the detergent from the magnetic particles, a 2-step 70% ethanol wash followed by 1-step ACN wash was performed until bubbles were no longer visible on the magnetic particles. Magnetic particles were reconstituted in a trypsin to total protein digest ratio of 1:50 (from 0.2 µg/µl trypsin protease in acetic acid stock) overnight. The following day, sample tubes were added to the magnetic rack and peptide-containing supernatant was removed. Remaining peptides were removed from magnetic particles with 2% dimethyl sulfoxide (Sigma-Aldrich) in Milli-Q and incubated for 2 minutes at RT off the rack. Both supernatants were combined and acidified with 1 µl 10% formic acid (FA – reagent grade) prior to analysis on the mass spectrometer.

3.3.5 Proteomics methods components

Desalted samples were separated on an UltiMate 3000 UHPLC system (Thermo Fischer Scientific, UK) and electro-sprayed directly into a Q-Exactive Mass Spectrometer (Thermo Fischer Scientific) through an EASY-Spray nano-electrospray ion source (Thermo Fischer Scientific). The peptides were trapped on a C18 Acclaim™ PepMap™ 100 pre-column (300 µm i.d. × 5 mm, 100Å, Thermo Fisher Scientific) using solvent A (0.1% FA in Milli-Q) at a pressure of 500 bar. The peptides were separated on an in-house packed analytical column (75 µm i.d. × 50cm packed with ReproSil-Pur 120 C18-AQ, 1.9 µm, 120 Å, Dr.Maisch GmbH, Germany) using a linear gradient (length: 65 minutes, 15% to 35% solvent B (0.1% FA in ACN), flow rate: 200 nL/min). Data were acquired in a data-dependent mode (DDA). Full scan MS spectra were acquired in the Orbitrap (scan range 350–1500 m/z, resolution 70000, AGC target 3E6, maximum injection time 50 ms^{-1}). The 3 or 20 most intense peaks were selected for HCD fragmentation at 30% of normalised collision energy (resolution 17500, AGC target 5E4,

maximum injection time 120 ms^{-1}) with first fixed mass at 180 m/z. A Top 3 method (3 MS/MS collected per MS scan) was used for the label-free quantitative comparisons while a separate run was performed using a Top 20 method for qualitative analysis.

3.3.6 Data analysis pipeline

Identification of peptides was performed using MaxQuant computational proteomics platform (version 1.5.3.30) with the implemented Andromeda algorithm (Wiśniewski et al. 2013; Cox & Mann, 2008) by searching MS/MS spectra against a database consisting of the protein translation of the *N. maritimus* genome obtained from UniProt (uniprot.org/proteomes/UP000000792). Protein matches were filtered to an FDR of 1% at the PSM (peptide to spectrum match), peptide and protein levels. Measured intensities were converted to LFQ (label-free quantification) intensities using MaxLFQ algorithm (Cox et al. 2014) integrated within MaxQuant (using default parameters), using both unique and razor peptides for protein quantification. The MaxLFQ algorithm uses a non-linear optimisation model to normalise the peptide intensities thereby ensuring that profiles of LFQ intensities across samples accurately reflect the relative amounts of the proteins — taking into account all the peptide ratios for each protein measured in all pairwise comparisons of the different quantified samples and removing outliers (Cox et al. 2014). Protein LFQ intensities do not equate to protein abundance, and therefore intensities of the same protein across treatments are only robustly comparable — intensities of different proteins within treatments cannot be accurately compared. Mean LFQ intensities for Fe-limited and Fe-replete treatments were calculated from replicates and tested for significant differences using a Student's *T* test at an FDR-adjusted *p* value of 0.05 in Perseus software (version 1.5.1.6). All differentially intense proteins are listed in Table A2.1. No statistical analysis was performed for proteins which were absent or below the limit of detection, and instead a presence-absence response was assigned.

3.3.7 Biological function groups and Fe-containing proteins

Biological function categories (Table A2.1) were assigned to proteins using the Gene Ontology (GO database). Where GO terms were not available, we used the Kyoto Encyclopaedia of Genes and Genomes (KEGG; Kanehisa et al. 2007) reference pathways or InterPro to assign putative biological functions. In order to gain an insight into the effect of Fe limitation specifically on the Fe-containing proteome, we identified the Fe-containing proteins within the *N. maritimus* proteome. A full list of proteins encoded by the *N. maritimus* genome was downloaded from UniProt (proteome ID: UP000000792) which was subsequently submitted to the PHYRE2 protein fold recognition server to identify homologues for known protein structures (Kelley et al. 2015). Significant matches (> 95% confidence) were submitted to metalPDB (Putignano et al. 2018; Andreini et al. 2012) which models the 3D minimal functional sites surrounding metals. Trace metals were assigned if the search returned significant sequence similarity to metal-binding sites in other proteins (E value < 10^{-5}). This identification is underpinned by the assumption that the genome-predicted proteome of *N. maritimus* has been accurately annotated and that any archaeal proteins which are homologous to characterised bacterial Fe proteins also have similar Fe stoichiometry. By identifying homologues based on predicted 3D protein structures which are highly conserved, we have greater confidence that Fe stoichiometry will also be conserved.

3.4 RESULTS & DISCUSSION

3.4.1 Growth rates, cellular Fe quota and protein detection

Low concentrations of unchelated iron ([Fe′]) led to a 59% reduction in specific growth rate (μ) and a decline in the final nitrite (NO_2^-) concentration from 913 μmol L^{-1} to 185 μmol L^{-1} NO_2^-(Figure 3.1; Figure A2.2) between treatments. In Fe-replete *N. maritimus* cells we measured an intracellular-Fe quota of 1.1×10^{-10} μmol Fe $cell^{-1}$ ($\pm$ 4.2×10^{-11}) which reduced to 2.25×10^{-12} μmol Fe $cell^{-1}$ ($\pm$ 3.9×10^{-13}) in Fe-limited cells (Figure 3.1). Of the 1,795 predicted protein-encoding genes in the *N. maritimus* genome (www.jgi.doe.gov), 1,346 discrete proteins were detected in the Fe-replete proteome (74.9%) and 1,337 proteins in the Fe-limited proteome (74.5%) (at a 1% FDR). Biological replicates showed strong reproducibility with r^2 values exceeding 0.8 in all comparisons (Figure A2.3). The detected proteome coverage was greater or consistent with previous proteomic recovery of *N. maritimus* (68% in Bayer et al. 2019; 74% in Qin et al. 2018) and *Candidatus* Nitrosopelagicus brevis (~70% in Santoro et al. 2015) and supports the notion that AOA have streamlined genomes with a high proportion of predicted protein expression. Sixty-nine proteins showed a significant difference in label-free quantitation (LFQ) intensity between Fe treatments (FDR-adjusted p value < 0.05). All differential protein intensities discussed in this study are statistically significant at an FDR-adjusted p value < 0.05. Relative to the Fe-replete treatment, 34 proteins increased significantly in LFQ intensity and 35 decreased in intensity in the Fe-limited treatment. Three proteins that were detected in the Fe-limited proteome were absent in all replicates (or below L.O.D) of the Fe-replete proteome, whereas 12 proteins were detected in the Fe-replete proteome that were absent from all replicates of the Fe-limited proteome (Table A2.1). Proteins with predicted functions in the surface layer (S-layer; Nmar_1547), ammonia oxidation (Nmar_1102), carbon fixation (Nmar_0273), and genetic information

processing (Nmar_1034) showed the highest LFQ intensities in both Fe-limited and Fe-replete proteomes (Table 3.1).

3.4.2 Ammonia monooxygenase

Ammonia monooxygenase (AMO), the hallmark enzyme of ammonia-oxidising microorganisms, is comprised of three subunits: AmoA, B and C (Nmar_1500, Nmar_1503, Nmar_1502). Under Fe limitation, total AMO subunit LFQ intensity increased as a proportion of the total signal from 1.75% to 2.37% with AmoB among the top 10 most intense proteins in the Fe-limited proteome (Table 3.1). Additionally, we found that AmoA (Nmar_1500) intensity increased with statistical significance in Fe-limited treatments — suggesting that *N. maritimus*' core ammonia oxidation machinery remains intact even when Fe is scarce. This highlights that the availability of the AMO complex may not be the rate-limiting factor which leads to the observed decline in ammonia oxidation rate and μ when Fe′ is low (Figure 3.1, Figure A2.2). In contrast, energy and Cu limitation reduces the transcription of all AMO subunits (Qin et al. 2018; Reyes et al. 2020), apart from *amoC* which is preferentially retained under NH_4^+ starvation (Qin et al. 2018). The ostensible greater impact of Cu and NH_4^+ limitation on the AMO complex may be expected given the larger predicted Cu requirement of AMO (based on AMO homology to methane monooxygenase) and the fact NH_4^+ is required as its substrate: AmoC and AmoA putatively bind 7 Cu atoms collectively compared to AmoB which only binds 3 Fe atoms. However, it cannot be ruled out that transcriptional changes under Fe limitation are not apparent at the proteomic level due to differential rates of post-translational protein degradation. This potential is highlighted by the divergence in AMO subunit abundance between metatranscriptomic and metaproteomic analyses: marine *amoC* and *amoA* transcripts typically outnumber *amoB* transcripts in metatranscriptomes (Shi et al. 2011; Feike et al. 2012) but initial metaproteomic surveys

show that *Nitrosopumilus*-like AmoA and AmoB proteins are ~ three-fold more abundant and widespread compared with AmoC (Saunders et al. unpublished; Saito et al. 2020; Figure A2.4). This disparity highlights the importance of complementary proteomic and transcriptomic characterisation of AMO stoichiometry in future research.

Protein	GO Category	Protein description	LFQ intensity	% of Group	% of total
Fe-limited *N. maritimus* (250 pmol L^{-1} Fe′)					
Nmar_1547	S-layer, cell wall & membrane	Uncharacterized protein	1.9×10^{11}	76.1	19.0
Nmar_0875	ABC transporters	Phosphonate ABC transporter, periplasmic phosphonate-binding protein	5.2×10^{10}	74.1	5.3
Nmar_1034	Genetic information processing	Elongation factor 1-alpha	3.3×10^{10}	20.0	3.4
Nmar_0478	Uncharacterised protein	Uncharacterized protein	1.6×10^{10}	12.1	1.6
Nmar_1622	Carbon fixation	Alcohol dehydrogenase zinc-binding domain protein	1.4×10^{10}	19.8	1.4
Nmar_0331	Uncharacterised protein	ABC-3 protein	1.3×10^{10}	18.2	1.3
Nmar_0559	Metabolism (other)	Trans-sialidase	1.2×10^{10}	19.4	1.2
Nmar_0273	Carbon fixation	Carbamoyl-phosphate synthase L chain ATP-binding	1.1×10^{10}	15.8	1.1
Nmar_1503	Ammonia oxidation/assimilation/N-processing	Ammonia monooxygenase B (AMO)	1.1×10^{10}	9.6	1
Nmar_1102	Ammonia oxidation/assimilation/N-processing	Blue (Type 1) copper domain protein	1×10^{10}	9.3	1
Fe-replete *N. maritimus* (1050 pmol L^{-1} Fe′)					
Nmar_1547	S-layer, cell wall & membrane	Uncharacterized protein	2.2×10^{11}	88.5	21.8
Nmar_1034	Genetic information processing	Elongation factor 1-alpha	3.3×10^{10}	19.6	3.4
Nmar_1537	Ammonia oxidation/assimilation/N-processing	4Fe-4S ferredoxin iron-sulphur binding domain protein	2.7×10^{10}	19.1	2.6
Nmar_1622	Carbon fixation	Alcohol dehydrogenase zinc-binding domain protein	1.6×10^{10}	22.5	1.6
Nmar_0239	Ammonia oxidation/assimilation/N-processing	4Fe-4S ferredoxin iron-sulphur binding domain protein	1.3×10^{10}	9.4	1.3
Nmar_1691	Ammonia oxidation/assimilation/N-processing	ATP synthase alpha chain	1.1×10^{10}	8.0	1.1
Nmar_1102	Ammonia oxidation/assimilation/N-processing	Blue (Type 1) copper domain protein	1.1×10^{10}	7.5	1
Nmar_1577	Protein folding/Chaperones	Thermosome	1×10^{10}	17.8	1
Nmar_0273	Carbon fixation	Carbamoyl-phosphate synthase L chain ATP-binding	1×10^{10}	13.8	1
Nmar_1638	S-layer, cell wall & membrane	Uncharacterized protein	1×10^{10}	4.0	1

Table 3.1 Top 10 proteins based on LFQ spectral counts in Fe-replete and Fe-limited treatments

LFQ intensity refers to the label free quantitation intensity, % of group refers to the percentage that the intensity contributions relative to the total intensity in that biological functional group, % of total refers to the intensity relative to the total sum of intensities measured by all proteins in the treatment.

3.4.3 Ammonia oxidation and the electron transport chain

In Fe-replete treatments, Complex I proteins were among the most intensely detected proteins in the *N. maritimus* proteome (Table 3.1) and are also predicted to be the most Fe-dense based on our analysis of Fe-binding proteins in *N. maritimus*' genome-predicted proteome (Table A2.2). Complex I and putatively-associated ferredoxins require a predicted 16 atoms of Fe compared with AmoC, complex III and complex IV which we predict in total require only 11 Fe atoms (Table A2.2). Complex I is responsible for the generation of NAD(P)H — a reducing agent involved in numerous cellular processes including nutrient assimilation, biosynthesis, carbon fixation, and metabolism. In Fe-limited treatments, we observed a significant reduction in the intensity of complex I proteins and ferredoxins (Nmar_0279; Nmar_0284; Nmar_1765; Nmar_1537, Nmar_0239) but no change in the intensity of Fe-containing complexes III and IV or AmoC (Figure 3.2). Complex III and *amoC* transcripts were also retained in *N. maritimus* under energy and nutrient limitation (Qin et al. 2018), pointing to their crucial roles in generating a proton motive force and stabilising the AMO holoenzyme under resource limitation. Qin and colleagues (2018) also found ferredoxins (specifically Nmar_1765 and Nmar_0239) to be among the most downregulated genes under Cu and NH_4^+ limitation (Figure A2.5). This suggests that the eschewal of Fe-containing ferredoxins may be a general, rather than an Fe-specific limitation response (Table A2.3). This assumes that the reduced intensity of ferredoxins in our study is primarily underpinned by a downregulation of ferredoxin genes as opposed to differential protein degradation rates between Fe treatments. In Fe-limited treatments we also observed a significant increase in the LFQ intensity of riboflavin synthase (Nmar_1617), flavodoxin (Nmar_1356) and a putative Cu-binding plastocyanin-like protein (Nmar_0815) suggesting that when starved for Fe, *N. maritimus* may functionally replace ferredoxins

for Fe-free electron carriers as has been observed in numerous marine microorganisms under Fe limitation (Sepúlveda Cisternas et al. 2018; Snow et al. 2015; La Roche et al. 1996; Peers & Price, 2006). Both flavodoxin (Nmar_1356) and the Cu-binding plastocyanin-like protein (Nmar_0815) are downregulated in response to Cu-limitation in *N. maritimus* (Qin et al. 2018) thereby suggesting that these proteins may potentially form part of an Fe-specific limitation response (Figure A2.5).

Taken together, we posit that a reduction in Complex I ferredoxins and the potential substitution with Fe-free electron carriers, combined with the retention of Complex III and IV proteins, and AmoC presents a potential compensatory strategy designed to most efficiently reduce Fe demand while keeping energy production as intact as possible. A comparable compensatory strategy has been observed in cosmopolitan marine phytoplankton such as *Trichodesmium* (Shi et al. 2007; Snow et al. 2015). Yet despite such functional replacements there is still a significant decline in growth rate under low Fe (Figure 3.1) suggesting that such potential functional substitution is not perfect and/or that the rate of Fe uptake is still insufficient under low Fe′ to meet the lowered Fe demand — signalling *N. maritimus*' integral need for greater extracellular [Fe′] to maintain a high growth rate.

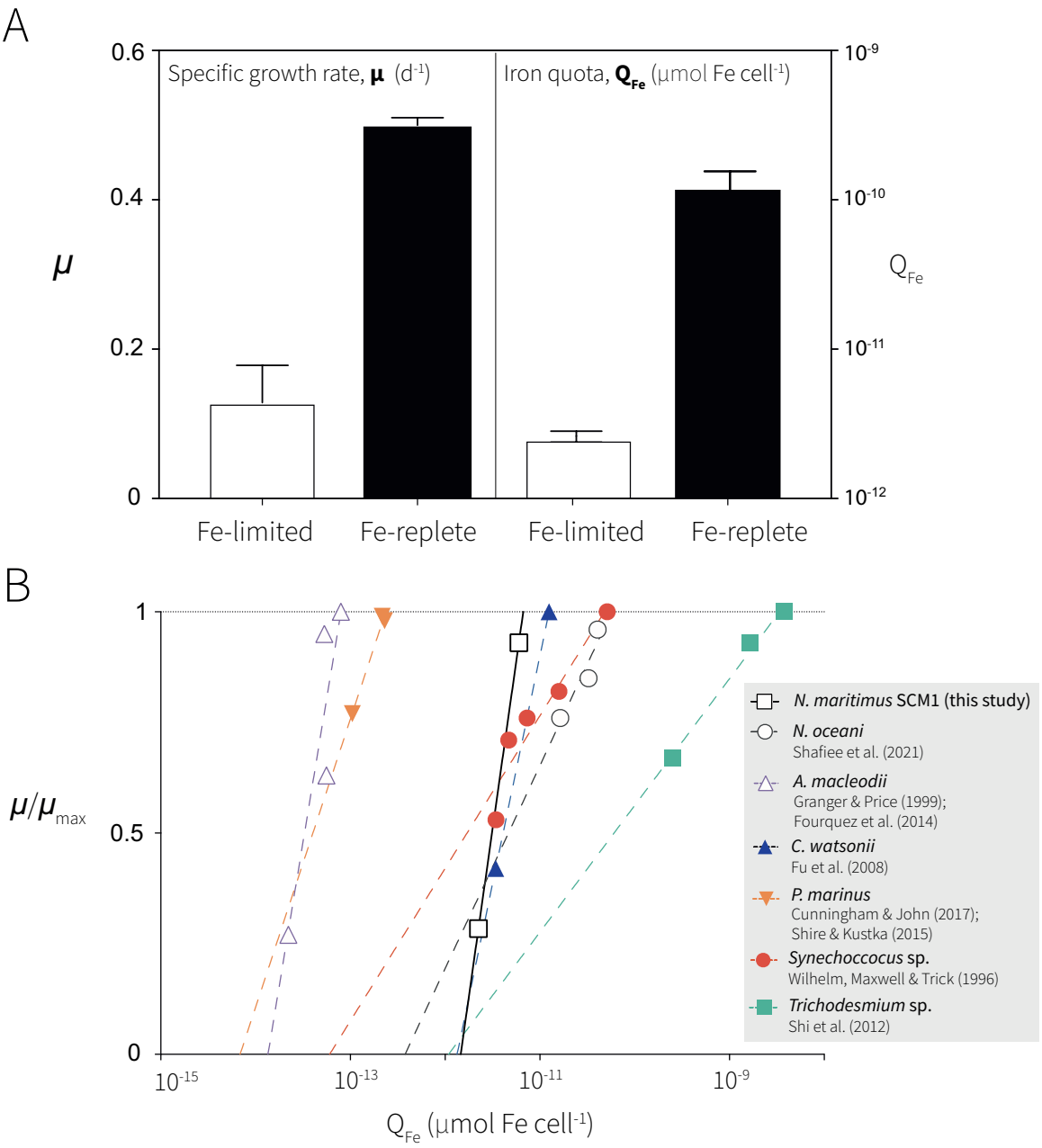


Figure 3.1 *N. maritimus* growth rate and intracellular Fe quota under Fe replete and deplete treatments

A) *Nitrosopumilus maritimus* strain SCM1 growth rate and cellular quota (Q_{Fe}) under Fe-replete and Fe-limited growth, corresponding to 250 and 1050 pmol L^{-1} Fe′. **B)** Relative growth rate (μ/μ_{max}) as a function of intracellular Fe quota (Q_{Fe}) in *N. maritimus* and other marine microorganisms (Shafiee et al. 2021a; Granger & Price, 1999; Fourquez et al. 2014; Fu et al. 2008; Cunningham & John, 2017; Shire & Kustka, 2015; Wilhelm, Maxwell & Trick, 1996; Shi et al. 2012). Copyright © 2021, Shafiee et al.

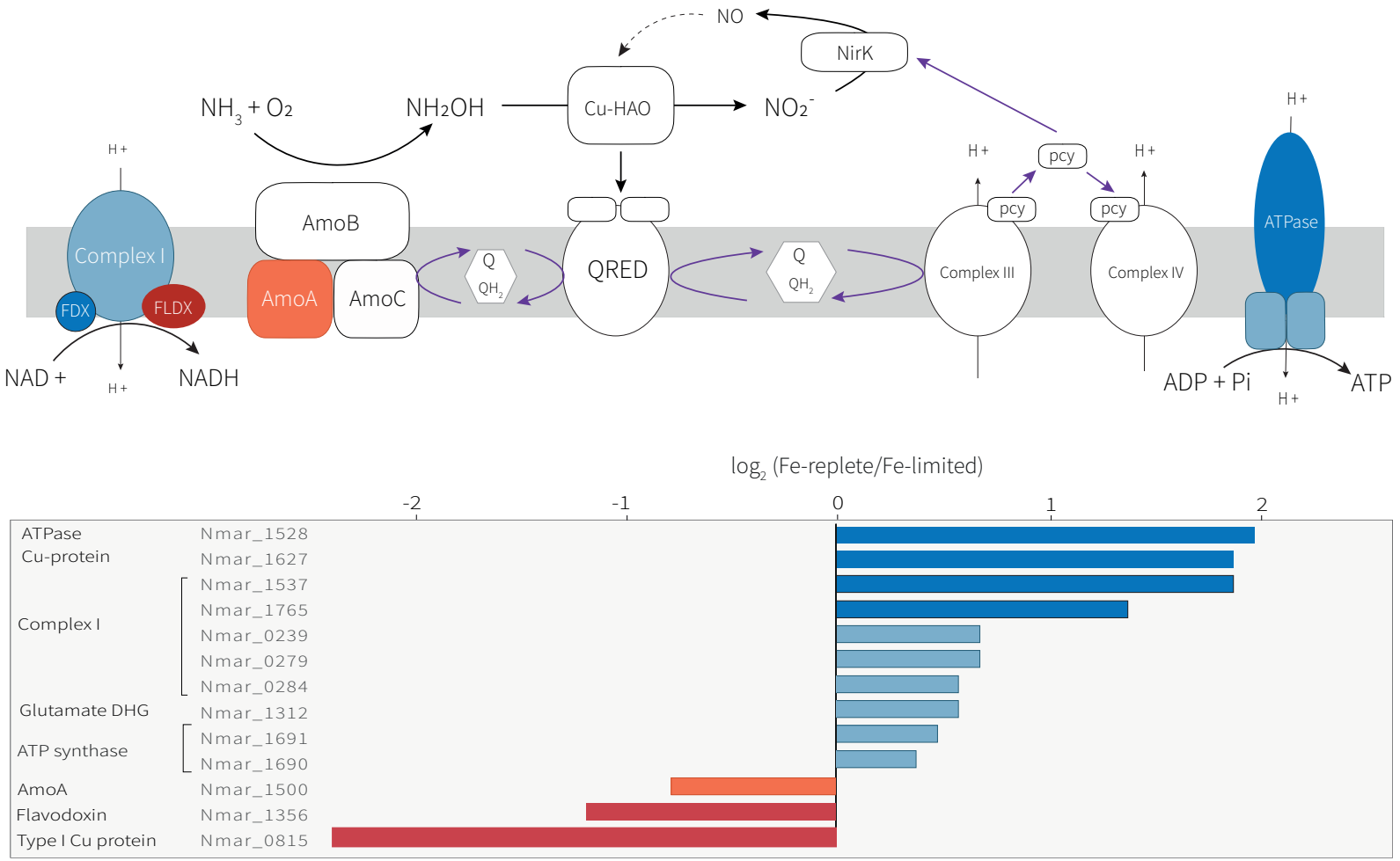


Figure 3.2 Significant intensity changes to proteins involved in ammonia oxidation under Fe limitation

Proteins involved in the electron transport chain of *N. maritimus*, with proteins showing significant $\log_2$-fold changes ($p < 0.05$) between Fe-replete and Fe-limited proteome shown in colour, corresponding to bar chart below. Abbreviations: pcy: plastocyanin; FDX: Ferredoxin; FLDX: Flavodoxin, QRED: quinone reductase. Purple arrows indicate possible electron flow. Copyright © 2021, Shafiee et al.

3.4.4 Carbon fixation, TCA cycle and biosynthesis

The HP/HB cycle adopted by *N. maritimus* to fix carbon contains only one predicted Fe-binding protein (Nmar_1110), which we did not find to change significantly in intensity between Fe treatments. In contrast, we found that several predicted Fe-containing and Fe-free proteins involved in the TCA cycle and biosynthesis processes changed significantly in intensity between Fe-treatments (expanded discussion below). Taken together, this supports the previous notion that Fe retrenchment targets the processes which are densest in their Fe use allowing *N. maritimus*' carbon fixing capacity to remain intact.

In Fe-limited treatments, we observed significant changes to the intensity of proteins involved in the TCA cycle and biosynthesis, indicating the presence of potential strategies to mitigate the effects of Fe depletion (Figure 3.3). The TCA cycle is central to metabolism — releasing stored energy through the oxidation of acetyl-CoA and providing essential intermediates for biosynthesis. In marine phytoplankton, TCA intermediates are estimated to account for one-third of the total Fe requirement (Raven, 1988) and must be substituted for Fe-free alternatives under low Fe (Cohen et al. 2018). Enzymes with Fe-containing and Fe-free variants include fumarate hydratases and fructose biphosphate aldolases (Horecker et al. 1972; Picaud et al. 2011). *N. maritimus* only has the genetic capability to produce the Fe-free variants of these enzymes indicating that the TCA cycle already has a parsimonious Fe demand irrespective of extracellular Fe. In Fe-limited treatments we observed a significant drop in the intensity of a ferredoxin (Nmar_0413) predicted to mediate the breakdown of pyruvate to acetyl-CoA — a key step in acetyl-CoA supply to the TCA cycle (Figure 3.3). Concurrently 4-hydroxy-2-oxovalerate aldolase (Nmar_0149), which supplies pyruvate to Nmar_0413 and Nmar_0414 from the breakdown of pentanoic acid, increased in intensity (Figure 3.3). Considered together, we

speculate that in order to compensate for the decline in ferredoxins under Fe limitation, *N. maritimus* may instead increase substrate supply (pyruvate) to the ferredoxins — thus saturating these enzymes with pyruvate and in doing so maintaining crucial acetyl-CoA supply to the TCA cycle under Fe limitation.

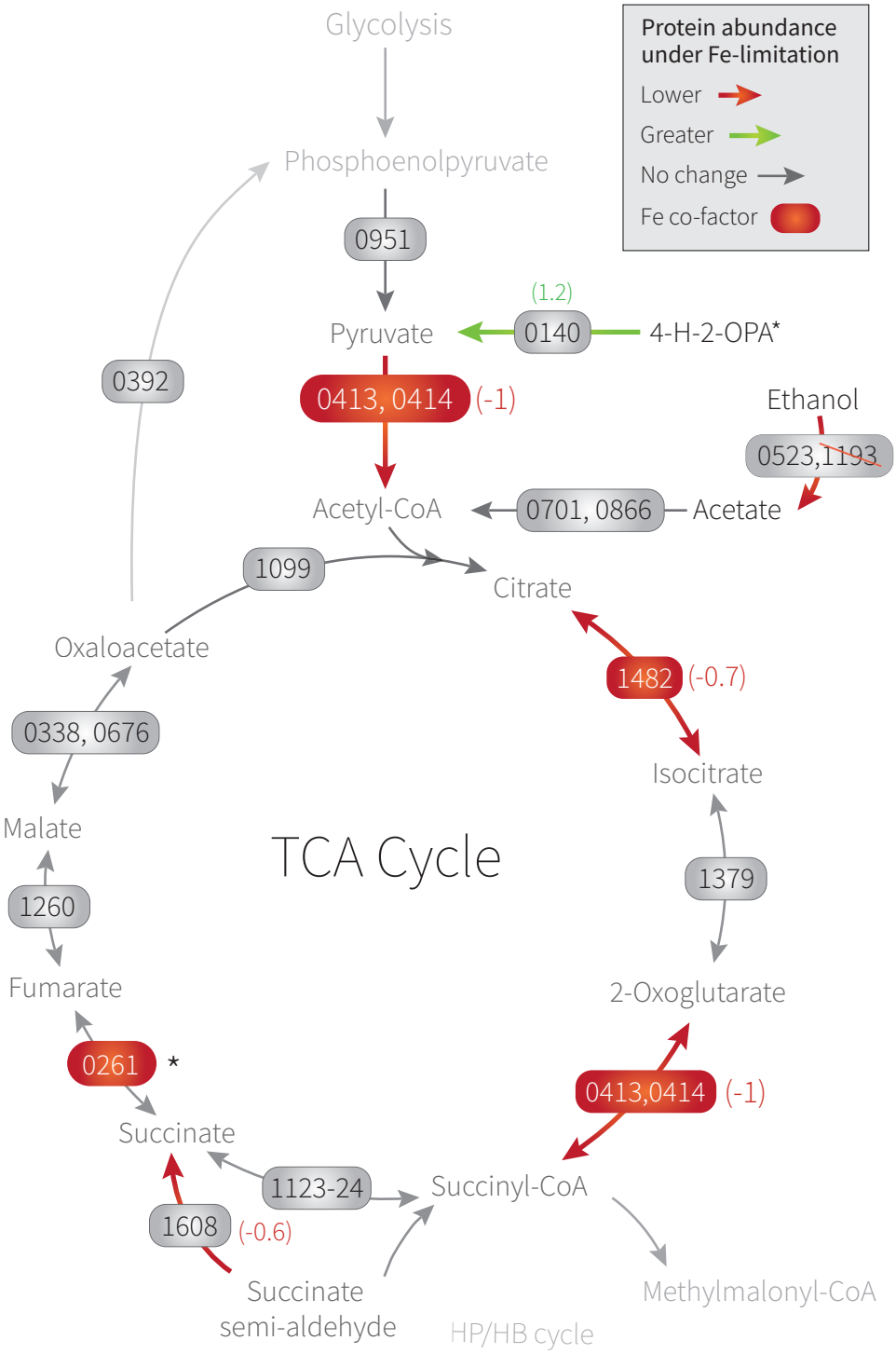


Figure 3.3 Significant intensity changes to proteins involved in the TCA cycle under Fe limitation

Tricarboxylic acid cycle (TCA) in *N. maritimus*. Protein names are shown without 'Nmar' prefix. Proteins showing a significant increase in abundance in Fe-limited treatments are indicated with a green arrow and those showing a significant decrease in abundance ($p < 0.05$) are indicated with a red arrow (For definition of significance refer to *Data analysis pipeline*). Log_2-fold changes are shown in brackets. Proteins in coloured in red are Fe-containing based on metalPDB analysis (see Section 3.3.7). Copyright © 2021, Shafiee et al.

3.4.5 Detoxification of reactive oxygen species

In addition to their role in ammonia oxidation and the TCA cycle, ferredoxins participate in cellular defence against oxidative stress (Krapp et al. 1997), signifying the potential for a reduced capacity of Fe-limited *N. maritimus* to deal with oxidative stress. Additionally, the breakdown of Fe-S proteins under Fe limitation has been shown to directly generate excess oxidative stress (Liochev & Fridovich, 1994; Keyer & Imlay, 1996; Jang & Imlay, 2010). In our study, the breakdown of Fe-S clusters is implied by a significant reduction in the intensity of both Fe-containing proteins throughout the cell and the Suf protein family which are responsible for Fe-S cluster biosynthesis and repair (Figure A2.6: Nmar_0516; Nmar_0496; Nmar_0495). The potential for increased oxidative stress in Fe-limited cells is suggested by a significant increase in Nmar_1386 intensity, a protein annotated as RadA (Figure A2.6), shown to be responsible for DNA damage repair across the archaeal domain (Seitz & Kowalczykowsk, 2000; Komori et al. 2000). RadA was also found to increase significantly in the proteomes of AOA exposed to hydrogen peroxide — H_2O_2 (Bayer et al. 2019). We observed a concomitant increase in the intensity of proteins homologous to the Fe-free detoxification proteins thioredoxin reductase (Nmar_0672) and alkyl hydroperoxide (Nmar_1252). This suggests that *N. maritimus* may be reconfiguring its detoxification mechanisms to Fe-free alternatives — a common strategy employed by Fe-limited microorganisms to mitigate enhanced oxidative stress (Holmes et al. 2005; Yingping et al. 2014). We also found that a protein belonging to the universal stress family of proteins, UspA (Nmar_1659) showed a significant 1.7 $\log_2$ fold increase in intensity in Fe-limited treatments (Figure A2.6). UspA proteins in *E. coli* play a role in defence against superoxide-generating agents and in cell growth retardation during stationary phase (Nachin et al. 2005; Nyström & Neidhardt, 1994). However, Bayer et al. (2019) found that UspA family proteins were almost

completely absent in cultures exposed to H_2O_2 in *N. maritimus,* increasing in abundance only when grown in co-culture with a heterotrophic bacterium or supplemented with catalase — suggesting that UspA is regulated by something other than general, cellular oxidative stress. As *uspA* (Nmar_1659) was found to be downregulated in response to Cu and NH_4^+ limitation by Qin et al. (2018), we postulate that this UspA family protein may function as an Fe-specific response protein although it's exact role in protecting against Fe-induced stress remains to be explored.

3.4.6 S-layer proteins

In both Fe treatments, Nmar_1547 shows the greatest LFQ intensity in the *N. maritimus* proteome, contributing 18.9–21.7% of all intensities (Table 3.1), consistent with previous work finding that surface layer (S-layer) proteins dominate expressed AOA proteomes (Qin et al. 2018; Bayer et al. 2019; Santoro et al. 2015). Nmar_1547 forms part of the distinctive S-layer of *N. maritimus* and other archaea (Urakawa et al. 2011; Sára and Sleytr, 2000; Santoro et al. 2015) and is a substantial proportion of environmental marine AOA metatranscriptomes and metaproteomes (Hollibaugh et al. 2011; Saunders et al. unpubl). The S-layer serves as the first selective barrier between the cell interior and the environment which includes interactions with proteins, nutrients and energy substrates (Rodrigues-Oliveira et al. 2017). The chemical properties of the S-layer proteins (SLP) are hypothesised to enhance *N. maritimus*' access to its energy substrate (NH_4^+) and Cu (Gorman-Lewis et al. 2014, 2019; Li et al. 2018). The key role played by the S-layer in nutrient and energy acquisition sheds clarity on why there is significant proteomic investment in S-layer biosynthesis. However, we did not observe a significant change in the intensity of detected SLP, signalling that the S-layer does not respond to changing Fe.

3.4.7 Fe-reductase activity and ABC transport

Spatially, following SLP, transmembrane proteins are the next selective barrier between the *N. maritimus* cell interior and external environment. In response to Fe limitation, microorganisms may implement numerous strategies to enhance access to extracellular Fe including altering the number or composition of transmembrane proteins, secreting compounds which solubilise inaccessible Fe, or increasing the activity of ferric reductases. The genome of *N. maritimus* has little diversity in metal transport proteins, consistent with characterised oligotrophs (Hogle et al. 2016) and further supports genome streamlining in AOA (Santoro et al. 2015). The majority of AOA isolates, including *N. maritimus*, only encode general cation transporters (Shafiee et al. 2019 — Chapter two; Walker et al. 2010; Amin et al. 2013) which were not found to change in intensity under Fe limitation (Figure 3.4). Physiological experiments indicate that *N. maritimus* reduces Fe^{3+} to Fe^{2+} prior to uptake (Shafiee et al. 2019 — Chapter two), but the ferric reductase protein responsible has yet to be identified. One of the only Fe-containing proteins to increase in intensity under Fe limitation was Nmar_0679, currently annotated as a haem and Fe-S binding sulphite reductase. Sulphite reductases have been shown to reduce a broad range of Fe-chelated substrates via a similar mechanism to NAD(P)H:flavin oxidoreductase (Coves et al. 1993). If Nmar_0679 is indeed responsible for the Fe-reductase activity in *N. maritimus*, its elevated intensity in response to Fe limitation may signal a potential strategy to increase the bioavailability of dissolved Fe to transmembrane uptake proteins.

In Fe-limited treatments, several components of the ABC phosphonate transporter (PhnCDE) increased significantly in LFQ intensity (Nmar_0250, Nmar_0874, Nmar_0875) or were only detected in Fe-limited treatments (Nmar_0876 – Figure 3.4). Further, a putative transcriptional regulator in the same operon as the phosphate pstSCAB

transport system (Nmar_0478) shows the greatest log_2 fold increase in intensity out of all proteins analysed in our study by an order of magnitude (Figure 3.4). Out of these proteins PhnD (Nmar_0875) and the putative transcriptional regulator of the phosphate pstSCAB transport system (Nmar_0478) show the greatest LFQ intensity in Fe-limited cultures, individually representing 5% and 1.5% of total signal, respectively (Table 3.1). Previous work has shown that *phnD* is downregulated under Cu limitation and NH_4^+ starvation in *N. maritimus* (Qin et al. 2018), and that Phn proteins decrease in abundance in numerous *Nitrosopumilus* strains upon exposure to H_2O_2 (Bayer et al. 2019). Therefore, we suggest that the significant increase in PhnD intensity observed in our study may be an Fe-specific limitation response (Figure A2.6; Table A2.1). Phosphonates can be a significant source of phosphorus (P) to microbial communities starved of inorganic P (Dyhrman et al. 2006; Cook et al. 1978; Clark et al. 1999). As *N. maritimus* does not possess proteins with known C-P lyase activity and inorganic P limitation is not alleviated by supplementation with phosphonates (Metcalf et al. 2012; Walker et al. 2010), a link between Fe limitation and P nutritional status is unlikely. An analysis of the spent media from *N. maritimus* cultures shows that *N. maritimus* produces weak ligands as by-products of natural growth — biomaterials hypothesised to be similar to exopolysaccharides (EPS) (Amin et al. 2013). EPS are effective scavengers of cations such as Fe^{2+}/Fe^{3+} (Hassler et al. 2011; Hassler et al. 2015; Gutierrez et al. 2012) owing in part to the negative charge carried by P-bearing groups of the EPS (Ozdemir et al. 2003). P-bearing functional groups have been thermodynamically characterised in Cu^{2+} complexation at the *N. maritimus* cell surface (Gorman-Lewis et al. 2019) and are proposed to be due to the presence of EPS-associated methylphosphonate, which is produced endogenously by *N. maritimus* (Metcalf et al. 2012). The hallmark enzyme of methylphosphonate (Mpn) biosynthesis in *N. maritimus,* methylphosphonic acid synthase (MpnS), binds two Fe atoms (Metcalf et

al. 2012) and the final step in the pathway requires free Fe^{2+} as an electron donor (Figure A2.7). We speculate that the observed increase in PhnCDE intensity under Fe limitation may represent a strategy to enhance the uptake of exogenous phosphonates thereby compensating for a reduction in the cells own methylphosphonate biosynthesis capacity which relies on Fe. While we did not observe any significant change in the intensity of proteins in *N. maritimus'* putative Mpn biosynthesis pathway (Figure A2.7), recent analyses of AOA *mpnS* gene biogeography (Qin et al. 2020) highlight the potential for Fe to play a role in regulating Mpn production by acting as a selective pressure for the presence of *mpnS* genes in AOA populations. The analysis showed that *mpnS* genes are enriched in open ocean AOA populations in the mesopelagic (> 200 m) relative to surface waters (< 200 m), thereby mirroring profiles of dissolved Fe which shows an increase in concentration with depth (Figure A2.8). Based on the results presented in this study, it may be expected for *phnD* gene abundance to follow an inverse trend to *mpnS* abundance, showing an enrichment in shallow AOA populations wherein Fe is scarce relative to deeper populations which have excess to more plentiful Fe. To test this hypothesis, we performed a similar analysis to Qin et al. (2020) using the *Tara* oceans database to investigate the trend in *phnD*: *amoA* with depth (see Appendix II for full details). We found that *phnD*: *amoA* copies per cell in shallow water samples (< 200m) were statistically indistinguishable (Wilcoxon-Test, $p > 0.05$) from mesopelagic samples (> 200 m) (Figure A2.9). However, we found that shallow water *phnD:amoA* showed greater variance compared with deep samples (Levene's test, f-ratio value = 16.4, $p << 0.01$) — with *phnD:amoA* ranging over 3 orders of magnitude below 200 m (Figure A2.9). A greater variance in *phnD:amoA* in shallow water AOA communities is consistent with the high variability in dissolved Fe concentrations in the surface waters compared with depth (Figure A2.8), driven by more intensive biogeochemical cycling of Fe in surface

waters. Additional analyses would be required to rule out that *mpnS* and *phnD* gene biogeography are not driven by other physicochemical factors or ecological factors, such as the dominance of deep-water AOA ecotypes (WCB) at depth (Santoro et al. 2019).

An alternative hypothesis is that the marked increase of PhnCDE intensity under Fe limitation is to drive greater phosphonate uptake as a means of enhancing (not compensating for) *N. maritimus*' methylphosphonate production — potentially explaining why methylphosphonate biosynthesis proteins remain unchanged in response to Fe limitation. In doing so, more P-bearing groups may be provided to the EPS making the cell surface more chemically attractive to extracellular Fe (Figure A2.7). We speculate that increased Fe binding to P-bearing functional groups on the *N. maritimus* cell surface could provide more Fe substrate to *N. maritimus*' ferric reductase, consistent with an increase in the intensity of the aforementioned ferric reductase candidate under Fe limitation (Nmar_0679). In both instances these conjectures highlight that a more detailed characterisation of the EPS of *N. maritimus* and its relationship with Fe cycling and phosphonates is required to robustly explain the increase in PhnCDE under Fe-limitation observed in our study.

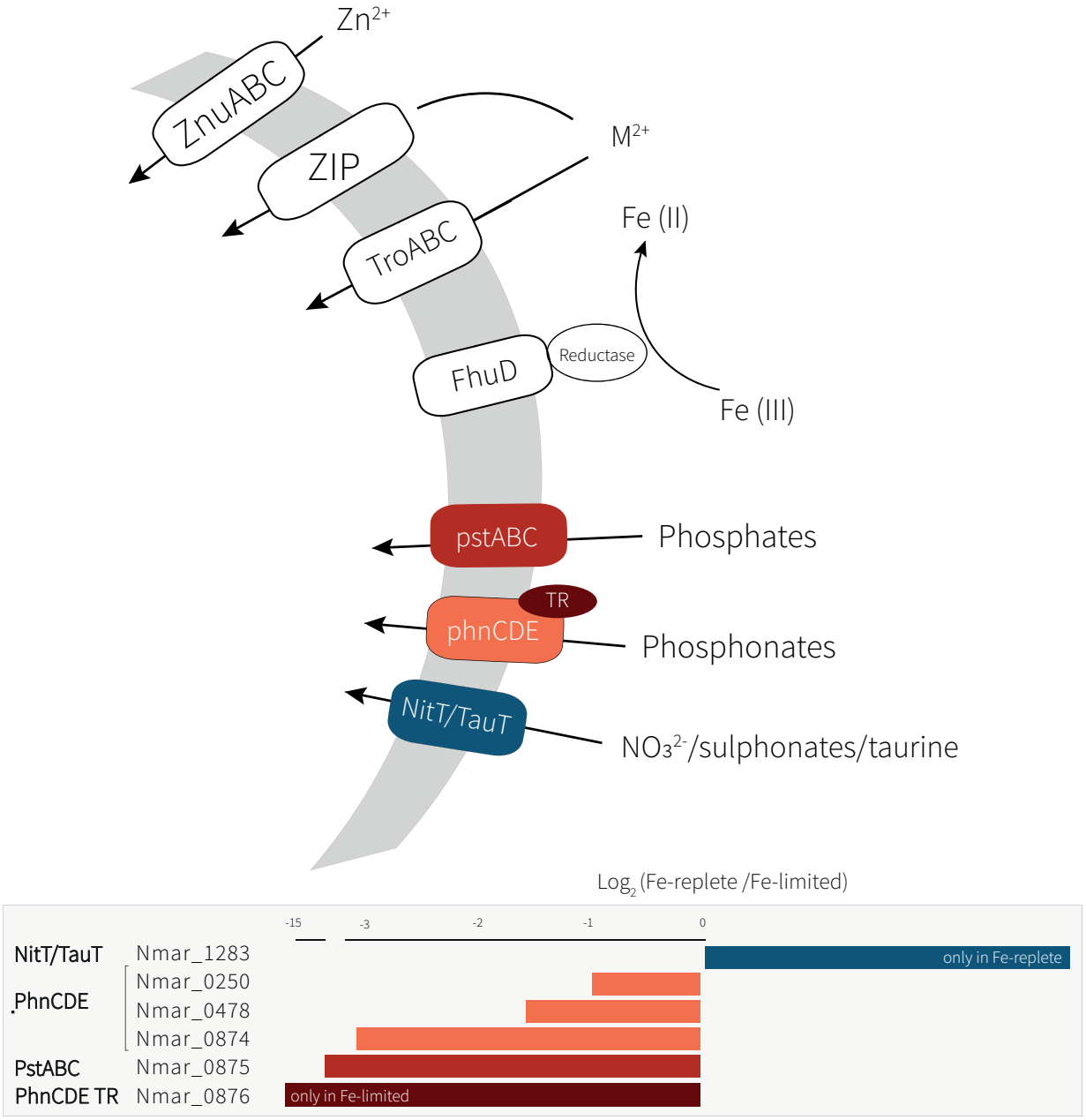


Figure 3.4 Significant intensity changes to proteins involved in transmembrane uptake

Proteins involved in membrane transport encoded by *N. maritimus* genome, with proteins showing significant log_2-fold changes in LFQ intensity between Fe-replete and Fe-limited treatments shown in colour. Protein colour on schematic corresponds to the bars on the plot below. Copyright © 2021, Shafiee et al.

3.5 CONCLUSION

When growth is limited by Fe, *N. maritimus* primarily minimises Fe demand by reducing Fe-dense ferredoxins which putatively interact with Complex I to generate the reduced co-factor NAD(P)H — potentially functionally substituting these ferredoxins for Fe-free alternatives. In doing so, Fe-binding proteins which play a more central role in electron transfer and ammonia oxidation can be preferentially retained, allowing *N. maritimus* to continue in supporting key energy-yielding pathways under Fe limitation. We observed additional compensatory strategies within the TCA cycle, biosynthesis and detoxification demonstrating efforts to maintain the activity of these pathways whilst significantly reducing Fe requirements. Further, in response to Fe limitation we observed a significant increase in the intensity of proteins with a putative role in the uptake of exogenous phosphonates. We speculate this reflects a potential strategy to enhance or compensate for a reduction in *N. maritimus*' endogenous methylphosphonate

3.6 STATEMENT OF AUTHORSHIP

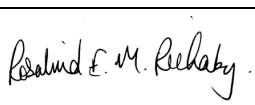
Title of Paper	Proteomic response of the marine ammonia-oxidising archaeon, *Nitrosopumilus maritimus* to iron limitation reveals strategies to compensate for nutrient scarcity
Publication Status	✓ **Published** □ Accepted for Publication □ Submitted for Publication □ Unpublished and unsubmitted work written in a manuscript style
Publication Details	Shafiee, R. T., Snow, J. T., Hester, S., Zhang, Q., & Rickaby, R. E. (2021). Proteomic response of the marine ammonia-oxidising archaeon, Nitrosopumilus maritimus to iron limitation reveals strategies to compensate for nutrient scarcity. *Environmental Microbiology*.

Student Confirmation

Student Name:	Roxana T Shafiee	
Contribution to the Paper	• Conceived idea (in cooperation with RR, JS) • Made trace metal clean culture media and prepared all acid-cleaned culture apparatus. • Cultured AOA under Fe limited and Fe replete conditions (informed from previous work in Chapter two) • Harvested cells for ICP-MS analysis, performed ICP-MS analysis (with QZ) • Performed trial of protein extraction efficiencies • Harvested cells and performed protein extraction • Performed protein digestion/SP3 protocol (with JS) • Performed statistical analysis of data in Perseus, performed additional annotation of protein data and assigned biological function groups • Performed analysis (including and interpretation of proteomic data, including comparison with previous proteomic/transcriptomic studies. • Performed analysis of *Tara* oceans dataset • Performed analysis of metal-binding genome/proteome • Performed statistical analyses • Made all paper figures/graphs • Discussed/interpreted broad scale implications of results (with JS and RR) • Wrote and revised manuscript in response to reviewers' comments.	
Signature:		**Date:** 21/05/2021

Supervisor Confirmation

By signing the Statement of Authorship, you are certifying that the candidate made a substantial contribution to the publication, and that the description described above is accurate.

Supervisor name:	Professor Rosalind Rickaby	
Supervisor signature:		**Date:** 21/05/2021

4 MARINE AMMONIA-OXIDISING ARCHAEA AND BACTERIA OCCUPY DISTINCT IRON AND COPPER NICHES

This chapter provides a physiological characterisation of the Fe and Cu requirements (including uptake strategies) of the marine AOB isolate, *Nitrosococcus oceani*. These data are compared with data provided in chapter two of the Fe requirements of the marine AOA isolate *Nitrosopumilus maritimus* and previously published data. These data are used to examine how contrasting trophic strategies for Fe and Cu contribute to the niche separation of AOA and AOB, the success of AOA in the oceans and the potential for widespread Cu limitation of ammonia oxidation.

This chapter is a reprint of material as it appears in ISME Communications (2021, doi.org/10.1038/s43705-021-00001-7), co-authored by Miss Poppy Diver, Dr. Joseph Snow, Dr Qiong Zhang and Professor Rosalind Rickaby. All supporting material is located in Appendix III.

4.1 ABSTRACT

Ammonia oxidation by archaea and bacteria (AOA and AOB), is the first step of nitrification in the oceans. As AOA have an ammonium (NH_4^+) affinity 200-fold higher than AOB isolates, the chemical niche allowing AOB to persist in the oligotrophic ocean remains unclear. Here we show that marine isolates, *Nitrosopumilus maritimus* strain SCM1 (AOA) and *Nitrosococcus oceani* strain C-107 (AOB) have contrasting physiologies in response to the trace metals iron (Fe) and copper (Cu), holding potential implications for their niche separation in the oceans. A greater affinity for unchelated Fe may allow AOB to inhabit shallower, euphotic waters where NH_4^+ supply is high, but competition for Fe is rife. In contrast to AOB, AOA isolates have a greater affinity and

toxicity threshold for unchelated Cu providing an additional explanation to the greater success of AOA in the marine environment where Cu availability can be highly variable. Using comparative genomics, we predict that the proteomic and metal transport basis giving rise to contrasting physiologies in isolates is widespread across phylogenetically diverse marine AOA and AOB that are not yet available in pure culture. Our results develop the testable hypothesis that ammonia oxidation may be limited by Cu in large tracts of the open ocean and suggest a relatively earlier emergence of AOB than AOA when considered in the context of evolving trace metal availabilities over geologic time.

4.2 INTRODUCTION

Ammonia-oxidising archaea (AOA) and bacteria (AOB) mediate the first step of nitrification, the stepwise oxidation of ammonium (NH_4^+) to nitrite (NO_2^-) and nitrate (NO_3^-) — the central component of biogeochemical nitrogen (N) cycling. A third group of aerobic ammonia oxidisers has also been identified, mediating complete aerobic ammonia oxidation to nitrate (comammox) (Daims et al. 2015). AOA widely outnumber their bacterial counterparts in a range of environments including soils (Leininger et al. 2006) freshwater streams and lakes (Merbt et al. 2011; Jiang et al. 2009; Auguet et al. 2011) and the oceans (Mincer et al. 2007; Wuchter et al. 2006; Santoro et al. 2010; Santoro et al. 2013; Horak et al. 2013; Newell et al. 2013; Peng et al. 2016). In the oligotrophic open ocean, archaeal *amoA* genes, an indicator of cell abundance, are up to three orders of magnitude greater than those of AOB (Wuchter et al. 2006; Horak et al. 2013; Newell et al. 2013; Peng et al. 2016; Shiozaki et al. 2016) hypothesised to be due to the greater affinity of AOA for their shared substrate NH_4^+ (Martens-Habbena et al. 2009). Yet NH_4^+ growth kinetics are unable to solely account for the dominance of AOA in some coastal, estuarine and open ocean environments (Abell et al. 2010; Bernhard et al. 2010; Urakawa et al. 2014) where NH_4^+ supply is enough to support AOB growth, indicating that additional adaptive mechanisms contribute to the greater success of AOA. Further, the coexistence of AOB with AOA in marine environments albeit at low abundances of AOB (Mincer et al. 2007; Wuchter et al. 2006; Santoro et al. 2010; Santoro et al. 2013; Horak et al. 2013; Newell et al. 2013; Peng et al. 2016; Shiozaki et al. 2016) suggests that AOB occupy a distinct chemical niche allowing them to persist despite a low affinity for NH_4^+ (Martens-Habbena et al. 2009).

The genome sequence of the marine AOA isolate, *Nitrosopumilus maritimus* strain SCM1 revealed the presence of numerous copper (Cu)-rich halo- and plastocyanin

enzymes (Walker et al. 2010) in lieu of Fe-dense cytochromes typically found in AOB (Blainey et al. 2011; Zannoni, 2004) alluding to a potential role for trace metals in the niche separation between AOA and AOB. Subsequent studies (Amin et al. 2013; Shafiee et al. 2019 — Chapter two) have revealed that the cupric ion (Cu^{2+}) and unchelated Fe (Fe′) requirement for optimal growth in *N. maritimus* (1 pmol L^{-1} Cu^{2+} and 550 pmol L^{-1} Fe′) are above those typically measured in the marine environment (~0.01–0.1 pmol L^{-1} Cu^{2+} and ~1 pmol L^{-1} Fe′), presenting the potential for marine nitrification to be limited by these trace metals in the open oceans. Growth limitation by Fe or Cu is well documented in other components of the marine N cycle including N_2 fixation (Moore et al. 2009; Richier et al. 2012), NO_3^- assimilation (Timmermans et al. 1994) and denitrification (Granger & Ward, 2003). There has yet to be an equivalent physiological analysis of marine AOB Fe and Cu requirements for growth, precluding an accurate assessment of the role of these trace metals in modulating marine ammonia oxidation rates and shaping the niche separation between AOA and AOB. Comparison of Fe and Cu requirements also provides a new perspective on the longstanding question of AOA and AOB relative emergence, drawing on the idea that extant microorganisms contain imprints of shifting trace metal bioavailabilities over geologic time at the cellular level (da Silva & Williams, 2001; Saito et al. 2003; Dupont et al. 2006; Williams & Rickaby, 2012).

Here, we provide the first physiological examination of the trace metal requirements of any marine AOB isolate, reporting the free inorganic Fe and Cu requirements of *Nitrosococcus oceani* strain C-107 (ATCC 19707). *N. oceani* belongs to the γ-subdivision of the Proteobacteria, an omnipresent AOB group in seawater (Ward & O'Mullan, 2002; Wang et al. 2020). We compare the physiological response of *N. oceani* to unchelated Fe and Cu availability with that of the cultured marine AOA

isolate, *Nitrosopumilus maritimus* strain SCM1 from previous work (Amin et al. 2013; Shafiee et al. 2019 — Chapter two) supplementing the published data with the intracellular Cu quota of *N. maritimus*. To explore whether the physiologies and uptake strategies of *N. oceani* and *N. maritimus* reflect broader marine AOA and AOB communities, pure isolates for which are not yet available, we perform a two-pronged bioinformatic analysis of the metal-binding sites and metal transporter systems in marine AOA and AOB genomes.

4.3 MATERIALS & METHODS

4.3.1 *Nitrosococcus oceani* cultures and growth media

Polycarbonate culture vessels and culturing apparatus were acid-cleaned in 10% (v/v) TraceMetal™ grade HCl (Fisher Scientific, Loughborough, UK) for 24 h and UV-sterilised before use. Triplicate 10 ml cultures of *Nitrosococcus oceani* strain C-107 (ATCC 19707 originally isolated from the open North Atlantic) herein referred to as *N. oceani*, were grown in modified SCM medium (Könneke et al. 2005) amended with additional NH_4Cl (final NH_4^+ concentration 10mM) and maintained at 30 °C in the dark on a rotary shaker (150 r.p.m.). Basal salt medium and macronutrients were treated with Chelex 100 resin (BioRad, Watford, UK) to remove trace metal contaminants (Price et al. 1989) and passed through an acid-washed (10% HCl as before) 0.2 µm polycarbonate filter to sterilise in a trace metal-free clean laboratory. The final pH of the media was 7.5 and was buffered with HEPES. To investigate the effect of unchelated inorganic Fe (Fe′) and copper (Cu′) concentrations on *N. oceani* growth, ethylenediaminetetraacetic acid (EDTA, Merck, Darmstadt, Germany) was used to buffer Fe, Cu and other trace metals in cultures. Fe′ and Cu′ concentrations were controlled by varying the addition of $FeCl_3$ or $CuCl_2$ from filter-sterilised concentrated stocks made using > 99.999% trace metal basis salts (Sigma Aldrich, UK) and maintaining a constant concentration of EDTA

at 25 µmol L^{-1} (Fe experiments) or 120 µmol L^{-1} (Cu experiments)—EDTA concentrations which have been shown to be non-toxic to *N. oceani* in previous work (Hozuki et al. 2014; Gorman-Lewis et al. 2019). Fe′, Cu′ and cupric ion (Cu^{2+}) concentrations were calculated using Visual Minteq software (Gustafsson, 2010). Cu^{2+} is presented in main figures, in order to allow for comparison with previous Cu growth experiments of AOA and phytoplankton and measurements made in the field, which use Cu^{2+}. Cu′ values are given in Table 4.1 and Figure A3.1. Background Fe and Cu blank levels of 1.4 and 12.5 nmol L^{-1}, respectively, from basal SCM medium, were measured using inductively coupled plasma mass spectrometry (ICP-MS) (Zhang et al. 2018) and included in the calculation of trace metal speciation. Cultures were acclimated to Fe′ and Cu′/Cu^{2+} by transferring cultures consecutively during the late exponential growth phase into new media until growth rates did not vary with statistical significance (ANOVA, $p < 0.05$). The growth rate was determined by measuring nitrite (NO_2^-) spectrophotometrically over time as in previous studies (Figure A3.2, Könneke et al. 2005; Lehtovirta-Morley et al. 2011; Powell & Prosser, 1992; Griess, 1879) the production of which correlates with cell counts (Shafiee et al. 2019 — Chapter two). Specific growth rate, μ (d^{-1}) was calculated over the linear phase of semi-log plots of NO_2^- concentration over time.

4.3.2 *Nitrosopumilus maritimus* SCM1 cultures

To supplement previously published data with the intracellular Cu quota of *Nitrosopumilus maritimus* strain SCM1 (herein referred to as *N. maritimus*), *N. maritimus* cultures were maintained as previously described (Shafiee et al. 2019 — Chapter two). In brief, triplicate cultures of *N. maritimus* were grown in SCM media (Könneke et al. 2005) treated with Chelex 100 resin, with 1 mM NH_4Cl (final concentration) and maintained in the dark at 28 °C. Cultures were acclimated to optimal

Cu^{2+} concentrations (1 pmol L^{-1} Cu^{2+}) determined in a previous study (Amin et al. 2013).

Full details of *N. maritimus* culturing methods are provided in Appendix III.

4.3.3 Trace metal quota analysis of cells

All samples and reagents were processed using trace metal clean techniques and acid-washed plasticware in a clean laboratory before trace element analysis. *N. oceani* and *N. maritimus* cells growing at μ_{max} (see Appendix III for full discussion of Fe′ and Cu^{2+} chosen for trace metal analysis) were harvested in mid-exponential phase by centrifugation at 5000 × *g* for 25 min and then rinsed three times with Chelex 100-treated SCM media to remove weakly bound surface metals (Zhang et al. 2018). Cells were digested in acid-cleaned Teflon as follows: refluxing at 100 °C with 16N quartz-distilled (q.d.) HNO_3 (produced in-house) and H_2O_2 (ROMIL UpA™, Cambridge, UK) in a ratio of 3:2 overnight. The liquid was then allowed to evaporate to dryness and 2% q.d. HNO_3 was added to reflux for an hour to resuspend the dried samples. ^{56}Fe, ^{31}P and ^{63}Cu concentrations were determined using a Quadrupole ICP-MS Perkin Elmer NexION 350 with Elemental Scientific Flow Injection Auto-sampler (FIAS) in a method optimised for high-salt matrices (Zhang et al. 2018).

4.3.4 Steady-state Fe uptake rate

The steady-state Fe′ uptake rate (ρ_{ss} – intracellular Fe quota in mol $cell^{-1}$ · specific growth rate in hr^{-1}) and steady-state uptake constant ($k_{in} - \rho_{ss}$ normalised to Fe′ in the medium) were calculated for *N. oceani* as per previous work (Shafiee et al. 2019 — Chapter two; Shaked et al. 2005) using Fe-limited cellular quotas (Figure 4.1). Cellular quotas measured in *N. oceani* cells cultured at 100 pmol L^{-1} Fe′ (66% of μ_{max}) and 376 pmol L^{-1} Fe′ (78% of μ_{max}) were used in calculations. To obtain a steady-state uptake constant per unit surface area (S.A.), S.A. was calculated based on a spherical cell shape and using a radius of 1 μm obtained from SEM imaging (Figure A3.3), preparing cells using the same protocol as in Shafiee et al. (2019)/Chapter two, which is fully outlined in Appendix III.

4.3.5 FeDFB and ferrozine experiments

To examine whether *N. oceani* can utilise organically chelated Fe, *N. oceani* was cultured in medium with the addition of the siderophore desferrioxamine B mesylate (DFB, Merck) to buffer Fe. *N. oceani* was cultured under high and low concentrations of total dissolved Fe (dFe) corresponding to 5006 pmol L^{-1} dFe and 100 pmol L^{-1} dFe. A 1.3-fold excess of DFB was added over Fe, in order to reduce Fe′ to negligible concentrations ($< 1 \times 10^{-9}$ pmol L^{-1} Fe′). EDTA was added in a low concentration (12 µmol L^{-1} EDTA) to buffer other trace metals. We used the ferrozine assay (Shaked et al. 2005) to identify whether *N. oceani* adopts a reductive Fe-uptake pathway in Fe acquisition. Ferrozine (FZ, 5,6-diphenyl-3-(2-pyridyl)-1,2,4-triazine) binds with any available Fe^{2+} in the medium forming an Fe^{2+}–FZ_3 complex which is unavailable for uptake across the outer cell membrane (Lis et al. 2015b). Inhibition of growth with the addition of FZ therefore indicates that cells are actively reducing Fe^{3+} to Fe^{2+} during Fe acquisition. *N. oceani* cultures were acclimated to replete and deplete Fe′ (5006 pmol L^{-1} Fe′ and 100 pmol L^{-1} Fe′), then transferred to new media with 200 µmol L^{-1} FZ. Growth rate (μ) was determined as previously outlined.

4.3.6 Bioinformatic predictions of AOA and AOB physiology in wider communities

The limited number of marine AOA and AOB species isolated into pure culture precludes an extensive physiological analysis of the trace metal requirements across the wider AOA/AOB community using culture-based approaches. To explore whether the physiologies of *N. oceani* and *N. maritimus* may reflect broader marine AOA and AOB communities, we used available genome-predicted proteomes (downloaded from UniProt: https://www.uniprot.org) to annotate the hypothetical Cu- and Fe-binding sites in marine AOA and AOB, on the basis that physiological requirement typically scales with the number of metal-binding sites. In addition, we annotated the presence of metal

transporter systems to explore whether the genetic basis for the contrasting trace metal affinities of *N. oceani* and *N. maritimus* in culture is ubiquitous among the broader AOA and AOB community.

For both analyses, only genome-predicted proteomes with a high genome completeness (> 96%) were used (full search criteria outlined in Appendix III). For annotation of Cu and Fe binding sites, protein sequences were submitted to the PHYRE2 protein fold recognition server to identify homologues for known protein structures (Kelley et al. 2015). Significant matches (> 95% confidence) were submitted to metalPDB (Putignano et al. 2018) which models the 3D minimal functional sites (MFSs) surrounding metals. Metals were assigned if the search returned significant sequence similarity to metal-binding sites in other proteins (*E* value < 10^{-5}). To confirm that genome-predicted proteomes were reflective of expressed proteome trace metal demands, we performed the same analyses with available published expressed proteomes (Figure A3.4 and Figure A3.5). We used both marine and coastal AOA and AOB in our analyses as they were shown to be statistically indistinguishable in terms of genome-predicted proteome trace metal demand (see Figure A3.4 and Appendix III for further clarification).

To annotate trace metal transporter families, we adopted an approach similar to previous studies (Hogle et al. 2016) where conserved domains were identified using the NCBI-conserved domains database (Marchler-Bauer et al. 2015) and then searched against currently characterised trace metal transport systems (Table A3.5). Orthologues were identified using a BLAST search (*E* value < 10^{-5}). Each presence of a transporter family gene was considered as a 'count' and count numbers were plotted against species. Genomes and transporter families included in this analysis are discussed in greater detail in Appendix III.

4.3.7 Data analysis

All statistical analyses were performed using Minitab v.13.1. Data were examined for normality and equal variance prior to Student's *T* test and analysis of variance (ANOVA) statistical tests. Significant results are reported at the 95% confidence level unless otherwise stated ($p < 0.05$).

4.4 RESULTS AND DISCUSSION

4.4.1 Comparison of *N. maritimus* and *N. oceani* response to Fe′ and Cu^{2+}

We examined and compared the effect of unchelated Fe′ and Cu^{2+} on the growth of the ammonia-oxidising bacterium, *N. oceani* strain C-107 with that of the archaeal isolate, *N. maritimus* strain SCM1 previously published (Amin et al. 2013; Shafiee et al. 2019 — Chapter two). *N. oceani* required 0.09 pmol L^{-1} Cu^{2+} to reach maximum specific growth rates (μ_{max}) of 0.61 d^{-1} (± 0.04), becoming growth limited at < 0.09 pmol L^{-1} Cu^{2+} and ceasing all growth at ≤ 0.05 pmol L^{-1} Cu^{2+} (Figure 4.1).

At μ_{max}, *N. oceani* cells contained 3.1×10^{-19} mol Cu $cell^{-1}$ ($\pm 1.9 \times 10^{-19}$), equating to a Cu:P of 0.13 mmol mol^{-1}. In contrast, *N. maritimus* required a greater [Cu^{2+}] to reach μ_{max} (1 pmol L^{-1} Cu^{2+}) but was able to maintain growth at < 0.05 pmol L^{-1} Cu^{2+} (Amin et al. 2013). At μ_{max}, we found that *N. maritimus* had a greater cellular Cu quota of 4.9×10^{-18} mol Cu $cell^{-1}$ ($\pm 1.9 \times 10^{-19}$) compared with *N.oceani* at μ_{max} (Mann–Whitney *U* test). To our knowledge, *N. maritimus* has the greatest cellular Cu:P quota (1.89 mmol mol^{-1}) documented for any marine microorganism growing at μ_{max}. Maximum growth rates in *N. oceani* between 0.09 and 0.14 pmol L^{-1} Cu^{2+} may appear to result from the expression of a high-affinity Cu uptake system in a similar mechanism to that demonstrated for Fe (Wilhelm & Trick, 1994). As *N. oceani* does not possess any known genes for high-affinity Cu uptake (e.g. CTR or *ctaA*—see below for further discussion), we posit that the

reduction in μ at > 0.14 pmol L^{-1} Cu^{2+} is more likely a toxicity response. Our results suggest that *N. oceani* is more susceptible to Cu^{2+} toxicity than *N. maritimus*: at 53.54 pmol L^{-1} Cu^{2+}, *N. oceani* growth was 28% below μ_{max} compared with *N. maritimus* growth rate that was only reduced by 10% at the equivalent [Cu^{2+}].

While *N. maritimus* requires an elevated [Cu^{2+}] to reach μ_{max} and is able to maintain growth at lower [Cu^{2+}] compared with *N. oceani*, we observed the opposite trend between the two microorganisms with respect to Fe′. *N. oceani* reached μ_{max} at 5006 pmol L^{-1} Fe′ and became partially growth limited in treatments with ≤ 828 pmol L^{-1} (Figure 4.1). *N. oceani* growth was not detected in treatments with < 100 pmol L^{-1} Fe′. At μ_{max}, the intracellular Fe quota of *N. oceani* cells was 6.1×10^{-17} mol Fe $cell^{-1}$ ($\pm$ 1.1×10^{-17}). In contrast, *N. maritimus* reaches μ_{max} at a lower [Fe′] of 550 pmol L^{-1} and is unable to grow at < 250 pmol L^{-1} Fe′ (Shafiee et al. 2019 — Chapter two). At μ_{max}, *N. maritimus* cells have an intracellular Fe quota of 6.5×10^{-18} mol Fe $cell^{-1}$ ($\pm 1.3 \times 10^{-18}$) — an order of magnitude less than intracellular Fe quota of *N. oceani* at μ_{max} (Student's *T* test, two-tailed, $p < 0.01$). The *N. oceani* steady-state Fe′ uptake rate constant (k_{in}), an indicator of Fe affinity, is typical based on the linear relationship between k_{in} and S.A. in marine phytoplankton and heterotrophic bacteria (Lis et al. 2015a). *N. maritimus* deviates from the linear relationship between k_{in} and S.A. with a lower k_{in} of 4.5×10^{-13} L $cell^{-1}$ h^{-1} ($\pm 1.2 \times 10^{-13}$) and therefore per unit S.A. *N. maritimus* has a lower Fe′ uptake rate compared with *N. oceani* and cosmopolitan marine microorganisms (Figure A3.5).

dCu nmol L^{-1}	**dFe** µmol L^{-1}	**Fe´** pmol L^{-1}	**Cu´** pmol L^{-1}	**Cu^{2+}** pmol L^{-1}	**μ** d^{-1}	**μ/μ_{max}**	**Cell Fe** mol $cell^{-1}$	**Cell P** mol $cell^{-1}$	**Cell Cu** mol $cell^{-1}$	**Fe:P** mmol mol L^{-1}	**Cu:P** mmol mol L^{-1}	**ρ_{ss}** mol Fe $cell^{-1}$ hr^{-1}	**k_{in}** L $cell^{-1}$ hr^{-1}	**k_{in}/S.A.**
***N. oceani* strain C-107**														
2.5	0.05	9	0.15	0.10	n.g.	0								
2.5	0.2	35	0.15	0.10	n.g.	0								
2.5	0.57	100	0.16	0.10	0.41* (0.01)	0.66	1.6×10^{-17} (1.4×10^{-18})	3×10^{-15} (1.2×10^{-15})		6.1		2.8×10^{-19} (2.4×10^{-20})	2.8×10^{-9} (2.4×10^{-10})	2.2×10^{-10}
2.5	1	179	0.16	0.11	0.41* (0.01)	0.66								
2.5	2	376	0.16	0.11	0.46** (0.01)	0.78	3×10^{-17} (1.1×10^{-17})	3×10^{-15} (2.7×10^{-15})		10.9		6.2×10^{-19} (2.1×10^{-19})	1.7×10^{-9} (5.5×10^{-10})	1.3×10^{-10}
2.5	4	825	0.16	0.10	0.52** (0.02)	0.85	4.1×10^{-17} (1.9×10^{-17})	2×10^{-15} (6.1×10^{-16})		19.8				
2.5	**13**	**5006**	**0.20**	**0.10**	**0.61*** (0.01)**	**1.00**	**6.1×10^{-17} (1.1×10^{-17})**	**2.2×10^{-15} (3.6×10^{-15})**		**27.9**				
2.5	17	10063	0.21	0.10	0.54*** (0.03)	0.93								
1.4	7.5	6500	0.07	0.05	n.g.	0.00								
2	7.5	6500	0.10	0.07	0.44 * (0.02)	0.72								
2.5	**7.5**	6500	**0.13**	**0.09**	**0.61** (0.04)**	**1.00**		**2.5×10^{-15} (1.7×10^{-15})**	**3.1×10^{-19} (1.9×10^{-19})**		**0.13**			
4.9	7.5	6500	0.21	0.14	0.55** (0.08)	0.90								

7.9	7.5	6501	0.40	0.27	0.52 *** (0.08)	0.85			
32.5	7.5	6505	1.68	1.01	0.43 † (0.05)	0.71			
68	7.5	6510	3.49	2.37	0.48 † (0.04)	0.78			
125	7.5	6519	6.89	4.68	0.48 † (0.07)	0.78			
680	7.5	6604	35.93	24.63	0.47 † (0.06)	0.77	6.8×10^{-14} (1.3×10^{-14})	6.9×10^{-19} (8.6×10^{-19})	**0.7**
52.00	7.5	6734	78.84	53.54	0.44 † (0.05)	0.72			
N. maritimus									
7×10^{-8}	**7500**	**7585**	**1.66**	**1.00**	**0.51 (0.02)**	**1.00**	**2.6×10^{-15} (1.3×10^{-15})**	**4.9×10^{-18} (1.9×10^{-19})**	**1.89**

Table 4.1 *N. oceani* growth and intracellular quota in response to changing Fe and Cu

Relationships among total and inorganic unchelated Fe (dFe and Fe′), total, unchelated and cupric ion (dCu, Cu′ and Cu^{2+}), growth rate (μ), relative growth rate (μ/μ_{max}), Fe, Cu and P quota per cell and Cu and Fe normalised to cellular P, Fe′ steady-state uptake rate (ρ_{ss}) and steady-state uptake rate normalised to Fe′ (k_{in}). Values in brackets indicate standard deviation. Treatments in bold indicate the first instance that μ_{max} is reached, quotas for which are used for comparison in Figure 4.1. Treatments are grouped by the symbols *, **, *** and † – treatments with the same symbols are statistically indistinguishable from each other ($p < 0.05$, two-tailed *T* test or one way ANOVA) but vary with statistical significance from other treatments ($p < 0.05$, two-tailed *T* test or one way ANOVA.

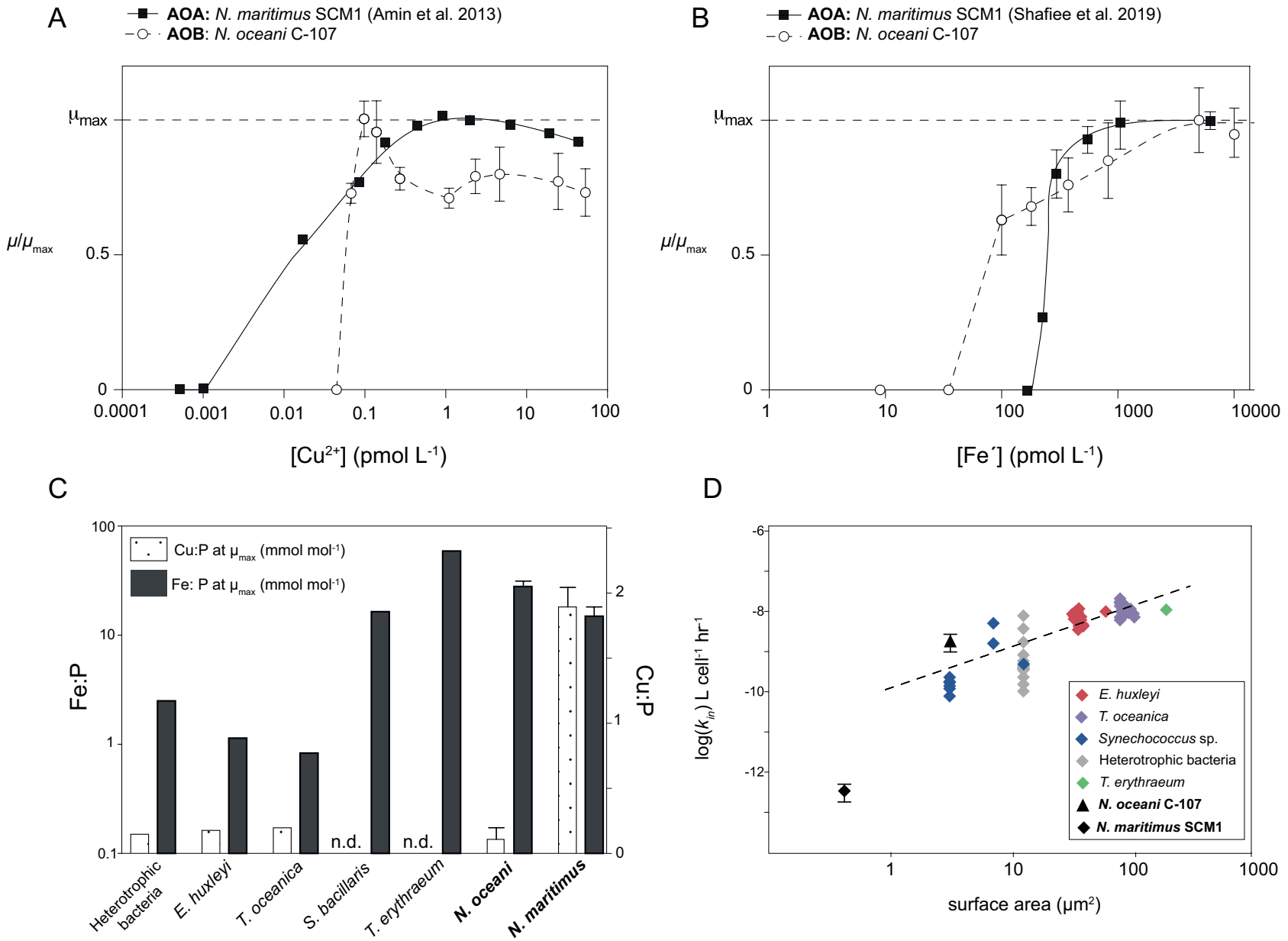

A
AOA: N. maritimus SCM1 (Amin et al. 2013)
AOB: N. oceani C-107
μmax
μ/μmax
0.5
0
0.0001
0.001
0.01
0.1
1
10
100
[Cu2+] (pmol L-1)
B
AOA: N. maritimus SCM1 (Shafiee et al. 2019)
AOB: N. oceani C-107
μmax
μ/μmax
0.5
0
1
10
100
1000
10000
[Fe´] (pmol L-1)
C
Cu:P at μmax (mmol mol-1)
Fe: P at μmax (mmol mol-1)
Fe:P
Cu:P
100
10
1
0.1
2
1
0
n.d.
n.d.
Heterotrophic bacteria
E. huxleyi
T. oceanica
S. bacillaris
T. erythraeum
N. oceani
N. maritimus
D
log(kin) L cell-1 hr-1
-6
-8
-10
-12
1
10
100
1000
surface area (μm2)
E. huxleyi
T. oceanica
Synechococcus sp.
Heterotrophic bacteria
T. erythraeum
N. oceani C-107
N. maritimus SCM1

Figure 4.1 Cu and Fe requirements of *N. oceani* compared with AOA and other marine microorganisms

Effect of **(A)** cupric ion concentration [Cu^{2+}] (pmol L^{-1}) **(B)** unchelated Fe concentration (Fe′) on the relative growth rate (μ/μ_{max}) of the ammonia-oxidising bacterium *N. oceani* strain C-107 (open circles and dashed line) compared with previously published data on the ammonia-oxidising archaeon *N. maritimus* strain SCM1 (Amin et al. 2013; Shafiee et al. 2019 — Chapter two) (closed squares and solid black line - error bars within points on *N. maritimus* data). Error bars on *N. oceani* points represent standard deviation calculated on $n = 21$ (3 replicates were conducted for each treatment in a total of 7 acclimated sub-cultures – calculated to be statistically indistinguishable, ANOVA, $p < 0.01$). Error bars on *N. maritimus* strain SCM1 data points in 1B) represent standard deviation on $n = 20$, as calculated previously (Shafiee et al. 2019 – Chapter two) **(C)** Intracellular Cu and Fe quota in mol $cell^{-1}$ normalised to mol $cell^{-1}$ P at maximum relative growth rate, μ_{max}, in *N. oceani* and *N. maritimus* (Cu quota calculated in this study, Fe quota calculated in Shafiee et al. 2019 – Chapter two) compared with published quota data of numerous marine phytoplankton (data and references provided in Table A3.1). Fe:P and Cu:P at μ_{max} in *N. oceani* was measured at 5006 pmol L^{-1} Fe′ and 0.07 pmol L^{-1} Cu^{2+}, respectively. Cu:P at μ_{max} in *N. maritimus* strain SCM1 was measured at 0.97 pmol L^{-1} Cu^{2+}. Additional Fe and Cu quota under varying [Fe′] and [Cu^{2+}] is provided in Table 4.1 and Figure A3.1. See Appendix III for further discussion on the use of quota data at μ_{max}. Error bars on *N. oceani* data represent standard deviation, $n = 3$ **(D)** log k_{in}, Fe′ steady-state uptake constant, in L $cell^{-1}$ hr^{-1} as a function of cellular surface area (μm^3) in *N. oceani* (filled diamond) compared with published data of *N. maritimus* (Shafiee et al. 2019 — Chapter two) and other marine phytoplankton (Lis et al. 2015a). Error bars represent standard deviation, $n = 6$. Copyright © 2021, Shafiee et al.

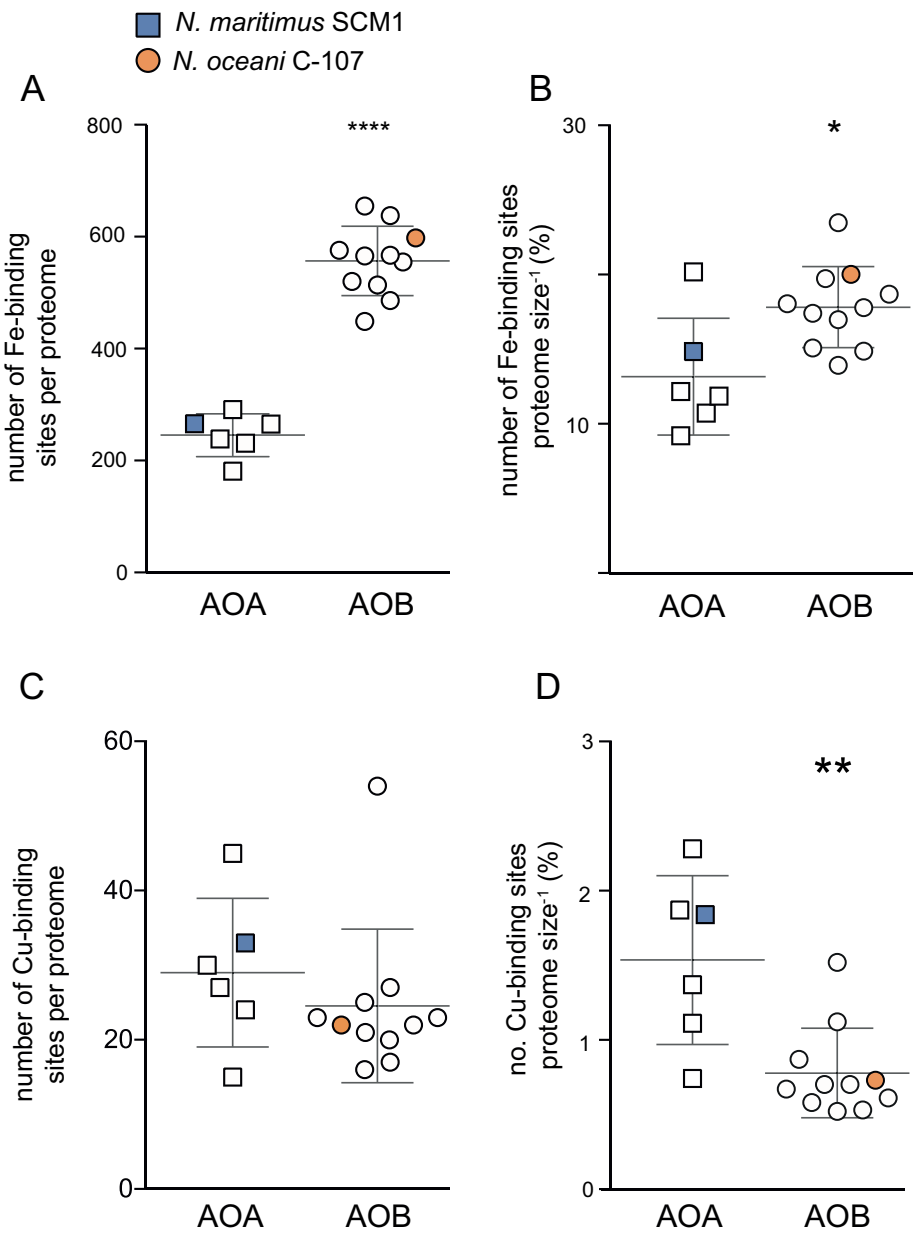


Figure 4.2 AOA and AOB Cu and Fe requirements based on genome-predicted proteomes

A) Absolute number of Fe-binding sites per genome-predicted proteome of marine (coastal and open ocean) AOA and AOB. See Appendix III for full discussion of included species. **** denotes that values are significantly different between AOA and AOB (*T* test, two-tailed, $p < 0.0001$) **B)** Number of Fe-binding sites annotated in genome-predicted proteome of marine AOA and AOB relative to proteome size (number of proteins predicted from genome) as a percentage. * denotes that values are significantly different between AOA and AOB (*T* test, two-tailed, $p < 0.05$**) C)** Absolute number of Cu-binding sites annotated in genome-predicted proteome of marine (coastal and open ocean) AOA and AOB. See Appendix III for full discussion of included species. **D)** Number of Cu-binding sites annotated on genome-predicted proteome of marine AOA and

AOB relative to proteome size (number of proteins predicted from genome) as a percentage. ** denotes those values are significantly different between AOA and AOB (*T* test, two-tailed, $p < 0.01$). For plots A – D, AOA $n = 6$, AOB $n = 11$. Error bars indicate standard deviation and middle line indicates mean. All data available in Table A3.1. Copyright © 2021, Shafiee et al.

4.4.2 Metal requirements and uptake strategies across AOA and AOB communities

To explore whether Cu and Fe quotas in *N. oceani* and *N. maritimus* at μ_{max} (Figure 4.1) are likely to be representative of broader AOA and AOB communities, we analysed the number of Cu- and Fe-binding sites in available marine AOA and AOB genome-predicted proteomes. We found that the number of hypothetical Fe-binding sites in genome-predicted proteomes were significantly greater in marine AOB compared to AOA (Figure 4.2, Student's *T* test, $p < 0.0001$). As such, it is plausible that the greater measured Fe quota at μ_{max} in *N. oceani* is reflective of broader marine AOA and AOB communities, supporting the notion that a greater utilisation of cytochromes (Blainey et al. 2011; Zannoni, 2004) burdens AOB with a significant additional Fe demand relative to AOA. The same trend is evident when normalised to proteome size ($p = 0.006$), indicating that the greater number of Fe-binding sites is not an artefact of the larger average genome size in AOB. We did not observe a significant difference between the absolute number of Cu-binding sites in genome-predicted proteomes of AOA and AOB (Figure 4.2). Individually *N. oceani* and *N. maritimus* differ in their number of Cu-binding sites per genome —33 in *N. maritimus* versus only 22 in *N. oceani*. Therefore, we speculate that the greater Cu quota per cell in *N. maritimus* compared with *N. oceani* reflects species-level differences and does not necessarily represent trends among the wider AOA and AOB community. However, when normalised to proteome size, AOA are significantly enriched in Cu-binding proteins, suggesting that the greater Cu:P in *N.*

maritimus compared with *N. oceani* (Figure 4.1) may be reflective of broader AOA and AOB communities. A greater Cu:P in *N. maritimus* compared to AOB supports genome and proteome analysis revealing relative to their small proteome/genome size, AOA have an unusually high number of Cu proteins, including plastocyanins and multi-Cu oxidases with a putative role in electron transport (Walker et al. 2010; Santoro et al. 2015).

4.4.3 Inorganic Fe uptake

The Fe′ uptake rate constant normalised to S.A. in *N. oceani* exceeds numerous marine microorganisms including *N. maritimus* (Figure A3.5), suggesting that if illustrative of wider AOB physiologies, AOB may be effective competitors for Fe′ in the marine environment. Analyses of the trace metal uptake complement of available AOB genomes support the case for *N. oceani* strain C-107 as a suitable representative for wider AOB physiologies: all AOB in our analysis had at least one inorganic Fe-specific uptake system, compared with only 40% of AOA (Figure 4.3 and Figure A3.6). The genomes of all *Nitrosococcus* species encode proteins for the high-affinity FTR/Fet3p Fe^{2+} uptake system (Figure 4.3), comprising a multi-Cu oxidase (Fet3p) that oxidises Fe^{2+} to Fe^{3+} prior to uptake across the inner membrane by FTR (Lis et al. 2015a). Given that the main Fe′ substrate in EDTA-buffered systems is Fe^{3+}, we predict that Fe^{3+} is reduced prior to being delivered to the FTR/Fet3p system for re-oxidation as demonstrated in previous work (Kwok & Kosman, 2005). FTR has high substrate specificity for Fe^{3+} which has been oxidised by the Fet3p multi-Cu oxidase and as such exogenous Fe^{3+} cannot be provided directly to FTR for uptake (Kwok & Kosman, 2005). As we did not observe any reduction in growth rate with the addition of ferrozine (FZ) (Figure A3.7), any Fe^{3+} reduction does likely not occur extracellularly but rather in the periplasmic space before uptake.

In contrast, *N. maritimus* does not possess any genes diagnostic of known inorganic Fe-uptake systems suggesting a reliance on general cation ZIP transporters for Fe^{2+} uptake or the utilisation of a hitherto uncharacterised Fe-specific transporter. A low Fe′ steady-state uptake rate in *N. maritimus* (Shafiee et al. 2019 — Chapter two) points to Fe uptake by non-specific ZIP transporters rather than an uncharacterised Fe-specific transporter. *N. maritimus* strain SCM1 was isolated from a marine aquarium (Könneke et al. 2005) calling into question whether the Fe-uptake strategies seen in *N. maritimus* are reflective of the environmental AOA populations or whether species such as *Ca*. Nitrosopelagicus brevis, (Santoro et al. 2015) with Fe-specific uptake transporters (Figure 4.3) are in fact more typical of oceanic AOA. Previous work shows that *N. maritimus* is closely related to marine AOA (*in situ* and those recovered in enrichment cultures) based on gene content and sequence (Wuchter et al. 2006; Santoro et al. 2010; Walker et al. 2010; Agogué et al. 2008; Santoro & Casciotti, 2011) and metagenomic and metatranscriptomic analyses point to the dominance of *Thaumarchaeota* belonging to '*Nitrosopumilus*-type' *Nitrospumilales* in the oceans (Reji et al. 2019; King et al. 2013; Stewart et al. 2012). In addition, Thaumarcheotal genes homologous to non-specific metal transporters in *N. maritimus* have been shown to be more prevalent in the *Tara* metagenomic database compared with *Ca.* N. brevis-related Fe transporters (Shafiee et al. 2019 — Chapter two). Together these results suggest that *N. maritimus* may be more representative of broader marine AOA Fe-uptake dynamics; however, it is still plausible that Fe-uptake strategies play into the niche separation of AOA 'ecotypes' or clades in a manner similar to NH_4^+, light and O_2 concentrations (Sintes et al. 2013, 2015, 2016; Francis et al. 2005; Luo et al. 2014; Qin et al. 2017b) and provide interesting avenues for future research.

4.4.4 Chelated Fe uptake and siderophore biosynthesis

Despite that fact that AOB isolates appear to be more competitive for Fe′ compared with AOA isolates, Fe′ is still exceedingly scarce in the marine environments with > 99.9% Fe complexed to organic ligands (Gledhill & Buck, 2012). *N. maritimus* has been shown to be able to utilise Fe even when strongly chelated to the siderophore desferrioxamine B mesylate (DFB), using an extracellular reductive uptake strategy, but shows no physiological and bioinformatic evidence of producing siderophores endogenously (Shafiee et al. 2019 — Chapter two; Figure 4.3). An inability to produce siderophores across the *Thaumarchaeota* phylum is suggested by the absence of known siderophore biosynthesis genes in all AOA genomes we examined (Figure 4.3; Figure A3.6). In contrast, the *N. oceani* genome encodes an aerobactin biosynthesis pathway (Klotz et al. 2006) a capability likely widespread across AOB: 88% of marine AOB genomes have at least one gene diagnostic of a siderophore biosynthetic pathway (Figure 4.3). We did not observe any growth of *N. oceani* in medium wherein all Fe was chelated to a xenosiderophore, desferrioxamine B (Figure A3.7). However, all but one of the AOB genomes examined encoded multiple TonB-dependent transporters and at least one periplasmic substrate-binding protein capable of transporting siderophores across the outer and inner bacterial membrane (e.g. *fecCD, fhuD, fiu*—see Table A3.5 for full list). The only AOA genome that encodes TonB-dependent transport is *N. maritimus*—the function of this transporter remains to be investigated given that *N. maritimus* likely reduces Fe extracellularly (Shafiee et al. 2019 — Chapter two). However, all AOB genomes that we examined (except *N. halophilia* Nm 1) encode multiple TonB-dependent transporters and at least one periplasmic substrate-binding protein capable of transporting siderophores across the outer and inner bacterial membrane, respectively

(Figure 4.3 and Figure A3.6). Addition of ferrozine (FZ) in EDTA-buffered cultures did not inhibit *N. oceani* growth rates (Figure A3.7), suggesting that *N. oceani* does not employ a reductive Fe-uptake strategy and we did not find any bioinformatic evidence for extracellular ferric reductases in *N. oceani* or AOB genomes. Taken together, these results suggest that AOB are only able to access specific forms of Fe chelates, utilising a direct uptake strategy rather than reducing Fe^{3+} to Fe^{2+} from Fe chelates extracellularly as suggested for *N. maritimus* (Shafiee et al. 2019 — Chapter two). The ferric reductase responsible for reductive uptake in *N. maritimus* has not yet been identified and other AOA genomes do not encode typical ferric reductases (e.g. FRE or SIP), hampering efforts to explore the extent of a reductive uptake strategy among the wider AOA community. If a non-discriminate reductive uptake strategy is widespread among AOA, it may provide a key competitive advantage over AOB that are constrained to specific Fe chelates and Fe′ to satisfy Fe demand. Although AOB are able to respond to Fe scarcity by producing siderophores, siderophores are subject to diffusive losses in the marine environment (Völker & Wolf-Gladrow, 1999) and can be taken up by other 'cheating' microorganisms. In the oligotrophic ocean a 'generalist' reductive strategy as seen in *N. maritimus*, allowing access to a broader range of Fe substrates, may be a favourable strategy over the siderophore production (Kranzler et al. 2011; Blaby-Haas & Merchant, 2012) and direct uptake of distinct Fe complexes of *N. oceani* and other AOB.

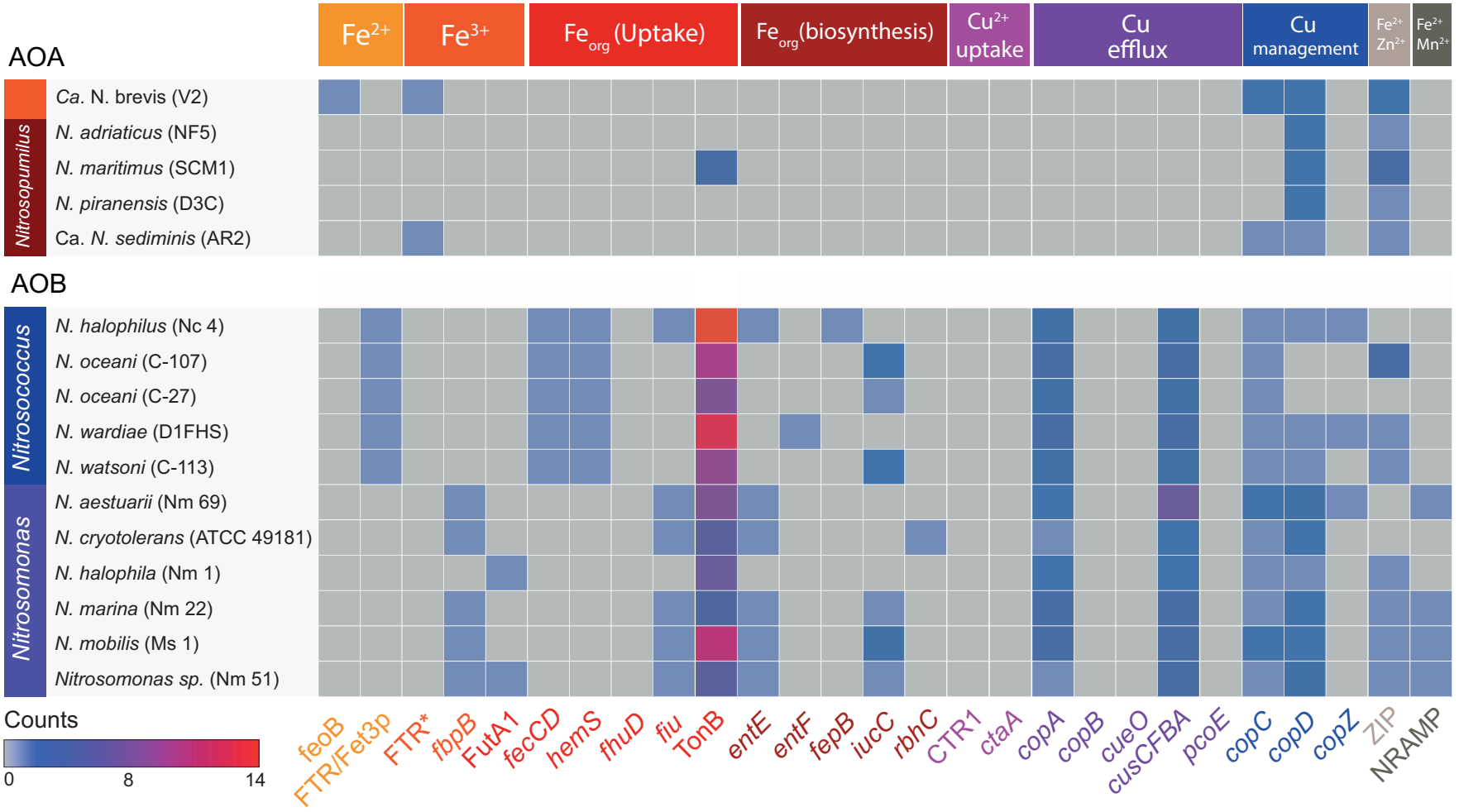

AOA
AOB
Nitrosopumilus
Nitrososcoccus
Nitrosomonas
Ca. N. brevis (V2)
N. adriaticus (NF5)
N. maritimus (SCM1)
N. piranensis (D3C)
Ca. N. sediminis (AR2)
N. halophilus (Nc 4)
N. oceani (C-107)
N. oceani (C-27)
N. wardiae (D1FHS)
N. watsoni (C-113)
N. aestuarii (Nm 69)
N. cryotolerans (ATCC 49181)
N. halophila (Nm 1)
N. marina (Nm 22)
N. mobilis (Ms 1)
Nitrosomonas sp. (Nm 51)
Fe2+
Fe3+
Feorg (Uptake)
Feorg(biosynthesis)
Cu2+ uptake
Cu efflux
Cu management
Fe2+ Zn2+
Fe2+ Mn2+
feoB
FTR/Fet3p
FTR*
fbpB
FutA1
fecCD
hemS
fhuD
fiu
TonB
entE
entF
fepB
iucC
rbhC
CTR1
ctaA
copA
copB
cueO
cusCFBA
pcoE
copC
copD
copZ
ZIP
NRAMP
Counts
0
8
14

Figure 4.3 Abundance of metal transport systems in marine AOA and AOB

Abundance of trace metal transport systems in marine AOA and AOB. Each respective trace metal uptake, siderophore uptake and biosynthesis or Cu toxicity management system per genome, with colours responding to the number of counts. Trace metal uptake systems are partitioned by colour into their metal substrate. A full description of trace metal transport systems searched in the analysis and data is outlined in Table A3.5. AOA and AOB are partitioned by genus. Strains are given in brackets alongside species names. *FTR – refers to presence of FTR1 gene only without corresponding fet3p gene which constitutes high-affinity Fe^{3+} uptake. Copyright © 2021, Shafiee et al.

4.4.5 Cu uptake and management

The ability of *N. maritimus* to maintain growth under lower [Cu^{2+}] compared with *N. oceani* points to the presence of a high-affinity Cu uptake system such as CTR1, yet our analysis did not reveal the presence of such systems in either of the examined AOA or AOB genomes across all environments (Figure 4.3). A higher affinity for Cu^{2+} in *N. maritimus* has been hypothesised to be due to the chemical characteristics of their S-layer: Cu^{2+} is characterised as a 'soft' metal and is therefore attracted to polarisable 'soft' thiol ligands within the archaeal S-layer, allowing Cu^{2+} to accumulate at the cell surface to greater concentrations (Gorman-Lewis et al. 2019; Gorman-Lewis et al. 2014; Li et al. 2018). The distinctive S-layer is common to AOA and absent from AOB across all environments — indicating that an ability to grow under low Cu^{2+} may be widespread among *Thaumarchaeota*. Indeed, the soil archaeon *Nitrososphaera viennensis* and other AOA can maintain growth at [Cu^{2+}] as low as 10^{-4} pmol L^{-1} Cu^{2+} (Gwak et al. 2020; Reyes et al. 2020; Kerou et al. 2016) nearly two orders of magnitude lower than [Cu^{2+}] needed to support *N. maritimus* growth. Previous work shows that the soil AOB, *Nitrosomonas europaea*, can maintain growth at [Cu^{2+}] below that which is limiting to soil AOA (Gwak et al. 2020) signifying that environment-specific selection pressures may be at play and that there is likely species-specific physiological diversity

within AOA and AOB groups. For instance, high nutrient environments may be less likely to select for S-layer proteins that are more chemically attractive to cations, contributing to the high diversity observed in S-layer proteins (Li et al. 2018). Compared with *N. oceani, N. maritimus* is able to tolerate greater [Cu^{2+}] before an inhibitory effect on growth is observed (Amin et al. 2013). Environmental studies mirror these results, showing that elevated Cu in marine sediments, river sediments and soils drives a greater reduction in AOB *amoA* gene abundances compared to AOA *amoA* (Li et al. 2009; Besaury et al. 2014; Mertens et al. 2010; Kim et al. 2016). Elevated intracellular Cu^{2+} leads to the production of reactive oxygen species (ROS) that can cause lipid peroxidation, protein oxidation and DNA damage necessitating the production of oxidative defence mechanisms such as superoxide dismutases or catalases. While both AOA and AOB encode genes for superoxide dismutase, the ability to produce the hydrogen peroxide-detoxifying enzyme catalase is absent from the genomes of AOA (Kim et al. 2016) suggesting this is not the mechanism conferring increased Cu^{2+} resistance to AOA.

Our analysis revealed the presence of at least two known Cu efflux and internal Cu management systems in all AOB. These systems include the Cu-exporting CopA (Odermatt et al. 1994) and CusA (Outten et al. 2001) families and the cytoplasmic Cu chaperone CopC, CopD (Lawton et al. 2016), and CopZ (Solioz & Odermatt, 1995) families. In contrast, AOA genomes do not encode any Cu efflux proteins, and only contain *copC* or *copD* genes that play a putative role in chaperoning Cu within the cell (Lawton et al. 2016). The rarity of Cu efflux systems is not unique to *Thaumarchaeota*: genomes across the Archaeal domain encode significantly fewer Cu efflux genes compared to genomes of the Bacterial domain (Ridge et al. 2008) calling into question the mechanism allowing AOA isolates to tolerate greater [Cu^{2+}] in culture (Figure 4.1).

Amin et al. (2013) found that under Cu-replete conditions, *N. maritimus* produced weak ligands that were not produced under Cu-limiting conditions. The production of ligands with a range of stability constants, which form complexes with free Cu^{2+} thereby preventing it from accumulating on cell surfaces, is a common indirect strategy among marine microorganisms to manage high Cu^{2+} (Azenha et al. 1995; Croot et al. 2000; Moffett & Brand, 1996). If the ligands produced by *N. maritimus* are playing a similar role in lowering cupric ion activity, it explains how *N. maritimus* is able to tolerate higher (calculated) $[Cu^{2+}]$, despite the lack of known Cu-detoxification genes in its genome.

4.5 IMPLICATIONS FOR MARINE AMMONIA OXIDATION, NICHE SEPARATION AND EVOLUTION

4.5.1 Copper limitation of ammonia oxidation

While 'omics approaches are useful in making initial predictions about microbial niche separation, the effect of genotypic variation on physiology is more robustly gleaned from examining pure isolates in controlled culture conditions—a non-trivial task given that pure isolates of AOA and AOB are lacking. If representative of *in-situ* communities, as suggested by our bioinformatic analysis of available genomes, our physiological characterisation of *N. oceani* and *N. maritimus* provides testable hypotheses and new avenues to be explored in future research.

To our knowledge the cupric ion concentration ($[Cu^{2+}]$) required for minimum growth in *N. oceani* and *N. maritimus*, is greater than all other microbial components of the marine N cycle (Amin et al. 2013; Granger & Ward, 2003; Lopez et al. 2019; Brand et al. 1986; Kim & Price, 2017; Sunda & Huntsman, 1995– Table A3.1 and Figure A3.8) examined to date, suggesting that ammonia oxidation may act as a bottleneck in marine biogeochemical N cycling when $[Cu^{2+}]$ is low. We hypothesise that ammonia oxidation

in the Pacific Ocean may be susceptible to Cu limitation, as [Cu^{2+}] measured in the Pacific can be spatially and temporally below the AOA and AOB Cu-limiting threshold (< 0.01 pmol L^{-1} Cu^{2+} — Figure 4.4). In the North East Pacific, where [Cu^{2+}] has been documented to be < 0.001 pmol L^{-1} Cu^{2+} at all depths (Coale & Bruland, 1988; Whitby et al. 2018), Cu limitation may extend throughout the water column, contributing to the low observed ammonia oxidation rates and *amoA* gene abundances despite otherwise replete NH_4^+ (Shiozaki et al. 2016). Cu-amendment experiments conducted *in situ* will be necessary in order to test this hypothesis as open-ocean ecotypes may harbour physiologies distinct to those demonstrated here.

The observation that AOB become completely growth limited at greater [Cu^{2+}] relative to the AOA aligns with observations of lower AOB: AOA abundances under Cu-deplete regimes in the North East Pacific (0.0001–0.01 pmol L^{-1} Cu^{2+}), despite concentrations of NH_4^+ which are otherwise sufficient to support AOB growth (Martens-Habbena et al. 2009). [Cu^{2+}] ranges over five orders of magnitude between the surface and deep ocean (Figure 4.4 — 0.0001–10 pmol L^{-1} Cu^{2+}) and varies three orders of magnitude between ocean basins (0.0010 pmol L^{-1} Cu^{2+} in the Pacific (Coale & Bruland, 1988; Whitby et al. 2018) to 0.2 pmol L^{-1} Cu^{2+} in the North Atlantic (Heller & Croot, 2015). The ability of *N. maritimus* to support growth over a broader [Cu^{2+}] range, may provide an additional adaptation, in addition to a higher affinity for NH_4^+ (Martens-Habbena et al. 2009), which contributes to the greater success of AOA in the environment.

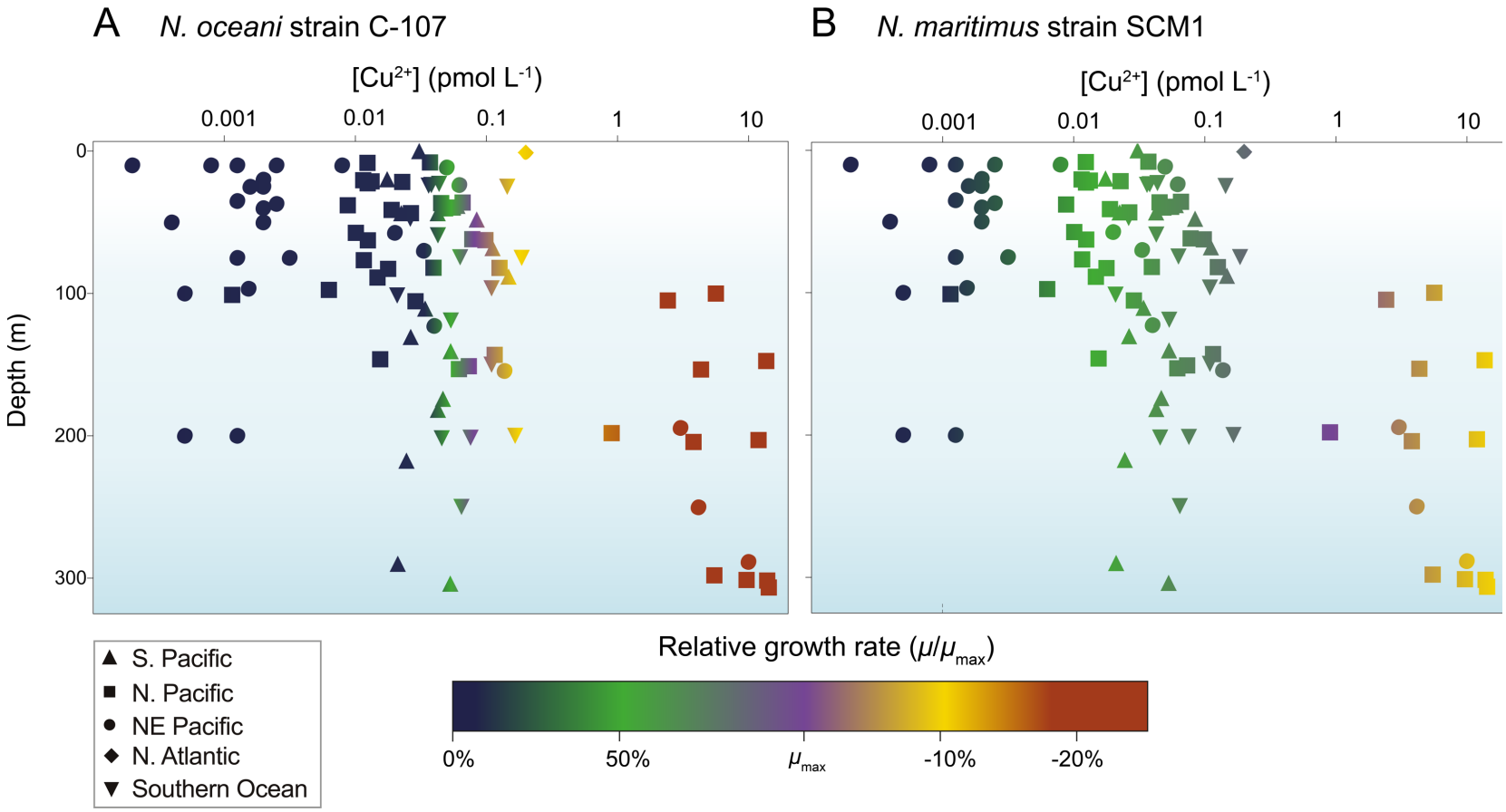


Figure 4.4 Predicted effect of oceanic [Cu^{2+}] on AOA and AOB growth rates based on laboratory growth cultures

Published oceanic cupric ion concentrations ([Cu^{2+}]) (See Appendix III for all references) plotted against a colour gradient reflecting the relative growth rate of **(A)** *N. oceani* strain C-107 and **(B)** *N. maritimus* strain SCM1 in culture at the given [Cu^{2+}]. For instance, at [Cu^{2+}] measured in the North East Pacific (on average between 0.001 – 0.01 pmol L^{-1} Cu^{2+}) no growth of *N. oceani* is observed in culture hence NE Pacific data points are largely dark

blue (no growth). Growth data for *N. oceani* were obtained from this study and data for *N. maritimus* were previously published (Amin et al. 2013).

Copyright © 2021, Shafiee et al.

4.5.2 AOA and AOB trace metal niche separation

As AOB have a lower affinity for NH_4^+ compared with AOA (Martens-Habbena et al. 2009) it follows that AOB must occupy a niche with a high NH_4^+ supply to fulfil their NH_4^+ demand. NH_4^+ depth profiles show that NH_4^+ begins to accumulate to appreciable levels within the euphotic zone between 50–100m (Figure 4.5), as light limitation of phytoplankton growth causes NH_4^+ consumption to slow (Gruber, 2008; Diaz & Raimbault, 2000). Compiled depth profiles show that AOB *amoA* abundances also peak below 100m depth (Figure 4.5 and Figure A3.9), shallower than AOA, pointing to the greater role of NH_4^+ supply in governing the vertical distribution of AOB. A need to be proximal to high NH_4^+ supply in shallower waters would force AOB to conform to the trace metal environment of sunlit surface waters: scarce Fe with fierce competition with phytoplankton and heterotrophic bacteria. A high affinity for Fe′ demonstrated in *N. oceani* and the presence of Fe-specific transporters among the wider AOB community (Figure 4.3), suggests that AOB would be effective competitors with marine phytoplankton and bacteria for unchelated Fe in the euphotic zone. AOB would also be able to respond to chronic Fe scarcity in upper surface waters by producing their own siderophores to enhance access to Fe. A niche for AOB in the sunlit upper water column is also supported by evidence indicating that AOB have a higher tolerance to irradiance than AOA (Merbt et al. 2011; French et al. 2012). At shallower depths, AOB would avoid any toxic effects of Cu^{2+} deeper in the water column: below 200m depth [Cu^{2+}] (> 1 pmol L^{-1} Cu^{2+}) is sufficient to cause partial inhibition of *N. oceani* growth in culture (Figure 4.4). The potential for Cu toxicity is supported by observations of environmental genes and transcripts homologous to AOB Cu efflux proteins which show a general scaling between Cu^{2+} concentration (shown in Figure 4.4) and read abundance (Figure A3.12 and

Figure A3.13). For example, highest reads (as a percentage of total reads) are observed in the North Atlantic and North Pacific where Cu^{2+} can reach 0.2 pmol L^{-1} Cu^{2+}.

In addition to explaining why AOA widely outnumber AOB, a higher affinity for NH_4^+ compared with AOB (Martens-Habbena et al. 2009) affords AOA the luxury of occupying greater depths wherein the NH_4^+ supply is lower, but photoinhibitory effects are substantially reduced. Indeed, AOA maxima are commonly at the base of the euphotic zone (Santoro et al. 2010; Newell et al. 2013) deeper than AOB maxima (Figure 4.5 and Figure A3.9). With increasing depth, competition for Fe would lessen as phytoplankton, heterotrophic bacteria and AOB become limited by light, DOC (Kirchman et al. 1990) or NH_4^+, respectively. As such, below the euphotic zone, there would be little selective pressure to develop a high-affinity Fe′ uptake system—reflected in the rarity of inorganic Fe′ transporters among marine AOA and the low steady-state uptake rate of Fe′ in *N. maritimus*. As well as the reduction in competition for Fe, with increasing depth, the water column becomes naturally richer in dissolved Fe as organic matter remineralises (Figure 4.5). The capacity to reduce Fe chelates via a reductive strategy (Shafiee et al. 2019 — Chapter two) would make AOA well adapted to utilise organic Fe chelates from remineralising organic matter, which are heterogeneous in nature (Gledhill & Buck, 2012). An ecological niche driven by Fe remineralisation, which is deeper than N remineralisation, potentially explains why AOA abundances and nitrification rates correlate with depth-integrated primary productivity but often do not respond to additions of NH_4^+ in open-ocean environments (Newell et al. 2013; Shiozaki et al. 2016).

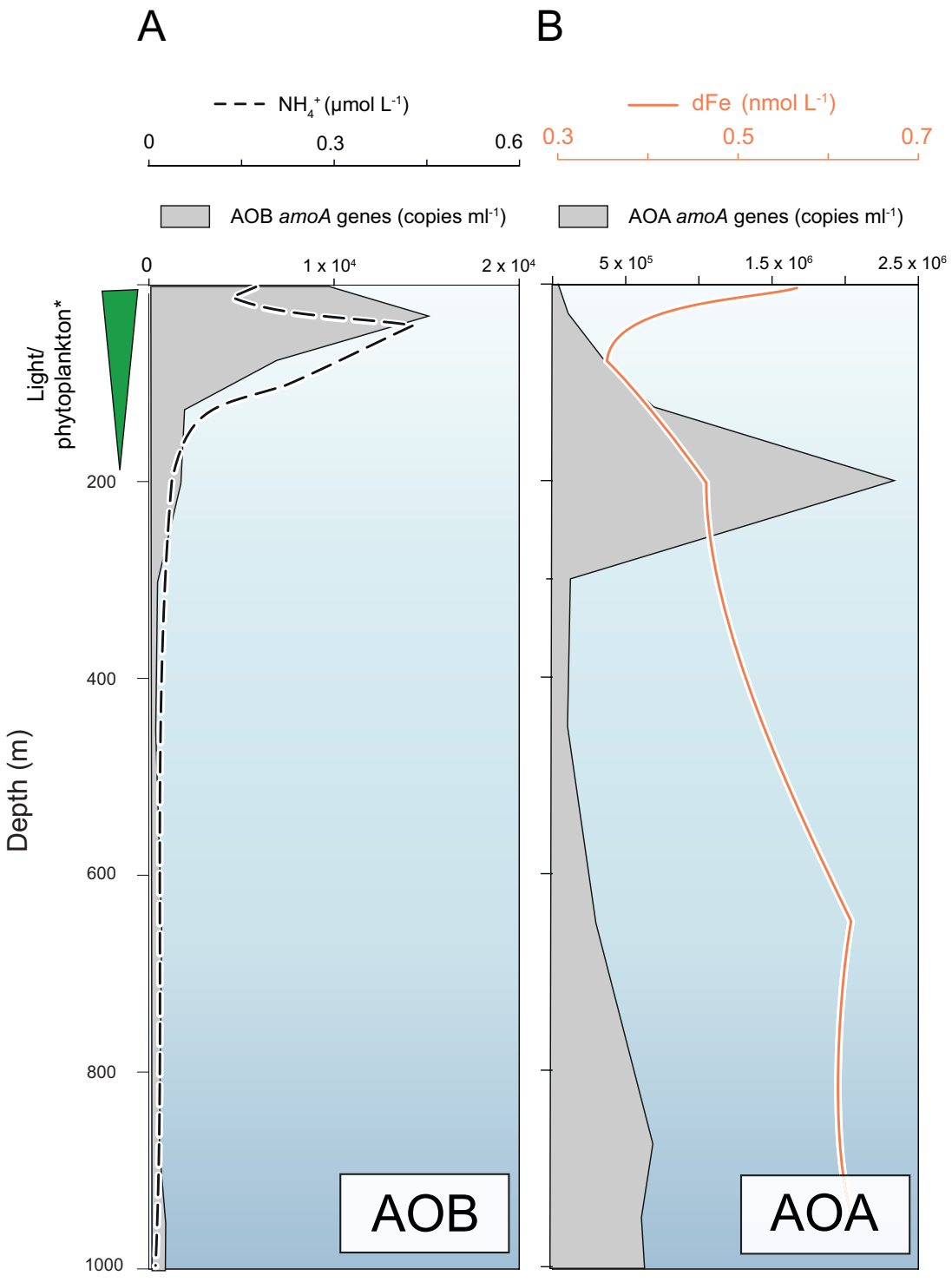


Figure 4.5 Schematic showing hypothesised spatial niches of AOB and AOA

Published *amoA* gene abundance depth profiles (shaded grey area – copies ml^{-1} references provided in Table A3.7) are plotted against NH_4^+ depth profiles (black dashed line - µmol l^{-1} from Gruber, 2008) and dissolved Fe, dFe (orange solid line - nmol L^{-1} , data from GEOTRACES Intermediate Data Product 2017). Green wedge labelled light/phytoplankton* reflects the relative decrease in light, phytoplankton and marine bacteria with increasing depth. AOB *amoA*

sequences are based on those belonging to the Betaproteobacteriales. Copyright © 2021, Shafiee et al.

4.5.3 Geological implications

Molecular clock analyses constrain the timing of marine AOA and AOB emergence to 1084–959 million years ago (Mya) and 1169–596 Mya, (Ward et al. 2021; Ren et al. 2019) respectively. The overlapping error of such approaches demands additional tools to constrain the emergence of archaeal and bacterial ammonia oxidisers. Consideration of evolving trace metal availabilities in the ocean over geologic time offers an approach that may complement molecular clock analyses and provide new insight into the relative timing of the emergence of AOA and AOB. The progressive oxygenation of the oceans over geologic time has driven changes in the bioavailability of essential trace metals, notably enhancing the availability of Cu and Zn due to metal sulphide dissolution but drastically reducing the availability of Fe, Co and Mn that are insoluble under oxic conditions (da Silva & Williams, 2001; Saito et al. 2003). The result is a shift in microbial trace metal usage as organisms evolve to utilise more accessible metals, leaving imprints in the genomes, proteomes and metallomes of extant microorganisms (da Silva & Williams, 2001; Saito et al. 2003; Dupont et al. 2006; Williams & Rickaby, 2012; Zerkle et al. 2005). Considered in this context, a greater metallomic Fe demand at μ_{max} and higher sensitivity to Cu points to an earlier emergence of the AOB and additionally supports a major transition in trace metal availability between 1084 and 596 Mya driven by oxygenation (Saito et al. 2003) to impart such differences in AOA and AOB trace metal composition. Although AOA extensively outnumber AOB in the modern open oceans, the greater availability of Fe may have allowed AOB to play a more prominent role in the Precambrian aerobic N cycle. The role of oxygenation in liberating bio-essential trace metals such as Cu and Mo, thereby lifting limitation of certain metabolic pathways and allowing microorganisms to flourish into new trace metal niches, has previously been suggested for N_2 fixation (Anbar & Knoll, 2002) but may have also influenced

nitrification. A drawdown in bioavailable Fe and increase in Cu availability with oxygenation would allow AOA to proliferate into the newly available chemical niche thereby becoming the key players in the aerobic N cycle, owing to their lower Fe cellular quota at μ_{max} and greater tolerance of Cu. At this point, the contribution of AOB may have been reduced due to their greater Fe demand at μ_{max}, now scarce in a widely oxygenated ocean.

4.6 CONCLUSION

The results presented here provide the first parallel physiological, metallomic and bioinformatic comparison of marine AOA and AOB Fe and Cu requirements. We hypothesise that a greater affinity for unchelated Fe allows AOB to occupy shallower waters to fulfil their high NH_4^+ demand, while the strategy of reducing Fe chelates would make AOA better suited to below the euphotic zone where Fe supply from remineralisation is greater. Further, we posit that the ability of AOA to tolerate a broad range of Cu^{2+} concentrations compared with AOB contributes to the global success of AOA as Cu^{2+} concentrations are highly variable in the marine environment. Considered in the context of evolving trace metal availability over geologic time, our results offer a new perspective to an ongoing debate—suggesting that the greater Fe demand at maximum growth but lower Cu tolerance of AOB compared with AOA is vestigial to the dominance of AOB in the Precambrian when Fe availability was greater, but Cu availability was lower.

4.7 STATEMENT OF AUTHORSHIP

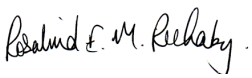
Title of Paper	Marine ammonia-oxidising archaea and bacteria occupy distinct iron and copper niches
Publication Status	✓ **Published** □ Accepted for Publication □ Submitted for Publication work written in a manuscript style □ Unpublished and unsubmitted
Publication Details	Shafiee, R. T., Diver, P. J., Snow, J. T., Zhang, Q., & Rickaby, R. E. (2021). Marine ammonia-oxidising archaea and bacteria occupy distinct iron and copper niches. ISME Communications, 1(1), 1-12.

Student Confirmation

Student Name:	Roxana T Shafiee	
Contribution to the Paper	• Conceived idea (in cooperation with RR, JS) • Made trace metal clean culture media and prepared all acid-cleaned culture apparatus. • Established AOB growth, growth curves and nitrite growth assay (growth rates measured by PD) • Harvested and digested cells for ICP-MS analysis • Analysed cells via ICP-MS (with QZ) • Performed siderophore and reductase experiments • Prepared cells for SEM analysis and performed SEM imaging (with PD) • Analysed growth rate data • Analysed quota data • Performed comparative genomics of metal transporters • Performed analysis of metal-binding genome/proteome • Performed statistical analyses • Made all paper figures/graphs • Compiled gene abundance data/Fe/NH_4^+ biogeochemistry • Discussed/interpretated broad scale implications of results (with PD and RR) • Wrote and revised manuscript in response to reviewers' comments.	
Signature:		**Date:** 21/05/2021

Supervisor Confirmation

By signing the Statement of Authorship, you are certifying that the candidate made a substantial contribution to the publication, and that the description described above is accurate.

Supervisor name:	Professor Rosalind Rickaby	
Supervisor signature:		**Date:** 21/05/2021

5 CONCLUDING REMARKS AND OUTLOOK

The following sections summarise the key findings of this research thesis, the wider significance and contribution of the results and finally the areas in which further research is necessary. In particular, discussion focuses on how the new perspective on trace metals gleaned from this work fits into the wider context of other physicochemical factors known to influence ammonia oxidation in the oceans.

5.1 KEY FINDINGS

The research presented in this thesis brings together approaches in microbial physiology, metallomics, proteomics and comparative genomics to ask if there is physiological precedent for iron (Fe) and copper (Cu) availability to govern the growth, distribution and niche separation of AOA and AOB in the oceans.

In chapter two**, the Fe requirements and uptake strategies of the marine ammonia-oxidising archaeal isolate *Nitrosopumilus maritimus* are examined, in order to understand the potential role of Fe in the growth and distribution of AOA in the oceans.** The results show that *N. maritimus* has the greatest unchelated Fe (Fe′) half-saturation constant for growth of any marine microorganism examined to date. Analyses of the intracellular Fe quota and Fe′ steady-state uptake rate of *N. maritimus* indicate that the high Fe′ required for growth in culture is the result of a low affinity for Fe′ and not an intrinsically great metalloproteomic Fe demand. This physiological result is potentially explained by the lack of Fe-specific transporters encoded in *N. maritimus'* genome. *N. maritimus* cannot synthesise siderophores but can access Fe bound to an organic siderophore (desferrioxamine B) — likely through a reductive uptake mechanism. Using available metagenomic datasets, it is shown that *N. maritimus*-like metal uptake genes are widespread in the marine environment and are likely representative of the Fe-uptake

kinetics among *in-situ* marine AOA communities. Based on these physiological traits, the hypothesis is presented that Fe availability contributes to the vertical niche occupied by AOA in the oceans, characterised by low surface abundances and maxima at the base of the euphotic zone. It is proposed that AOA are outcompeted for Fe in sunlit surface waters by phytoplankton and heterotrophic bacteria with a greater affinity for important Fe substrates. At the base of the euphotic zone, where phytoplankton and heterotrophic bacteria are limited by other physicochemical factors, and Fe is released through organic matter remineralisation, AOA can proliferate. The lack of specificity in AOA Fe-uptake systems supports the evolution of AOA in an environment with low selective pressure to develop sophisticated Fe-uptake strategies.

As the flux of organically-bound Fe delivered to the base of the euphotic zone can be sporadic, AOA may undergo long periods of Fe limitation. Molecular level strategies to cope with prolonged Fe limitation are central to the ecological success of cosmopolitan marine microorganisms. Therefore, as one of the most successful microorganisms in the oceans, the biochemical strategies to deal with Fe limitation may offer insight into how AOA came to be ubiquitous in the modern oceans. Chapter three **examines the proteomic response of *N. maritimus* when limited for Fe, shedding light on the potential molecular strategies adopted by AOA to survive Fe scarcity.** When Fe limits growth, *N. maritimus* primarily minimises Fe demand by reducing Fe-dense ferredoxins, potentially substituting these ferredoxins for Fe-free alternatives. In doing so, Fe-binding proteins which play a more central role in electron transfer and ammonia oxidation can be preferentially retained thereby allowing *N. maritimus* to continue in supporting key energy-yielding pathways under Fe limitation. Additional compensatory strategies within the TCA cycle, biosynthesis and detoxification are also observed, demonstrating efforts to maintain the activity of these pathways whilst significantly reducing Fe requirements.

Further, in response to Fe limitation, there is a significant increase in the intensity of proteins with a putative role in the uptake of exogenous phosphonates. This potentially reflects a strategy to enhance or compensate for a reduction in *N. maritimus*' endogenous methylphosphonate biosynthesis pathway, which requires Fe-binding proteins.

A greater affinity for their shared substrate ammonium (NH_4^+) is typically evoked to explain why AOA widely outnumber AOB in the oligotrophic oceans — yet cannot fully account for the dominance of AOA in high energy environments (e.g., coastal and estuarine environments and select open ocean regimes). In 2005, the first ammonia-oxidising archaeal genome was published — of *N. maritimus* strain SCM1 — revealing numerous copper (Cu)-rich enzymes in lieu of Fe-dense proteins used by AOB. This finding sparked a hypothesis that a Cu rather than Fe-centric metabolism confers AOA with a competitive advantage over AOB in the marine environment where Fe is chronically scarce. **In** chapter four**, the role of Fe and Cu in the niche separation of marine AOA and AOB in oceans is investigated, by characterising and comparing the Fe and Cu requirements of marine AOB with those of AOA at the physiological, metallomic and genomic levels.** Chapter four demonstrates that the marine isolates, *N. maritimus* strain SCM1 (AOA) and *Nitrosococcus oceani* strain C-107 (AOB) have contrasting physiologies in response to Fe and Cu, holding potential implications for their niche separation in the oceans. Growth experiments demonstrate that *N. oceani* is able to grow at lower Fe′ but that *N. maritimus* can grow over a broader range of Cu^{2+} concentrations (Cu data previously published by Amin et al. 2013): showing both a lower limitation and higher toxicity threshold for this trace metal. These data challenge the assertion that the Cu-centric biochemistry of AOA provides a physiological advantage to AOA over AOB in an ocean wherein Fe is exceedingly rare, by showing that an AOB isolate in fact survives better at low Fe′. Using comparative genomics, the proteomic and

trace metal transport basis giving rise to contrasting physiologies in isolates is predicted to be widespread across phylogenetically diverse marine AOA and AOB which are not yet available in pure culture. This suggests that the physiological comparison of marine isolates presented in this thesis may be representative of *in-situ* AOA and AOB communities.

When considered with previously published work on AOA Cu requirements (Amin et al. 2013), the results provide the physiological basis and develop the testable hypothesis that Cu^{2+} availability may limit overall ammonia oxidation rates in large tracts of the open ocean — particularly the NE Pacific. Based on the physiological data, it is hypothesised that Fe and Cu ecophysiologies contribute to the success of AOA over AOB, and the niche separation of these microorganisms. The ability of *N. maritimus* to grow over a broad range of Cu^{2+} is potentially advantageous to AOA in an ocean wherein Cu^{2+} varies over 5 orders of magnitude, providing another line of physiological evidence showing that AOA are well adapted to the open ocean. Contrasting trophic strategies for Cu and Fe provide physiological support for the role of trace metals in the niche separation of AOA and AOB. A greater affinity for unchelated Fe may allow AOB to inhabit shallower, euphotic waters where NH_4^+ supply is high but competition for Fe is rife. The physiological strategy of reducing Fe chelates, demonstrated in *N. maritimus*, would make AOA better suited to living at the base of the euphotic zone where heterogenous Fe supply from remineralisation is greater. A high Fe niche for AOA explains the lack of selective pressure to develop Fe-specific uptake systems (outlined in Chapter two). Finally, the greater cellular Fe demand of AOB at μ_{max} compared with AOA suggests the relatively earlier emergence of AOB than AOA when considered in the context of evolving trace metal availabilities over geologic time.

5.2 TRACE METALS WITHIN THE CONTEXT OF OTHER PHYSICOCHEMICAL FACTORS

The prevailing paradigm is that NH_4^+ and irradiance are the first-order controls on AOA and AOB growth and niche separation in the marine environment. While other factors have also been shown to have quantifiable effects on AOA and AOB growth (summarised in Table 1.1), their role in governing the distribution and niche separation of ammonia oxidisers is generally considered to be less significant than that of NH_4^+ and irradiance (Ward, 2008). In light of this, it may be questioned how significantly trace metals contribute to the growth and niche separation of ammonia oxidisers in the marine environment, compared with and in addition to other physicochemical factors — including NH_4^+, O_2, irradiance and reactive oxygen species (Table 1.1). Is it likely that trace metal availability acts as a first-order control on the growth and niche separation of AOA and AOB in the oceans, as suggested for NH_4^+ and irradiance? How does trace metal availability contribute to AOA/AOB growth and distribution within the wider context of other physicochemical factors known to govern their growth (Table 1.1)?

Of course, without *in-situ* experimentation, it is not possible to answer this question with direct certainty (discussed in greater detail in section 5.4.2). The experiments conducted in this research were performed under energy (NH_4^+) replete conditions and therefore are best suited to provide insight into the role of trace metals in environments where AOA and AOB are not energy limited. On this basis, it can be suggested that trace metal availability likely plays a significant role in governing ammonia oxidation rates in oceanic regimes where NH_4^+ requirements have already been met — particularly where low AOA and AOB abundances have been observed, indicating that additional factors limit growth. For instance, trace metals may play a first-order control on ammonia oxidation in regions such as the NE Pacific, where ammonia oxidation is NH_4^+ saturated but Cu^{2+} has been documented to be scarce (Shiozaki et al. 2016). Trace metal availability

may also play a significant role in AOA and AOB growth in regions where low ammonia oxidation rates are observed despite the euphotic zone being relatively low lit (Beman et al. 2011; Lipschultz et al. 2001). Theoretically NH_4^+ is less likely to be limiting to AOA and AOB in lowly lit surface waters as light-limited phytoplankton reduce their NH_4^+ uptake — therefore trace metals may exert a larger influence on ammonia oxidation in these regions. A pertinent region in which to study these interactions is the Southern Ocean, where light and Fe limitation control phytoplankton NH_4^+ uptake and productivity (Boyd, 2002), theoretically increasing NH_4^+ supply to ammonia oxidisers (Zakem et al. 2018). However, in a similar manner to phytoplankton, Fe scarcity may limit surface AOA and AOB communities (with greater effects felt by AOA) and provoke even greater competition between phytoplankton and ammonia oxidiser communities for this micronutrient.

The research presented here is not able to indicate that trace metals are the *primary* determinants of niche differentiation between AOA and AOB throughout the oligotrophic oceans and energy supply is likely to be the first-order control on the niche separation of ammonia-oxidising microorganisms (Martens-Habbena et al. 2009). Yet the distinct trace metal ecophysiologies demonstrated in this work are still useful in providing potential explanations for *how* AOA and AOB can occupy distinct NH_4^+ niches. This is because trace metal ecophysiologies likely reflect how these microorganisms have conformed to the chemical environment that allows them to best fulfil their NH_4^+ demand. For instance, in chapter four it is predicted that their greater affinity for Fe′ may allow AOB to occupy shallower depths in the water column, wherein they are more likely to fulfil their higher NH_4^+ demand due to the greater rates of ammonification at these depths. In contrast, a higher affinity for NH_4^+, which allows AOA to sit deeper in the water column at the base of the euphotic zone, means that AOA must use more remineralised forms of Fe as

organic matter undergoes remineralisation at these depths. As remineralised Fe is chemically complex and heterogeneous (Hansell, 2013), the ability of AOA to utilise chelated Fe via generalist Fe reductive uptake strategy would allow AOA access to this heterogeneous Fe pool. This suggests that AOA are well adapted to their spatial niche — which is ultimately controlled by NH_4^+ supply. However, distinct trace metal trophic strategies may be more important in regions where NH_4^+ supply is greater — for instance in high energy coastal environments. The ability of AOA isolates to tolerate greater Cu^{2+} compared with AOB isolates provides a potential explanation to why AOA still dominate in coastal regions despite a high NH_4^+ availability theoretically sufficient to support high AOB abundances.

The above discussion outlines the separate effect of NH_4^+ and trace metal requirements, yet it is plausible that NH_4^+ requirements and trace metal acquisition strategies in AOA and AOB are directly linked through the preference for a particle-attached or free-living lifestyle in a similar manner to heterotrophic bacteria (see Section 1.6.2 for further clarification). While initial research indicates that there is likely niche separation both within the AOA and AOB based on preferences for a particle-attached versus planktonic lifestyle, generally AOB appear to show a preference towards a particle-attached lifestyle (Section 1.5.3). By living proximal to particles, AOB would theoretically have greater access to NH_4^+ liberated through the hydrolysing activity of heterotrophic bacteria — allowing them to fulfil their greater NH_4^+ demand. In return, AOB would provide a fixed source of carbon to heterotrophs — outlining the potential for synergistic relationship between ammonia-oxidising microorganisms and heterotrophic bacteria rather than simply competing for Fe resources.

The greater proportion of TonB-dependent transporters in AOB relative to AOA (Chapter four) — known to transport high molecular weight organically-complexed Fe across the cell membrane — aligns with previous research showing that particle-attached heterotrophs utilise TonB-dependent transport more relative to their free-living counterparts. The greater proportion of TonB-dependent transport allows microorganisms to access the high molecular weight Fe complexes (e.g. siderophore bound Fe) associated with particle remineralisation. The ability of AOB to also play an active role in producing siderophores would also allow AOB to effectively sequester inorganic forms of Fe as they become available through the hydrolysing activity of heterotrophs. Further, the ability to take up different inorganic Fe species across AOB genera (Fe^{2+} in the *Nitrosococcus* and Fe^{3+} *Nitrosomonas* and *Nitrosospira*) may allow AOB to occupy distinct Fe microniches on particles, which are known to exhibit gradients in pH and oxygen levels (Alldredge & Cohen, 1987; Ploug et al. 1997) promoting the activity of Fe^{3+} reducing microorganisms to produce Fe^{2+} (Balzano et al. 2009). In either case, further work is needed to clarify the preference for particle-attached versus free-living lifestyle of the AOA and AOB, before these trophic strategies can be linked to the mechanisms for metal uptake as performed in Hogle et al. 2018. This may be investigated, for example, through metagenomic or transcriptomic surveys of AOA and AOB communities obtained from environmental particles or water samples.

The preceding discussion illustrates how trace metals may fit into the wider context of physicochemical factors known to govern the growth and niche separation of ammonia oxidisers, particularly NH_4^+ and irradiance (Table 1.1). Further research will be necessary to corroborate the hypotheses presented here, with *in-situ* and laboratory experimentation looking at the: (1) interrelated but individual contribution of these factors and the (2) interrelated but combined effect of multiple variables (see section 5.4.3).

5.3 CONTRIBUTION AND WIDER SIGNIFICANCE

The work presented in this thesis advances our understanding of the physicochemical factors governing ammonia oxidation in the oceans by showing that there is a physiological basis for trace metals to separate the marine AOA and AOB into distinct niches and limit their growth in some parts of the oceans. By demonstrating trace metal requirements and uptake strategies at the physiological level, the research presented here goes further in characterising the role of trace metals in AOA/AOB ecophysiology in a way that has not been previously possible through comparative genomic analyses alone. While it will be essential to corroborate the results presented here with further strains and *in-situ* experimentation, this work contributes testable hypotheses for future research, particularly by predicting the regions in which Cu^{2+} may widely limit ammonia oxidation.

The increasing abundance of marine meta'omic datasets has been met with the ability to map microbial biogeography against gradients in key environmental variables such as nutrients, temperature, O_2 and light. Therefore, it might be asked, what is the purpose of characterising the physiological response of microorganisms to environmental variables in culture? While meta'omic datasets offer a valuable static snapshot of microbial ecology, they lack the dynamic nature of physiological studies. This dynamic aspect makes physiological work central to predicting how microbial communities will respond to ongoing perturbations to ocean chemistry. The work presented in this thesis — characterising the growth response of marine AOA to trace metal availability — is particularly pertinent as trace metal bioavailability is sensitive to changing oceanic pH and oxygenation levels. Given the central role that AOA and AOB play in the biogeochemical N and C cycles (outlined in the Introduction), shifts in the growth and structure of AOA/AOB communities have far-reaching consequences beyond simply the provision of oxidised N in the oceans.

5.4 FUTURE RESEARCH

The research presented here emphasises that there is a clear physiological basis to continue the investigation into the role of trace metals in the growth and niche separation of AOA and AOB — both through laboratory culture work and *in-situ* experimentation. The following sections outline the areas in which work should be prioritised to advance the understanding of the role of trace metals in marine ammonia oxidation.

5.4.1 Pure isolates

Decades of research into phytoplankton trace metal ecophysiology demonstrate vast phenotypic diversity in how microorganisms respond and adapt to trace metal scarcity — even among genetically related groups (Lis et al. 2015a; Lis et al. 2015b; Rocap et al. 2003). It is probable that the trace metal demands and uptake strategies — and therefore ecophysiology — varies *within* the AOA and AOB, as they do between these two groups. For instance, there is emerging evidence that marine AOA group into distinct 'ecotypes' which dominate at different depths (See Box 3) with the potential for trace metal driven niche separation (Santoro et al. 2019). Currently, there are no isolated representatives of the deep-water clade to test this hypothesis. To date, there is only a handful of marine AOA and AOB cultures, and even fewer still which are in the pure culture form necessary to perform the trace metal analyses presented in this research. While this thesis has aimed to overcome some of this limitation using comparative genomics, it will be essential to examine the physiological trace metal requirements of more AOA and AOB isolates — if and when — they become available. Isolating these fastidious microorganisms is a non-trivial task, often taking years of meticulous work, but will be essential to better understand ammonia-oxidising microorganisms. It will be especially important to examine whether the physiological traits uncovered from this research are prevalent among wider AOA/AOB isolates, through a similar approach to those adopted here. Additionally, by determining the underpinning biochemical and genetic basis which gives rise to the distinct physiologies it will be possible to assess whether trace metal physiologies are likely widespread among AOA/AOB species and strains that cannot be brought into pure culture. The following questions — with suggested experimental means of addressing them — should be prioritised to increase the confidence of the conclusions drawn from this research.

OUTSTANDING QUESTIONS FOR FUTURE RESEARCH

*Questions are followed by potential approache*s

(1) Are other AOA isolates able to utilise organically chelated Fe?

While this study has demonstrated that one AOA isolate can use one type of chemically complexed Fe (likely via a reductive-uptake strategy), it will be essential to examine whether different AOA strains can access a variety of chelated Fe forms. This holds implications for the ability of AOA to access Fe in the marine environment where ~99.9% of Fe is chelated and chelates are chemically heterogenous and complex (Gledhill & Buck, 2012). To examine this, other AOA pure isolates should be cultured in the presence of a range of different chemical forms of organically-complexed Fe (including FeDFB as used in this study) – assessing the growth response in different treatments.

(2) What is the ferric reductase responsible for Fe uptake in AOA?

First and foremost, gene knock-out/knock-down experiments should be performed with the candidate ferric reductases presented in chapter two and chapter three, assessing the ability of *N. maritimus* to grow in the presence of different chemical forms of Fe. The key challenge associated with this work will be developing a genetically tractable *N. maritimus* system in which genes can be manipulated (e.g. through transposon mutagenesis).

(3) How widespread is the reductive Fe-uptake strategy among AOA isolates?

Once the underlying protein/gene responsible for reductase activity has been determined, it can be assessed how widespread its encoding genes are among *in-situ* microbial communities (e.g. by using metagenomic and metatranscriptomic datasets).

(4) What is the role of the increased abundance of phosphonate (PhnD) transporters (shown in chapter three**) under low Fe?**

Firstly, it will be essential to determine whether the increase in phosphonate transporters is an Fe-specific response, by performing similar proteomic analyses under a range of limitation states (e.g. NH_4^+ limitation or Cu^{2+} limitation). Following this, hypotheses presented in chapter three can be tested. For instance, the hypothesis that under low Fe, phosphonates are used in cell surface exopolymeric substances (EPS) to increase Fe binding, can be tested by:

a) Isolating and purifying AOA cell surface EPS associated with Fe-limited and Fe-replete *N. maritimus* cells and measuring the phosphonate content using Nuclear Magnetic Resonance (NMR).

b) Measuring the trace metal concentration of isolated EPS under a spectrum of Fe-physiological states (Fe-limited to very Fe replete) using Inductively Coupled Plasma-Mass Spectrometry (ICP-MS).

c) Finally, determining the strength of Fe binding to the EPS using competitive ligand exchange-adsorptive cathodic stripping voltammetry (CLE-ACSV).

(5) Do other cultured isolates display the same contrasting responses to Fe and Cu as those demonstrated in *N. maritimus* and *N. oceani*?

Particular trends to assess through generating dose-response curves will be:

a) The ability of AOA to grow over a broader range of Cu^{2+}

b) The ability of AOA to grow at low Cu^{2+} but requiring greater Fe′

c) The ability of AOB to grow at low Fe′ but not low Cu^{2+}

It will be particularly important to assess this using AOA and AOB isolates which show the genetic potential to have different physiologies (i.e. *Ca.* N. brevis which has an Fe^{2+} transporter).

(6) What is the mechanism conferring AOA a high Cu^{2+} affinity and resistance to high Cu^{2+}? Is it related to the S-layer in AOA?

This can be assessed using a similar protocol as Gorman-Lewis et al. (2019) in which isothermal titration calorimetry combined with surface complexation modelling is used to assess the role of the AOA S-layer in complexing Cu^{2+} under high Cu^{2+} — compared with the cell surface response of AOB.

5.4.2 *In-situ* experimentation

The primary focus of this work has been to examine whether there is a physiological basis for trace metals to control the growth and niche separation of ammonia-oxidising microorganisms in the oceans. In this regard, this thesis has been successful in showing that the growth of AOA and AOB respond in contrasting ways to the availability of Fe and Cu in a controlled laboratory setting — indicating the potential for their growth limitation and niche separation in the marine environment. These data have allowed for conjecture about how trace metals shape the growth and niche separation of AOA and AOB in the marine environment. Yet *in-situ* experimentation will be ultimately required to corroborate the presented hypotheses. A typical approach to assessing for nutrient limitation *in situ* is the addition of nutrients to a sample taken from the environment — so-called 'bottle' experiments. Bottle incubation experiments can confirm whether the growth of AOA/AOB communities is trace metal limited *in situ*, but these approaches are geographically restricted and often alter the native community composition. However, the potentially Fe-specific proteomic response presented in Chapter three (the

phosphonate transporter, PhnD) highlights a prospective proteomic tool that could be developed to assess Fe limitation across spatial gradients in physicochemical factors using metaproteomic datasets. Additional analyses are required to confirm the role of PhnD in the AOA Fe limitation response and assess whether it is indeed Fe-specific, cross-examining the results presented here with proteomic responses to other stressors (e.g. Cu, NH_4^+ or light).

5.4.3 Multiple variables

The research presented in this thesis isolates the effect of trace metal micronutrients on the growth of marine AOA and AOB isolates in a controlled laboratory setting. In reality, AOA and AOB growth is influenced by a myriad of often interrelated variables, including NH_4^+, light, O_2 and as suggested in this body of work — trace metals. In particular, it is not yet known whether trace metal requirements change under different NH_4^+, O_2 or light regimes. Similar interrelated effects have been demonstrated in phytoplankton, whereby Fe requirements increase under low light (Sunda & Huntsman, 1997). Low O_2 is known to promote distinct pathways in AOA and AOB (nitrifier denitrification and N_2O production – see Box 1), which often utilise different enzymes and trace metal co-factors. Therefore, changing O_2 availability may be associated with a shift in cellular trace metal requirements. As low O_2 pathways are active in oxygen minimum zones (OMZs), where trace metal availability is also altered due to low O_2, there may be combined effects on AOA and AOB growth and community structure. Investigating trace metal requirements under low O_2 will not be a straightforward endeavour, as the techniques adopted to investigate trace metals and O_2 are typically at odds with one another. While trace metal culturing requires acid-washed plasticware to minimise trace metal blanks, anaerobic culturing demands airtight glassware to keep cultures strictly anoxic. However, as AOA/AOB are obligate aerobes, it will not be

necessary to achieve the low O_2 concentrations typically required for obligate anaerobes, providing an opportunity to develop culturing apparatus that can lower O_2 in a trace metal clean fashion. Investigating the interdependence of trace metal requirements and oxygen availability will also provide better insight into the relative emergence and evolution of ammonia oxidation in the early, pre-oxygenated Earth. This combined O_2-trace metal approach is superior to simply altering trace metal availability to its predicted availability in low O_2 environments, which does not consider the effect O_2 may have on the intrinsic metal demand of microorganisms.

5.5 CLOSING REMARKS

This body of work represents a concerted effort to bring trace metal biogeochemical approaches — historically focused on the marine primary producers— to a critically underexplored component of the biogeochemical nitrogen cycle. In doing so, this research demonstrates the utility of cross-fertilising techniques and concepts between disciplines, in this case adopting trace metal clean approaches nearly a century in the making to the microbial ecology of ammonia-oxidising microorganisms. My hope is that this research highlights the absolute imperative and continued relevance of physiology-based characterisations, in a world which is increasingly 'omics centred. When used together, these approaches may unlock the full potential of the other.

6 REFERENCES

Abell, G.C., Revill, A.T., Smith, C., Bissett, A.P., Volkman, J.K. and Robert, S.S., 2010. Archaeal ammonia oxidizers and nirS-type denitrifiers dominate sediment nitrifying and denitrifying populations in a subtropical macrotidal estuary. *The ISME Journal*, *4*(2), pp.286-300.

Abell, G.C., Banks, J., Ross, D.J., Keane, J.P., Robert, S.S., Revill, A.T. and Volkman, J.K., 2011. Effects of estuarine sediment hypoxia on nitrogen fluxes and ammonia oxidizer gene transcription. *FEMS Microbiology Ecology*, *75*(1), pp.111-122.

Adhikari, P., Berish, S.A., Nowalk, A.J., Veraldi, K.L., Morse, S.A. and Mietzner, T.A., 1996. The fbpABC locus of Neisseria gonorrhoeae functions in the periplasm-to-cytosol transport of iron. *Journal of Bacteriology*, *178*(7), pp.2145-2149.

Agogué, H., Brink, M., Dinasquet, J. and Herndl, G.J., 2008. Major gradients in putatively nitrifying and non-nitrifying Archaea in the deep North Atlantic. *Nature*, *456*(7223), pp.788-791.

Ahlgren, N.A., Chen, Y., Needham, D.M., Parada, A.E., Sachdeva, R., Trinh, V., Chen, T. and Fuhrman, J.A., 2017. Genome and epigenome of a novel marine Thaumarchaeota strain suggest viral infection, phosphorothioation DNA modification and multiple restriction systems. *Environmental Microbiology*, *19*(6), pp.2434-2452.

Alldredge, A.L. and Cohen, Y., 1987. Can microscale chemical patches persist in the sea? Microelectrode study of marine snow, fecal pellets. Science, 235(4789), pp.689-691.

Allen, A.E., LaRoche, J., Maheswari, U., Lommer, M., Schauer, N., Lopez, P.J., Finazzi, G., Fernie, A.R. and Bowler, C., 2008. Whole-cell response of the pennate diatom Phaeodactylum tricornutum to iron starvation. *Proceedings of the National Academy of Sciences*, *105*(30), pp.10438-10443.

Alonso-Sáez, L., Waller, A.S., Mende, D.R., Bakker, K., Farnelid, H., Yager, P.L., Lovejoy, C., Tremblay, J.É., Potvin, M., Heinrich, F. and Estrada, M., 2012. Role for urea in nitrification by polar marine Archaea. *Proceedings of the National Academy of Sciences*, *109*(44), pp.17989-17994.

Aluwihare, L.I. and Meador, T., 2008. Chemical composition of marine dissolved organic nitrogen. *Nitrogen in the marine environment*, pp.95-140.

Alves, R.J.E., Minh, B.Q., Urich, T., von Haeseler, A. and Schleper, C., 2018. Unifying the global phylogeny and environmental distribution of ammonia-oxidising archaea based on amoA genes. *Nature Communications*, *9*(1), pp.1-17.

Amin, S.A., Moffett, J.W., Martens-Habbena, W., Jacquot, J.E., Han, Y., Devol, A., Ingalls, A.E., Stahl, D.A. and Armbrust, E.V., 2013. Copper requirements of the ammonia-oxidizing archaeon Nitrosopumilus maritimus SCM1 and implications for nitrification in the marine environment. *Limnology and Oceanography*, *58*(6), pp.2037-2045.

Anbar, A.D., 2008. Elements and evolution. *Science*, *322* (5907), pp.1481-1483.

Anbar, A.D. and Knoll, A.H., 2002. Proterozoic ocean chemistry and evolution: a bioinorganic bridge? *Science*, *297*(5584), pp.1137-1142.

Andreini, C., Cavallaro, G., Lorenzini, S. and Rosato, A., 2012. MetalPDB: a database of metal sites in biological macromolecular structures. *Nucleic Acids Research*, *41:*D312-D319.

Andrews, N.C., 2002. Metal transporters and disease. *Current opinion in chemical biology*, *6*(2), pp.181-186.

Armstrong, R.A., 1999. An optimization-based model of iron—light—ammonium colimitation of nitrate uptake and phytoplankton growth. *Limnology and Oceanography*, *44*(6), pp.1436-1446.

Arp, D.J., Chain, P.S. and Klotz, M.G., 2007. The impact of genome analyses on our understanding of ammonia-oxidizing bacteria. *Annual Review of Microbiology*, 61, pp.503-528.

Arp, D.J., Sayavedra-Soto, L.A. and Hommes, N.G., 2002. Molecular biology and biochemistry of ammonia oxidation by Nitrosomonas europaea. *Archives of Microbiology*, *178*(4), pp.250-255.

Auguet, J.C., Nomokonova, N., Camarero, L. and Casamayor, E.O., 2011. Seasonal changes of freshwater ammonia-oxidizing archaeal assemblages and nitrogen species in oligotrophic alpine lakes. *Applied and Environmental Microbiology*, *77*(6), pp.1937-1945.

Azenha, M., Vasconcelos, M.T. and Cabral, J.P., 1995. Organic ligands reduce copper toxicity in Pseudomonas syringae. *Environmental Toxicology and Chemistry: An International Journal*, *14*(3), pp.369-373.

Balzano, S., Statham, P.J., Pancost, R.D. and Lloyd, J.R., 2009. Role of microbial populations in the release of reduced iron to the water column from marine aggregates. *Aquatic Microbial Ecology*, 54(3), pp.291-303.

Bano, N. and Hollibaugh, J.T., 2000. Diversity and distribution of DNA sequences with affinity to ammonia-oxidizing bacteria of the β subdivision of the class Proteobacteria in the Arctic Ocean. *Applied and Environmental Microbiology*, *66*(5), pp.1960-1969.

Barbeau, K., 2006. Photochemistry of organic iron (III) complexing ligands in oceanic systems. *Photochemistry and Photobiology*, *82*(6), pp.1505-1516.

Bayer, B., Pelikan, C., Bittner, M.J., Reinthaler, T., Könneke, M., Herndl, G.J. and Offre, P., 2019. Proteomic response of three marine ammonia-oxidizing archaea to hydrogen peroxide and their metabolic Interactions with a heterotrophic alphaproteobacterium. *Msystems*, *4*(4), e00181-19.

Bayer, B., Vojvoda, J., Reinthaler, T., Reyes, C., Pinto, M. and Herndl, G.J., 2019. Nitrosopumilus adriaticus sp. nov. and Nitrosopumilus piranensis sp. nov., two ammonia-

oxidizing archaea from the Adriatic Sea and members of the class Nitrososphaeria. *International Journal of Systematic and Evolutionary Microbiology*, 69(7), pp.1892-1902.

Bayer, B., Vojvoda, J., Offre, P., Alves, R.J., Elisabeth, N.H., Garcia, J.A., Volland, J.M., Srivastava, A., Schleper, C. and Herndl, G.J., 2016. Physiological and genomic characterization of two novel marine thaumarchaeal strains indicates niche differentiation. *The ISME Journal, 10*(5), pp.1051-1063.

Beman, J.M., Chow, C.E., King, A.L., Feng, Y., Fuhrman, J.A., Andersson, A., Bates, N.R., Popp, B.N. and Hutchins, D.A., 2011. Global declines in oceanic nitrification rates as a consequence of ocean acidification. *Proceedings of the National Academy of Sciences*, *108*(1), pp.208-213.

Beman, J.M., Popp, B.N. and Francis, C.A., 2008. Molecular and biogeochemical evidence for ammonia oxidation by marine Crenarchaeota in the Gulf of California. *The ISME Journal*, *2*(4), pp.429-441.

Berg, C., Vandieken, V., Thamdrup, B. and Jürgens, K., 2015. Significance of archaeal nitrification in hypoxic waters of the Baltic Sea. *The ISME Journal*, *9*(6), pp.1319-1332.

Berg, G.M., Balode, M., Purina, I., Bekere, S., Béchemin, C. and Maestrini, S.Y., 2003. Plankton community composition in relation to availability and uptake of oxidized and reduced nitrogen. *Aquatic Microbial Ecology*, *30*(3), pp.263-274.

Berg, I.A., Kockelkorn, D., Buckel, W. and Fuchs, G., 2007. A 3-hydroxypropionate/4-hydroxybutyrate autotrophic carbon dioxide assimilation pathway in Archaea. *Science*, *318*(5857), pp.1782-1786.

Bergquist, B.A. and Boyle, E.A., 2006. Dissolved iron in the tropical and subtropical Atlantic Ocean. *Global Biogeochemical Cycles*, *20*(1).

Bergquist, B.A., Wu, J. and Boyle, E.A., 2007. Variability in oceanic dissolved iron is dominated by the colloidal fraction. *Geochimica et Cosmochimica Acta*, 71(12), pp.2960-2974.

Berman-Frank, I., Cullen, J.T., Shaked, Y., Sherrell, R.M. and Falkowski, P.G., 2001. Iron availability, cellular iron quotas, and nitrogen fixation in Trichodesmium. *Limnology and Oceanography*, *46*(6), pp.1249-1260.

Berman-Frank, I., Quigg, A., Finkel, Z.V., Irwin, A.J. and Haramaty, L., 2007. Nitrogen-fixation strategies and Fe requirements in cyanobacteria. *Limnology and Oceanography*, *52*(5), pp.2260-2269.

Bernhard, A.E. and Bollmann, A., 2010. Estuarine nitrifiers: new players, patterns and processes. *Estuarine, Coastal and Shelf Science*, *88*(1), pp.1-11.

Bernhard, A.E., Landry, Z.C., Blevins, A., José, R., Giblin, A.E. and Stahl, D.A., 2010. Abundance of ammonia-oxidizing archaea and bacteria along an estuarine salinity gradient in

relation to potential nitrification rates. *Applied and Environmental Microbiology*, *76*(4), pp.1285-1289.

Bertagnolli, A.D. and Stewart, F.J., 2018. Microbial niches in marine oxygen minimum zones. *Nature Reviews Microbiology*, *16*(12), pp.723-729.

Besaury, L., Ghiglione, J.F. and Quillet, L., 2014. Abundance, activity, and diversity of archaeal and bacterial communities in both uncontaminated and highly copper-contaminated marine sediments. *Marine Biotechnology*, *16*(2), pp.230-242.

Bianchi, M., Fosset, C. and Conan, P., 1999. Nitrification rates in the NW Mediterranean Sea. *Aquatic Microbial Ecology*, *17*(3), pp.267-278.

Blaby-Haas, C.E. and Merchant, S.S., 2012. The ins and outs of algal metal transport. *Biochimica et Biophysica Acta (BBA)-Molecular Cell Research*, *1823*(9), pp.1531-1552.

Blainey, P.C., Mosier, A.C., Potanina, A., Francis, C.A. and Quake, S.R., 2011. Genome of a low-salinity ammonia-oxidizing archaeon determined by single-cell and metagenomic analysis. *PloS One*, *6*(2), p.e16626.

Boatman, T.G., Oxborough, K., Gledhill, M., Lawson, T. and Geider, R.J., 2018. An integrated response of Trichodesmium erythraeum IMS101 growth and photo-physiology to iron, CO2, and light intensity. *Frontiers in Microbiology*, *9*, p.624.

Boiteau, R.M., Mende, D.R., Hawco, N.J., McIlvin, M.R., Fitzsimmons, J.N., Saito, M.A., Sedwick, P.N., DeLong, E.F. and Repeta, D.J., 2016. Siderophore-based microbial adaptations to iron scarcity across the eastern Pacific Ocean. *Proceedings of the National Academy of Sciences*, *113*(50), pp.14237-14242.

Botebol, H., Lelandais, G., Six, C., Lesuisse, E., Meng, A., Bittner, L., Lecrom, S., Sutak, R., Lozano, J.C., Schatt, P. and Vergé, V., 2017. Acclimation of a low iron adapted Ostreococcus strain to iron limitation through cell biomass lowering. *Scientific Reports*, *7*(1), pp.1-11.

Bouskill, N.J., Eveillard, D., Chien, D., Jayakumar, A. and Ward, B.B., 2012. Environmental factors determining ammonia-oxidizing organism distribution and diversity in marine environments. *Environmental Microbiology*, *14*(3), pp.714-729.

Boyd, P.W., 2002. Environmental factors controlling phytoplankton processes in the Southern Ocean1. *Journal of Phycology*, *38*(5), pp.844-861.

Boyd, P.W. and Ellwood, M.J., 2010. The biogeochemical cycle of iron in the ocean. *Nature Geoscience*, 3(10), pp.675-682.

Boyd, P.W., Jickells, T., Law, C.S., Blain, S., Boyle, E.A., Buesseler, K.O., Coale, K.H., Cullen, J.J., De Baar, H.J., Follows, M. and Harvey, M., 2007. Mesoscale iron enrichment experiments 1993-2005: synthesis and future directions. *Science*, *315*(5812), pp.612-617.

Boyd, P.W., Law, C.S., Hutchins, D.A., Abraham, E.R., Croot, P.L., Ellwood, M., Frew, R.D., Hadfield, M., Hall, J., Handy, S. and Hare, C., 2005. FeCycle: Attempting an iron biogeochemical budget from a mesoscale SF6 tracer experiment in unperturbed low iron waters. *Global Biogeochemical Cycles*, 19(4).

Boyle, E.A., Edmond, J.M. and Sholkovitz, E.R., 1977. The mechanism of iron removal in estuaries. Geochimica et Cosmochimica Acta, 41(9), pp.1313-1324.

Boyle, E.A., Sclater, F.R. and Edmond, J.M., 1977. The distribution of dissolved copper in the Pacific. *Earth and Planetary Science Letters*, 37(1), pp.38-54.

Brand, L.E., Sunda, W.G. and Guillard, R.R., 1983. Limitation of marine phytoplankton reproductive rates by zinc, manganese, and iron 1. *Limnology and Oceanography*, *28*(6), pp.1182-1198.

Brand, L.E., Sunda, W.G. and Guillard, R.R., 1986. Reduction of marine phytoplankton reproduction rates by copper and cadmium. *Journal of Experimental Marine Biology and Ecology*, *96*(3), pp.225-250.

Braun, V. and Herrmann, C., 2007. Docking of the periplasmic FecB binding protein to the FecCD transmembrane proteins in the ferric citrate transport system of Escherichia coli. *Journal of Bacteriology*, *189*(19), pp.6913-6918.

Bristow, L.A., Dalsgaard, T., Tiano, L., Mills, D.B., Bertagnolli, A.D., Wright, J.J., Hallam, S.J., Ulloa, O., Canfield, D.E., Revsbech, N.P. and Thamdrup, B., 2016. Ammonium and nitrite oxidation at nanomolar oxygen concentrations in oxygen minimum zone waters. *Proceedings of the National Academy of Sciences*, *113*(38), pp.10601-10606.

Brochier-Armanet, C., Boussau, B., Gribaldo, S. and Forterre, P., 2008. Mesophilic Crenarchaeota: proposal for a third archaeal phylum, the Thaumarchaeota. *Nature Reviews Microbiology*, 6(3), pp.245-252.

Bronk, D.A., See, J.H., Bradley, P. and Killberg, L., 2007. DON as a source of bioavailable nitrogen for phytoplankton. *Biogeosciences*, *4*(3), pp.283-296.

Brown, N.L., Barrett, S.R., Camakaris, J., Lee, B.T. and Rouch, D.A., 1995. Molecular genetics and transport analysis of the copper-resistance determinant (pco) from Escherichia coli plasmid pRJ1004. *Molecular Microbiology*, *17*(6), pp.1153-1166.

Brown, M.T., Landing, W.M. and Measures, C.I., 2005. Dissolved and particulate Fe in the western and central North Pacific: Results from the 2002 IOC cruise. *Geochemistry, Geophysics, Geosystems*, 6(10). Q10001.

Bruland, K., and R. Franks. 1983. Mn, Ni, Cu, Zn and Cd in the western North Atlantic, p. 395–414. In C.S. Wong, E. Boyle, K.W. Bruland, J.D. Burton, and E.D. Goldberg [eds.], Trace metals in sea water. Springer US

Brun, P., Vogt, M., Payne, M.R., Gruber, N., O'brien, C.J., Buitenhuis, E.T., Le Quéré, C., Leblanc, K. and Luo, Y.W., 2015. Ecological niches of open ocean phytoplankton taxa. *Limnology and Oceanography*, *60*(3), pp.1020-1038.

Buckley, P.J. and van den Berg, C.M., 1986. Copper complexation profiles in the Atlantic Ocean: A comparative study using electrochemical and ion exchange techniques. *Marine Chemistry*, *19*(3), pp.281-296.

Bundy, R.M., Boiteau, R.M., McLean, C., Turk-Kubo, K.A., McIlvin, M.R., Saito, M.A., Van Mooy, B.A. and Repeta, D.J., 2018. Distinct siderophores contribute to iron cycling in the mesopelagic at station ALOHA. *Frontiers in Marine Science*, *5*, p.61.

Burton, S.A. and Prosser, J.I., 2001. Autotrophic ammonia oxidation at low pH through urea hydrolysis. *Applied and Environmental Microbiology*, 67(7), pp.2952-2957.

Campbell, L., Liu, H., Nolla, H.A. and Vaulot, D., 1997. Annual variability of phytoplankton and bacteria in the subtropical North Pacific Ocean at Station ALOHA during the 1991–1994 ENSO event. *Deep Sea Research Part I: Oceanographic Research Papers*, *44*(2), pp.167-192.

Canfield, D.E., Glazer, A.N. and Falkowski, P.G., 2010. The evolution and future of Earth's nitrogen cycle. *Science*, *330*(6001), pp.192-196.

Caranto, J.D. and Lancaster, K.M., 2017. Nitric oxide is an obligate bacterial nitrification intermediate produced by hydroxylamine oxidoreductase. *Proceedings of the National Academy of Sciences*, 114(31), pp.8217-8222.

Caranto, J.D., Vilbert, A.C. and Lancaster, K.M., 2016. Nitrosomonas europaea cytochrome P460 is a direct link between nitrification and nitrous oxide emission. *Proceedings of the National Academy of Sciences*, *113*(51), pp.14704-14709.

Carini, P., Dupont, C.L. and Santoro, A.E., 2018. Patterns of thaumarchaeal gene expression in culture and diverse marine environments. *Environmental Microbiology*, *20*(6), pp.2112-2124.

Casciotti, K.L. and Ward, B.B., 2001. Dissimilatory nitrite reductase genes from autotrophic ammonia-oxidizing bacteria. *Applied and Environmental Microbiology*, *67*(5), pp.2213-2221.

Casciotti, K.L. and Ward, B.B., 2005. Phylogenetic analysis of nitric oxide reductase gene homologues from aerobic ammonia-oxidizing bacteria. *FEMS Microbiology Ecology*, *52*(2), pp.197-205.

Cavagna, A.J., Fripiat, F., Elskens, M., Mangion, P., Chirurgien, L., Closset, I., Lasbleiz, M., Florez-Leiva, L., Cardinal, D., Leblanc, K. and Fernandez, C., 2015. Production regime and associated N cycling in the vicinity of Kerguelen Island, Southern Ocean. *Biogeosciences*, *12*(21), pp.6515-6528.

Chappell, P.D. and Webb, E.A., 2010. A molecular assessment of the iron stress response in the two phylogenetic clades of Trichodesmium. *Environmental Microbiology*, *12*(1), pp.13-27.

Chappell, P.D., Whitney, L.P., Wallace, J.R., Darer, A.I., Jean-Charles, S. and Jenkins, B.D., 2015. Genetic indicators of iron limitation in wild populations of Thalassiosira oceanica from the northeast Pacific Ocean. *The ISME journal*, *9*(3), pp.592-602.

Church, M.J., DeLong, E.F., Ducklow, H.W., Karner, M.B., Preston, C.M. and Karl, D.M., 2003. Abundance and distribution of planktonic Archaea and Bacteria in the waters west of the Antarctic Peninsula. *Limnology and Oceanography*, *48*(5), pp.1893-1902.

Church, M.J., Hutchins, D.A. and Ducklow, H.W., 2000. Limitation of bacterial growth by dissolved organic matter and iron in the Southern Ocean. *Applied and Environmental Microbiology*, *66*(2), pp.455-466.

Church, M.J., Wai, B., Karl, D.M. and DeLong, E.F., 2010. Abundances of crenarchaeal amoA genes and transcripts in the Pacific Ocean. *Environmental Microbiology*, *12*(3), pp.679-688.

Clark, D.R., Rees, A.P. and Joint, I., 2008. Ammonium regeneration and nitrification rates in the oligotrophic Atlantic Ocean: Implications for new production estimates. *Limnology and Oceanography*, *53*(1), pp.52-62.

Clark, L.L., Ingall, E.D. and Benner, R., 1999. Marine organic phosphorus cycling; novel insights from nuclear magnetic resonance. *American Journal of Science*, *299*(7-9), pp.724-737.

Coale, K.H. and Bruland, K.W., 1988. Copper complexation in the Northeast Pacific. *Limnology and Oceanography*, *33*(5), pp.1084-1101.

Coale, K.H. and Bruland, K.W., 1990. Spatial and temporal variability in copper complexation in the North Pacific. *Deep Sea Research Part A. Oceanographic Research Papers*, *37*(2), pp.317-336.

Cochlan, W.P., 2001. The heterotrophic bacterial response during a mesoscale iron enrichment experiment (IronEx II) in the eastern equatorial Pacific Ocean. *Limnology and Oceanography*, *46*(2), pp.428-435.

Cohan, F.M., 2001. Bacterial species and speciation. *Systematic biology*, *50*(4), pp.513-524.

Cohen, N.R., Gong, W., Moran, D.M., McIlvin, M.R., Saito, M.A. and Marchetti, A., 2018. Transcriptomic and proteomic responses of the oceanic diatom Pseudo-nitzschia granii to iron limitation. *Environmental Microbiology*, *20*(8), pp.3109-3126.

Cook, A.M., Daughton, C.G. and Alexander, M., 1978. Phosphonate utilization by bacteria. *Journal of Bacteriology*, *133*(1), pp.85-90.

Coulton, J.W., Mason, P.A. and Allatt, D.D., 1987. fhuC and fhuD genes for iron (III)-ferrichrome transport into Escherichia coli K-12. *Journal of Bacteriology*, *169*(8), pp.3844-3849.

Coves, J., Eschenbrenner, M. and Fontecave, M., 1993. Sulfite reductase of Escherichia coli is a ferrisiderophore reductase. *Biochemical and Biophysical Research Communications*, *192*(3), pp.1403-1408.

Cox, J. and Mann, M., 2008. MaxQuant enables high peptide identification rates, individualized ppb-range mass accuracies and proteome-wide protein quantification. *Nature Biotechnology*, *26*(12), pp.1367-1372.

Cox, J., Hein, M.Y., Luber, C.A., Paron, I., Nagaraj, N. and Mann, M., 2014. Accurate proteome-wide label-free quantification by delayed normalization and maximal peptide ratio extraction, termed MaxLFQ. *Molecular & Cellular Proteomics*, *13*(9), pp.2513-2526.

Croot, P.L., Moffett, J.W. and Brand, L.E., 2000. Production of extracellular Cu complexing ligands by eucaryotic phytoplankton in response to Cu stress. *Limnology and Oceanography*, *45*(3), pp.619-627.

Cunningham, B.R. and John, S.G., 2017. The effect of iron limitation on cyanobacteria major nutrient and trace element stoichiometry. *Limnology and Oceanography*, *62*(2), pp.846-858.

Cvetkovic, A., Menon, A.L., Thorgersen, M.P., Scott, J.W., Poole II, F.L., Jenney Jr, F.E., Lancaster, W.A., Praissman, J.L., Shanmukh, S., Vaccaro, B.J. and Trauger, S.A., 2010. Microbial metalloproteomes are largely uncharacterized. *Nature*, *466*(7307), pp.779-782.

Da Silva, J.F. and Williams, R.J.P., 2001. The biological chemistry of the elements: the inorganic chemistry of life. Oxford University Press.

Daims, H., Lebedeva, E.V., Pjevac, P., Han, P., Herbold, C., Albertsen, M., Jehmlich, N., Palatinszky, M., Vierheilig, J., Bulaev, A. and Kirkegaard, R.H., 2015. Complete nitrification by Nitrospira bacteria. *Nature*, *528*(7583), pp.504-509.

Dalsgaard, T., Thamdrup, B. and Canfield, D.E., 2005. Anaerobic ammonium oxidation (anammox) in the marine environment. *Research in Microbiology*, *156*(4), pp.457-464.

De Baar, H.J., Boyd, P.W., Coale, K.H., Landry, M.R., Tsuda, A., Assmy, P., Bakker, D.C., Bozec, Y., Barber, R.T., Brzezinski, M.A. and Buesseler, K.O., 2005. Synthesis of iron fertilization experiments: From the Iron Age in the Age of Enlightenment. *Journal of Geophysical Research: Oceans*, 110(C9).

De Lorenzo, V. and Neilands, J.B., 1986. Characterization of iucA and iucC genes of the aerobactin system of plasmid ColV-K30 in Escherichia coli. *Journal of Bacteriology*, *167*(1), pp.350-355.

DeLong, E.F., 1992. Archaea in coastal marine environments. *Proceedings of the National Academy of Sciences*, *89*(12), pp.5685-5689.

DeLong, E.F., Franks, D.G. and Alldredge, A.L., 1993. Phylogenetic diversity of aggregate-attached vs. free-living marine bacterial assemblages. *Limnology and oceanography*, 38(5), pp.924-934.

Di, H.J., Cameron, K.C., Shen, J.P., Winefield, C.S., O'Callaghan, M., Bowatte, S. and He, J.Z., 2009. Nitrification driven by bacteria and not archaea in nitrogen-rich grassland soils. *Nature Geoscience*, *2*(9), pp.621-624.

Di, H.J., Cameron, K.C., Shen, J.P., Winefield, C.S., O'Callaghan, M., Bowatte, S. and He, J.Z., 2010. Ammonia-oxidizing bacteria and archaea grow under contrasting soil nitrogen conditions. *FEMS Microbiology Ecology*, *72*(3), pp.386-394.

Diaz, F. and Raimbault, P., 2000. Nitrogen regeneration and dissolved organic nitrogen release during spring in a NW Mediterranean coastal zone (Gulf of Lions): implications for the estimation of new production. *Marine Ecology Progress Series*, *197*, pp.51-65.

Donat, J.R. and Bruland, K.W., 1990. A comparison of two voltammetric techniques for determining zinc speciation in Northeast Pacific Ocean waters. *Marine Chemistry*, *28*(4), pp.301-323.

Dore, J.E. and Karl, D.M., 1996. Nitrification in the euphotic zone as a source for nitrite, nitrate, and nitrous oxide at Station ALOHA. *Limnology and Oceanography*, *41*(8), pp.1619-1628.

Doxey, A.C., Kurtz, D.A., Lynch, M.D., Sauder, L.A. and Neufeld, J.D., 2015. Aquatic metagenomes implicate Thaumarchaeota in global cobalamin production. *The ISME Journal*, *9*(2), pp.461-471.

Duce, R.A., Liss, P.S., Merrill, J.T., Atlas, E.L., Buat-Menard, P., Hicks, B.B., Miller, J.M., Prospero, J.M., Arimoto, R.C.T.M., Church, T.M. and Ellis, W., 1991. The atmospheric input of trace species to the world ocean. *Global biogeochemical cycles*, 5(3), pp.193-259.

Duff, A.M., Zhang, L.M. and Smith, C.J., 2017. Small-scale variation of ammonia oxidisers within intertidal sediments dominated by ammonia-oxidising bacteria Nitrosomonas sp. amoA genes and transcripts. *Scientific Reports*, *7*(1), pp.1-13.

Dugdale, R.C. and Goering, J.J., 1967. Uptake of new and regenerated forms of nitrogen in primary productivity 1. *Limnology and Oceanography*, *12*(2), pp.196-206.

Dupont, C.L., Yang, S., Palenik, B. and Bourne, P.E., 2006. Modern proteomes contain putative imprints of ancient shifts in trace metal geochemistry. *Proceedings of the National Academy of Sciences*, *103*(47), pp.17822-17827.

Dupont, C.L., Butcher, A., Valas, R.E., Bourne, P.E. and Caetano-Anollés, G., 2010. History of biological metal utilization inferred through phylogenomic analysis of protein structures. *Proceedings of the National Academy of Sciences*, *107*(23), pp.10567-10572.

Dyhrman, S.T., Chappell, P.D., Haley, S.T., Moffett, J.W., Orchard, E.D., Waterbury, J.B. and Webb, E.A., 2006. Phosphonate utilization by the globally important marine diazotroph Trichodesmium. *Nature*, *439*(7072), pp.68-71.

Eide, D., 1997. Molecular biology of iron and zinc uptake in eukaryotes. *Current Opinion in Cell Biology*, *9*(4), pp.573-577.

Eiler, A., Langenheder, S., Bertilsson, S. and Tranvik, L.J., 2003. Heterotrophic bacterial growth efficiency and community structure at different natural organic carbon concentrations. *Applied and Environmental Microbiology*, *69*(7), pp.3701-3709.

Eldridge, M.L., Trick, C.G., Alm, M.B., DiTullio, G.R., Rue, E.L., Bruland, K.W., Hutchins, D.A. and Wilhelm, S.W., 2004. Phytoplankton community response to a manipulation of bioavailable iron in HNLC waters of the subtropical Pacific Ocean. *Aquatic Microbial Ecology, 35*(1), pp.79-91.

Erdner, D.L., Price, N.M., Doucette, G.J., Peleato, M.L. and Anderson, D.M., 1999. Characterization of ferredoxin and flavodoxin as markers of iron limitation in marine phytoplankton. *Marine Ecology Progress Series*, *184*, pp.43-53.

Falkowski, P.G., 1994. The role of phytoplankton photosynthesis in global biogeochemical cycles. *Photosynthesis Research*, *39*(3), pp.235-258.

Fawcett, S.E., Lomas, M.W., Casey, J.R., Ward, B.B. and Sigman, D.M., 2011. Assimilation of upwelled nitrate by small eukaryotes in the Sargasso Sea. *Nature Geoscience*, *4*(10), pp.717-722.

Fawcett, S.E., Ward, B.B., Lomas, M.W. and Sigman, D.M., 2015. Vertical decoupling of nitrate assimilation and nitrification in the Sargasso Sea. *Deep Sea Research Part I: Oceanographic Research Papers*, *103*, pp.64-72.

Feike, J., Jürgens, K., Hollibaugh, J.T., Krüger, S., Jost, G. and Labrenz, M., 2012. Measuring unbiased metatranscriptomics in suboxic waters of the central Baltic Sea using a new in situ fixation system. *The ISME Journal*, *6*(2), pp.461-470.

Fernández, C., Farías, L. and Alcaman, M.E., 2009. Primary production and nitrogen regeneration processes in surface waters of the Peruvian upwelling system. *Progress in Oceanography*, *83*(1-4), pp.159-168.

Fisher, O.S., Kenney, G.E., Ross, M.O., Ro, S.Y., Lemma, B.E., Batelu, S., Thomas, P.M., Sosnowski, V.C., DeHart, C.J., Kelleher, N.L. and Stemmler, T.L., 2018. Characterization of a long-overlooked copper protein from methane-and ammonia-oxidizing bacteria. *Nature Communications*, *9*(1), pp.1-12.

Fitzsimmons, J.N., Conway, T.M., Lee, J.M., Kayser, R., Thyng, K.M., John, S.G. and Boyle, E.A., 2016. Dissolved iron and iron isotopes in the southeastern Pacific Ocean. *Global Biogeochemical Cycles*, *30*(10), pp.1372-1395.

Fontanez, K.M., Eppley, J.M., Samo, T.J., Karl, D.M. and DeLong, E.F., 2015. Microbial community structure and function on sinking particles in the North Pacific Subtropical Gyre. *Frontiers in Microbiology*, *6*, p.469.

Fourquez, M., Devez, A., Schaumann, A., Guéneuguès, A., Jouenne, T., Obernosterer, I. and Blain, S., 2014. Effects of iron limitation on growth and carbon metabolism in oceanic and coastal heterotrophic bacteria. *Limnology and Oceanography*, *59*(2), pp.349-360.

Francis, C.A., Roberts, K.J., Beman, J.M., Santoro, A.E. and Oakley, B.B., 2005. Ubiquity and diversity of ammonia-oxidizing archaea in water columns and sediments of the ocean. *Proceedings of the National Academy of Sciences*, *102*(41), pp.14683-14688.

Franke, S., Grass, G., Rensing, C. and Nies, D.H., 2003. Molecular analysis of the copper-transporting efflux system CusCFBA of Escherichia coli. *Journal of Bacteriology*, *185*(13), pp.3804-3812.

Freing, A., Wallace, D.W. and Bange, H.W., 2012. Global oceanic production of nitrous oxide. *Philosophical Transactions of the Royal Society B: Biological Sciences*, *367*(1593), pp.1245-1255.

French, E., Kozlowski, J.A., Mukherjee, M., Bullerjahn, G. and Bollmann, A., 2012. Ecophysiological characterization of ammonia-oxidizing archaea and bacteria from freshwater. *Applied and Environmental Microbiology*, *78*(16), pp.5773-5780.

Fripiat, F., Elskens, M., Trull, T.W., Blain, S., Cavagna, A.J., Fernandez, C., Fonseca-Batista, D., Planchon, F., Raimbault, P., Roukaerts, A. and Dehairs, F., 2015. Significant mixed layer nitrification in a natural iron-fertilized bloom of the Southern Ocean. *Global Biogeochemical Cycles*, *29*(11), pp.1929-1943.

Fu, F.X., Mulholland, M.R., Garcia, N.S., Beck, A., Bernhardt, P.W., Warner, M.E., Sanudo-Wilhelmy, S.A. and Hutchins, D.A., 2008. Interactions between changing pCO2, N2 fixation, and Fe limitation in the marine unicellular cyanobacterium Crocosphaera. *Limnology and Oceanography*, *53*(6), pp.2472-2484.

Fuhrman, J.A. and Davis, A.A., 1997. Widespread Archaea and novel Bacteria from the deep sea as shown by 16S rRNA gene sequences. *Marine Ecology Progress Series*, *150*, pp.275-285.

Fuhrman, J.A., McCallum, K. and Davis, A.A., 1992. Novel major archaebacterial group from marine plankton. *Nature*, *356*(6365), pp.148-149.

Gaiero, D.M., Probst, J.L., Depetris, P.J., Bidart, S.M. and Leleyter, L., 2003. Iron and other transition metals in Patagonian riverborne and windborne materials: geochemical control and transport to the southern South Atlantic Ocean. *Geochimica et Cosmochimica Acta*, 67(19), pp.3603-3623.

Ganesh, S., Bertagnolli, A.D., Bristow, L.A., Padilla, C.C., Blackwood, N., Aldunate, M., Bourbonnais, A., Altabet, M.A., Malmstrom, R.R., Woyke, T. and Ulloa, O., 2018. Single cell genomic and transcriptomic evidence for the use of alternative nitrogen substrates by anammox bacteria. *The ISME Journal*, *12*(11), pp.2706-2722.

Gehring, A.M., Mori, I. and Walsh, C.T., 1998. Reconstitution and characterization of the Escherichia coli enterobactin synthetase from EntB, EntE, and EntF. *Biochemistry*, *37*(8), pp.2648-2659.

Geider, R. and La Roche, J., 2002. Redfield revisited: variability of C: N: P in marine microalgae and its biochemical basis. *European Journal of Phycology*, *37*(1), pp.1-17.

Glass, J.B., Axler, R.P., Chandra, S. and Goldman, C.R., 2012. Molybdenum limitation of microbial nitrogen assimilation in aquatic ecosystems and pure cultures. *Frontiers in Microbiology*, *3*, p.331.

Gledhill, M. and Buck, K.N., 2012. The organic complexation of iron in the marine environment: a review. *Frontiers in Microbiology*, *3*, p.69.

Gledhill, M. and van den Berg, C.M., 1994. Determination of complexation of iron (III) with natural organic complexing ligands in seawater using cathodic stripping voltammetry. Marine Chemistry, 47(1), pp.41-54.

Glibert, P.M., Wilkerson, F.P., Dugdale, R.C., Raven, J.A., Dupont, C.L., Leavitt, P.R., Parker, A.E., Burkholder, J.M. and Kana, T.M., 2016. Pluses and minuses of ammonium and nitrate uptake and assimilation by phytoplankton and implications for productivity and community composition, with emphasis on nitrogen-enriched conditions. *Limnology and Oceanography*, *61*(1), pp.165-197.

Goreau, T.J., Kaplan, W.A., Wofsy, S.C., McElroy, M.B., Valois, F.W. and Watson, S.W., 1980. Production of NO2-and N2O by nitrifying bacteria at reduced concentrations of oxygen. *Applied and Environmental Microbiology, 40*(3), pp.526-532.

Gorman-Lewis, D., Martens-Habbena, W. and Stahl, D.A., 2014. Thermodynamic characterization of proton-ionizable functional groups on the cell surfaces of ammonia-oxidizing bacteria and archaea. *Geobiology*, *12*(2), pp.157-171.

Gorman-Lewis, D., Martens-Habbena, W. and Stahl, D.A., 2019. Cu (II) adsorption onto ammonia-oxidizing bacteria and archaea. *Geochimica et Cosmochimica Acta*, *255*, pp.127-143.

Grabowski, M.N., Church, M.J. and Karl, D.M., 2008. Nitrogen fixation rates and controls at Stn ALOHA. *Aquatic Microbial Ecology*, *52*(2), pp.175-183.

Granger, J. and Price, N.M., 1999. The importance of siderophores in iron nutrition of heterotrophic marine bacteria. *Limnology and Oceanography*, *44*(3), pp.541-555.

Granger, J. and Ward, B.B., 2003. Accumulation of nitrogen oxides in copper-limited cultures of denitrifying bacteria. *Limnology and Oceanography*, *48*(1), pp.313-318.

Graziano, L.M., Geider, R.J., Li, W.K.W. and Olaizola, M., 1996. Nitrogen limitation of North Atlantic phytoplankton: Analysis of physiological condition in nutrient enrichment experiments. *Aquatic Microbial Ecology*, *11*(1), pp.53-64.

Griess, P., 1879. Griess reagent: a solution of sulphanilic acid and α-naphthylamine in acetic acid which gives a pink colour on reaction with the solution obtained after decomposition of nitrosyl complexes. *Chemische Berichte, 12*, p.427.

Grinter, R. and Lithgow, T., 2019. The structure of the bacterial iron–catecholate transporter Fiu suggests that it imports substrates via a two-step mechanism. *Journal of Biological Chemistry*, *294*(51), pp.19523-19534.

Gruber, N., 2008. The marine nitrogen cycle: overview and challenges. *Nitrogen in the marine environment*, *2*, pp.1-50.

Guidi, L., Jackson, G.A., Stemmann, L., Miquel, J.C., Picheral, M. and Gorsky, G., 2008. Relationship between particle size distribution and flux in the mesopelagic zone. *Deep Sea Research Part I: Oceanographic Research Papers*, *55*(10), pp.1364-1374.

Gustafsson, J.P., 2010. Visual MINTEQ ver. 3.0. http://www2. lwr. kth. se/English/OurSoftware/vminteq/index. htm.

Gutierrez, T., Biller, D.V., Shimmield, T. and Green, D.H., 2012. Metal binding properties of the EPS produced by Halomonas sp. TG39 and its potential in enhancing trace element bioavailability to eukaryotic phytoplankton. *Biometals*, *25*(6), pp.1185-1194.

Gwak, J.H., Jung, M.Y., Hong, H., Kim, J.G., Quan, Z.X., Reinfelder, J.R., Spasov, E., Neufeld, J.D., Wagner, M. and Rhee, S.K., 2020. Archaeal nitrification is constrained by copper complexation with organic matter in municipal wastewater treatment plants. *The ISME Journal*, *14*(2), pp.335-346.

Hallam, S.J., Mincer, T.J., Schleper, C., Preston, C.M., Roberts, K., Richardson, P.M. and DeLong, E.F., 2006. Pathways of carbon assimilation and ammonia oxidation suggested by environmental genomic analyses of marine Crenarchaeota. *PLoS Biol, 4*(4), p.e95.

Hamm, C.E., Merkel, R., Springer, O., Jurkojc, P., Maier, C., Prechtel, K. and Smetacek, V., 2003. Architecture and material properties of diatom shells provide effective mechanical protection. *Nature*, *421*(6925), pp.841-843.

Hansell, D.A., 2013. Recalcitrant dissolved organic carbon fractions. Annual Review of Marine Science, 5, pp.421-445.

Hansen, J.I., Henriksen, K. and Blackburn, T.H., 1981. Seasonal distribution of nitrifying bacteria and rates of nitrification in coastal marine sediments. *Microbial Ecology*, *7*(4), pp.297-304.

Hassler, C.S. and Schoemann, V., 2009. Bioavailability of organically bound Fe to model phytoplankton of the Southern Ocean. *Biogeosciences*, *6*(10), pp.2281-2296.

Hassler, C.S., Norman, L., Nichols, C.A.M., Clementson, L.A., Robinson, C., Schoemann, V., Watson, R.J. and Doblin, M.A., 2015. Iron associated with exopolymeric substances is highly bioavailable to oceanic phytoplankton. *Marine Chemistry*, *173*, pp.136-147.

Hassler, C.S., Schoemann, V., Nichols, C.M., Butler, E.C. and Boyd, P.W., 2011. Saccharides enhance iron bioavailability to Southern Ocean phytoplankton. *Proceedings of the National Academy of Sciences*, *108*(3), pp.1076-1081.

Hatzenpichler, R., 2012. Diversity, physiology, and niche differentiation of ammonia-oxidizing archaea. *Applied and Environmental Microbiology*, *78*(21), pp.7501-7510

Hatzenpichler, R., Lebedeva, E.V., Spieck, E., Stoecker, K., Richter, A., Daims, H. and Wagner, M., 2008. A moderately thermophilic ammonia-oxidizing crenarchaeote from a hot spring. *Proceedings of the National Academy of Sciences, 105*(6), pp.2134-2139.

Heal, K.R., Qin, W., Ribalet, F., Bertagnolli, A.D., Coyote-Maestas, W., Hmelo, L.R., Moffett, J.W., Devol, A.H., Armbrust, E.V., Stahl, D.A. and Ingalls, A.E., 2017. Two distinct pools of B12 analogs reveal community interdependencies in the ocean. *Proceedings of the National Academy of Sciences*, *114*(2), pp.364-369.

Heggie, D., Klinkhammer, G. and Cullen, D., 1987. Manganese and copper fluxes from continental margin sediments. *Geochimica et Cosmochimica Acta*, 51(5), pp.1059-1070.

Heller, M.I. and Croot, P.L., 2015. Copper speciation and distribution in the Atlantic sector of the Southern Ocean. *Marine Chemistry*, *173*, pp.253-268.

Hogle, S.L., Thrash, J.C., Dupont, C.L. and Barbeau, K.A., 2016. Trace metal acquisition by marine heterotrophic bacterioplankton with contrasting trophic strategies. *Applied and Environmental Microbiology*, *82*(5), pp.1613-1624.

Hollibaugh, J.T., Gifford, S., Sharma, S., Bano, N. and Moran, M.A., 2011. Metatranscriptomic analysis of ammonia-oxidizing organisms in an estuarine bacterioplankton assemblage. *The ISME Journal*, *5*(5), pp.866-878.

Holmes, A.J., Costello, A., Lidstrom, M.E. and Murrell, J.C., 1995. Evidence that participate methane monooxygenase and ammonia monooxygenase may be evolutionarily related. *FEMS Microbiology Letters, 132*(3), pp.203-208.

Holmes, K., Mulholland, F., Pearson, B.M., Pin, C., McNicholl-Kennedy, J., Ketley, J.M. and Wells, J.M., 2005. Campylobacter jejuni gene expression in response to iron limitation and the role of Fur. *Microbiology*, *151*(1), pp.243-257.

Hommes, N.G., Sayavedra-Soto, L.A. and Arp, D.J., 2003. Chemolithoorganotrophic growth of Nitrosomonas europaea on fructose. *Journal of bacteriology*, 185(23), pp.6809-6814.

Hooper, A.B. and Terry, K.R., 1973. Specific inhibitors of ammonia oxidation in Nitrosomonas. *Journal of Bacteriology*, *115*(2), pp.480-485.

Horak, R.E., Qin, W., Bertagnolli, A.D., Nelson, A., Heal, K.R., Han, H., Heller, M., Schauer, A.J., Jeffrey, W.H., Armbrust, E.V. and Moffett, J.W., 2018. Relative impacts of light, temperature, and reactive oxygen on thaumarchaeal ammonia oxidation in the North Pacific Ocean. *Limnology and Oceanography*, *63*(2), pp.741-757.

Horak, R.E., Qin, W., Schauer, A.J., Armbrust, E.V., Ingalls, A.E., Moffett, J.W., Stahl, D.A. and Devol, A.H., 2013. Ammonia oxidation kinetics and temperature sensitivity of a natural marine community dominated by Archaea. *The ISME Journal*, *7*(10), pp.2023-2033.

Horecker, B.L., Tsolas, O.J. and Lai, C.Y., 1972. Aldolases. The Enzymes.

Horrigan, S.G. and Springer, A.L., 1990. Oceanic and estuarine ammonium oxidation: effects of light. *Limnology and Oceanography*, *35*(2), pp.479-482.

Hozuki, T., Ohtsuka, T., Arai, K., Yoshimatsu, K., Tanaka, S. and Fujiwara, T., 2014. Effect of Salinity on Hydroxylamine Oxidation in a Marine Ammonia-Oxidizing Gammaproteobacterium, Nitrosococcus oceani strain NS58: Molecular and Catalytic Properties of Tetraheme Cytochrome c-554. *Microbes and Environments*, *29*(2), p.236.

Hsu, S.C., Wong, G.T., Gong, G.C., Shiah, F.K., Huang, Y.T., Kao, S.J., Tsai, F., Lung, S.C.C., Lin, F.J., Lin, I.I. and Hung, C.C., 2010. Sources, solubility, and dry deposition of aerosol trace elements over the East China Sea. *Marine Chemistry*, 120(1-4), pp.116-127.

Hudson, R.J. and Morel, F.M., 1990. lron transport in marine phytoplankton: Kinetics of cellular and medium coordination reactions. *Limnology and Oceanography*, *35*(5), pp.1002-1020.

Hudson, R.J., Covault, D.T. and Morel, F.M., 1992. Investigations of iron coordination and redox reactions in seawater using 59Fe radiometry and ion-pair solvent extraction of amphiphilic iron complexes. *Marine Chemistry*, *38*(3-4), pp.209-235.

Hughes, C.S., Moggridge, S., Müller, T., Sorensen, P.H., Morin, G.B. and Krijgsveld, J., 2019. Single-pot, solid-phase-enhanced sample preparation for proteomics experiments. *Nature Protocols*, *14*(1), pp.68-85.

Hügler, M. and Sievert, S.M., 2011. Beyond the Calvin cycle: autotrophic carbon fixation in the ocean. *Annual Review of Marine Science, 3,* pp.261-289.

Hutchins, D.A., Hare, C.E., Weaver, R.S., Zhang, Y., Firme, G.F., DiTullio, G.R., Alm, M.B., Riseman, S.F., Maucher, J.M., Geesey, M.E. and Trick, C.G., 2002. Phytoplankton iron limitation in the Humboldt Current and Peru Upwelling. *Limnology and Oceanography*, *47*(4), pp.997-1011.

Hutchins, D.A., Witter, A.E., Butler, A. and Luther, G.W., 1999. Competition among marine phytoplankton for different chelated iron species. *Nature, 400*(6747), pp.858-861.

Hutner, S.H., Provasoli, L., Schatz, A. and Haskins, C.P., 1950. Some approaches to the study of the role of metals in the metabolism of microorganisms. *Proceedings of the American Philosophical Society, 94*(2), pp.152-170.

Ingalls, A.E., Shah, S.R., Hansman, R.L., Aluwihare, L.I., Santos, G.M., Druffel, E.R. and Pearson, A., 2006. Quantifying archaeal community autotrophy in the mesopelagic ocean using natural radiocarbon. *Proceedings of the National Academy of Sciences, 103(*17), pp.6442-6447.

Jacquot, J.E. and Moffett, J.W., 2015. Copper distribution and speciation across the International GEOTRACES Section GA03. *Deep Sea Research Part II: Topical Studies in Oceanography*, 116, pp.187-207.

Jacquot, J.E., Kondo, Y., Knapp, A.N. and Moffett, J.W., 2013. The speciation of copper across active gradients in nitrogen-cycle processes in the eastern tropical South Pacific. *Limnology and Oceanography, 58*(4), pp.1387-1394.

Jang, S. and Imlay, J.A., 2010. Hydrogen peroxide inactivates the Escherichia coli Isc iron-sulphur assembly system, and OxyR induces the Suf system to compensate. *Molecular Microbiology*, *78*(6), pp.1448-1467.

Jia, Z. and Conrad, R., 2009. Bacteria rather than Archaea dominate microbial ammonia oxidation in an agricultural soil. *Environmental Microbiology*, *11*(7), pp.1658-1671.

Jiang, H., Dong, H., Yu, B., Lv, G., Deng, S., Berzins, N. and Dai, M., 2009. Diversity and abundance of ammonia-oxidizing archaea and bacteria in Qinghai Lake, Northwestern China. *Geomicrobiology Journal*, *26*(3), pp.199-211.

Jiang, D., Khunjar, W.O., Wett, B., Murthy, S.N. and Chandran, K., 2015. Characterizing the metabolic trade-off in Nitrosomonas europaea in response to changes in inorganic carbon supply. *Environmental Science & Technology*, *49*(4), pp.2523-2531.

Jin, X., Gruber, N., Dunne, J.P., Sarmiento, J.L. and Armstrong, R.A., 2006. Diagnosing the contribution of phytoplankton functional groups to the production and export of particulate organic carbon, CaCO3, and opal from global nutrient and alkalinity distributions. *Global Biogeochemical Cycles*, *20*(2).

Jing, H., Cheung, S., Xia, X., Suzuki, K., Nishioka, J. and Liu, H., 2017. Geographic distribution of ammonia-oxidizing archaea along the Kuril Islands in the Western Subarctic Pacific. *Frontiers in Microbiology*, *8*, p.1247.

Johnson, K.S., Gordon, R.M. and Coale, K.H., 1997. What controls dissolved iron concentrations in the world ocean? *Marine Chemistry*, *57*(3-4), pp.137-161.

Jordi, A., Basterretxea, G., Tovar-Sánchez, A., Alastuey, A. and Querol, X., 2012. Copper aerosols inhibit phytoplankton growth in the Mediterranean Sea. *Proceedings of the National Academy of Sciences*, 109(52), pp.21246-21249.

Kalvelage, T., Lavik, G., Lam, P., Contreras, S., Arteaga, L., Löscher, C.R., Oschlies, A., Paulmier, A., Stramma, L. and Kuypers, M.M., 2013. Nitrogen cycling driven by organic matter export in the South Pacific oxygen minimum zone. *Nature Geoscience, 6*(3), pp.228-234.

Kanehisa, M., Araki, M., Goto, S., Hattori, M., Hirakawa, M., Itoh, M., Katayama, T., Kawashima, S., Okuda, S., Tokimatsu, T. and Yamanishi, Y., 2007. KEGG for linking genomes to life and the environment. *Nucleic Acids Research*, *36*,pp.D480-D484.

Karner, M.B., DeLong, E.F. and Karl, D.M., 2001. Archaeal dominance in the mesopelagic zone of the Pacific Ocean. *Nature*, *409*(6819), pp.507-510.

Kartal, B., Kuypers, M.M., Lavik, G., Schalk, J., Op den Camp, H.J., Jetten, M.S. and Strous, M., 2007. Anammox bacteria disguised as denitrifiers: nitrate reduction to dinitrogen gas via nitrite and ammonium. *Environmental Microbiology*, *9*(3), pp.635-642.

Katoh, H., Hagino, N. and Ogawa, T., 2001. Iron-binding activity of FutA1 subunit of an ABC-type iron transporter in the cyanobacterium Synechocystis sp. strain PCC 6803. *Plant and Cell Physiology*, *42*(8), pp.823-827.

Kelley, L.A., Mezulis, S., Yates, C.M., Wass, M.N. and Sternberg, M.J., 2015. The Phyre2 web portal for protein modeling, prediction and analysis. *Nature Protocols*, *10*(6), pp.845-858.

Kerou, M., Offre, P., Valledor, L., Abby, S.S., Melcher, M., Nagler, M., Weckwerth, W. and Schleper, C., 2016. Proteomics and comparative genomics of Nitrososphaera viennensis reveal the core genome and adaptations of archaeal ammonia oxidizers. *Proceedings of the National Academy of Sciences*, *113*(49), pp.E7937-E7946.

Keyer, K. and Imlay, J.A., 1996. Superoxide accelerates DNA damage by elevating free-iron levels. *Proceedings of the National Academy of Sciences*, *93*(24), pp.13635-13640.

Kiefer, P., Buchhaupt, M., Christen, P., Kaup, B., Schrader, J. and Vorholt, J.A., 2009. Metabolite profiling uncovers plasmid-induced cobalt limitation under methylotrophic growth conditions. *PLoS One*, *4*(11), p.e7831.

Kim, J.G., Park, S.J., Damsté, J.S.S., Schouten, S., Rijpstra, W.I.C., Jung, M.Y., Kim, S.J., Gwak, J.H., Hong, H., Si, O.J. and Lee, S., 2016. Hydrogen peroxide detoxification is a key mechanism for growth of ammonia-oxidizing archaea. *Proceedings of the National Academy of Sciences*, *113*(28), pp.7888-7893.

Kim, J.W. and Price, N.M., 2017. The influence of light on copper-limited growth of an oceanic diatom, Thalassiosira oceanica (Coscinodiscophyceae). *Journal of Phycology*, *53*(5), pp.938-950.

King, G.M., Smith, C., Tolar, B. and Hollibaugh, J.T., 2013. Analysis of composition and structure of coastal to mesopelagic bacterioplankton communities in the northern Gulf of Mexico. *Frontiers in Microbiology*, *3*, p.438.

Kirchman, D.L., 1994. The uptake of inorganic nutrients by heterotrophic bacteria. *Microbial Ecology*, *28*(2), pp.255-271.

Kirchman, D.L., Keil, R.G. and Wheeler, P.A., 1990. Carbon limitation of ammonium uptake by heterotrophic bacteria in the subarctic Pacific. *Limnology and Oceanography*, *35*(6), pp.1258-1266.

Kirchman, D.L., Meon, B., Cottrell, M.T., Hutchins, D.A., Weeks, D. and Bruland, K.W., 2000. Carbon versus iron limitation of bacterial growth in the California upwelling regime. *Limnology and Oceanography*, *45*(8), pp.1681-1688.

Kitzinger, K., Padilla, C.C., Marchant, H.K., Hach, P.F., Herbold, C.W., Kidane, A.T., Könneke, M., Littmann, S., Mooshammer, M., Niggemann, J. and Petrov, S., 2019. Cyanate and urea are substrates for nitrification by Thaumarchaeota in the marine environment. *Nature Microbiology*, *4*(2), pp.234-243.

Klotz, M.G., Arp, D.J., Chain, P.S., El-Sheikh, A.F., Hauser, L.J., Hommes, N.G., Larimer, F.W., Malfatti, S.A., Norton, J.M., Poret-Peterson, A.T. and Vergez, L.M., 2006. Complete genome sequence of the marine, chemolithoautotrophic, ammonia-oxidizing bacterium Nitrosococcus oceani ATCC 19707. *Applied and Environmental Microbiology*, *72*(9), pp.6299-6315.

Klunder, M.B., Bauch, D., Laan, P., De Baar, H.J., van Heuven, S.M.A.C. and Ober, S., 2012. Dissolved iron in the Arctic shelf seas and surface waters of the central Arctic Ocean: Impact of Arctic river water and ice-melt. *Journal of Geophysical Research: Oceans*, *117*(C1).

Klunder, M.B., Laan, P., Middag, R., De Baar, H.J.W. and Van Ooijen, J.C., 2011. Dissolved iron in the Southern Ocean (Atlantic sector). *Deep Sea Research Part II: Topical Studies in Oceanography*, 58(25-26), pp.2678-2694.

Komori, K., Miyata, T., DiRuggiero, J., Holley-Shanks, R., Hayashi, I., Cann, I.K., Mayanagi, K., Shinagawa, H. and Ishino, Y., 2000. Both RadA and RadB are involved in homologous recombination inPyrococcus furiosus. *Journal of Biological Chemistry*, *275*(43), pp.33782-33790.

Könneke, M., Bernhard, A.E., José, R., Walker, C.B., Waterbury, J.B. and Stahl, D.A., 2005. Isolation of an autotrophic ammonia-oxidizing marine archaeon. *Nature*, *437*(7058), pp.543-546.

Könneke, M., Schubert, D.M., Brown, P.C., Hügler, M., Standfest, S., Schwander, T., von Borzyskowski, L.S., Erb, T.J., Stahl, D.A. and Berg, I.A., 2014. Ammonia-oxidizing archaea use the most energy-efficient aerobic pathway for CO2 fixation. *Proceedings of the National Academy of Sciences*, *111*(22), pp.8239-8244.

Koops, H.P. and Stehr, G., 1991. Classification of eight new species of ammonia-oxidizing bacteria: Nitrosomonas communis sp. nov., Nitrosomonas ureae sp. nov., Nitrosomonas aestuarii sp. nov., Nitrosomonas marina sp. nov., Nitrosomonas nitrosa sp. nov., Nitrosomonas eutropha sp. nov., Nitrosomonas oligotropha sp. nov. and Nitrosomonas halophila sp. nov. *Microbiology*, 137(7), pp.1689-1699.

Korkhov, V.M., Mireku, S.A. and Locher, K.P., 2012. Structure of AMP-PNP-bound vitamin B 12 transporter BtuCD–F. *Nature*, *490*(7420), pp.367-372.

Kowalchuk, G.A. and Stephen, J.R., 2001. Ammonia-oxidizing bacteria: a model for molecular microbial ecology. *Annual Reviews in Microbiology, 55*(1), pp.485-529.

Kozlowski, J.A., Kits, K.D. and Stein, L.Y., 2016. Comparison of nitrogen oxide metabolism among diverse ammonia-oxidizing bacteria. *Frontiers in Microbiology, 7*, p.1090.

Kranzler, C., Lis, H., Shaked, Y. and Keren, N., 2011. The role of reduction in iron uptake processes in a unicellular, planktonic cyanobacterium. *Environmental Microbiology*, *13*(11), pp.2990-2999.

Krapp, A.R., Tognetti, V.B., Carrillo, N. and Acevedo, A., 1997. The Role of Ferredoxin-NADP+ Reductase in the Concerted Cell Defense Against Oxidative Damage: Studies using Escherichia Coli Mutants and Cloned Plant Genes. *European Journal of Biochemistry*, *249*(2), pp.556-563.

Krümmel, A. and Harms, H., 1982. Effect of organic matter on growth and cell yield of ammonia-oxidizing bacteria. *Archives of Microbiology*, 133(1), pp.50-54.

Kuo, Y.M., Zhou, B., Cosco, D. and Gitschier, J., 2001. The copper transporter CTR1 provides an essential function in mammalian embryonic development. *Proceedings of the National Academy of Sciences*, *98*(12), pp.6836-6841.

Kustka, A.B., Allen, A.E. and Morel, F.M., 2007. Sequence analysis and transcriptional regulation of iron acquisition genes in two marine diatoms. *Journal of Phycology*, *43*(4), pp.715-729.

Kuypers, M.M., Marchant, H.K. and Kartal, B., 2018. The microbial nitrogen-cycling network. *Nature Reviews Microbiology*, *16*(5), p.263.

Kwok, E. and Kosman, D., 2005. Iron in yeast: Mechanisms involved in homeostasis. In *Molecular biology of metal homeostasis and detoxification* (pp. 59-99). Springer, Berlin, Heidelberg.

La Roche, J., Boyd, P.W., McKay, R.M.L. and Geider, R.J., 1996. Flavodoxin as an in situ marker for iron stress in phytoplankton. *Nature*, *382*(6594), pp.802-805.

Lam, P. and Kuypers, M.M., 2011. Microbial nitrogen cycling processes in oxygen minimum zones. *Annual Review of Marine Science, 3*, pp.317-345.

Lam, P., Jensen, M.M., Lavik, G., McGinnis, D.F., Müller, B., Schubert, C.J., Amann, R., Thamdrup, B. and Kuypers, M.M., 2007. Linking crenarchaeal and bacterial nitrification to anammox in the Black Sea. *Proceedings of the National Academy of Sciences, 104*(17), pp.7104-7109.

Lam, P., Lavik, G., Jensen, M.M., van de Vossenberg, J., Schmid, M., Woebken, D., Gutiérrez, D., Amann, R., Jetten, M.S. and Kuypers, M.M., 2009. Revising the nitrogen cycle in the Peruvian oxygen minimum zone. *Proceedings of the National Academy of Sciences, 106*(12), pp.4752-4757.

Lane, E.S., Semeniuk, D.M., Strzepek, R.F., Cullen, J.T. and Maldonado, M.T., 2009. Effects of iron limitation on intracellular cadmium of cultured phytoplankton: Implications for surface dissolved cadmium to phosphate ratios. *Marine Chemistry*, *115*(3-4), pp.155-162.

Lannuzel, D., Schoemann, V., De Jong, J., Chou, L., Delille, B., Becquevort, S. and Tison, J.L., 2008. Iron study during a time series in the western Weddell pack ice. *Marine Chemistry*, 108(1-2), pp.85-95.

Laperriere, S.M., Morando, M., Capone, D.G., Gunderson, T., Smith, J.M. and Santoro, A.E., 2020. Nitrification and nitrous oxide dynamics in the Southern California Bight. *Limnology and Oceanography,66*(4), pp.1099-1112.

Lauro, F.M., McDougald, D., Thomas, T., Williams, T.J., Egan, S., Rice, S., DeMaere, M.Z., Ting, L., Ertan, H., Johnson, J. and Ferriera, S., 2009. The genomic basis of trophic strategy in marine bacteria. *Proceedings of the National Academy of Sciences*, 106(37), pp.15527-15533.

Lawton, T.J., Kenney, G.E., Hurley, J.D. and Rosenzweig, A.C., 2016. The CopC family: structural and bioinformatic insights into a diverse group of periplasmic copper binding proteins. *Biochemistry*, *55*(15), pp.2278-2290.

Lehtovirta-Morley, L.E., 2018. Ammonia oxidation: Ecology, physiology, biochemistry and why they must all come together. *FEMS Microbiology Letters*, *365*(9), fny058.

Lehtovirta-Morley, L.E., Stoecker, K., Vilcinskas, A., Prosser, J.I. and Nicol, G.W., 2011. Cultivation of an obligate acidophilic ammonia oxidizer from a nitrifying acid soil. *Proceedings of the National Academy of Sciences*, *108*(38), pp.15892-15897.

Lehtovirta-Morley, L.E., Verhamme, D.T., Nicol, G.W. and Prosser, J.I., 2013. Effect of nitrification inhibitors on the growth and activity of Nitrosotalea devanaterra in culture and soil. *Soil Biology and Biochemistry*, *62*, pp.129-133.

Leininger, S., Urich, T., Schloter, M., Schwark, L., Qi, J., Nicol, G.W., Prosser, J.I., Schuster, S.C. and Schleper, C., 2006. Archaea predominate among ammonia-oxidizing prokaryotes in soils. *Nature*, *442*(7104), pp.806-809.

Levitus, S., Conkright, M.E., Reid, J.L., Najjar, R.G. and Mantyla, A., 1993. Distribution of nitrate, phosphate and silicate in the world oceans. *Progress in Oceanography, 31*(3), pp.245-273.

Li, P.N., Herrmann, J., Tolar, B.B., Poitevin, F., Ramdasi, R., Bargar, J.R., Stahl, D.A., Jensen, G.J., Francis, C.A., Wakatsuki, S. and van den Bedem, H., 2018. Nutrient transport suggests an evolutionary basis for charged archaeal surface layer proteins. *The ISME Journal*, *12*(10), pp.2389-2402.

Li, X., Zhu, Y.G., Cavagnaro, T.R., Chen, M., Sun, J., Chen, X. and Qiao, M., 2009. Do ammonia-oxidizing archaea respond to soil Cu contamination similarly asammonia-oxidizing bacteria? *Plant and Soil*, *324*(1), pp.209-217.

Liochev, S.I. and Fridovich, I., 1994. The role of O2.− in the production of HO.: in vitro and in vivo. *Free Radical Biology and Medicine*, *16*(1), pp.29-33.

Lipschultz, F., 2001. A time-series assessment of the nitrogen cycle at BATS. *Deep Sea Research Part II: Topical Studies in Oceanography, 48*(8-9), pp.1897-1924.

Lipschultz, F., Wofsy, S.C., Ward, B.B., Codispoti, L.A., Friedrich, G. and Elkins, J.W., 1990. Bacterial transformations of inorganic nitrogen in the oxygen-deficient waters of the Eastern Tropical South Pacific Ocean. *Deep Sea Research Part A. Oceanographic Research Papers, 37*(10), pp.1513-1541.

Lis, H., Shaked, Y., Kranzler, C., Keren, N. and Morel, F.M., 2015a. Iron bioavailability to phytoplankton: an empirical approach. *The ISME Journal*, *9*(4), pp.1003-1013.

Lis, H., Kranzler, C., Keren, N. and Shaked, Y., 2015b. A comparative study of iron uptake rates and mechanisms amongst marine and fresh water cyanobacteria: prevalence of reductive iron uptake. *Life*, *5*(1), pp.841-860.

Litchman, E., 2007. Resource competition and the ecological success of phytoplankton. In *Evolution of primary producers in the sea* (pp. 351-375). Academic Press.

Lomas, M.W. and Glibert, P.M., 1999. Temperature regulation of nitrate uptake: A novel hypothesis about nitrate uptake and reduction in cool-water diatoms. *Limnology and Oceanography*, *44*(3), pp.556-572.

Lomas, M.W. and Lipschultz, F., 2006. Forming the primary nitrite maximum: nitrifiers or phytoplankton? *Limnology and Oceanography*, *51*(5), pp.2453-2467.

Lomas, M.W., Lipschultz, F., Nelson, D.M., Krause, J.W. and Bates, N.R., 2009. Biogeochemical responses to late-winter storms in the Sargasso Sea, I—Pulses of primary and new production. *Deep Sea Research Part I: Oceanographic Research Papers, 56*(6), pp.843-860.

López-García, P., Moreira, D., López-López, A. and Rodríguez-Valera, F., 2001. A novel haloarchaeal-related lineage is widely distributed in deep oceanic regions. *Environmental Microbiology, 3*(1), pp.72-78.

Lopez, J.S., Lee, L. and Mackey, K.R., 2019. The toxicity of copper to Crocosphaera watsonii and other marine phytoplankton: a systematic review. *Frontiers in Marine Science*, *5*, p.511.

Löscher, C.R., Kock, A., Könneke, M., LaRoche, J., Bange, H.W. and Schmitz, R.A., 2012. Production of oceanic nitrous oxide by ammonia-oxidizing archaea. *Biogeosciences, 9*(7), pp.2419-2429.

Luo, H., Tolar, B.B., Swan, B.K., Zhang, C.L., Stepanauskas, R., Moran, M.A. and Hollibaugh, J.T., 2014. Single-cell genomics shedding light on marine Thaumarchaeota diversification. *The ISME Journal*, *8*(3), pp.732-736.

Maldonado, M.T. and Price, N.M., 2001. Reduction and transport of organically bound iron by Thalassiosira oceanica (Bacillariophyceae). *Journal of Phycology*, *37*(2), pp.298-310.

Maldonado, M.T., Allen, A.E., Chong, J.S., Lin, K., Leus, D., Karpenko, N. and Harris, S.L., 2006. Copper-dependent iron transport in coastal and oceanic diatoms. *Limnology and Oceanography*, *51*(4), pp.1729-1743.

Maldonado, M.T., Strzepek, R.F., Sander, S. and Boyd, P.W., 2005. Acquisition of iron bound to strong organic complexes, with different Fe binding groups and photochemical reactivities, by plankton communities in Fe-limited subantarctic waters. *Global Biogeochemical Cycles*, *19*(4).

Marchetti, A., Maldonado, M.T., Lane, E.S. and Harrison, P.J., 2006. Iron requirements of the pennate diatom Pseudo-nitzschia: Comparison of oceanic (high-nitrate, low-chlorophyll waters) and coastal species. *Limnology and Oceanography*, *51*(5), pp.2092-2101.

Manck, L.E., Espinoza, J.L., Dupont, C.L. and Barbeau, K.A., 2020. Transcriptomic Study of Substrate-Specific Transport Mechanisms for Iron and Carbon in the Marine Copiotroph Alteromonas macleodii. *MSystems*, 5(2), pp.e00070-20.

Marchetti, A., Schruth, D.M., Durkin, C.A., Parker, M.S., Kodner, R.B., Berthiaume, C.T., Morales, R., Allen, A.E. and Armbrust, E.V., 2012. Comparative metatranscriptomics identifies molecular bases for the physiological responses of phytoplankton to varying iron availability. *Proceedings of the National Academy of Sciences*, *109*(6), pp.E317-E325.

Marchler-Bauer, A., Derbyshire, M.K., Gonzales, N.R., Lu, S., Chitsaz, F., Geer, L.Y., Geer, R.C., He, J., Gwadz, M., Hurwitz, D.I. and Lanczycki, C.J., 2015. CDD: NCBI's conserved domain database. *Nucleic Acids Research*, *43*(D1), pp.D222-D226.

Martens-Habbena, W., Berube, P.M., Urakawa, H., José, R. and Stahl, D.A., 2009. Ammonia oxidation kinetics determine niche separation of nitrifying Archaea and Bacteria. *Nature*, *461*(7266), pp.976-979.

Martens-Habbena, W. and Stahl, D.A., 2011. Nitrogen metabolism and kinetics of ammonia-oxidizing archaea. *Methods in enzymology*, *496*, pp.465-487.

Martens-Habbena, W., Qin, W., Horak, R.E., Urakawa, H., Schauer, A.J., Moffett, J.W., Armbrust, E.V., Ingalls, A.E., Devol, A.H. and Stahl, D.A., 2015. The production of nitric oxide by marine ammonia-oxidizing archaea and inhibition of archaeal ammonia oxidation by a nitric oxide scavenger. *Environmental Microbiology*, *17*(7), pp.2261-2274.

Martin, J.H. and Fitzwater, S.E., 1988. Iron deficiency limits phytoplankton growth in the north-east Pacific subarctic. *Nature*, *331*(6154), pp.341-343.

Martin, J.H. and Gordon, R.M., 1988. Northeast Pacific iron distributions in relation to phytoplankton productivity. Deep Sea Research Part A. Oceanographic Research Papers, 35(2), pp.177-196.

Melis, A., 1989. Spectroscopic methods in photosynthesis: photosystem stoichiometry and chlorophyll antenna size. *Philosophical Transactions of the Royal Society of London. B, Biological Sciences*, *323*(1216), pp.397-409.

Merbt, S.N., Auguet, J.C., Casamayor, E.O. and Marti, E., 2011. Biofilm recovery in a wastewater treatment plant-influenced stream and spatial segregation of ammonia-oxidizing microbial populations. *Limnology and Oceanography*, *56*(3), pp.1054-1064.

Merbt, S.N., Stahl, D.A., Casamayor, E.O., Martí, E., Nicol, G.W. and Prosser, J.I., 2012. Differential photoinhibition of bacterial and archaeal ammonia oxidation. *FEMS Microbiology Letters*, *327*(1), pp.41-46.

Mertens, J., Wakelin, S.A., Broos, K., McLaughlin, M.J. and Smolders, E., 2010. Extent of copper tolerance and consequences for functional stability of the ammonia-oxidizing community in long-term copper-contaminated soils. *Environmental Toxicology and Chemistry*, *29*(1), pp.27-37.

Metcalf, W.W., Griffin, B.M., Cicchillo, R.M., Gao, J., Janga, S.C., Cooke, H.A., Circello, B.T., Evans, B.S., Martens-Habbena, W., Stahl, D.A. and Van Der Donk, W.A., 2012. Synthesis of methylphosphonic acid by marine microbes: a source for methane in the aerobic ocean. *Science*, *337*(6098), pp.1104-1107.

Mills, M.M., Ridame, C., Davey, M., La Roche, J. and Geider, R.J., 2004. Iron and phosphorus co-limit nitrogen fixation in the eastern tropical North Atlantic. *Nature*, *429*(6989), pp.292-294.

Millero, F.J., 1998. Solubility of Fe (III) in seawater. Earth and Planetary Science Letters, 154(1-4), pp.323-329.

Mincer, T.J., Church, M.J., Taylor, L.T., Preston, C., Karl, D.M. and DeLong, E.F., 2007. Quantitative distribution of presumptive archaeal and bacterial nitrifiers in Monterey Bay and the North Pacific Subtropical Gyre. *Environmental Microbiology*, *9*(5), pp.1162-1175.

Moeck, G.S. and Coulton, J.W., 1998. TonB-dependent iron acquisition: mechanisms of siderophore-mediated active transport. *Molecular Microbiology*, *28*(4), pp.675-681.

Moffett, J.W. and Brand, L.E., 1996. Production of strong, extracellular Cu chelators by marine cyanobacteria in response to Cu stress. *Limnology and Oceanography*, *41*(3), pp.388-395.

Moffett, J.W. and Dupont, C., 2007. Cu complexation by organic ligands in the sub-arctic NW Pacific and Bering Sea. *Deep Sea Research Part I: Oceanographic Research Papers*, *54*(4), pp.586-595

Moore, J.K., Doney, S.C., Glover, D.M. and Fung, I.Y., 2001. Iron cycling and nutrient-limitation patterns in surface waters of the World Ocean. *Deep Sea Research Part II: Topical Studies in Oceanography*, 49(1-3), pp.463-507.

Moore, C.M., Mills, M.M., Achterberg, E.P., Geider, R.J., LaRoche, J., Lucas, M.I., McDonagh, E.L., Pan, X., Poulton, A.J., Rijkenberg, M.J. and Suggett, D.J., 2009. Large-scale

distribution of Atlantic nitrogen fixation controlled by iron availability. *Nature Geoscience*, *2*(12), pp.867-871.

Moore, C.M., Mills, M.M., Arrigo, K.R., Berman-Frank, I., Bopp, L., Boyd, P.W., Galbraith, E.D., Geider, R.J., Guieu, C., Jaccard, S.L. and Jickells, T.D., 2013. Processes and patterns of oceanic nutrient limitation. *Nature Geoscience*, *6*(9), pp.701-710.

Moore, C.M., Mills, M.M., Langlois, R., Milne, A., Achterberg, E.P., La Roche, J. and Geider, R.J., 2008. Relative influence of nitrogen and phosphorous availability on phytoplankton physiology and productivity in the oligotrophic sub-tropical North Atlantic Ocean. *Limnology and Oceanography*, *53*(1), pp.291-305.

Moore, J.K., Doney, S.C., Glover, D.M. and Fung, I.Y., 2001. Iron cycling and nutrient-limitation patterns in surface waters of the World Ocean. *Deep Sea Research Part II: Topical Studies in Oceanography, 49*(1-3), pp.463-507.

Moore, L.R., Rocap, G. and Chisholm, S.W., 1998. Physiology and molecular phylogeny of coexisting Prochlorococcus ecotypes. *Nature, 393*(6684), pp.464-467.

Morel, F.M. and Price, N.M., 2003. The biogeochemical cycles of trace metals in the oceans. *Science, 300*(5621), pp.944-947.

Morrissey, J. and Bowler, C., 2012. Iron utilization in marine cyanobacteria and eukaryotic algae. *Frontiers in Microbiology*, *3*, p.43.

Mosier, A.C. and Francis, C.A., 2011. Determining the distribution of marine and coastal ammonia-oxidizing archaea and bacteria using a quantitative approach. *Methods in Enzymology, 486*, pp.205-221.

Mulholland, M.R. and Lomas, M.W., 2008. Nitrogen uptake and assimilation. *Nitrogen in the marine environment*, pp.303-384.

Nachin, L., Nannmark, U. and Nyström, T., 2005. Differential roles of the universal stress proteins of Escherichia coli in oxidative stress resistance, adhesion, and motility. *Journal of Bacteriology*, *187*(18), pp.6265-6272.

Needoba, J.A., Foster, R.A., Sakamoto, C., Zehr, J.P. and Johnson, K.S., 2007. Nitrogen fixation by unicellular diazotrophic cyanobacteria in the temperate oligotrophic North Pacific Ocean. *Limnology and Oceanography, 52*(4), pp.1317-1327.

Newell, S.E., Babbin, A.R., Jayakumar, A. and Ward, B.B., 2011. Ammonia oxidation rates and nitrification in the Arabian Sea. *Global Biogeochemical Cycles*, *25*(4).

Newell, S.E., Fawcett, S.E. and Ward, B.B., 2013. Depth distribution of ammonia oxidation rates and ammonia-oxidizer community composition in the Sargasso Sea. *Limnology and Oceanography*, *58*(4), pp.1491-1500.

Niegowski, D. and Eshaghi, S., 2007. The CorA family: structure and function revisited. *Cellular and Molecular Life Sciences*, *64*(19), pp.2564-2574.

Nishioka, J., Ono, T., Saito, H., Nakatsuka, T., Takeda, S., Yoshimura, T., Suzuki, K., Kuma, K., Nakabayashi, S., Tsumune, D. and Mitsudera, H., 2007. Iron supply to the western subarctic Pacific: Importance of iron export from the Sea of Okhotsk. *Journal of Geophysical Research: Oceans*, 112(C10).

Nyström, T. and Neidhardt, F.C., 1994. Expression and role of the universal stress protein, UspA, of Escherichia coli during growth arrest. *Molecular Microbiology*, *11*(3), pp.537-544.

O'Mullan, G.D. and Ward, B.B., 2005. Relationship of temporal and spatial variabilities of ammonia-oxidizing bacteria to nitrification rates in Monterey Bay, California. *Applied and Environmental Microbiology, 71*(2), pp.697-705.

Odermatt, A., Krapf, R. and Solioz, M., 1994. Induction of the putative copper ATPases, CopA and CopB, of Enterococcus hirae by Ag+ and Cu2+, and Ag+ extrusion by CopB. *Biochemical and Biophysical Research Communications*, *202*(1), pp.44-48.

Olson, R.J., 1981a. ^{15}N tracer studies of the primary nitrite maximum. *Journal of Marine Research, 39*, pp.203-226.

Olson, R.J., 1981b. Differential photoinhibition of marine nitrifying bacteria: a possible mechanism for the formation of the primary nitrite maximum. *Journal of Marine Research, 39,* pp. 227-238.

Outten, F.W., Huffman, D.L., Hale, J.A. and O'Halloran, T.V., 2001. The independent cue and cusSystems confer copper tolerance during aerobic and anaerobic growth inEscherichia coli. *Journal of Biological Chemistry*, *276*(33), pp.30670-30677.

Ozdemir, G., Ozturk, T., Ceyhan, N., Isler, R. and Cosar, T., 2003. Heavy metal biosorption by biomass of Ochrobactrum anthropi producing exopolysaccharide in activated sludge. *Bioresource Technology*, *90*(1), pp.71-74.

Pakulski, J.D., Coffin, R.B., Kelley, C.A., Holder, S.L., Downer, R., Aas, P., Lyons, M.M. and Jeffrey, W.H., 1996. Iron stimulation of Antarctic bacteria. *Nature*, *383*(6596), pp.133-134.

Palatinszky, M., Herbold, C., Jehmlich, N., Pogoda, M., Han, P., von Bergen, M., Lagkouvardos, I., Karst, S.M., Galushko, A., Koch, H. and Berry, D., 2015. Cyanate as an energy source for nitrifiers. *Nature*, *524*(7563), pp.105-108.

Park, S., Bae, W. and Rittmann, B.E., 2010. Operational boundaries for nitrite accumulation in nitrification based on minimum/maximum substrate concentrations that include effects of oxygen limitation, pH, and free ammonia and free nitrous acid inhibition. *Environmental Science & Technology, 44*(1), pp.335-342.

Parks, D.H., Chuvochina, M., Waite, D.W., Rinke, C., Skarshewski, A., Chaumeil, P.A. and Hugenholtz, P., 2018. A standardized bacterial taxonomy based on genome phylogeny substantially revises the tree of life. *Nature biotechnology*, 36(10), pp.996-1004.

Parks, D.H., Chuvochina, M., Chaumeil, P.A., Rinke, C., Mussig, A.J. and Hugenholtz, P., 2020. A complete domain-to-species taxonomy for Bacteria and Archaea. *Nature Biotechnology*, *38*(9), pp.1079-1086.

Peers, G. and Price, N.M., 2006. Copper-containing plastocyanin used for electron transport by an oceanic diatom. *Nature*, *441*(7091), pp.341-344.

Pellitteri-Hahn, M.C., Halligan, B.D., Scalf, M., Smith, L. and Hickey, W.J., 2011. Quantitative proteomic analysis of the chemolithoautotrophic bacterium Nitrosomonas europaea: comparison of growing-and energy-starved cells. *Journal of Proteomics*, *74*(4), pp.411-419.

Peng, X., Fawcett, S.E., Van Oostende, N., Wolf, M.J., Marconi, D., Sigman, D.M. and Ward, B.B., 2018. Nitrogen uptake and nitrification in the subarctic North Atlantic Ocean. *Limnology and Oceanography*, *63*(4), pp.1462-1487.

Peng, X., Fuchsman, C.A., Jayakumar, A., Oleynik, S., Martens-Habbena, W., Devol, A.H. and Ward, B.B., 2015. Ammonia and nitrite oxidation in the Eastern Tropical North Pacific. *Global Biogeochemical Cycles*, *29*(12), pp.2034-2049.

Peng, X., Fuchsman, C.A., Jayakumar, A., Warner, M.J., Devol, A.H. and Ward, B.B., 2016. Revisiting nitrification in the Eastern Tropical South Pacific: a focus on controls. *Journal of Geophysical Research: Oceans*, *121*(3), pp.1667-1684.

Peterson, M.L., Wakeham, S.G., Lee, C., Askea, M.A. and Miquel, J.C., 2005. Novel techniques for collection of sinking particles in the ocean and determining their settling rates. *Limnology and Oceanography: Methods*, *3*(12), pp.520-532.

Phillips, C.J., Smith, Z., Embley, T.M. and Prosser, J.I., 1999. Phylogenetic differences between particle-associated and planktonic ammonia-oxidizing bacteria of the β subdivision of the class Proteobacteria in the northwestern Mediterranean Sea. *Applied and Environmental Microbiology*, 65(2), pp.779-786.

Picaud, S., Kavanagh, K.L., Yue, W.W., Lee, W.H., Muller-Knapp, S., Gileadi, O., Sacchettini, J. and Oppermann, U., 2011. Structural basis of fumarate hydratase deficiency. *Journal of Inherited Metabolic Disease*, *34*(3), pp.671-676.

Planquette, H., Statham, P.J., Fones, G.R., Charette, M.A., Moore, C.M., Salter, I., Nedelec, F.H., Taylor, S.L., French, M., Baker, A.R. and Mahowald, N., 2007. Dissolved iron in the vicinity of the Crozet Islands, Southern Ocean. *Deep Sea Research Part II: Topical Studies in Oceanography*, *54*(18-20), pp.1999-2019.

Ploug, H., Kühl, M., Buchholz-Cleven, B. and Jørgensen, B.B., 1997. Anoxic aggregates-an ephemeral phenomenon in the pelagic environment? Aquatic Microbial Ecology, 13(3), pp.285-294.

Poindexter, J.S., 1981. Oligotrophy. In *Advances in Microbial Ecology* (pp. 63-89). Springer, Boston, MA.

Posacka, A.M., Semeniuk, D.M. and Maldonado, M.T., 2019. Effects of copper availability on the physiology of marine heterotrophic bacteria. *Frontiers in Marine Science*, *5*, p.523.

Powell, S.J. and Prosser, J.I., 1992. Inhibition of biofilm populations of Nitrosomonas europaea. *Microbial Ecology*, *24*(1), pp.43-50.

Price, N.M., Harrison, G.I., Hering, J.G., Hudson, R.J., Nirel, P.M., Palenik, B. and Morel, F.M., 1989. Preparation and chemistry of the artificial algal culture medium Aquil. *Biological Oceanography*, *6*(5-6), pp.443-461.

Prosser, J.I. and Nicol, G.W., 2012. Archaeal and bacterial ammonia-oxidisers in soil: the quest for niche specialisation and differentiation. *Trends in Microbiology*, *20*(11), pp.523-531.

Prosser, J.I., Head, I.M. and Stein, L.Y., 2014. The family Nitrosomonadaceae. In *The Prokaryotes: Alphaproteobacteria and Betaproteobacteria* (pp. 901-918). Springer Berlin/Heidelberg.

Purkhold, U., Wagner, M., Timmermann, G., Pommerening-Röser, A. and Koops, H.P., 2003. 16S rRNA and amoA-based phylogeny of 12 novel betaproteobacterial ammonia-oxidizing isolates: extension of the dataset and proposal of a new lineage within the nitrosomonads. *Journal of Medical Microbiology, 53*(5), pp.1485-1494.

Putignano, V., Rosato, A., Banci, L. and Andreini, C., 2018. MetalPDB in 2018: a database of metal sites in biological macromolecular structures. *Nucleic Acids Research*, *46*(D1), pp.D459-D464.

Qin, W., Amin, S.A., Lundeen, R.A., Heal, K.R., Martens-Habbena, W., Turkarslan, S., Urakawa, H., Costa, K.C., Hendrickson, E.L., Wang, T. and Beck, D.A., 2018. Stress response of a marine ammonia-oxidizing archaeon informs physiological status of environmental populations. *The ISME Journal*, *12*(2), pp.508-519.

Qin, W., Amin, S.A., Martens-Habbena, W., Walker, C.B., Urakawa, H., Devol, A.H., Ingalls, A.E., Moffett, J.W., Armbrust, E.V. and Stahl, D.A., 2014. Marine ammonia-oxidizing archaeal isolates display obligate mixotrophy and wide ecotypic variation. *Proceedings of the National Academy of Sciences*, *111*(34), pp.12504-12509.

Qin, W., Meinhardt, K.A., Moffett, J.W., Devol, A.H., Virginia Armbrust, E., Ingalls, A.E. and Stahl, D.A., 2017a. Influence of oxygen availability on the activities of ammonia-oxidizing archaea. *Environmental Microbiology Reports*, *9*(3), pp.250-256.

Qin, W., Heal, K.R., Ramdasi, R., Kobelt, J.N., Martens-Habbena, W., Bertagnolli, A.D., Amin, S.A., Walker, C.B., Urakawa, H., Könneke, M. and Devol, A.H., 2017b. Nitrosopumilus maritimus gen. nov., sp. nov., Nitrosopumilus cobalaminigenes sp. nov., Nitrosopumilus oxyclinae sp. nov., and Nitrosopumilus ureiphilus sp. nov., four marine ammonia-oxidizing archaea of the phylum Thaumarchaeota. *International Journal of Systematic and Evolutionary Microbiology*, *67*(12), pp.5067-5079.

Qin, W., Zheng, Y., Zhao, F., Wang, Y., Urakawa, H., Martens-Habbena, W., Liu, H., Huang, X., Zhang, X., Nakagawa, T. and Mende, D.R., 2020. Alternative strategies of nutrient acquisition and energy conservation map to the biogeography of marine ammonia-oxidizing archaea. *The ISME Journal*, *14*(10), pp.2595-2609.

Raimbault, P., Slawyk, G., Boudjellal, B., Coatanoan, C., Conan, P., Coste, B., Garcia, N., Moutin, T. and Pujo-Pay, M., 1999. Carbon and nitrogen uptake and export in the equatorial Pacific at 150 W: Evidence of an efficient regenerated production cycle. *Journal of Geophysical Research: Oceans*, *104*(C2), pp.3341-3356.

Raven, J.A., 1988. The iron and molybdenum use efficiencies of plant growth with different energy, carbon and nitrogen sources. *New Phytologist*, *109*(3), pp.279-287.

Rees, A.P., Woodward, E.M.S. and Joint, I., 2006. Concentrations and uptake of nitrate and ammonium in the Atlantic Ocean between 60◦ N and 50◦ S. *Deep Sea Research Part II: Topical Studies in Oceanography*, *53*(14-16), pp.1649-1665.

Reinthaler, T., van Aken, H.M. and Herndl, G.J., 2010. Major contribution of autotrophy to microbial carbon cycling in the deep North Atlantic's interior. *Deep Sea Research Part II: Topical Studies in Oceanography*, *57*(16), pp.1572-1580.

Reji, L., Tolar, B.B., Smith, J.M., Chavez, F.P. and Francis, C.A., 2019. Differential co-occurrence relationships shaping ecotype diversification within Thaumarchaeota populations in the coastal ocean water column. *The ISME Journal, 13(*5), pp.1144-1158.

Ren, M., Feng, X., Huang, Y., Wang, H., Hu, Z., Clingenpeel, S., Swan, B.K., Fonseca, M.M., Posada, D., Stepanauskas, R. and Hollibaugh, J.T., 2019. Phylogenomics suggests oxygen availability as a driving force in Thaumarchaeota evolution. *The ISME Journal, 13*(9), pp.2150-2161.

Reyes, C., Hodgskiss, L.H., Kerou, M., Pribasnig, T., Abby, S.S., Bayer, B., Kraemer, S.M. and Schleper, C., 2020. Genome wide transcriptomic analysis of the soil ammonia oxidizing archaeon Nitrososphaera viennensis upon exposure to copper limitation. *The ISME Journal*, *14*(11), pp.2659-2674.

Richier, S., Macey, A.I., Pratt, N.J., Honey, D.J., Moore, C.M. and Bibby, T.S., 2012. Abundances of iron-binding photosynthetic and nitrogen-fixing proteins of Trichodesmium both in culture and in situ from the North Atlantic. *PLOS One*, *7*(5), p.e35571.

Ridge, P.G., Zhang, Y. and Gladyshev, V.N., 2008. Comparative genomic analyses of copper transporters and cuproproteomes reveal evolutionary dynamics of copper utilization and its link to oxygen. *PLoS One*, *3*(1), p.e1378.

Rijkenberg, M.J., Middag, R., Laan, P., Gerringa, L.J., van Aken, H.M., Schoemann, V., de Jong, J.T. and De Baar, H.J., 2014. The distribution of dissolved iron in the West Atlantic Ocean. *PloS One*, *9*(6), p.e101323.

Rinke, C., Chuvochina, M., Mussig, A.J., Chaumeil, P.A., Waite, D.W., Whitman, W.B., Parks, D.H. and Hugenholtz, P., 2020. A rank-normalized archaeal taxonomy based on genome phylogeny resolves widespread incomplete and uneven classifications. *BioRxiv*.

Robson, R.L., Eady, R.R., Richardson, T.H., Miller, R.W., Hawkins, M. and Postgate, J.R., 1986. The alternative nitrogenase of Azotobacter chroococcum is a vanadium enzyme. *Nature*, *322*(6077), pp.388-390.

Rocap, G., Larimer, F.W., Lamerdin, J., Malfatti, S., Chain, P., Ahlgren, N.A., Arellano, A., Coleman, M., Hauser, L., Hess, W.R. and Johnson, Z.I., 2003. Genome divergence in two Prochlorococcus ecotypes reflects oceanic niche differentiation. *Nature*, *424*(6952), pp.1042-1047.

Rodionov, D.A., Hebbeln, P., Gelfand, M.S. and Eitinger, T., 2006. Comparative and functional genomic analysis of prokaryotic nickel and cobalt uptake transporters: evidence for a novel group of ATP-binding cassette transporters. *Journal of Bacteriology*, *188*(1), pp.317-327.

Rodrigues-Oliveira, T., Belmok, A., Vasconcellos, D., Schuster, B. and Kyaw, C.M., 2017. Archaeal S-layers: overview and current state of the art. *Frontiers in Microbiology*, *8*, p.2597.

Rotthauwe, J.H., Witzel, K.P. and Liesack, W., 1997. The ammonia monooxygenase structural gene amoA as a functional marker: molecular fine-scale analysis of natural ammonia-oxidizing populations. *Applied and Environmental Microbiology, 63*(12), pp.4704-4712.

Roy, E.G., Wells, M.L. and King, D.W., 2008. Persistence of iron (II) in surface waters of the western subarctic Pacific. *Limnology and Oceanography*, *53*(1), pp.89-98.

Rueter, J.G., Ohki, K. and Fujita, Y., 1990. The effect of iron nutrition on photosynthesis and nitrogen fixation in cultures of Trichodesmium (cyanophyceae). *Journal of Phycology, 26*(1), pp.30-35.

Sabine, C.L., Feely, R.A., Gruber, N., Key, R.M., Lee, K., Bullister, J.L., Wanninkhof, R., Wong, C.S.L., Wallace, D.W., Tilbrook, B. and Millero, F.J., 2004. The oceanic sink for anthropogenic CO2. *Science*, *305*(5682), pp.367-371.

Saino, T., Otobe, H., Wada, E. and Hattori, A., 1983. Subsurface ammonium maximum in the northern North Pacific and the Bering Sea in summer. *Deep Sea Research Part A. Oceanographic Research Papers*, *30*(11), pp.1157-1171.

Saito, M.A., McIlvin, M.R., Moran, D.M., Santoro, A.E., Dupont, C.L., Rafter, P.A., Saunders, J.K., Kaul, D., Lamborg, C.H., Westley, M. and Valois, F., 2020. Abundant nitrite-oxidizing metalloenzymes in the mesopelagic zone of the tropical Pacific Ocean. *Nature Geoscience*, *13*(5), pp.355-362.

Saito, M.A., Dorsk, A., Post, A.F., McIlvin, M.R., Rappé, M.S., DiTullio, G.R. and Moran, D.M., 2015. Needles in the blue sea: Sub-species specificity in targeted protein biomarker analyses within the vast oceanic microbial metaproteome. *Proteomics*, *15*(20), pp.3521-3531.

Saito, M.A., McIlvin, M.R., Moran, D.M., Goepfert, T.J., DiTullio, G.R., Post, A.F. and Lamborg, C.H., 2014. Multiple nutrient stresses at intersecting Pacific Ocean biomes detected by protein biomarkers. *Science*, *345*(6201), pp.1173-1177.

Saito, M.A., Sigman, D.M. and Morel, F.M., 2003. The bioinorganic chemistry of the ancient ocean: the co-evolution of cyanobacterial metal requirements and biogeochemical cycles at the Archean–Proterozoic boundary? *Inorganica Chimica Acta*, *356*, pp.308-318.

Sander, S.G. and Koschinsky, A., 2011. Metal flux from hydrothermal vents increased by organic complexation. *Nature Geoscience*, 4(3), pp.145-150.

Santoro, A.E. and Casciotti, K.L., 2011. Enrichment and characterization of ammonia-oxidizing archaea from the open ocean: phylogeny, physiology and stable isotope fractionation. *The ISME Journal*, *5*(11), pp.1796-1808.

Santoro, A.E., Buchwald, C., McIlvin, M.R. and Casciotti, K.L., 2011. Isotopic signature of N2O produced by marine ammonia-oxidizing archaea. *Science*, *333*(6047), pp.1282-1285.

Santoro, A.E., Casciotti, K.L. and Francis, C.A., 2010. Activity, abundance and diversity of nitrifying archaea and bacteria in the central California Current. *Environmental Microbiology*, *12*(7), pp.1989-2006.

Santoro, A.E., Dupont, C.L., Richter, R.A., Craig, M.T., Carini, P., McIlvin, M.R., Yang, Y., Orsi, W.D., Moran, D.M. and Saito, M.A., 2015. Genomic and proteomic characterization of "Candidatus Nitrosopelagicus brevis": an ammonia-oxidizing archaeon from the open ocean. *Proceedings of the National Academy of Sciences*, *112*(4), pp.1173-1178.

Santoro, A.E., Richter, R.A. and Dupont, C.L., 2019. Planktonic marine archaea. *Annual Review of Marine Science*, *11*, pp.131-158.

Santoro, A.E., Saito, M.A., Goepfert, T.J., Lamborg, C.H., Dupont, C.L. and DiTullio, G.R., 2017. Thaumarchaeal ecotype distributions across the equatorial Pacific Ocean and their potential roles in nitrification and sinking flux attenuation. *Limnology and Oceanography*, *62*(5), pp.1984-2003.

Santoro, A.E., Sakamoto, C.M., Smith, J.M., Plant, J.N., Gehman, A.L., Worden, A.Z., Johnson, K.S., Francis, C.A. and Casciotti, K.L., 2013. Measurements of nitrite production in and around the primary nitrite maximum in the central California Current. *Biogeosciences*, *10*(11), pp.7395-7410.

Sára, M. and Sleytr, U.B., 2000. S-layer proteins. *Journal of Bacteriology*, *182*(4), pp.859-868.

Sarthou, G., Vincent, D., Christaki, U., Obernosterer, I., Timmermans, K.R. and Brussaard, C.P., 2008. The fate of biogenic iron during a phytoplankton bloom induced by natural fertilisation: Impact of copepod grazing. *Deep Sea Research Part II: Topical Studies in Oceanography*, 55(5-7), pp.734-751.

Sazinsky, M.H. and Lippard, S.J., 2015. Methane monooxygenase: functionalizing methane at iron and copper. *Sustaining life on planet earth: Metalloenzymes mastering dioxygen and other chewy gases*, pp.205-256.

Schleper, C., Jurgens, G. and Jonuscheit, M., 2005. Genomic studies of uncultivated archaea. *Nature Reviews Microbiology, 3*(6), pp.479-488.

Schneider, S., Sharp, K.H., Barker, P.D. and Paoli, M., 2006. An induced fit conformational change underlies the binding mechanism of the heme transport proteobacteria-protein HemS. *Journal of Biological Chemistry*, *281*(43), pp.32606-32610.

Schulz, K.G., Zondervan, I., Gerringa, L.J.A., Timmermans, K.R., Veldhuis, M.J.W. and Riebesell, U., 2004. Effect of trace metal availability on coccolithophorid calcification. *Nature*, *430*(7000), pp.673-676.

Schwyn, B. and Neilands, J.B., 1987. Universal chemical assay for the detection and determination of siderophores. *Analytical Biochemistry*, *160*(1), pp.47-56.

Sedlacek, C.J., McGowan, B., Suwa, Y., Sayavedra-Soto, L., Laanbroek, H.J., Stein, L.Y., Norton, J.M., Klotz, M.G. and Bollmann, A., 2019. A physiological and genomic comparison of Nitrosomonas cluster 6a and 7 ammonia-oxidizing bacteria. *Microbial ecology*, 78(4), pp.985-994.

Seitz, E.M. and Kowalczykowski, S.C., 2000. The DNA binding and pairing preferences of the archaeal RadA protein demonstrate a universal characteristic of DNA strand exchange proteins. *Molecular Microbiology*, *37*(3), pp.555-560.

Semeniuk, D.M., Bundy, R.M., Posacka, A.M., Robert, M., Barbeau, K.A. and Maldonado, M.T., 2016. Using 67Cu to study the biogeochemical cycling of copper in the Northeast Subarctic Pacific Ocean. *Frontiers in Marine Science*, *3*, p.78.

Sepúlveda Cisternas, I., Salazar, J.C. and García-Angulo, V.A., 2018. Overview on the bacterial iron-riboflavin metabolic axis. *Frontiers in Microbiology*, *9*, p.1478.

Shafiee, R.T., Diver, P.J., Snow, J.T., Zhang, Q. and Rickaby, R.E., 2021a. Marine ammonia-oxidising archaea and bacteria occupy distinct iron and copper niches. *ISME Communications*, *1*(1), pp.1-12.

Shafiee, R.T., Snow, J.T., Hester, S., Zhang, Q. and Rickaby, R.E., 2021b. Proteomic response of the marine ammonia-oxidising archaeon, Nitrosopumilus maritimus to iron limitation reveals strategies to compensate for nutrient scarcity. *Environmental Microbiology*.

Shafiee, R.T., Snow, J.T., Zhang, Q. and Rickaby, R.E., 2019. Iron requirements and uptake strategies of the globally abundant marine ammonia-oxidising archaeon, Nitrosopumilus maritimus SCM1. *The ISME Journal*, *13*(9), pp.2295-2305.

Shaked, Y. and Lis, H., 2012. Disassembling iron availability to phytoplankton. *Frontiers in Microbiology*, *3*, p.123.

Shaked, Y., Kustka, A.B. and Morel, F.M., 2005. A general kinetic model for iron acquisition by eukaryotic phytoplankton. *Limnology and Oceanography*, *50*(3), pp.872-882.

Shaked, Y., Kustka, A.B., Morel, F.M. and Erel, Y., 2004. Simultaneous determination of iron reduction and uptake by phytoplankton. *Limnology and Oceanography: Methods*, *2*(5), pp.137-145.

Shaw, L.J., Nicol, G.W., Smith, Z., Fear, J., Prosser, J.I. and Baggs, E.M., 2006. Nitrosospira spp. can produce nitrous oxide via a nitrifier denitrification pathway. *Environmental Microbiology*, *8*(2), pp.214-222.

Shen, T., Stieglmeier, M., Dai, J., Urich, T. and Schleper, C., 2013. Responses of the terrestrial ammonia-oxidizing archaeon Ca. Nitrososphaera viennensis and the ammonia-oxidizing bacterium Nitrosospira multiformis to nitrification inhibitors. *FEMS Microbiology Letters, 344*(2), pp.121-129.

Shi, D., Kranz, S.A., Kim, J.M. and Morel, F.M., 2012. Ocean acidification slows nitrogen fixation and growth in the dominant diazotroph Trichodesmium under low-iron conditions. *Proceedings of the National Academy of Sciences*, *109*(45), pp.E3094-E3100.

Shi, D., Xu, Y., Hopkinson, B.M. and Morel, F.M., 2010. Effect of ocean acidification on iron availability to marine phytoplankton. *Science*, *327*(5966), pp.676-679.

Shi, T., Sun, Y. and Falkowski, P.G., 2007. Effects of iron limitation on the expression of metabolic genes in the marine cyanobacterium Trichodesmium erythraeum IMS101. *Environmental Microbiology*, *9*(12), pp.2945-2956.

Shi, Y., Tyson, G.W., Eppley, J.M. and DeLong, E.F., 2011. Integrated metatranscriptomic and metagenomic analyses of stratified microbial assemblages in the open ocean. *The ISME Journal*, *5*(6), pp.999-1013.

Shiozaki, T., Ijichi, M., Isobe, K., Hashihama, F., Nakamura, K.I., Ehama, M., Hayashizaki, K.I., Takahashi, K., Hamasaki, K. and Furuya, K., 2016. Nitrification and its influence on biogeochemical cycles from the equatorial Pacific to the Arctic Ocean. *The ISME Journal*, *10*(9), pp.2184-2197.

Shire, D.M. and Kustka, A.B., 2015. Luxury uptake, iron storage and ferritin abundance in Prochlorococcus marinus (Synechococcales) strain MED4. *Phycologia*, *54*(4), pp.398-406.

Silver, S. and Phung, L.T., 2005. A bacterial view of the periodic table: genes and proteins for toxic inorganic ions. *Journal of Industrial Microbiology and Biotechnology*, *32*(11-12), pp.587-605.

Singh, S.K., Grass, G., Rensing, C. and Montfort, W.R., 2004. Cuprous oxidase activity of CueO from Escherichia coli. *Journal of Bacteriology*, *186*(22), pp.7815-7817.

Sintes, E., Bergauer, K., De Corte, D., Yokokawa, T. and Herndl, G.J., 2013. Archaeal amoA gene diversity points to distinct biogeography of ammonia-oxidizing Crenarchaeota in the ocean. *Environmental Microbiology*, *15*(5), pp.1647-1658.

Sintes, E., De Corte, D., Ouillon, N. and Herndl, G.J., 2015. Macroecological patterns of archaeal ammonia oxidizers in the Atlantic Ocean. *Molecular Ecology*, *24*(19), pp.4931-4942.

Sintes, E., De Corte, D., Haberleitner, E. and Herndl, G.J., 2016. Geographic distribution of archaeal ammonia oxidizing ecotypes in the Atlantic Ocean. *Frontiers in Microbiology*, *7*, p.77.

Smith, J.M., Chavez, F.P. and Francis, C.A., 2014. Ammonium uptake by phytoplankton regulates nitrification in the sunlit ocean. *PloS One*, *9*(9), p.e108173.

Smith, K.L., Robison, B.H., Helly, J.J., Kaufmann, R.S., Ruhl, H.A., Shaw, T.J., Twining, B.S. and Vernet, M., 2007. Free-drifting icebergs: hot spots of chemical and biological enrichment in the Weddell Sea. *Science*, 317(5837), pp.478-482.

Smith, D.C., Simon, M., Alldredge, A.L. and Azam, F., 1992. Intense hydrolytic enzyme activity on marine aggregates and implications for rapid particle dissolution. *Nature*, 359(6391), pp.139-142.

Snow, J.T., Polyviou, D., Skipp, P., Chrismas, N.A., Hitchcock, A., Geider, R., Moore, C.M. and Bibby, T.S., 2015. Quantifying integrated proteomic responses to iron stress in the globally important marine diazotroph Trichodesmium. *PLoS One*, *10*(11), p.e0142626.

Sohm, J.A., Webb, E.A. and Capone, D.G., 2011. Emerging patterns of marine nitrogen fixation. *Nature Reviews Microbiology*, *9*(7), pp.499-508.

Solioz, M. and Odermatt, A., 1995. Copper and silver transport by CopB-ATPase in membrane vesicles of Enterococcus hirae. *Journal of Biological Chemistry*, *270*(16), pp.9217-9221.

Solioz, M. and Stoyanov, J.V., 2003. Copper homeostasis in Enterococcus hirae. *FEMS Microbiology Reviews*, *27*(2-3), pp.183-195.

Sprencel, C., Cao, Z., Qi, Z., Scott, D.C., Montague, M.A., Ivanoff, N., Xu, J., Raymond, K.M., Newton, S.M. and Klebba, P.E., 2000. Binding of Ferric Enterobactin by theEscherichia coli Periplasmic Protein FepB. *Journal of Bacteriology*, *182*(19), pp.5359-5364.

Stein, L.Y., 2011. Heterotrophic nitrification and nitrifier denitrification. *Nitrification*, pp.95-114.

Stewart, F.J., Ulloa, O. and DeLong, E.F., 2012. Microbial metatranscriptomics in a permanent marine oxygen minimum zone. *Environmental Microbiology*, *14*(1), pp.23-40.

Stieglmeier, M., Mooshammer, M., Kitzler, B., Wanek, W., Zechmeister-Boltenstern, S., Richter, A. and Schleper, C., 2014. Aerobic nitrous oxide production through N-nitrosating hybrid formation in ammonia-oxidizing archaea. *The ISME Journal, 8*(5), pp.1135-1146.

Strzepek, R.F. and Harrison, P.J., 2004. Photosynthetic architecture differs in coastal and oceanic diatoms. *Nature*, *431*(7009), pp.689-692.

Strzepek, R.F., Maldonado, M.T., Hunter, K.A., Frew, R.D. and Boyd, P.W., 2011. Adaptive strategies by Southern Ocean phytoplankton to lessen iron limitation: Uptake of organically complexed iron and reduced cellular iron requirements. *Limnology and Oceanography*, *56*(6), pp.1983-2002.

Stüeken, E.E., Kipp, M.A., Koehler, M.C. and Buick, R., 2016. The evolution of Earth's biogeochemical nitrogen cycle. *Earth-Science Reviews*, *160*, pp.220-239.

Sunda, W.G. and Huntsman, S.A., 1995. Iron uptake and growth limitation in oceanic and coastal phytoplankton. *Marine Chemistry*, *50*(1-4), pp.189-206.

Sunda, W.G. and Huntsman, S.A., 1995. Regulation of copper concentration in the oceanic nutricline by phytoplankton uptake and regeneration cycles. *Limnology and Oceanography*, *40*(1), pp.132-137.

Sunda, W.G. and Huntsman, S.A., 1997. Interrelated influence of iron, light and cell size on marine phytoplankton growth. *Nature*, *390*(6658), pp.389-392.

Sunda, W.G. and Huntsman, S.A., 2015. High iron requirement for growth, photosynthesis, and low-light acclimation in the coastal cyanobacterium Synechococcus bacillaris. *Frontiers in Microbiology*, *6*, p.561.

Sutka, R.L., Ostrom, N.E., Ostrom, P.H. and Phanikumar, M.S., 2004. Stable nitrogen isotope dynamics of dissolved nitrate in a transect from the North Pacific Subtropical Gyre to the Eastern Tropical North Pacific. *Geochimica et Cosmochimica Acta*, *68*(3), pp.517-527.

Suzuki, I., Dular, U. and Kwok, S.C., 1974. Ammonia or ammonium ion as substrate for oxidation by Nitrosomonas europaea cells and extracts. *Journal of Bacteriology*, *120*(1), pp.556-558.

Tagliabue, A., Bowie, A.R., Boyd, P.W., Buck, K.N., Johnson, K.S. and Saito, M.A., 2017. The integral role of iron in ocean biogeochemistry. *Nature*, *543*(7643), pp.51-59.

Tagliabue, A., Mtshali, T., Aumont, O., Bowie, A.R., Klunder, M.B., Roychoudhury, A.N. and Swart, S., 2012. A global compilation of dissolved iron measurements: focus on distributions and processes in the Southern Ocean. *Biogeosciences*, *9*(6), pp.2333-2349.

Taylor, A.E., Zeglin, L.H., Dooley, S., Myrold, D.D. and Bottomley, P.J., 2010. Evidence for different contributions of archaea and bacteria to the ammonia-oxidizing potential of diverse Oregon soils. *Applied and Environmental Microbiology, 76*(23), pp.7691-7698.

Thomas, M.K., Kremer, C.T., Klausmeier, C.A. and Litchman, E., 2012. A global pattern of thermal adaptation in marine phytoplankton. *Science*, *338*(6110), pp.1085-1088.

Thompson, C.M. and Ellwood, M.J., 2014. Dissolved copper isotope biogeochemistry in the Tasman Sea, SW Pacific Ocean. *Marine Chemistry*, *165*, pp.1-9.

Timmermans, K.R., Stolte, W. and De Baar, H.J.W., 1994. Iron-mediated effects on nitrate reductase in marine phytoplankton. *Marine Biology*, *121*(2), pp.389-396.

Tolar, B.B., King, G.M. and Hollibaugh, J.T., 2013. An analysis of Thaumarchaeota populations from the Northern Gulf of Mexico. *Frontiers in Microbiology, 4*, p.72.

Tolar, B.B., Powers, L.C., Miller, W.L., Wallsgrove, N.J., Popp, B.N. and Hollibaugh, J.T., 2016. Ammonia oxidation in the ocean can be inhibited by nanomolar concentrations of hydrogen peroxide. *Frontiers in Marine Science*, *3*, p.237.

Tolar, B.B., Wallsgrove, N.J., Popp, B.N. and Hollibaugh, J.T., 2017. Oxidation of urea-derived nitrogen by thaumarchaeota-dominated marine nitrifying communities. *Environmental Microbiology, 19*(12), pp.4838-4850.

Tortell, P.D., Maldonado, M.T. and Price, N.M., 1996. The role of heterotrophic bacteria in iron-limited ocean ecosystems. *Nature*, *383*(6598), pp.330-332.

Treusch, A.H., Leininger, S., Kletzin, A., Schuster, S.C., Klenk, H.P. and Schleper, C., 2005. Novel genes for nitrite reductase and Amo-related proteins indicate a role of uncultivated mesophilic crenarchaeota in nitrogen cycling. *Environmental Microbiology, 7*(12), pp.1985-1995.

Tully, B.J., Nelson, W.C. and Heidelberg, J.F., 2012. Metagenomic analysis of a complex marine planktonic thaumarchaeal community from the Gulf of Maine. *Environmental Microbiology, 14*(1), pp.254-267.

Turley, C.M. and Mackie, P.J., 1994. Biogeochemical significance of attached and free-living bacteria and the flux of particles in the NE Atlantic Ocean. *Marine Ecology-Progress Series*, 115, pp.191-191.

Ulloa, O., Canfield, D.E., DeLong, E.F., Letelier, R.M. and Stewart, F.J., 2012. Microbial oceanography of anoxic oxygen minimum zones. *Proceedings of the National Academy of Sciences, 109*(40), pp.15996-16003.

Urakawa, H., Martens-Habbena, W., Huguet, C., de la Torre, J.R., Ingalls, A.E., Devol, A.H. and Stahl, D.A., 2014. Ammonia availability shapes the seasonal distribution and activity of archaeal and bacterial ammonia oxidizers in the Puget Sound Estuary. *Limnology and Oceanography, 59*(4), pp.1321-1335.

Urakawa, H., Martens-Habbena, W., Stahl, D.A., 2011. Physiology and genomics of ammonia-oxidizing archaea. In: Ward MK BB, Arp DJ (ed). Nitrification. ASM Press: Washington, DC,117–155.

Vadas, A., Monbouquette, H.G., Johnson, E. and Schröder, I., 1999. Identification and characterization of a novel ferric reductase from the hyperthermophilic archaeon Archaeoglobus fulgidus. *Journal of Biological Chemistry*, *274*(51), pp.36715-36721.

Valasatava, Y., Rosato, A., Banci, L. and Andreini, C., 2016. MetalPredator: a web server to predict iron–sulfur cluster binding proteomes. *Bioinformatics*, *32*(18), pp.2850-2852.

Valentine, D.L., 2007. Adaptations to energy stress dictate the ecology and evolution of the Archaea. *Nature Reviews Microbiology, 5*(4), pp.316-323.

Van de Graaf, A.A., Mulder, A., de Bruijn, P.E.T.E.R., Jetten, M.S., Robertson, L.A. and Kuenen, J.G., 1995. Anaerobic oxidation of ammonium is a biologically mediated process. *Applied and Environmental Microbiology, 61*(4), pp.1246-1251.

Van Kessel, M.A., Speth, D.R., Albertsen, M., Nielsen, P.H., den Camp, H.J.O., Kartal, B., Jetten, M.S. and Lücker, S., 2015. Complete nitrification by a single microorganism. *Nature, 528*(7583), pp.555-559.

Van Oostende, N., Fawcett, S.E., Marconi, D., Lueders-Dumont, J., Sabadel, A.J.M., Woodward, E.M.S., Jönsson, B.F., Sigman, D.M. and Ward, B.B., 2017. Variation of summer phytoplankton community composition and its relationship to nitrate and regenerated nitrogen assimilation across the North Atlantic Ocean. *Deep Sea Research Part I: Oceanographic Research Papers, 121*, pp.79-94.

Van Wambeke, F., Bonnet, S., Moutin, T., Raimbault, P., Alarcón, G. and Guieu, C., 2008. Factors limiting heterotrophic bacterial production in the southern Pacific Ocean. *Biogeosciences*, *5*(3), pp.833-845.

Velayudhan, J., Hughes, N.J., McColm, A.A., Bagshaw, J., Clayton, C.L., Andrews, S.C. and Kelly, D.J., 2000. Iron acquisition and virulence in Helicobacter pylori: a major role for FeoB, a high-affinity ferrous iron transporter. *Molecular Microbiology*, *37*(2), pp.274-286.

Venter, J.C., Remington, K., Heidelberg, J.F., Halpern, A.L., Rusch, D., Eisen, J.A., Wu, D., Paulsen, I., Nelson, K.E., Nelson, W. and Fouts, D.E., 2004. Environmental genome shotgun sequencing of the Sargasso Sea. *Science, 304*(5667), pp.66-74.

Verhamme, D.T., Prosser, J.I. and Nicol, G.W., 2011. Ammonia concentration determines differential growth of ammonia-oxidising archaea and bacteria in soil microcosms. *The ISME Journal, 5*(6), pp.1067-1071.

Veuger, B., Pitcher, A., Schouten, S., Sinninghe Damsté, J.S. and Middelburg, J.J., 2013. Nitrification and growth of autotrophic nitrifying bacteria and Thaumarchaeota in the coastal North Sea. *Biogeosciences*, 10(3), pp.1775-1785.

Villanueva, L., Schouten, S. and Sinninghe Damsté, J.S., 2015. Depth-related distribution of a key gene of the tetraether lipid biosynthetic pathway in marine Thaumarchaeota. *Environmental Microbiology, 17*(10), pp.3527-3539.

Völker, C. and Wolf-Gladrow, D.A., 1999. Physical limits on iron uptake mediated by siderophores or surface reductases. *Marine Chemistry*, *65*(3-4), pp.227-244.

Vulpe, C.D. and Packman, S., 1995. Cellular copper transport. *Annual review of nutrition*, *15*(1), pp.293-322.

Walker, C.B., De La Torre, J.R., Klotz, M.G., Urakawa, H., Pinel, N., Arp, D.J., Brochier-Armanet, C., Chain, P.S.G., Chan, P.P., Gollabgir, A. and Hemp, J., 2010. Nitrosopumilus maritimus genome reveals unique mechanisms for nitrification and autotrophy in globally distributed marine crenarchaea. *Proceedings of the National Academy of Sciences*, *107*(19), pp.8818-8823.

Wan, X.S., Sheng, H.X., Dai, M., Zhang, Y., Shi, D., Trull, T.W., Zhu, Y., Lomas, M.W. and Kao, S.J., 2018. Ambient nitrate switches the ammonium consumption pathway in the euphotic ocean. *Nature Communications, 9*(1), pp.1-9.

Wang, L., Lim, C.K. and Klotz, M.G., 2020. High Synteny and Sequence Identity between Genomes of Nitrosococcus oceani Strains Isolated from Different Oceanic Gyres Reveals Genome Economization and Autochthonous Clonal Evolution. *Microorganisms*, *8*(5), p.693.

Ward, B., 2008. Nitrification in Marine Systems. In: D. Capone, D. Bronk, M. Mulholland and E. Carpenter, ed., *Nitrogen in the marine environment*. Elsevier, Amsterdam.

Ward, B.B. and Kilpatrick, K.A., 1991. Nitrogen transformations in the oxic layer of permanent anoxic basins: the Black Sea and the Cariaco Trench. In Black Sea Oceanography (pp. 111-124). Springer, Dordrecht.

Ward, B.B. and O'Mullan, G.D., 2002. Worldwide distribution of Nitrosococcus oceani, a marine ammonia-oxidizing γ-proteobacterium, detected by PCR and sequencing of 16S rRNA and amoA genes. *Applied and Environmental Microbiology*, *68*(8), pp.4153-4157.

Ward, B.B. and Zafiriou, O.C., 1988. Nitrification and nitric oxide in the oxygen minimum of the eastern tropical North Pacific. *Deep Sea Research Part A. Oceanographic Research Papers, 35*(7), pp.1127-1142.

Ward, B.B., 1985. Light and substrate concentration relationships with marine ammonium assimilation and oxidation rates. *Marine Chemistry, 16*(4), pp.301-316.

Ward, B.B., Glover, H.E. and Lipschultz, F., 1989. Chemoautotrophic activity and nitrification in the oxygen minimum zone off Peru. *Deep Sea Research Part A. Oceanographic Research Papers, 36*(7), pp.1031-1051.

Ward, B.B., Tuit, C.B., Jayakumar, A., Rich, J.J., Moffett, J. and Naqvi, S.W.A., 2008. Organic carbon, and not copper, controls denitrification in oxygen minimum zones of the ocean. *Deep Sea Research Part I: Oceanographic Research Papers*, *55*(12), pp.1672-1683.

Ward, L.M., Johnston, D.T. and Shih, P.M., 2021. Phanerozoic radiation of ammonia oxidizing bacteria. *Scientific Reports*, *11*(1), pp.1-9.

Webb, E.A., Moffett, J.W. and Waterbury, J.B., 2001. Iron stress in open-ocean cyanobacteria (synechococcus, trichodesmium, andcrocosphaera spp.): Identification of the idia protein. *Applied and Environmental Microbiology*, *67*(12), pp.5444-5452.

Wei, X., Vajrala, N., Hauser, L., Sayavedra-Soto, L.A. and Arp, D.J., 2006. Iron nutrition and physiological responses to iron stress in Nitrosomonas europaea. *Archives of microbiology*, *186*(2), pp.107-118.

Whitby, H., Posacka, A.M., Maldonado, M.T. and van den Berg, C.M., 2018. Copper-binding ligands in the NE Pacific. *Marine Chemistry*, *204*, pp.36-48.

Wilhelm, S.W. and Trick, C.G., 1994. Iron-limited growth of cyanobacteria: multiple siderophore production is a common response. *Limnology and Oceanography*, *39*(8), pp.1979-1984.

Wilhelm, S.W., Maxwell, D.P. and Trick, C.G., 1996. Growth, iron requirements, and siderophore production in iron-limited Synechococcus PCC 72. *Limnology and Oceanography*, *41*(1), pp.89-97.

Williams, R.J.P. and Rickaby, R.E., 2012. *Evolution's destiny: co-evolving chemistry of the environment and life*. Royal Society of Chemistry.

Wilson, S.T., del Valle, D.A., Segura-Noguera, M. and Karl, D.M., 2014. A role for nitrite in the production of nitrous oxide in the lower euphotic zone of the oligotrophic North Pacific Ocean. *Deep Sea Research Part I: Oceanographic Research Papers, 85*, pp.47-55.

Winogradsky, S., 1890. Recherches sur les organisms de la nitrification. *Annales de l'Institut Pasteur*, *4*, pp.213-231.

Wiśniewski, J.R., Duś, K. and Mann, M., 2013. Proteomic workflow for analysis of archival formalin-fixed and paraffin-embedded clinical samples to a depth of 10 000 proteins. *PROTEOMICS–Clinical Applications*, *7*(3-4), pp.225-233.

Woodland, M.P. and Dalton, H., 1984. Purification and characterization of component A of the methane monooxygenase from Methylococcus capsulatus (Bath). *Journal of Biological Chemistry, 259*(1), pp.53-59.

Wrage, N., Velthof, G.L., Van Beusichem, M.L. and Oenema, O., 2001. Role of nitrifier denitrification in the production of nitrous oxide. *Soil Biology and Biochemistry, 33*(12-13), pp.1723-1732.

Wu, J. and Boyle, E., 2002. Iron in the Sargasso Sea: Implications for the processes controlling dissolved Fe distribution in the ocean. *Global Biogeochemical Cycles*, *16*(4), pp.33-1.

Wu, J., Boyle, E., Sunda, W. and Wen, L.S., 2001. Soluble and colloidal iron in the oligotrophic North Atlantic and North Pacific. *Science*, 293(5531), pp.847-849.

Wuchter, C., Abbas, B., Coolen, M.J., Herfort, L., van Bleijswijk, J., Timmers, P., Strous, M., Teira, E., Herndl, G.J., Middelburg, J.J. and Schouten, S., 2006. Archaeal nitrification in the ocean. *Proceedings of the National Academy of Sciences*, *103*(33), pp.12317-12322.

Xu, M.N., Li, X., Shi, D., Zhang, Y., Dai, M., Huang, T., Glibert, P.M. and Kao, S.J., 2019. Coupled effect of substrate and light on assimilation and oxidation of regenerated nitrogen in the euphotic ocean. *Limnology and Oceanography*, *64*(3), pp.1270-1283.

Yakimov, M.M., La Cono, V., Smedile, F., Crisafi, F., Arcadi, E., Leonardi, M., Decembrini, F., Catalfamo, M., Bargiela, R., Ferrer, M. and Golyshin, P.N., 2014. Heterotrophic bicarbonate assimilation is the main process of de novo organic carbon synthesis in hadal zone of the Hellenic Trench, the deepest part of Mediterranean Sea. *Environmental Microbiology Reports*, 6(6), pp.709-722.

Yingping, F., Lemeille, S., Talla, E., Janicki, A., Denis, Y., Zhang, C.C. and Latifi, A., 2014. Unravelling the cross-talk between iron starvation and oxidative stress responses highlights the key role of PerR (alr 0957) in peroxide signalling in the cyanobacterium Nostoc PCC 7120. *Environmental Microbiology Reports*, *6*(5), pp.468-475.

Yool, A., Martin, A.P., Fernández, C. and Clark, D.R., 2007. The significance of nitrification for oceanic new production. *Nature*, *447*(7147), pp.999-1002.

Yoshida, N., Morimoto, H., Hirano, M., Koike, I., Matsuo, S., Wada, E., Saino, T. and Hattori, A., 1989. Nitrification rates and 15 N abundances of N 2 O and NO 3− in the western North Pacific. *Nature*, *342*(6252), pp.895-897.

Yu, E., 2011. Crystal Structures of the CusA Efflux Pump Suggest Methionine Mediated Metal Transport. *Biophysical Journal*, *100*(3), p.382a.

Zakem, E.J., Al-Haj, A., Church, M.J., van Dijken, G.L., Dutkiewicz, S., Foster, S.Q., Fulweiler, R.W., Mills, M.M. and Follows, M.J., 2018. Ecological control of nitrite in the upper ocean. *Nature communications*, *9*(1), pp.1-13.

Zannoni, D. ed., 2004. *Respiration in archaea and bacteria*. Kluwer Academic.

Zerkle, A.L., House, C.H. and Brantley, S.L., 2005. Biogeochemical signatures through time as inferred from whole microbial genomes. *American Journal of Science*, *305*(6-8), pp.467-502.

Zerkle, A.L., House, C.H., Cox, R.P. and Canfield, D.E., 2006. Metal limitation of cyanobacterial N2 fixation and implications for the Precambrian nitrogen cycle. *Geobiology*, *4*(4), pp.285-297.

Zerkle, A.L. and Mikhail, S., 2017. The geobiological nitrogen cycle: from microbes to the mantle. *Geobiology*, *15*(3), pp.343-352.

Zerkle, A.L., Poulton, S.W., Newton, R.J., Mettam, C., Claire, M.W., Bekker, A. and Junium, C.K., 2017. Onset of the aerobic nitrogen cycle during the Great Oxidation Event. *Nature, 542*(7642), pp.465-467.

Zhang, L., Koay, M., Maher, M.J., Xiao, Z. and Wedd, A.G., 2006. Intermolecular transfer of copper ions from the CopC protein of Pseudomonas syringae. Crystal structures of fully loaded CuICuII forms. *Journal of the American Chemical Society*, *128*(17), pp.5834-5850.

Zhang, L.M., Offre, P.R., He, J.Z., Verhamme, D.T., Nicol, G.W. and Prosser, J.I., 2010. Autotrophic ammonia oxidation by soil thaumarchaea. *Proceedings of the National Academy of Sciences, 107*(40), pp.17240-17245.

Zhang, Q., Snow, J.T., Holdship, P., Price, D., Watson, P. and Rickaby, R.E., 2018. Direct measurement of multi-elements in high matrix samples with a flow injection ICP-MS: application to the extended Emiliania huxleyi Redfield ratio. *Journal of Analytical Atomic Spectrometry*, *33*(7), pp.1196-1208.

Zheng, B., Zhang, Q., Gao, J., Han, H., Li, M., Zhang, J., Qi, J., Yan, J. and Gao, G.F., 2011. Insight into the interaction of metal ions with TroA from Streptococcus suis. *PLoS One*, *6*(5), p.e19510.

Zhong, H., Lehtovirta-Morley, L., Liu, J., Zheng, Y., Lin, H., Song, D., Todd, J.D., Tian, J. and Zhang, X.H., 2020. Novel insights into the Thaumarchaeota in the deepest oceans: their metabolism and potential adaptation mechanisms. *Microbiome*, 8, pp.1-16.

Zhu, X., Burger, M., Doane, T.A. and Horwath, W.R., 2013. Ammonia oxidation pathways and nitrifier denitrification are significant sources of N2O and NO under low oxygen availability. *Proceedings of the National Academy of Sciences, 110*(16), pp.6328-6333.

Zorz, J.K., Kozlowski, J.A., Stein, L.Y., Strous, M. and Kleiner, M., 2018. Comparative proteomics of three species of ammonia-oxidizing bacteria. *Frontiers in Microbiology*, *9*, p.938.

APPENDIX I

1 SUPPLEMENTARY METHODS & RESULTS

1.1 Calculation of the critical cellular Fe:P required to reach μ_{max}

In comparing Fe quotas of microorganisms, it is necessary to distinguish between the intracellular Fe incorporated into functional proteins (needed to support growth) versus Fe quotas representing Fe storage and 'luxury uptake'. In our comparison, we were interested in intracellular Fe associated with supporting growth, as this is what is relevant in the context of Fe′ dose response curves. A first-order linear relationship in Fe-limited diatoms between [Fe′], Fe:C and growth rate (μ) — whereby the x-axis intercept (at the point where the linear regression crosses μ_{max} – Figure A1.5) — represents the minimum Fe:C required to achieve μ_{max} (herein referred to as critical cell Fe:P) has been previously demonstrated (Sunda & Huntsman, 1995). Assuming that the same applies for other marine microorganisms, we plotted relative growth rate (μ/μ_{max}) against cell Fe:P in Fe-limited cells and fitted the data with a linear regression. The critical cell Fe:P was defined as the x-intercept when y is equal to one (μ_{max}), calculated using the linear regression equation. Published data used in our comparison is available in Table A1.1. Original Fe:C data was converted to Fe:P data for comparison assuming a "Redfield" C:N:P stoichiometry of 106:16:1.

1.2 Search for candidate ferric reductases

To date, no genes in the genome of *N. maritimus* have been annotated with ferric reductase functionality. In order to identify potential ferric reductases, we compiled a database of known ferric reductases and proteins which have been annotated as having ferric-chelate reductase (NADPH) activity in the gene orthology (GO) database (Table A1.4) from archaea, eukaryotes, and bacteria. We performed a BLASTp search of ferric

reductase proteins against the *N. maritimus* genome to identify any candidate ferric reductases using an *E* value threshold of 10^{-25} (Table A1.5).

1.3 Flow cytometry

In order to corroborate the relationship between cell counts and [NO_2^-] under an Fe-limited growth state, we measured cell densities from 250 pmol L^{-1} Fe′ cultures at different points in the *N. maritimus* growth curve (equating to a range of [NO_2^-] from 9–750 μmol L^{-1}. Samples were stained with SYBR Green I (final concentration = 10^{-4} dilution from a concentrated stock of SYBR Green, Thermo Fisher Scientific) prior to imaging with an Amnis Imagestream MKII imaging flow cytometer housed in the Dunn School of Pathology, University of Oxford. We found that our data agrees well with previous published data under Fe replete conditions (Amin et al. 2013), showing that the changes in NO_2^- at low [Fe′] are driven by differences in cell density rather than just a constant number of cells actively oxidising NH_4^+ in culture (Figure A1.2).

1.4 Scanning electron microscopy (SEM)

Fe-limited (250 pmol L^{-1}) and Fe-replete (1000 pmol L^{-1}) cell cultures were harvested by centrifugation into a concentrated cell suspension. Cell suspensions were applied to poly-L-lysine coated glass coverslips and were then fixed with 2.5% glutaraldehyde and allowed to adhere for 5 min. Glass coverslips were rinsed 3 × with 0.1 M phosphate buffer (pH 7.2) and then underwent secondary fixation with 1% OsO_4 for 45 min. Cells on coverslips were rinsed with water, dehydrated through a graded ethanol series to absolute ethanol, and then dried chemically with HDMS. Coverslips were mounted on carbon adhesive tape and splutter coated with 10 nm Au. Cells were examined using a GeminiSEM at an accelerating voltage of 3 kV and magnifications of × 5,000–100,000. Cell dimensions used for calculation of cell surface area in uptake rates were used from

Fe-limited treatments (Figure A1.3) as it is a requirement that steady-state uptake rate is calculated under non-Fe saturating conditions.

1.5 Search of *Tara* metagenomic database

Candidatus Nitrosopelagicus brevis (herein referred to as *Ca.* N. brevis) is the only ammonia-oxidising archaeon which possesses a ferrous Fe transporter (encoded by T478_0963). We explored whether Fe-specific transporters play a more significant role in marine *Thaumarcheotal* Fe uptake in the open ocean, compared with non-specific metal transporters used by *N. maritimus* and related AOA (Table A1.3). Using the Ocean Gene Atlas search facility of the *Tara* oceans metagenomic database, we examined whether homologues of the *Ca.* N. brevis Fe^{2+} uptake gene (T478_0963) were present in greater abundances compared with the non-specific metal transporters used by *N. maritimus*. To investigate this, we searched the *Tara* oceans database using the ocean gene atlas (OGA – http://tara-oceans.mio.osupytheas.fr/ocean-gene-atlas/) for homologues of *N. maritimus* unspecific metal uptake transporter genes (Nmar_0328, Nmar_0330, Nmar_0331, Nmar_0329, Nmar_1130, Nmar_1662) and *Ca.* N. brevis *feoB* transporters (T478_0963) using FASTA sequences downloaded from UniProt. This search returned any homologous genes over the threshold *E* value of 10^{-10} and also ascribes taxonomic classification to hits, usually down to the order level. Our aim was to compare only hits belonging to *Thaumarchaeota*, as these represent the marine AOA community.

The analysis returned no hits of homologues of *Ca.* N. brevis T478_0963 ascribed to organisms belonging to the *Thaumarchaeota* phylum, indicating that the Fe-specific uptake proteins and their homologues of *Ca.* N. brevis are below the limit of detection in metagenomic studies across all *Tara* stations. The only archaeal T478_0963 homologue returned from the search were ascribed to the order *Halobacteria* within the phylum

Euryarchaeota **(**Figure A1.7**)**. The analysis however returned multiple *Thaumarchaeota* hits for homologues of all *N. maritimus* unspecific metal uptake genes (Nmar_0328, Nmar_0330, Nmar_0331, Nmar_0329, Nmar_1130, Nmar_1662): of these, 68–94% of all archaeal hits were ascribed to the *Nitrosopumilales* order. These results suggest that genes relating to *N. maritimus* metal transport systems are vastly more prevalent in the wider oceanic environment than those relating to the high-affinity *Ca*. N. brevis *feoB* which did not return any hits.

2 SUPPLEMENTARY FIGURES & TABLES

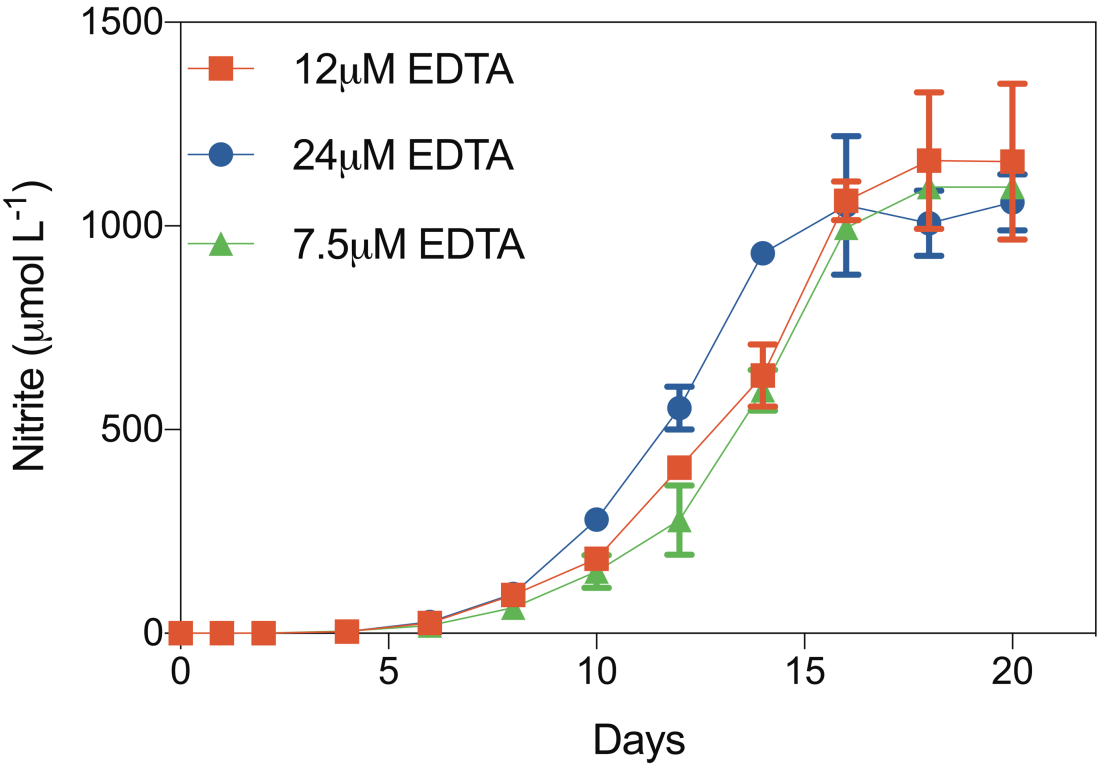


Figure A1.1 Effect of EDTA concentration on NO_2^- production by *N. maritimus*

Experiment to examine the toxicity effect of increased EDTA concentrations. Fe′ was kept constant at 7500 pmol L^{-1} in both treatments.

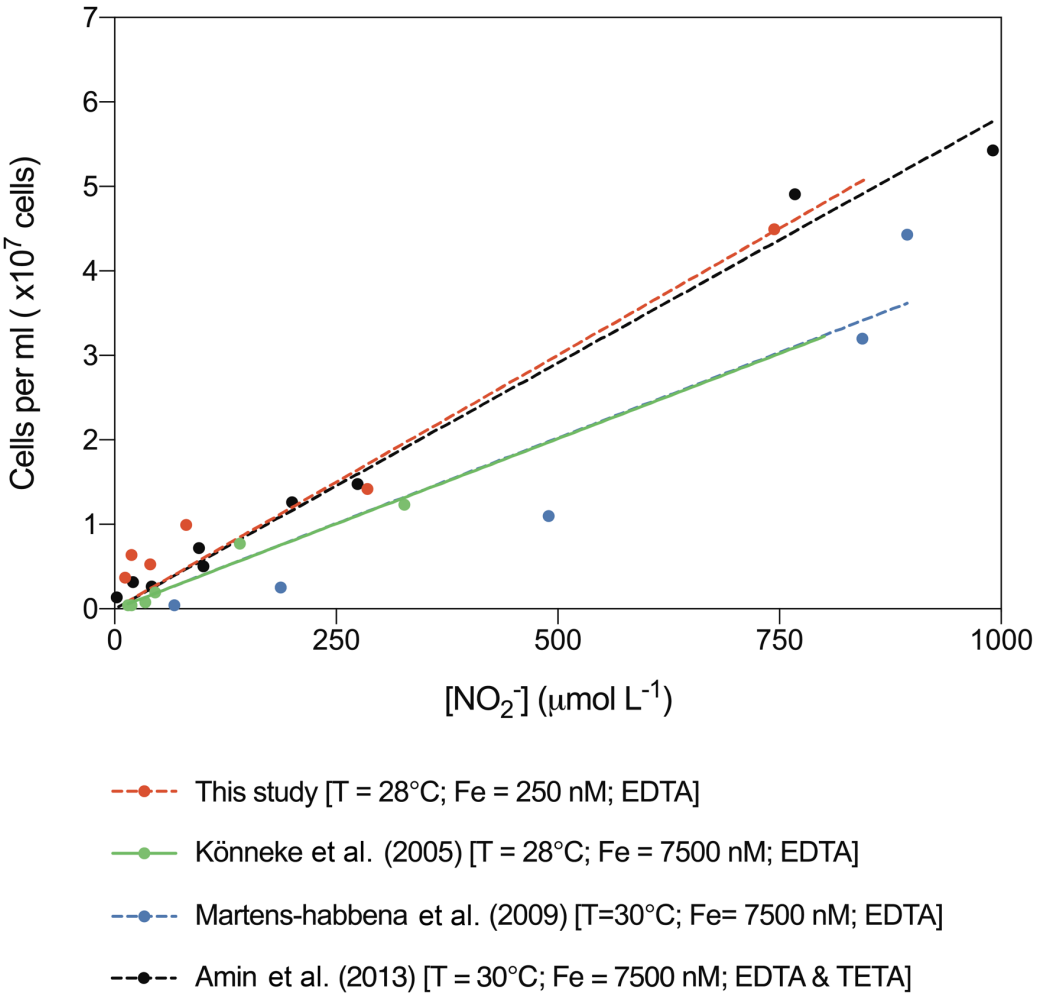


Figure A1.2 Correlation between cell counts and NO_2^- concentrations in *N. maritimus*

Correlation between cell counts and nitrite (NO_2^-) concentrations in *N. maritimus* cultures in 250 pmol L^{-1} experiments (red circles) compared with data from Amin et al. (2013), Martens-Habbena et al. (2009) and Könneke et al. (2005) in replete Fe conditions (7500 pmol L^{-1} Fe′).

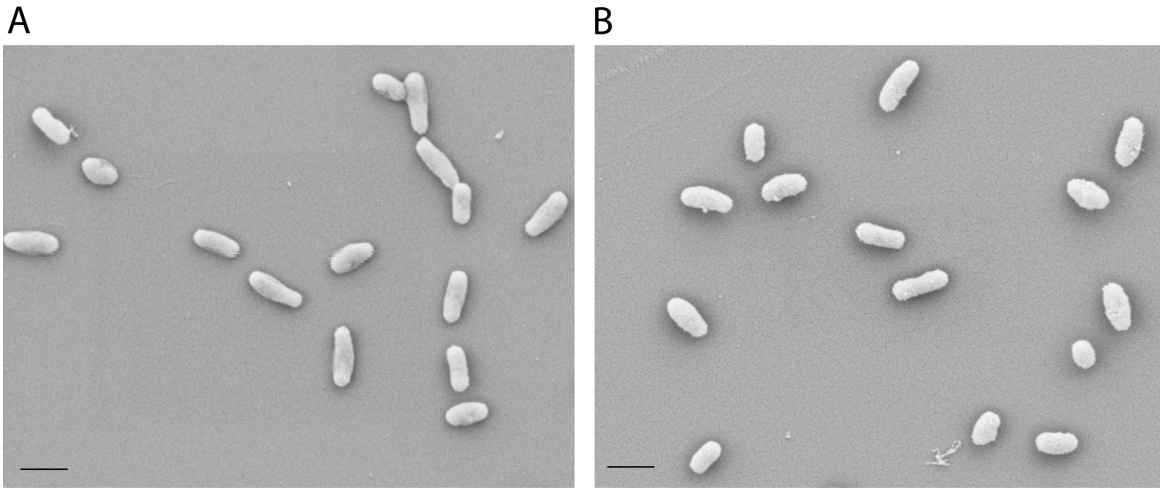


Figure A1.3 SEM images of *N. maritimus*

Scanning electron micrograph of **A)** *N. maritimus* cells grown under Fe-replete (1000 pmol L^{-1} Fe′) conditions and **B)** Fe-deplete (250 pmol L^{-1} Fe′) conditions. Scale bar in both images represents 0.5 µm.

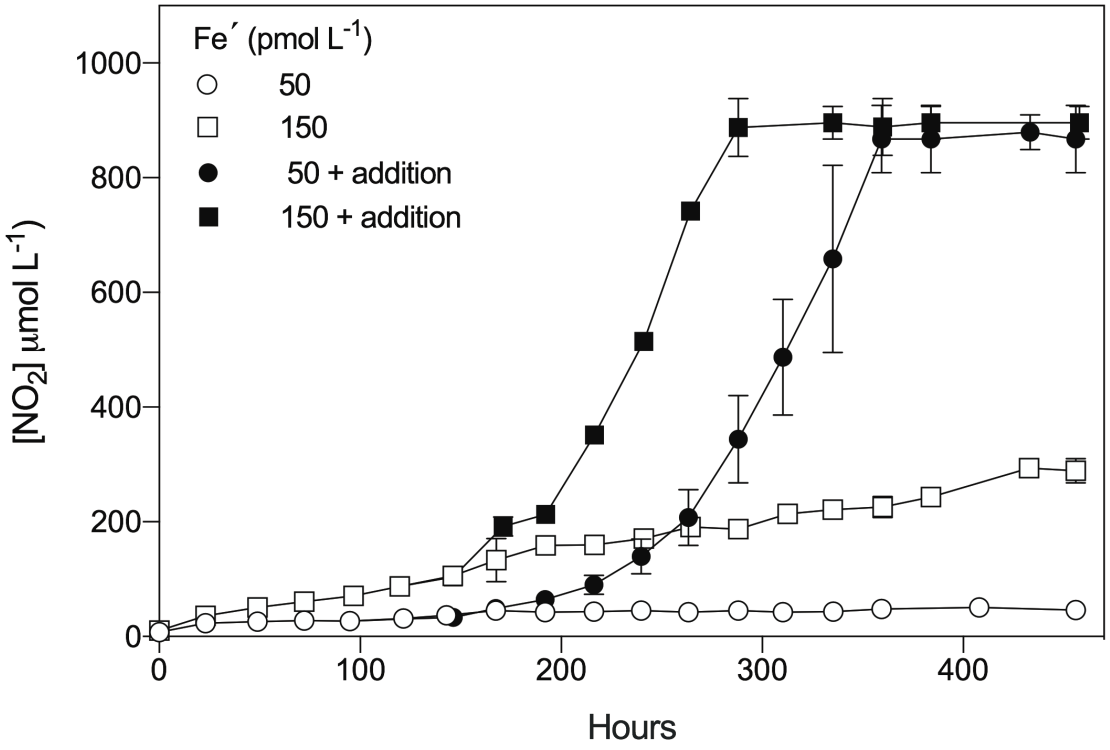


Figure A1.4 Effect of Fe re-addition on *N. maritimus* nitrite production

The effect of addition of Fe at 120 hours (prior to full growth acclimation) to cultures of *N. maritimus* originally treated with 50 pmol L^{-1} and 150 pmol L^{-1} Fe′. Final [Fe′] in amended cultures was 1000 pmol L^{-1}. Control cultures received no additional Fe. Error bars indicate standard deviation, $n = 3$.

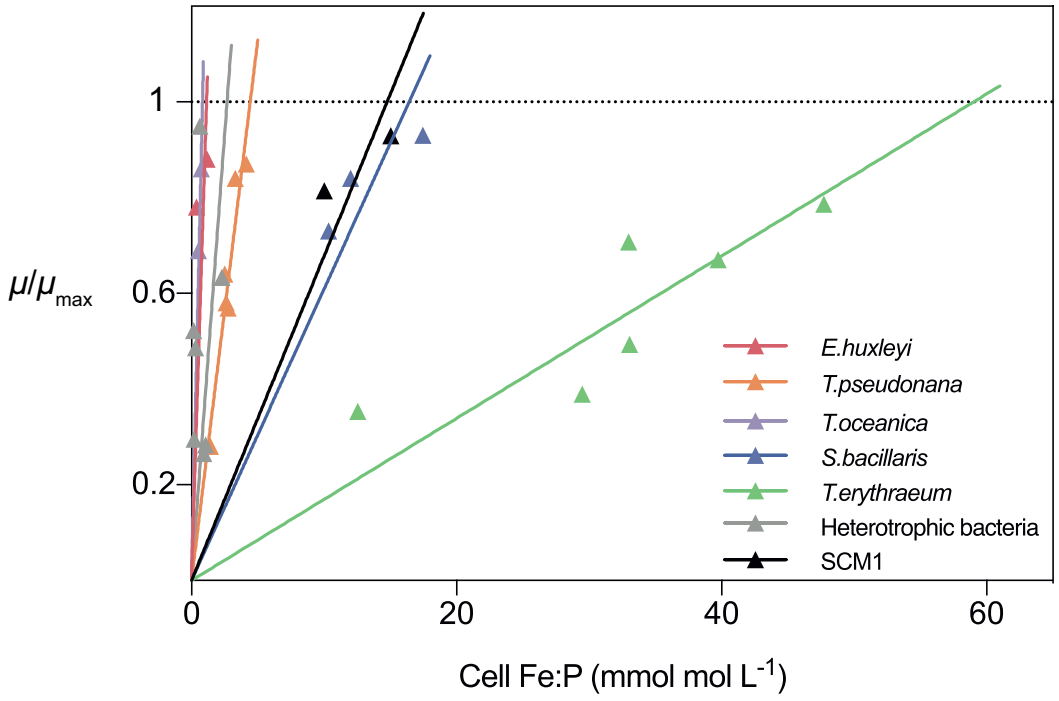


Figure A1.5 Relationship between Fe quota and growth rate in marine microorganisms

The linear relationship between specific growth rate (μ) and cellular Fe quota (Fe:P) in Fe-limited cells of phytoplankton and *N. maritimus* (i.e., below μ_{max}). X-axis intercept of the point at which linear regression lines crossed μ_{max} (y=1) were used as the Fe:P indicative to minimal Fe requirement to achieve maximum growth rates (critical Fe:P).

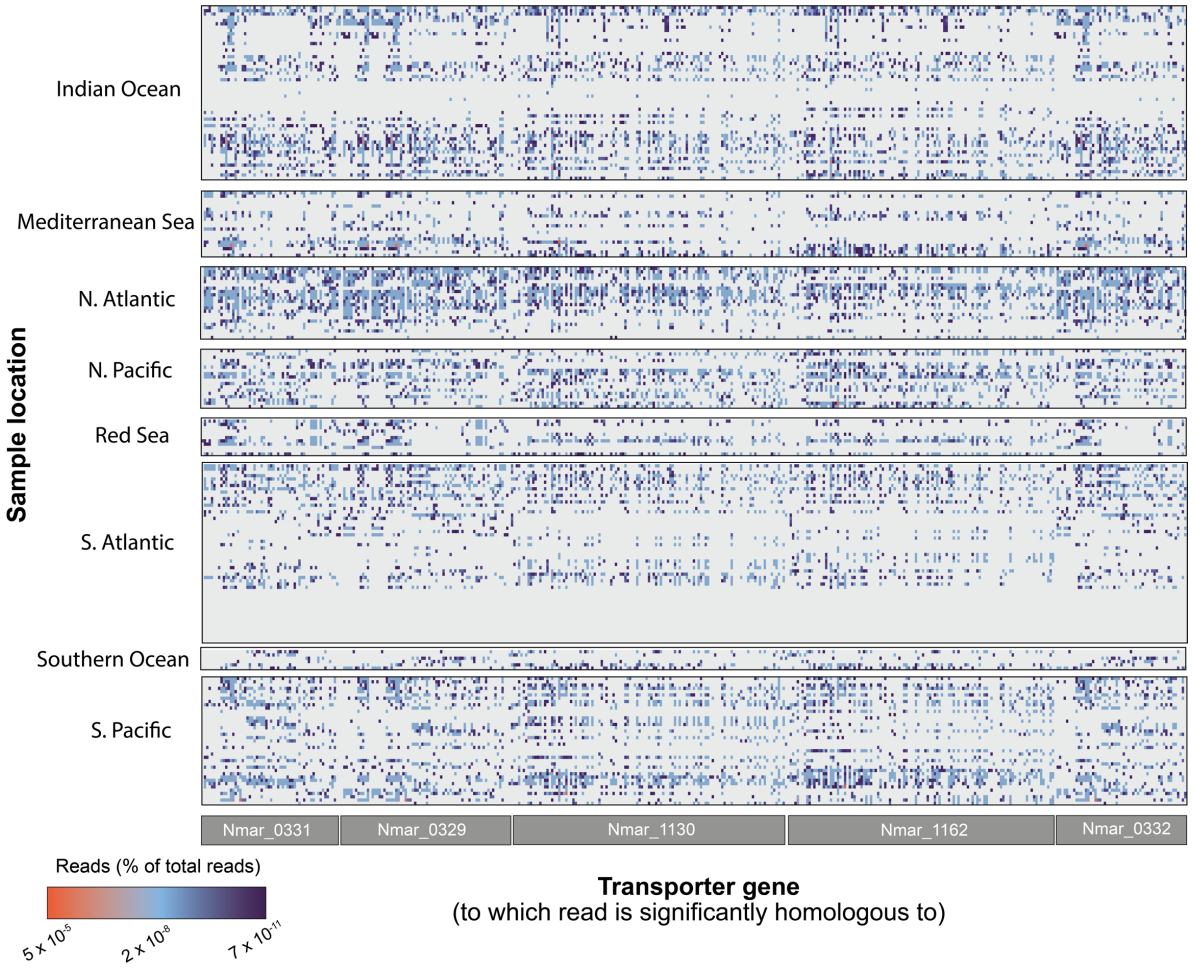


Figure A1.6 Reads homologous to *N. maritimus* transporter genes detected in *Tara* oceans database

Hits for genes showing significant homology to *N. maritimus* metal transport genes (Nmar_0331; Nmar_0329; Nmar_1130; Nmar_1162; Nmar_0332 – shown on the x-axis) in the *Tara* metagenomic database, as a percentage of total reads. Results are grouped into sample location.

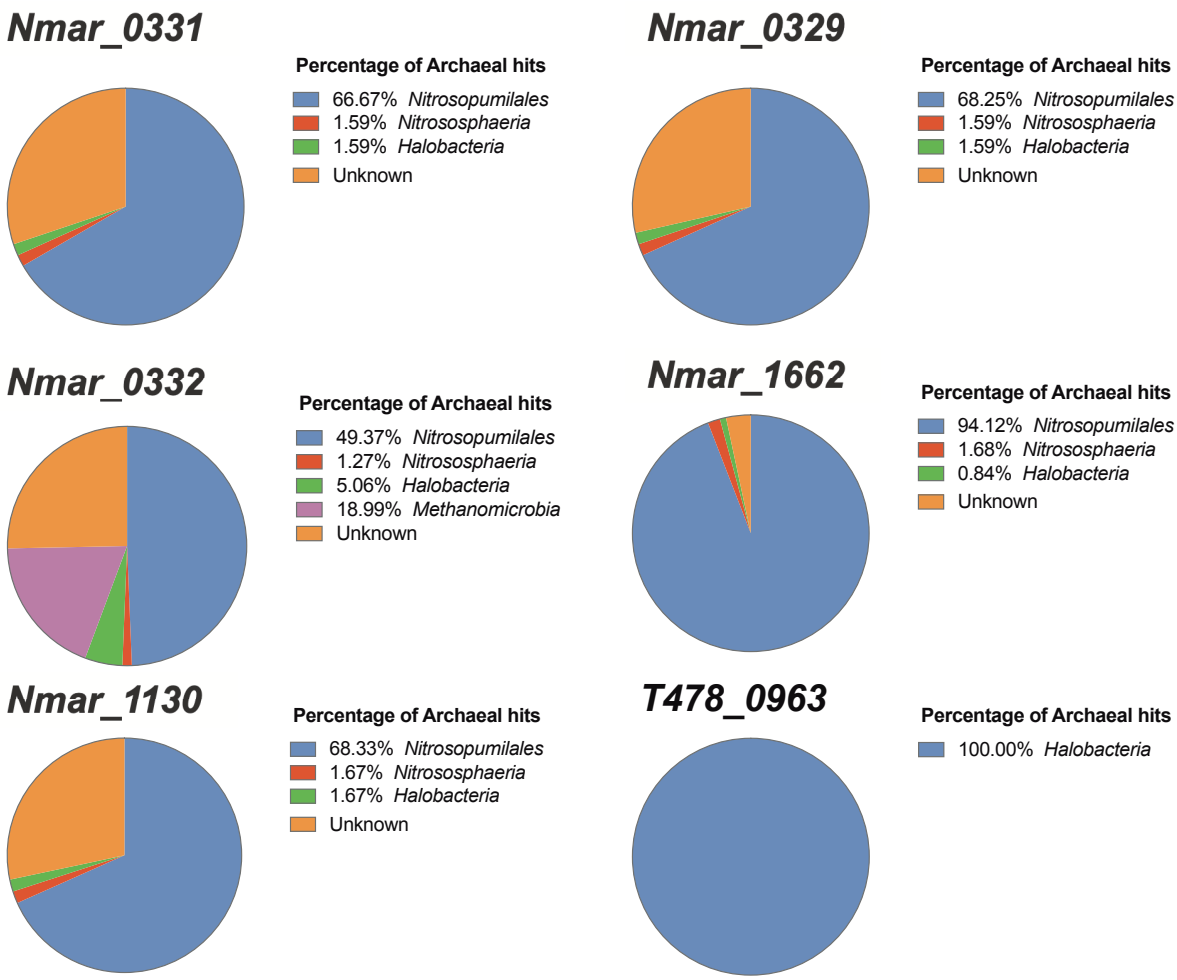


Figure A1.7 Archaeal hits from *Tara* oceans database homologous to metal uptake genes

Percentage of archaeal hits ascribed to orders *Nitrosopumililales*, *Nitrososphaeria*, *Halobacteria*, *Methanomicrobia* returned from *Tara* oceans database search of *N. maritimus* metal uptake genes (Nmar_0328, Nmar_0330, Nmar_0331, Nmar_0329, Nmar_1130, Nmar_1662) and *Ca*. N brevis (T478_0963).

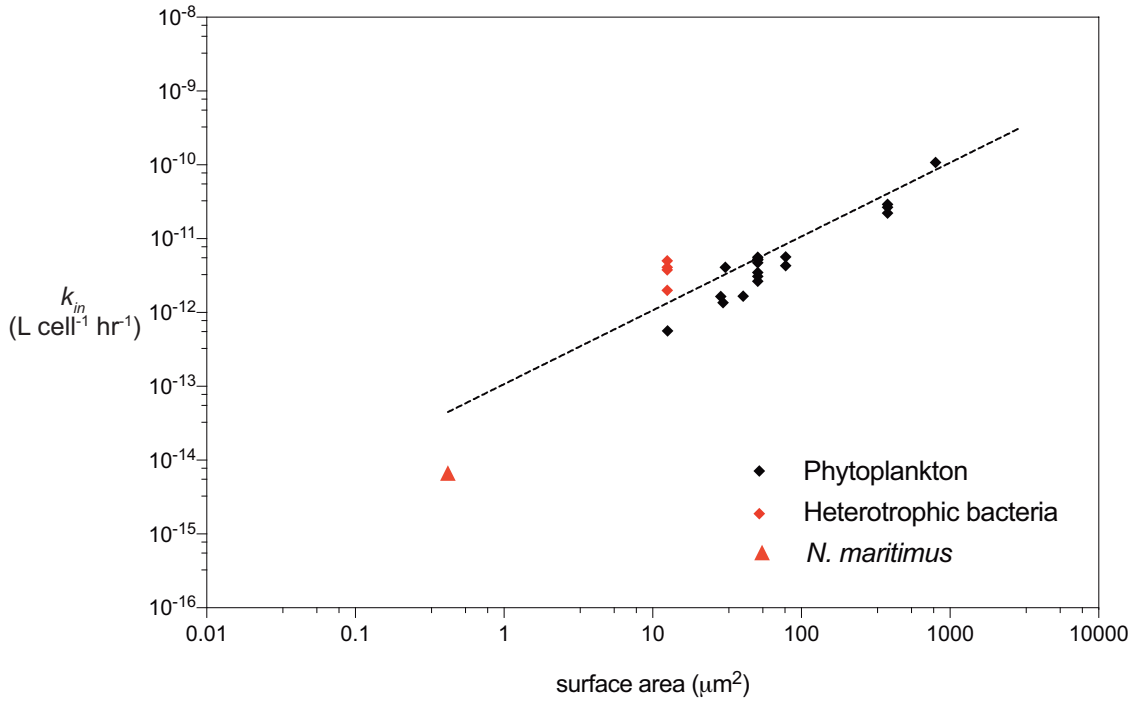


Figure A1.8 FeDFB uptake of *N. maritimus* and phytoplankton as a function of cell surface area

Steady-state uptake rate constant (k_{in} in units L cell^{-1} hr^{-1}) of marine phytoplankton (from Lis et al. 2015a), heterotrophic bacteria (Granger & Price, 1999) and *N. maritimus* (red triangle) as a function of cell surface area (S.A. in units μm^2). The general relationship between k_{in} and S.A. observed in phytoplankton and heterotrophic bacteria is denoted by the dashed line.

	Fe′ (pmol L^{-1})	μ (d^{-1})	μ/μ_{max} (d^{-1})	Fe:C (µmol mol^{-1})	Fe:P (mmol mol L^{-1})
Emiliania huxleyi					
Sunda & Huntsman (1995)	3.0	0.70	0.63		
	5.0	0.88	0.78	3.70	0.39
	9.7	0.99	0.88	11.00	1.17
	24.2	1.10	0.98	13.30	1.41
	71.0	1.07	0.95	26.30	2.79
	253.0	1.04	0.92	33.20	3.52
	750.0	1.12	1.00		
Schulz et al. (2004)	0.1	0.36	0.22		
	0.9	0.66	0.41		
	2.8	1.20	0.75		
	4.8	1.33	0.82		
	138.5	1.62	1.00		
Thalassiosira oceanica					
Sunda & Huntsman (1995)	3.0	0.73	0.46		
	10.6	1.10	0.69	4.90	0.52
	28.2	1.36	0.86	7.10	0.75
	78.0	1.55	0.98	11.30	1.20
	253.0	1.55	0.98	34.30	3.64
	760.0	1.58	1.00		
Thalassiosira pseudonana					
Sunda & Huntsman (1997)	9.8	0.00	0.00		
	23.8	0.51	0.28	13.33	1.41
	74.9	1.05	0.57	26.15	2.77
	79.8	0.99	0.54		
	122.2	1.19	0.64	23.78	2.52
	269.7	1.39	0.75		
	251.4	1.55	0.84	31.03	3.29
	413.0	1.60	0.86		
	797.6	1.66	0.90	69.71	7.39
	792.8	1.80	0.97		
	1221.3	1.85	1.00		
	2846.8	1.74	0.94		
	8242.5	1.67	0.90		
Sunda & Huntsman (1995)	23.9	0.50	0.28	12.50	1.33
	74.0	1.04	0.58	24.70	2.62
	244.0	1.57	0.87	39.00	4.13
	730.0	1.80	1.00		
		1.76	0.97	149.00	15.79
***Synechococcus bacillaris* (CCMP 1333)**					
Sunda & Huntsman (2015)	37.8	0.11	0.17		
	98.3	0.45	0.73	97.42	10.33
	328.0	0.52	0.84	113.30	12.01
	964.7	0.58	0.93	164.81	17.47
	3268.8	0.62	1.00	227.90	24.16
Trichodesmium erythraeum					
Berman-Frank et al. (2001)	16.4	0.04	0.34		
	32.6	0.05	0.38		
	128.1	0.06	0.49		
	386.9	0.09	0.71		
	15773.2	0.12	1.00		
Shi et al. (2012)	58.05	0.29	0.67		39.74
	530.16	0.40	0.93		211.75
	1411.25	0.43	1.00		367.74

Boatman et al. (2018)	584.81	0.18	0.51		
	584.81	0.21	0.58		
	417.72	0.28	0.77		
	706.33	0.26	0.73		
	3607.59	0.36	1.00		
	6174.68	0.32	0.88		
Marine Heterotrophic bacteria					
Tortell (1996)	40000	8.08	0.75		
	40000	10.06	0.94		
	40000	10.70	1.00		
	40000	10.61	0.99		
	40000	6.82	0.64		
	25	7.87	0.74		
	25	6.69	0.63		
	25	4.10	0.38		
	25	3.38	0.32		
	25	3.87	0.36		
Granger & Price (1999)	2.97	6.74	0.52		
	2166.00	12.90	1.00		0.15
	2.97	1.21	0.28		
	2166.00	4.27	1.00		1.06
	2.97	2.18	0.30		
	2166.00	7.37	1.00		0.20
	2.97	9.95	0.63		
	2166.00	15.70	1.00		2.28
	2.97	5.79	0.49		
	2166.00	11.90	1.00		0.29
	2.97	5.55	0.27		
	2166.00	20.90	1.00		0.91

Table A1.1 Fe requirements of marine phytoplankton and heterotrophs

Compiled data from published literature of the effect of Fe′ availability on the specific growth rate (μ), relative growth rate (μ_{max}), and intracellular Fe quota (Fe:C and Fe:P) of marine microorganisms. Values converted between Fe:P and Fe:C assuming a Redfield stoichiometry.

Organism/Study	S.A. (um^2)	Fe′ (pmol L^{-1})	Uptake rate (mol Fe $cell^{-1}$ hr^{-1})	k_{in} (L $cell^{-1}$ hr^{-1})	k_{in}/S.A.
Fe′					
***N. maritimus* strain SCM1**					
This study	0.42	250	1.6E-22	6.3E-13	1.5E-12
	0.42	250	8.2E-23	3.3E-13	7.8E-13
	0.42	500	9.7E-23	3.9E-13	9.2E-13
	0.42	500	1.3E-22	5.3E-13	1.3E-12
	0.42	500	9.4E-23	3.8E-13	9.0E-13
Emiliania huxleyi					
Sunda & Huntsman (1995)	32.8	5.0	3.2E-20	6.5E-09	2.0E-10
	32.8	5.0	3.8E-20	7.7E-09	2.3E-10
	31.8	5.1	4.4E-20	8.7E-09	2.7E-10
	33.9	5.1	5.1E-20	9.9E-09	2.9E-10
	33.3	9.3	8.7E-20	9.4E-09	2.8E-10
	35.2	9.3	8.9E-20	9.6E-09	2.7E-10
	35.9	9.7	1.1E-19	1.1E-08	3.2E-10
	35.9	9.7	1.1E-19	1.2E-08	3.3E-10
	37.4	19.3	1.4E-19	7.3E-09	2.0E-10

	37.4	19.3	1.2E-19	6.2E-09	1.7E-10
	36.1	24.2	1.5E-19	6.1E-09	1.7E-10
	36.1	24.2	1.5E-19	6.3E-09	1.7E-10
	36.1	71.0	3.2E-19	4.4E-09	1.2E-10
	36.1	71.0	3.0E-19	4.2E-09	1.2E-10
	35.5	73.0	2.6E-19	3.5E-09	9.9E-11
Shi et al. (2010)	38.2	9.7	4.5E-20	4.7E-09	1.2E-10
	38.2	12.2	5.8E-20	4.8E-09	1.2E-10
	38.2	14.9	7.3E-20	4.9E-09	1.3E-10
	39.0	27.6	1.3E-19	4.5E-09	1.2E-10
	39.0	34.3	1.5E-19	4.3E-09	1.1E-10
Lane et al. (2009)	59.9	8.2	8.2E-20	1.0E-08	1.7E-10
Thalassisosira oceanica					
Sunda & Huntsman (1995)	90.5	3.9	4.4E-20	1.1E-08	1.2E-10
	87.5	7.1	9.7E-20	1.4E-08	1.6E-10
	86.0	10.6	1.5E-19	1.4E-08	1.6E-10
	86.0	10.6	9.0E-20	8.5E-09	9.9E-11
	89.8	19.3	1.9E-19	1.0E-08	1.1E-10
	89.8	19.3	1.9E-19	1.0E-08	1.1E-10
	95.7	28.2	3.2E-19	1.1E-08	1.2E-10
	95.7	28.2	2.7E-19	9.6E-09	1.0E-10
	92.0	52.0	4.8E-19	9.2E-09	1.0E-10
	101.4	78.0	6.8E-19	8.8E-09	8.6E-11
	102.8	78.0	5.6E-19	7.2E-09	7.0E-11
Shi et al. (2010)	78.5	39.8	8.3E-19	2.1E-08	2.7E-10
	78.5	99.5	1.6E-18	1.6E-08	2.1E-10
	78.5	186.5	2.5E-18	1.4E-08	1.7E-10
	78.5	11.0	1.9E-19	1.7E-08	2.2E-10
	78.5	19.6	3.3E-19	1.7E-08	2.1E-10
Lane et al. (2009)	78.5	8.2	5.0E-20	6.1E-09	7.8E-11
Marchetti et al. (2006)	80.0	5.8	5.8E-20	1.0E-08	1.2E-10
Thalassiosira pseudonana					
Sunda & Huntsman (1995)	38.3	23.9	9.1E-20	3.8E-09	9.9E-11
	38.3	23.9	9.4E-20	3.9E-09	1.0E-10
	36.9	28.3	6.8E-20	2.4E-09	6.5E-11
	39.0	74.0	3.5E-19	4.8E-09	1.2E-10
	39.0	74.0	3.3E-19	4.4E-09	1.1E-10
	45.6	77.0	3.5E-19	4.6E-09	1.0E-10
	45.0	244.0	8.0E-19	3.3E-09	7.3E-11
	45.0	244.0	5.9E-19	2.4E-09	5.3E-11
Lane et al. (2009)	50.3	82.2	3.1E-19	3.7E-09	7.4E-11
***Synechococcus* sp. WH7803**					
Lis et al. (2015a)	3.1	24.7	4.4E-21	1.8E-10	5.6E-11
	3.1	18.5	2.3E-21	1.2E-10	3.9E-11
***Synechococcus* sp. WH8102**					
Lis et al. (2015a)	3.1	74.9	1.7E-20	2.3E-10	7.3E-11
	3.1	23.5	1.8E-21	7.8E-11	2.5E-11
	3.1	37.1	5.2E-21	1.4E-10	4.4E-11
	3.1	52.4	9.1E-21	1.7E-10	5.5E-11
***Synechococcus* sp. CCMP1183**					
Lis et al. (2015a)	12.6	19.8	9.6E-21	4.9E-10	3.9E-11
Synechococcus sp. PCC7002					
Lis et al. (2015a)	7.1	3.8	6.1E-21	1.6E-09	2.3E-10
	7.1	4.0	2.0E-20	5.1E-09	7.2E-10

Trichodesmium erythraeum					
Lis et al. (2015a)	188.5	77.5	8.8E-19	1.1E-08	6.0E-11
Marine heterotrophic bacteria					
Granger & Price (1999)	12.56	2.90	1.04E-21	3.49E-10	2.8E-11
	12.56	2.90	1.31E-21	4.42E-10	3.5E-11
	12.56	2.90	2.47E-21	8.30E-10	6.6E-11
	12.56	2.90	4.56E-22	1.54E-10	1.2E-11
	12.56	2.90	2.32E-20	7.82E-09	6.2E-10
	12.56	2.90	1.74E-21	5.86E-10	4.7E-11
	12.56	2.90	5.13E-21	1.73E-09	1.4E-10
FeDFB					
***N. maritimus* strain SCM1**					
This study	0.4	250000.0	7.13E-22	2.64E-15	6.3E-15
	0.4	250000.0	7.35E-22	2.85E-15	6.8E-15
	0.4	250000.0	7.35E-21	2.94E-15	7.0E-15
***Phaeocystis* sp.**					
Strzepek et al. (2011)	28.8	4000.0	6.61E-21	1.65E-12	5.7E-14
	29.8	4000.0	5.46E-21	1.36E-12	4.6E-14
	78.5	4000.0	2.28E-20	5.70E-12	7.3E-14
Thalasiossira oceanica					
Strzepek et al. (2011)	78.5	10000.0	4.33E-20	4.33E-12	5.5E-14
Maldonado & Price (2001)	380.0	45000.0	1.32E-18	2.93E-11	7.7E-14
Thalassiosira weissflogii					
Shaked et al. (2004)	380.0	70000.0	1.56E-18	2.22E-11	5.9E-14
Lis et al. (2015a)	380.0	90000.0	2.40E-18	2.67E-11	7.0E-14
Maldonado & Price (2001)	51.0	49000.0	2.75E-19	5.61E-12	1.1E-13
Thalasiossira pseudonana					
Lis et al. (2015a)	51.0	49000.0	1.30E-19	2.66E-12	5.2E-14
	51.0	49000.0	2.32E-19	4.74E-12	9.3E-14
	51.0	49000.0	1.70E-19	3.48E-12	6.8E-14
	51.0	49000.0	2.60E-19	5.31E-12	1.0E-13
	51.0	49000.0	2.55E-19	5.20E-12	1.0E-13
	51.0	49000.0	1.51E-19	3.08E-12	6.0E-14
	801.0	1000.0	1.08E-19	1.08E-10	1.3E-13
Thalassiosira antarctica					
Hassler & Schoemann (2009)	40.7	100000.0	1.67E-19	1.67E-12	4.1E-14
Emiliania huxleyi					
Lis et al. (2015a)	12.6	85900.2	4.86E-20	5.65E-13	4.5E-14
Nannochloropsis oculata					
Lis et al. (2015a)	12.6	10000	4.09E-21	4.086E-12	3.3E-13
Marine heterotrophic bacteria					
Granger & Price (1999)	12.6	10000	3.79E-21	3.786E-12	3.0E-13
	12.6	10000	5.02E-21	5.022E-12	4.0E-13
	12.6	10000	2.01E-21	2.01E-12	1.6E-13

Table A1.2 Steady-state Fe′ and FeDFB uptake rates of marine phytoplankton and heterotrophic bacteria

Steady-state uptake rates shown as a function of Fe′ substrate concentration and organismal surface area (S.A.) compiled from published literature.

Proteins	*Nitrosopumilus maritimus* strain SCM1	*Ca.* Nitrosopelagicus brevis	*Nitrosopumilus piranensis*	*Nitrosopumilus adriaticus*
Siderophore biosynthesis				
SIP				
EntE				
EntF				
rhbC				
Siderophore binding & uptake				
TBDT_MCL2				
FhuA/B/C				
FhuD/FepB	Nmar_0976		NPIRD3C_1178	NADRNF5_0974
TBDT_MCL3				
FatB				
Haem uptake				
TBDT_MCL1				
HemS				
HutB				
Fe^{2+}				
FeoA/B/C		T478_0963		
Fe^{3+}				
AfuA				
FTR1				
General divalent metal uptake				
TroA/B/C superfamily (Mn^{2+}/Zn^{2+}/Fe^{2+})	Nmar_0328; Nmar_0330; Nmar_0331;Nmar_0329		NPIRD3C_0731/0733/0734/ 0732	
ZIP (Zn^{2+}/Fe^{2+})	Nmar_1130, Nmar_1662	A7X95_06380	NPIRD3C_0398	NSED_01590
NRAMP				

Table A1.3 Metal transport systems encoded in marine AOA genomes

Genes for putative metal transport systems found in marine AOA.

Entry name	Gene names
FRO2_ARATH	FRO2 FRD1
FRE1_YEAST	FRE1 YLR214W L8167.2
FRE1_CANAL	CFL1
FRO7_ARATH	FRO7 At5g49740 K2I5.10
FRE6_YEAST	FRE6 YLL051C L0593
FRE3_YEAST	FRE3 YOR381W O6754
FRE2_YEAST	FRE2 YKL220C
CYBR1_HUMAN	CYBRD1 DCYTB FRRS3
FREB_ASPFU	freB fre2 AFUA_1G17270
FRE7_YEAST	FRE7 YOL152W AOB629
FRE4_YEAST	FRE4 YNR060W N3518
FRO6_ARATH	FRO6 At5g49730 K2I5.9
FERCR_ARCFU	feR AF_0830
FRO8_ARATH	FRO8 At5g50160 K6A12.2
FRP1_SCHPO	frp1 SPBC1683.09c
FRO3_ARATH	FRO3 FROHC
YQJH_ECOLI	yqjH b3070 JW3041
FRP2_SCHPO	frp2 SPBC947.05c
FRO5_ARATH	FRO5 At5g23990 MZF18.13
FRE5_YEAST	FRE5 YOR384W O6765
FRE8_YEAST	FRE8 YLR047C L2114
FRO4_ARATH	FRO4
FRO1_ARATH	FRO1 At1g01590 F22L4.13
FRRS1_MOUSE	FRRS1 Sdfr2 Sdr2
FRE7_YEAS7	FRE7 SCY_4929
FRRS1_HUMAN	FRRS1 SDFR2 SDR2
FRRS1_DROME	CG8399
FRE8_ASHGO	FRE8 ACL139W
CYBR1_MOUSE	Cybrd1 Dcytb
FRS1L_HUMAN	FRRS1L C9orf4
ARREH_SYNY3	arsH slr0945
ARREH_ACIF2	arsH AFE_2857
FERB_PARDE	ferB
STEA3_MOUSE	Steap3 Tsap6
FRRS1_BOVIN	FRRS1
STEA4_RAT	Steap4
STEA4_HUMAN	STEAP4
STEA2_HUMAN	STEAP2
STEA3_HUMAN	STEAP3 TSAP6
STEA4_MOUSE	Steap4 Tiarp
STEA2_MOUSE	Steap2
FRRS1_DANRE	frrs1 zgc:163022
FRRS1_XENLA	frrs1
FERA_PARDE	ferA
FRS1L_MOUSE	Frrs1l
STEA3_RAT	Steap3
CYAC3_MOUSE	Cyb561a3
FRS1L_RAT	Frrs1l
CYBR1_RAT	Cybrd1
CYBR1_XENTR	cybrd1
CYBR1_DANRE	cybrd1
AAR_SYNY3	sll0209
LEPG_ASPFN	lepG AFLA_066920
FNO_METJA	fno MJ1501
CY561_HUMAN	CYB561
CY561_BOVIN	CYB561
CYAC3_HUMAN	CYB561A3
CYBR1_XENLA	cybrd1
LEPD_ASPFN	lepD
CY561_MOUSE	Cyb561
LEPA_ASPFN	lepA
Q5KEL4_CRYNJ	CNG00110
Q5AZ80_EMENI	ANIA_06400
LEPH_ASPFN	lepH
CY561_PIG	CYB561
CY561_XENLA	cyb561
A3M0N1_PICST	FRE7
CYAC3_DANRE	cyb561a3
CYAC3_RAT	Cyb561a3
CYAC3_BOVIN	CYB561A3
CY561_SHEEP	CYB561
LEPF_ASPFN	AFLA_066910
LEPI_ASPFN	AFLA_066940
C0HB47_SALSA	FRRS1 frrs1
C8VIA2_EMENI	ANIA_03208
A0A2G9FYI7_9LAMI	CDL12_29386
B2ZDZ4_PIG	FRRS1
X8JA17_9HOMO	RSOL_348420
A0A074RTN9_9HOMO	V565_135900
A0JNK9_BOVIN	STEAP2
D4A6H3_RAT	Steap2
Q59PA1_CANAL	FRE10
E1BTX2_CHICK	STEAP2
CY561_PONAB	CYB561
E2RH63_CANLF	STEAP2
F7DFH6_HORSE	STEAP2
G1KRT4_ANOCA	STEAP2
F7A6U0_MONDO	STEAP2
A0A2B4SI88_STYPI	FRRS1
H0YT60_TAEGU	STEAP2
D2HE08_AILME	STEAP2 PANDA_008990

K2G4I9_9ZZZZ	ACD_2C00201G0009	B9WMD0_CANDC	Cd36_32920 CD36_32920
G1RYQ5_NOMLE	STEAP2	D4A8Z3_RAT	Frrs1
B9WJM6_CANDC	Cd36_70210 CD36_70210	B9WM91_CANDC	Cd36_32410 CD36_32410
G1T875_RABIT	STEAP2	G1SX94_RABIT	FRRS1
H2PMY8_PONAB	STEAP2	A0A0G2JFP4_MOUSE	Frrs1
R0JY43_ANAPL	STEAP2 Anapl_05178	M3XEV8_FELCA	FRRS1
K7G5A6_PELSI	STEAP2	H2PZG7_PANTR	FRRS1 CK820_G0020758
M3Z3N8_MUSPF	STEAP2	F1S555_PIG	FRRS1
W0TGA3_KLUMD	FRE1 KLMA_60520	F7E3G6_XENTR	frrs1
W5PQR1_SHEEP	STEAP2	H0V486_CAVPO	FRRS1
G7P1U9_MACFA	STEAP2 EGM_12791	Q4WXV4_ASPFU	AFUA_3G10820
G3WY55_SARHA	STEAP2	A0A0F4YF71_TALEM	T310_10138
H0XGI0_OTOGA	STEAP2	A0A165LRS8_RHOFA	yqjH_3 A3L23_02176
A0A287D9Q7_ICTTR	STEAP2	K7FHF7_PELSI	FRRS1
A0A286Y3Z1_CAVPO	STEAP2	A0A0K8TYT4_BACLA	CG8399_1
U3JZ30_FICAL	STEAP2	A0A0K8WG94_BACLA	CG8399_4
B2RX33_MOUSE	Steap2 mCG_2960	M3YLI5_MUSPF	FRRS1
B0VXE5_CALJA	STEAP2	F7B404_CIOIN	LOC100176500
A0A1D5Q2I1_MACMU	STEAP2	A0A2P6SN69_ROSCH	RchiOBHm_Chr1g0378111
A0A1D8PQM2_CANAL	CAALFM_C700430WA	A0A0F4YKM0_TALEM	T310_7268
G1N8N6_MELGA	STEAP2	H3AHK8_LATCH	FRRS1
G3T4M4_LOXAF	STEAP2	A0A0D2LQC9_9CHLO	MNEG_14018
A3LS62_PICST	FRE1.4 PICST_42867	W1QK25_OGAPD	HPODL_04953
F1R2F2_DANRE	frrs1a si:ch211-153l6.2	H0Z4S6_TAEGU	FRRS1
F1S336_PIG	STEAP2	U3J115_ANAPL	FRRS1
C0RW19_DASNO	STEAP2	H0X586_OTOGA	FRRS1
Q1EMS3_PLAMJ	fro1	G1LRB8_AILME	FRRS1
A0A1S3FYJ5_DIPOR	Steap2	F7G2H2_MACMU	FRRS1
G5BD67_HETGA	STEAP2 GW7_11113	G3WM81_SARHA	FRRS1
A3LP96_PICST	FRE1.2 PICST_40289	A0A2P6PC77_ROSCH	RchiOBHm_Chr7g0218171
A0A1U7QQN9_MESAU	Steap2	H2N6N8_PONAB	FRRS1
A0A0L8VNB7_9SACH	KO01_03221	A0A2P6SHV4_ROSCH	RchiOBHm_Chr1g0356951
A0A0L8VL73_9SACH	KO01_03463	A0A2P6SN91_ROSCH	RchiOBHm_Chr1g0378151
Q4PEM4_USTMA	fer9 UMAG_01439	A0A2P6SNA9_ROSCH	RchiOBHm_Chr1g0378171
Q4WLF1_ASPFU	AFUA_6G13750	A0A2P6PC82_ROSCH	RchiOBHm_Chr7g0218161
Q4W9S0_ASPFU	AFUA_4G03940	A0A2P6P5L8_ROSCH	RchiOBHm_Chr7g0192681
A0A0B2UQS1_TOXCA	frrs1 Tcan_06299	A0A2P6SN79_ROSCH	RchiOBHm_Chr1g0378121
G3HL79_CRIGR	I79_011464	A0A2P6PC73_ROSCH	RchiOBHm_Chr7g0218141
W1QA58_OGAPD	HPODL_01387	A0A2P6SHS0_ROSCH	RchiOBHm_Chr1g0356961
A0A0L8VK92_9SACH	KO01_03233	B9RIU2_RICCO	RCOM_1582800
A0A0D9RJ68_CHLSB	STEAP2	A0A2G9G393_9LAMI	CDL12_27709
K4Q884_STREQ	SDSE_0993	A0A0G2KE28_DANRE	frrs1b
E1C859_CHICK	FRRS1	K1RDF5_CRAGI	CGI_10025208
E2RSW3_CANLF	FRRS1	A0A2G9FVV8_9LAMI	CDL12_30327
B9WMD1_CANDC	Cd36_32930	Q7SEA5_NEUCR	NCU00829
B9W9A7_CANDC	Cd36_10340	Q7RY82_NEUCR	NCU00023

W5Q8F0_SHEEP	FRRS1
A0A023EXF7_AEDAL	109430546
F6U4Z1_HORSE	FRRS1
A0A096N3C9_PAPAN	FRRS1
A0A2G9G3A4_9LAMI	CDL12_27708
Q2LS83_SYNAS	SYN_02123
A0A2P6P5K5_ROSCH	RchiOBHm_Chr7g0192661
A0A2P6SN95_ROSCH	RchiOBHm_Chr1g0378131
I3MCG5_ICTTR	FRRS1
A0A0D9S6N6_CHLSB	FRRS1
L8X1P8_THACA	AG1IA_02941
A0A0W8AWI6_KLEPN	BB785_03295
A0A1D5NXG1_CHICK	FRRS1
G3WM82_SARHA	FRRS1
F7DU33_MONDO	FRRS1
A0A068XDC9_HYMMI	HmN_000278300
A0A068XYT4_ECHMU	EmuJ_000487700
A0A2K5TRI9_MACFA	FRRS1
G1KCE7_ANOCA	FRRS1
G1N5L1_MELGA	FRRS1
F6QN94_CALJA	FRRS1
G3T6I7_LOXAF	FRRS1
A0A166PFP5_9PEZI	CT0861_00553
A0A0L8VJV4_9SACH	KO01_04446
A0A165L7N1_RHOFA	A3L23_00823
A0A1D8PN54_CANAL	CFL4
A0A1D8PN52_CANAL	CFL5
A0A2K6TVQ6_SAIBB	FRRS1

Table A1.4 Ferric chelate reductases used in BLASTp analysis

Organism	Gene	Protein name	Homologous gene in *N.maritimus*	Protein name	% identity	alignment length	*E* value	bit score	% positives
Halobacterium salinarum	VNG_2607C	Uncharacterized protein (ferric-chelate reductase (NADPH) activity - GO: 0052851)	Nmar_0180	NADP oxidoreductase coenzyme F_{420}-dependent	29.72	212	1.9E-27	100	53
Methanocaldococcus jannaschii	FNO_METJA	F_{420}-dependent NADP reductase (ferric-chelate reductase (NADPH) activity - GO: 0052851)	Nmar_0180	NADP oxidoreductase coenzyme F_{420}-dependent	36.11	216	2.3E-27	100	54

Table A1.5 Candidate ferric reductases in *N. maritimus*

Candidate ferric reductases based on *N. maritimus* genes which show significant sequence homology with known ferric reductases from a BLASTp search.

APPENDIX II

1 SUPPLEMENTARY METHODS

1.1 Comparison of Fe limitation response to Cu and NH_4^+ stress

In order to gain insight into whether the differential protein intensities between Fe treatments reflect Fe-specific proteomic responses and strategies to deal with Fe limitation, or general cellular responses to changing nutrient or energy status, we compared our results to previously published transcriptomic work of Qin et al. 2018. We compared genes which were significantly differentially expressed in *N. maritimus* ($p < 0.05$) (obtained from Supplementary Table 4 of Qin et al. (2018)) with proteins showing significantly different intensities (FDR adjusted p value < 0.05) in our study. As we only compared significantly differentially expressed transcripts, not all differentially intense proteins in our study have corresponding data from Qin et al. (2018). Proteins are grouped into those postulated to be a general limitation response (proteins/genes show same directional response in all limitation experiments), a general trace metal response (proteins/genes show same directional response in trace metal limitation experiments), highly likely Fe-limitation response (only responsive to Fe and not NH_4^+ and Cu), likely Fe limitation response (responsive to Fe, not Cu – no data for NH_4^+), Fe and energy response (responsive to NH_4^+ and Fe only, not Cu). Results are shown in Table A2.3. We encourage a degree of caution in the interpretation of these results; this comparison is prefaced with the assumption that differential protein intensities between Fe treatments are largely underpinned by changing transcription rather than differential post-translational protein degradation rates. Although Qin et al. (2018) did not compare proteomes with changing nutrient status, their global proteome and transcriptome data show a general scaling between transcript abundance and protein abundance. For

instance, ferredoxins which are among the most abundant of transcripts in *N. maritimus* are also among the most abundant proteins.

1.2 Phosphonate transporter (*phnD*) gene biogeography

We used the *Tara* Oceans Gene Atlas to analyse marine AOA *phnD* gene abundances to compare with previously published analyses of *mpnS* gene biogeography (Qin et al. 2020). *N. maritimus' phnD* FASTA sequence (Nmar_0875) was used to search against the *Tara* database (OM-RGCv1 – *Tara* Oceans Microbiome Reference gene catalog v1 – prokaryotes) with significant homologous hits (1×10^{-10}) returned as average copies cell^{-1}. We took the mean *phnD* gene copies cell^{-1} for each *Tara* sample of Thaumarchaeal origin (only calculated from values > 0) and normalised it to the mean *amoA* abundance (also in copies cell^{-1}) at that site/sample using *N. maritimus amoA* (Nmar_1500) as the query sequence. DCM and surface *phnD: amoA* were grouped together to represent < 200 m and mesopelagic *phnD: amoA* were grouped to represent > 200 m (Figure A2.8). *phnD* gene copies cell^{-1} and *amoA* gene copies cell^{-1} in each sample (with their corresponding filter size and depth) are shown Table A2.4. Differences in mean values and variances between shallow and deep-water gene abundances were tested for statistical significance ($p < 0.05$) using Minitab software (version 19.2020.2.0).

2 SUPPLEMENTARY FIGURES & TABLES

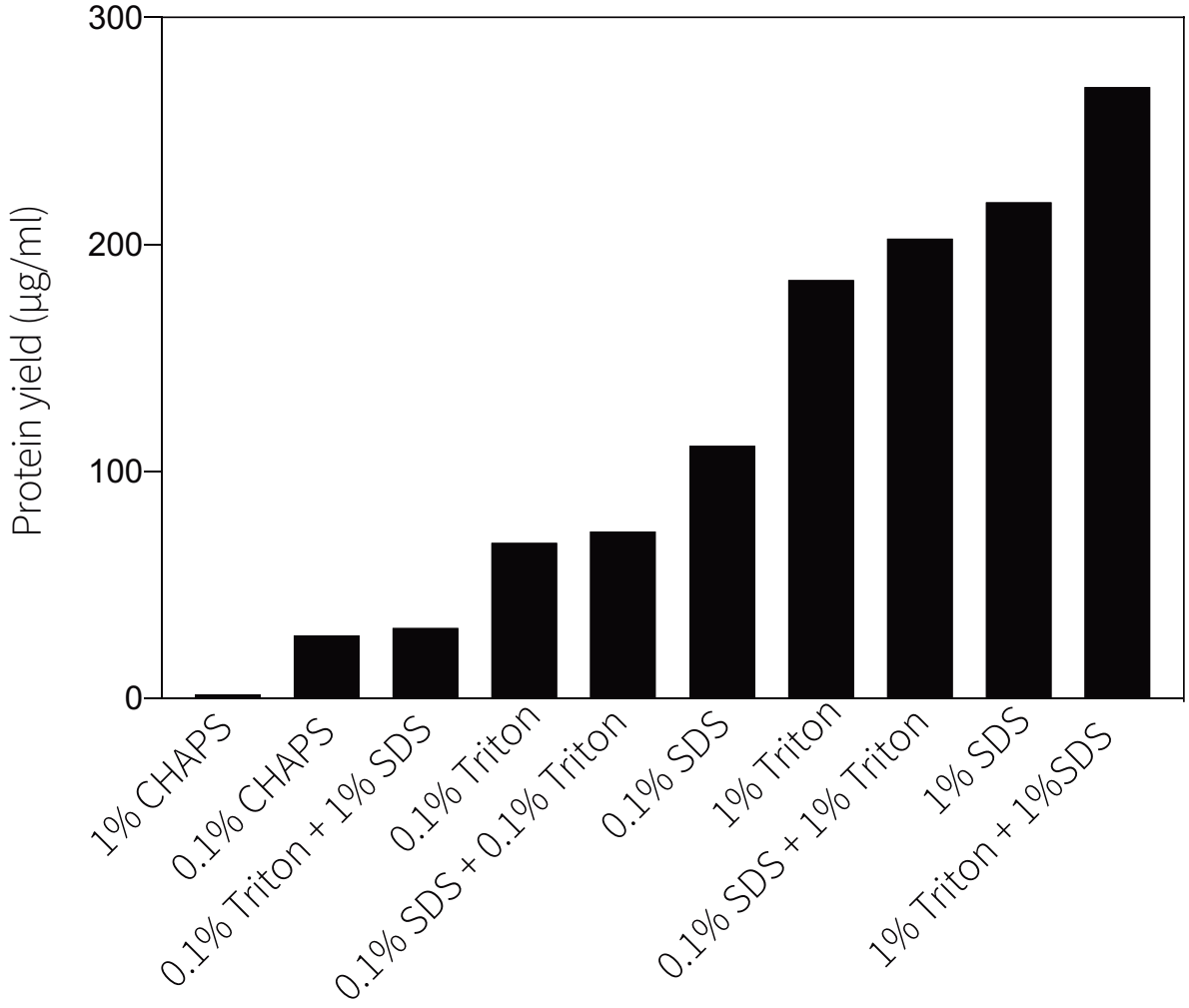


Figure A2.1 Effect of protein extraction buffer on *N. maritimus*' protein yield

Effect of different protein buffer solutions on the amount of protein extracted (in units of µg/ml) from *N. maritimus* cells, showing the greatest protein yield in 1% Triton +1% SDS extraction buffer.

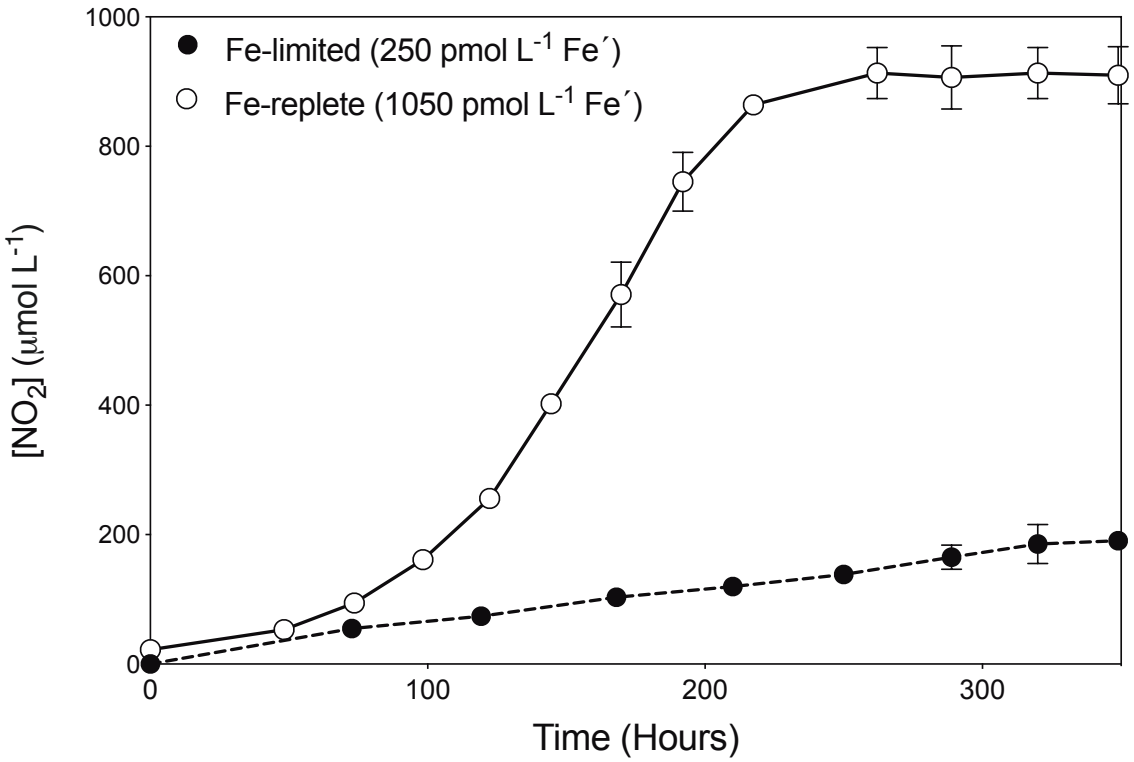


Figure A2.2 Production of NO_2^- by Fe-limited and Fe-replete *N. maritimus* cultures

Effect of Fe´ availability on the production of NO_2^- (µmol L^{-1}) in acclimated *N. maritimus* cultures over time. Error bars indicate standard deviation, $n = 3$.

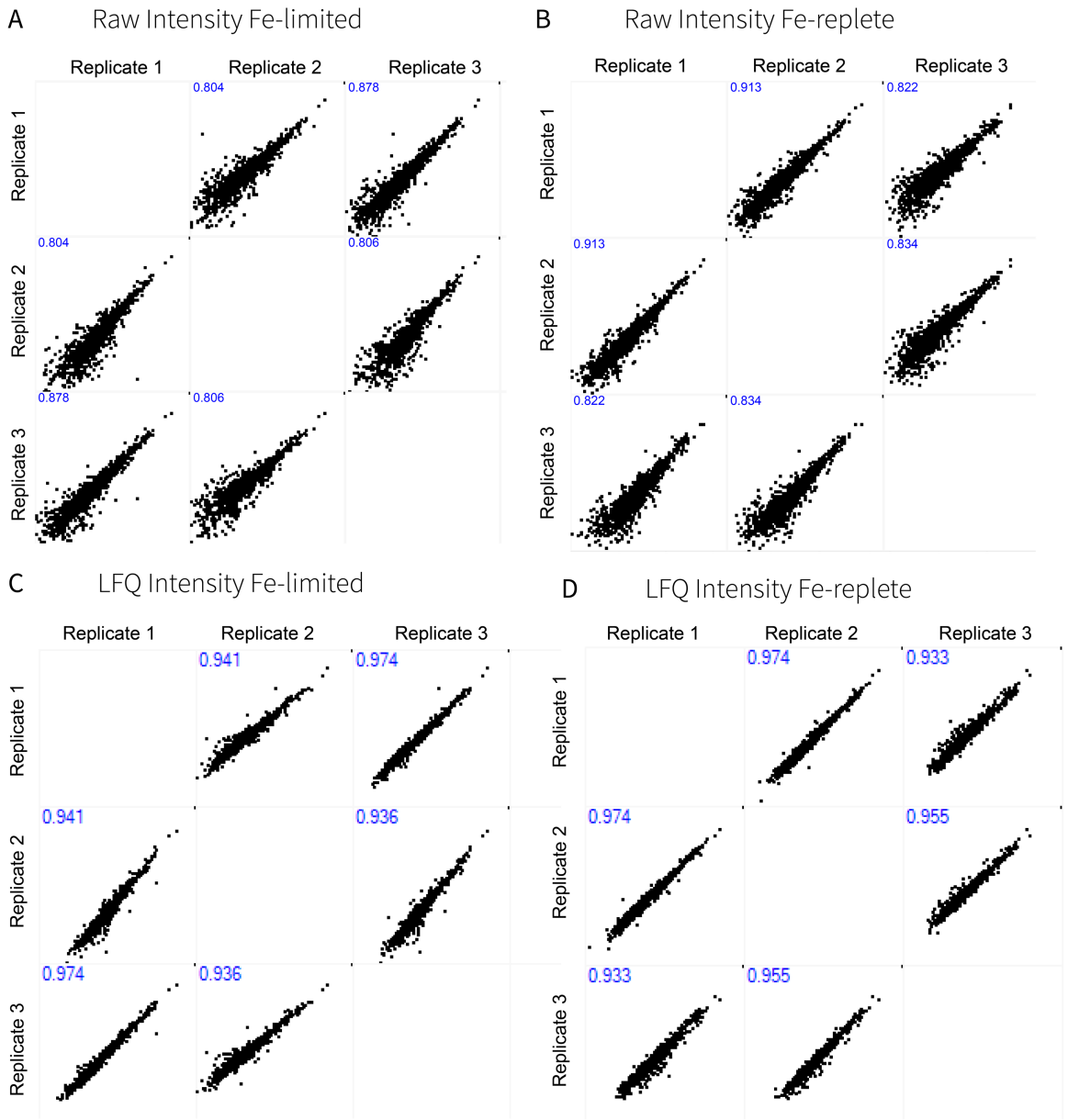


Figure A2.3 Log-log scatter plots of raw and LFQ protein intensities

Log-log scatter plots of raw and LFQ intensities in Fe-replete (1050 pmol L^{-1} Fe′) and Fe-limited (250 pmol L^{-1} Fe′) replicate treatments showing reproducibility of biological replicates. Correlation coefficient (r^2) values are shown on each plot. Plots generated in Perseus software (version 1.5.1.6).

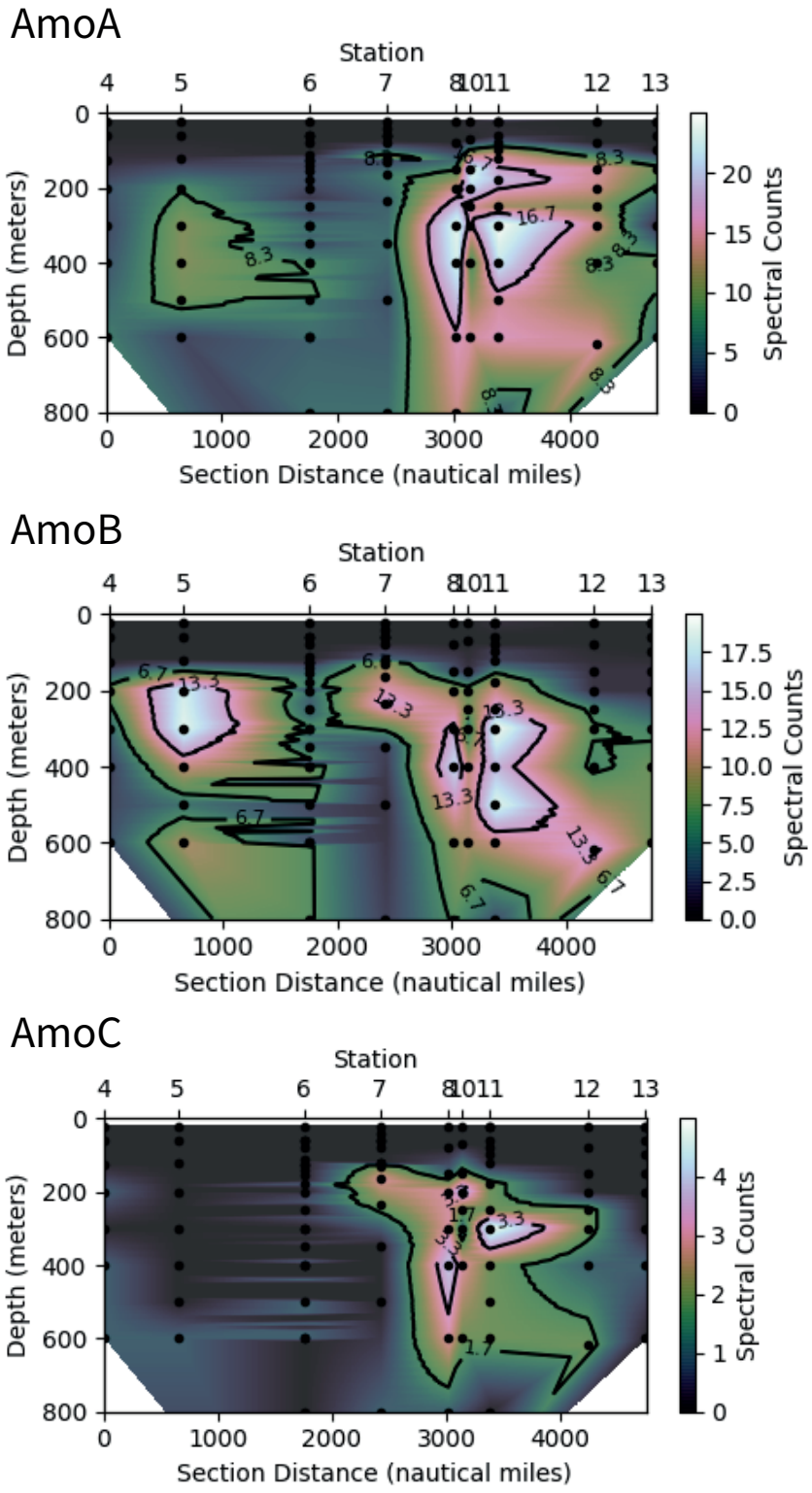


Figure A2.4 Spectral counts of AMO subunits generated using the Ocean Protein Portal

Spectral counts of AMO subunits generated using the Ocean Protein Portal (**Saito et al. 2020**) from the ProteOMZ metaproteomic dataset (FK160115 cruise to the central Pacific Ocean). *N. maritimus* AmoA (Nmar_1500), AmoB (Nmar_1503) and AmoC (Nmar_1502) FASTA sequences were used as search criteria to search against metaproteomic database.

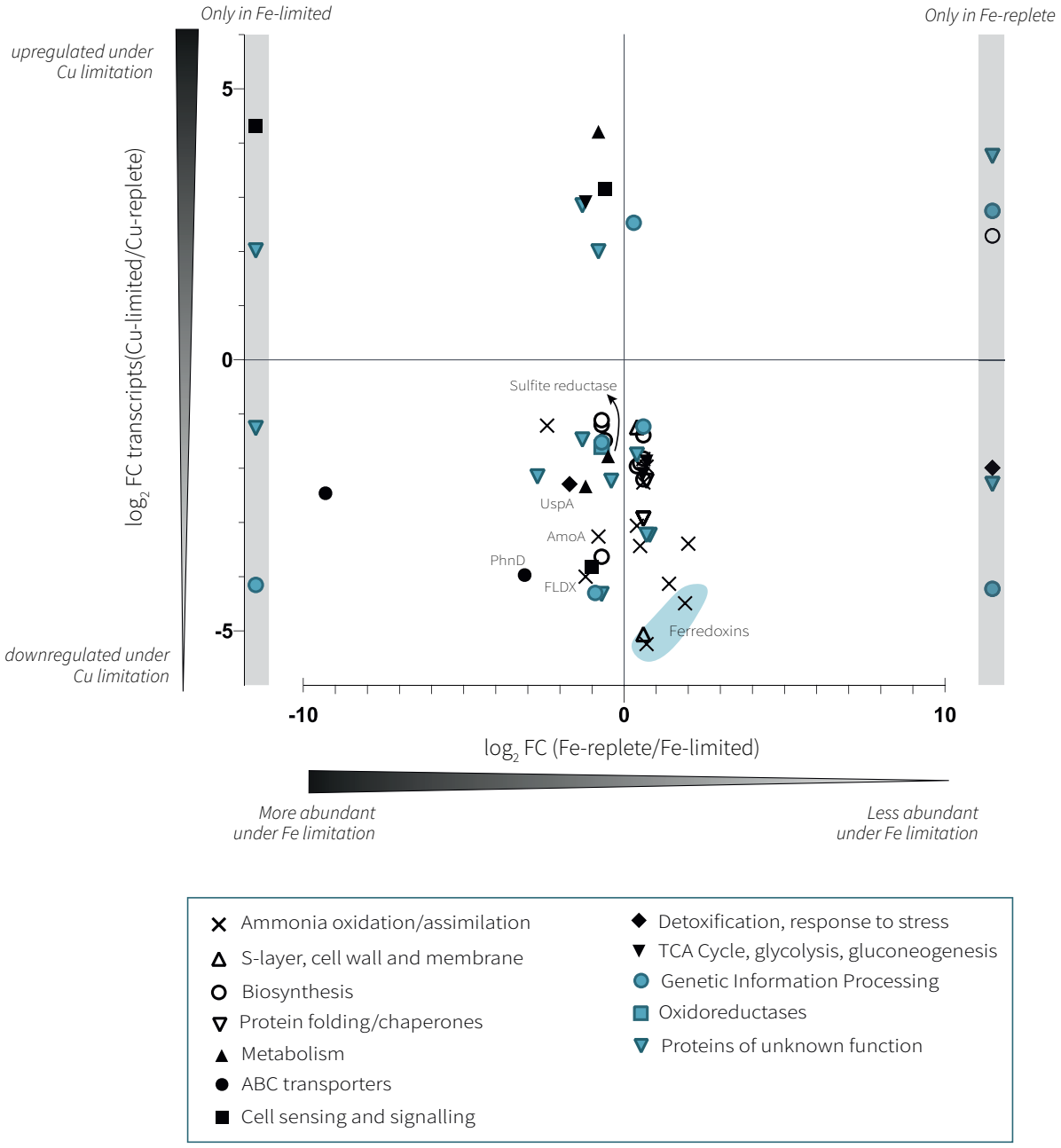


Figure A2.5 Comparison of Fe and Cu limitation on protein and gene expression

Significant $\log_2$ fold changes (5% FDR-adjusted *p* value) in protein intensity in this study plotted against the $\log_2$ fold change in that corresponding gene transcript under Cu limitation in Qin et al. (2018). Proteins in grey shaded area offset from x-axis represent proteins only detected in one of the Fe treatments. Proteins are grouped into their biological function groups. Labelled proteins/genes represent the following: AmoA: Nmar_1500, UspA: Nmar_1659, Sulfite reductase: Nmar_0679, PhnD: Nmar_0875, FLDX: Nmar_1356, Ferredoxins: Nmar_0239, Nmar_1537. Comparison of data shown in Table A2.3.

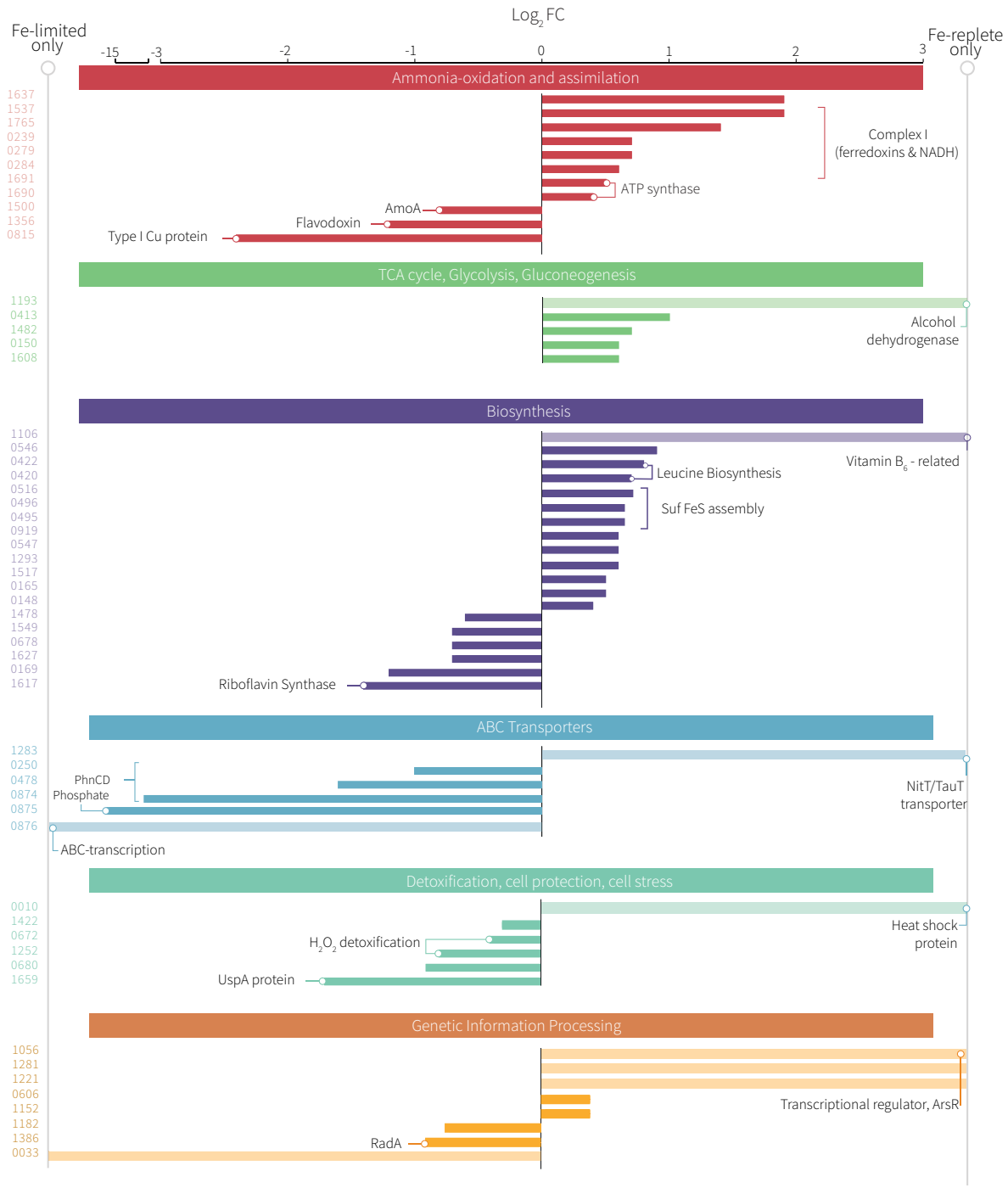


Figure A2.6 Proteins showing a significant LFQ intensity change under Fe limitation

Proteins showing significant changes in LFQ intensity on a $\log_2$ fold change scale assigned into different biological function groups. Bars reaching 'Fe-replete only' or 'Fe-limited only' indicate proteins which were only present under that treatment and absent from the contrasting treatment. Proteins of potential interest are labelled.

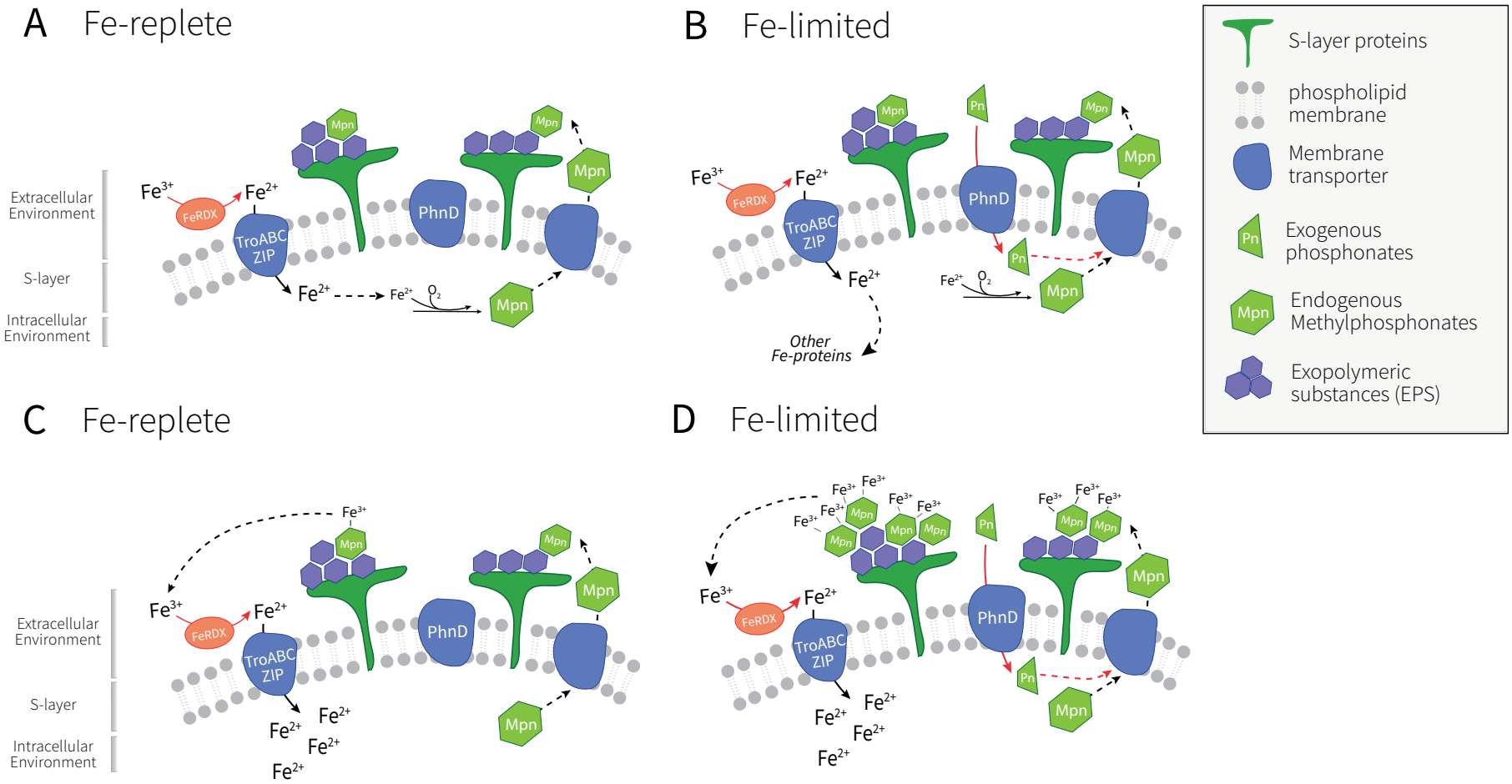


Figure A2.7 Hypothetical pathways linking increased Phn intensity under Fe limitation with Mpn production

Schematic Figure showing two hypothetical pathways linking increased Phn intensity under Fe limitation with methylphosphonate (Mpn) production. Hypothesis 1: **A)** Under Fe-replete conditions, there is sufficient Fe to allow for the production of the Fe-binding protein methylphosphonate synthase and

the final Fe^{2+} requiring step in *N. maritimus*' Mpn production. **B)** Under Fe limitation, there is not sufficient Fe to catalyse the final Fe^{2+} requiring step and thus *N. maritimus* increases the uptake of exogenous phosphonates to supplement the reduction in endogenous phosphonates. Hypothesis 2: **C)** Under Fe-replete conditions, the proportion of Mpn which decorates exopolymeric substances (EPS) is low, due to the abundance of extracellular Fe. **D)** Under Fe-limited conditions, increased exogenous phosphonate uptake is designed to enhance the cell's own Mpn production to increase the proportion of P-bearing groups on the EPS. In doing so, the EPS becomes more chemically attractive to Fe, thus supplying more Fe to the cell's putative ferric reductase (FeRDX) and increasing Fe uptake to the cell.

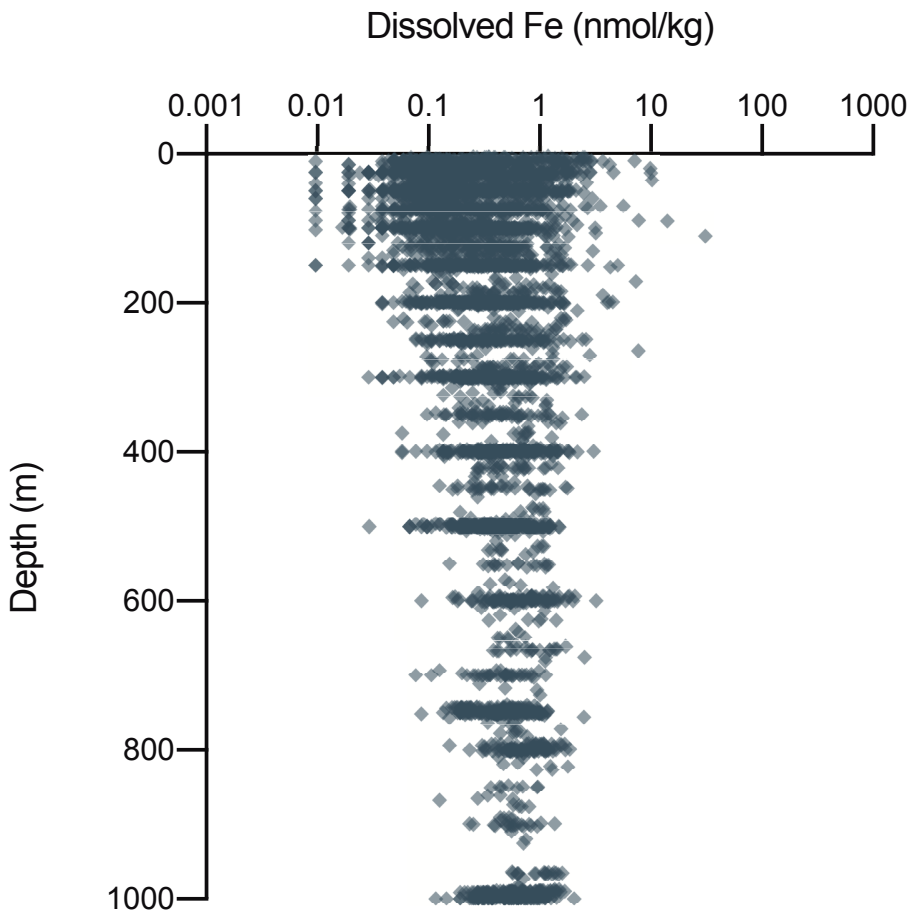


Figure A2.8 Oceanic dissolved Fe from GEOTRACES Intermediate Data Product 2017

Data downloaded from https://webodv.awi.de/geotraces in Jan 2021.

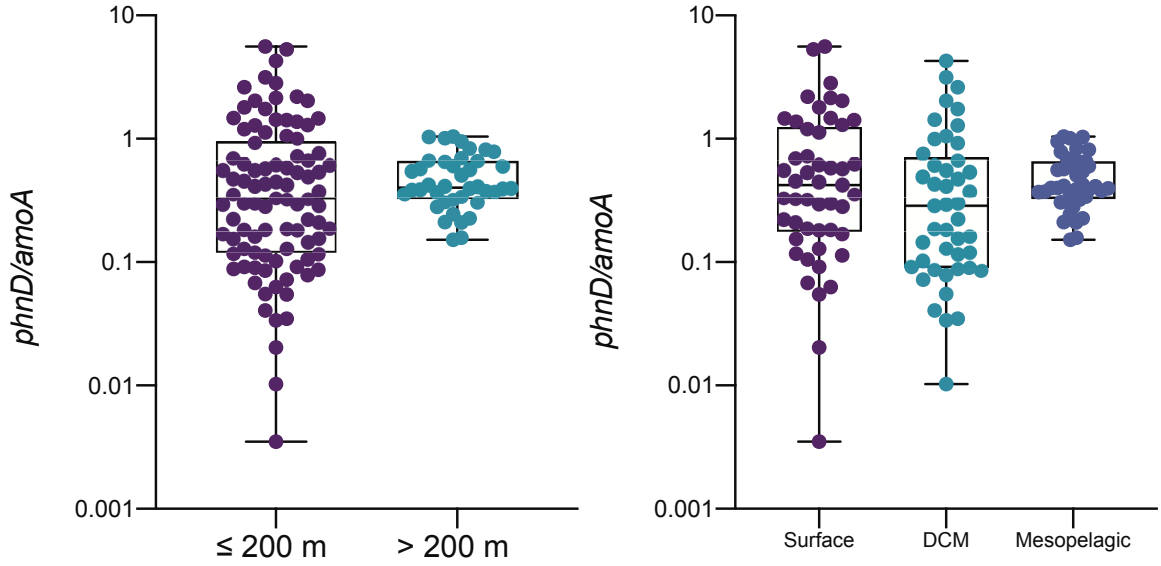


Figure A2.9 Analysis of *phnD* biogeography from *Tara* Oceans Gene Atlas

Analysis of *phnD* biogeography from *Tara* Oceans Gene Atlas. Figures show mean *phnD* copies per cell normalised to the mean *amoA* copies per cell from the same *Tara* sample (each point represents a different *Tara* sample – full data in Table A2.4). Left hand panel shows results grouped into ≤ 200m and 200 m for consistency of comparison with Qin et al. (2020) and right-hand panel shows the grouping based on *Tara* parameters (where surface and dissolved chlorophyll maximum, DCM, are ≤ 200m and mesopelagic is > 200 m). Error bars show range, box shows the standard deviation and line shows the mean.

				LFQ intensity		log_2 FC (Fe replete/Fe-limited)
Name	**q-value**	**Category**	**Name**	**Fe-limited**	**Fe-replete**	
Nmar_1283	0.00	ABC Transporters	NitT/TauT family transport permease protein (Sulfonate/Taurine/Nitrate transporter)	0.0E+00	2.4E+07	Fe-replete only
Nmar_0250	0.02	ABC Transporters	phnD; phosphonate transport system substrate-binding protein	9.0E+07	4.4E+07	-1.0
Nmar_0874	0.00	ABC Transporters	phnC; phosphonate transport system ATP-binding protein	3.7E+08	1.2E+08	-1.6
Nmar_0875	0.00	ABC Transporters	phnD; phosphonate transport system substrate-binding protein	5.2E+10	5.9E+09	-3.1
Nmar_0478	0.00	ABC Transporters	Hypothetical protein	1.5E+10	2.5E+07	-9.3
Nmar_0876	0.00	ABC Transporters	Hypothetical transcriptional regulatory protein	2.3E+08	0.0E+00	Fe-limited only
Nmar_1637	0.00	Ammonia oxidation/Assimilation	Copper binding proteins, plastocyanin/azurin family	1.7E+08	6.1E+08	1.9
Nmar_1537	0.00	Ammonia oxidation/Assimilation	4Fe-4S ferredoxin iron-sulphur binding domain protein	6.9E+09	2.7E+10	1.9
Nmar_1765	0.03	Ammonia oxidation/Assimilation	4Fe-4S ferredoxin iron-sulphur binding domain protein	8.3E+08	2.2E+09	1.4
Nmar_0239	0.03	Ammonia oxidation/Assimilation	Ferredoxin	7.8E+09	1.3E+10	0.7
Nmar_0279	0.03	Ammonia oxidation/Assimilation	NAD(P)H-quinone oxidoreductase	3.0E+08	4.9E+08	0.7
Nmar_0284	0.02	Ammonia oxidation/Assimilation	NADH-quinone oxidoreductase (transmembrane segment)	3.2E+08	5.0E+08	0.6
Nmar_1691	0.03	Ammonia oxidation/Assimilation	V-type ATP synthase alpha chain	7.8E+09	1.1E+10	0.5
Nmar_1690	0.03	Ammonia oxidation/Assimilation	V-type ATP synthase beta chain	3.3E+09	4.3E+09	0.4
Nmar_1500	0.02	Ammonia oxidation/Assimilation	Archaeal ammonia monooxygenase subunit A	3.7E+09	2.2E+09	-0.8
Nmar_1356	0.02	Ammonia oxidation/Assimilation	Flavodoxin	4.0E+08	1.8E+08	-1.2
Nmar_0815	0.00	Ammonia oxidation/Assimilation	Copper binding protein (plastocyanin/azurin family)	9.8E+09	1.8E+09	-2.4
Nmar_1106	0.00	Biosynthesis	Pyridoxamine 5'-phosphate oxidase-related FMN-binding	0.0E+00	1.9E+07	Fe-replete only
Nmar_0546	0.03	Biosynthesis	Aspartate transmaminase	2.2E+08	4.0E+08	0.9
Nmar_0422	0.00	Biosynthesis	3-isopropylmalate dehydratase, isozyme 1, large subunit	8.2E+07	1.5E+08	0.8
Nmar_0420	0.03	Biosynthesis	3-isopropylmalate dehydratase, isozyme 2, large subunit	2.7E+08	4.5E+08	0.7
Nmar_0919	0.01	Biosynthesis	CTP synthase	1.0E+08	1.6E+08	0.6
Nmar_0547	0.00	Biosynthesis	Chorismate synthase	2.7E+08	4.2E+08	0.6
Nmar_1293	0.03	Biosynthesis	Pyruvate carboxyltransferase OS	2.9E+08	4.3E+08	0.6
Nmar_0165	0.03	Biosynthesis	Glycosyltransferase	1.5E+08	2.1E+08	0.5
Nmar_0148	0.02	Biosynthesis	Glutamate-1-semialdehyde aminotransferase	6.5E+08	8.2E+08	0.3
Nmar_1478	0.03	Biosynthesis	Glutamine amidotransferase subunit PdxT	1.8E+08	1.2E+08	-0.6
Nmar_1549	0.02	Biosynthesis	Threonine synthase	4.2E+08	2.7E+08	-0.7
Nmar_0678	0.03	Biosynthesis	Thiazole biosynthesis enzyme	5.5E+08	3.4E+08	-0.7

Nmar_1627	0.03	Biosynthesis	ribonucleotide reductase	6.0E+08	3.7E+08	-0.7
Nmar_0169	0.03	Biosynthesis	Methylthioribose-1-phosphate isomerase	3.6E+08	1.5E+08	-1.2
Nmar_1617	0.01	Biosynthesis	Riboflavin synthase, alpha subunit	7.6E+07	2.9E+07	-1.4
Nmar_1481	0.00	Cell sensing and signalling	Putative signal transduction protein with CBS domains	0.0E+00	6.6E+07	Fe-replete only
Nmar_0764	0.01	Cell sensing and signalling	CBS domain containing protein	1.8E+08	3.3E+08	0.9
Nmar_1349	0.01	Cell sensing and signalling	Putative sensor with HAMP domain	6.5E+08	9.3E+08	0.5
Nmar_0164	0.01	Cell sensing and signalling	Putative signal transduction protein with CBS domains	1.4E+08	9.7E+07	-0.6
Nmar_1766	0.00	Cell sensing and signalling	hamp domain protein	1.8E+09	5.0E+08	-1.8
Nmar_0010	0.00	Detoxification	Small heat shock protein	0.0E+00	5.4E+07	Fe-replete only
Nmar_1422	0.02	Detoxification	Small heat shock protein	4.5E+08	3.6E+08	-0.3
Nmar_1252	0.03	Detoxification	Alkyl hydroperoxide reductase	3.8E+08	2.2E+08	-0.8
Nmar_0680	0.01	Detoxification	Rhodanese domain protein OS	9.7E+08	5.2E+08	-0.9
Nmar_1659	0.01	Detoxification	UspA domain protein OS	2.6E+09	8.1E+08	-1.7
Nmar_0672	0.04	Detoxification	Thioredoxin reductase OS	1.2E+09	9.1E+08	-0.4
Nmar_1056	0.00	Genetic information processing	DNA polymerase-related protein	0.0E+00	3.6E+07	Fe-replete only
Nmar_1281	0.00	Genetic information processing	Transcriptional regulator, ArsR family	0.0E+00	3.0E+07	Fe-replete only
Nmar_1221	0.00	Genetic information processing	Zn-ribbon RNA-binding protein	0.0E+00	1.1E+07	Fe-replete only
Nmar_0606	0.03	Genetic information processing	Type I restriction-modification system, M subunit	2.5E+08	3.1E+08	0.3
Nmar_1152	0.00	Genetic information processing	type I restriction-modification system, M subunit	2.5E+08	3.1E+08	0.3
Nmar_1182	0.01	Genetic information processing	Cold-shock deAd box protein	5.0E+08	3.1E+08	-0.7
Nmar_1386	0.00	Genetic information processing	DNA repair and recombination protein RadA	4.5E+08	2.5E+08	-0.9
Nmar_0033	0.00	Genetic information processing	DNA binding - Winged helix DNA-binding	1.6E+08	0.0E+00	Fe-limited only
Nmar_0883	0.03	Metabolism (other)	Histidine triad (HIT) proteins	3.9E+08	2.8E+08	-0.4
Nmar_0023	0.02	Metabolism (other)	Adenylylsulfate kinase	8.2E+08	3.6E+08	-1.2
Nmar_0679	0.04	Metabolism (other)	Sulfite reductase	2.4E+09	1.7E+09	-0.5
Nmar_1321	0.00	Oxidoreductases	Short-chain dehydrogenase/reductase SDR	1.1E+09	5.1E+08	-1.1
Nmar_1643	0.00	Protein folding/Chaperone	ATPase, MoxR family [ATP binding]	2.8E+08	1.4E+09	2.3
Nmar_0516	0.04	Protein folding/Chaperone	FeS assembly ATPase (SufC)	7.7E+08	1.2E+09	0.7
Nmar_0496	0.04	Protein folding/Chaperone	FeS assembly protein (SufB)	6.5E+08	9.6E+08	0.6
Nmar_0495	0.04	Protein folding/Chaperone	FeS assembly protein (SufB)	4.7E+08	6.9E+08	0.6
Nmar_1476	0.00	S-layer, cell wall and membrane	Cell wall protein	0.0E+00	1.8E+07	Fe-replete only
Nmar_1638	0.02	S-layer, cell wall and membrane	hypothetical protein	2.7E+09	1.0E+10	1.9

Nmar_0825	0.02	S-layer, cell wall and membrane	Band 7 protein	1.3E+09	9.0E+08	-0.5
Nmar_1193	0.00	TCA/Glycolysis/Gluconeogenesis	Alcohol dehydrogenase GroES domain protein	0.0E+00	2.6E+07	Fe-replete only
Nmar_1482	0.02	TCA/Glycolysis/Gluconeogenesis	Aconitate hydratase	7.4E+08	1.2E+09	0.7
Nmar_0150	0.02	TCA/Glycolysis/Gluconeogenesis	GDP-mannose 4,6-dehydratase	5.2E+08	7.7E+08	0.6
Nmar_1608	0.02	TCA/Glycolysis/Gluconeogenesis	Aldehyde dehydrogenase OS	3.3E+08	5.0E+08	0.6
Nmar_0413	0.04	TCA/Glycolysis/Gluconeogenesis	2-oxoacid: ferredoxin oxidoreductase, alpha subunit	1.6E+08	3.3E+08	1.0
Nmar_1483	0.03	Uncharacterised proteins	Uncharacterised protein	0.0E+00	4.1E+07	Fe-replete only
Nmar_0730	0.00	Uncharacterised proteins	Uncharacterised protein	0.0E+00	5.1E+07	Fe-replete only
Nmar_1159	0.00	Uncharacterised proteins	Uncharacterised protein	0.0E+00	4.4E+07	Fe-replete only
Nmar_0074	0.03	Uncharacterised proteins	Uncharacterised protein	1.1E+09	2.5E+09	1.1
Nmar_0130	0.00	Uncharacterised proteins	Uncharacterised protein	3.9E+08	7.7E+08	1.0
Nmar_0195	0.03	Uncharacterised proteins	Uncharacterised protein	1.0E+08	1.8E+08	0.8
Nmar_0196	0.02	Uncharacterised proteins	Uncharacterised protein	7.8E+08	1.3E+09	0.7
Nmar_0448	0.00	Uncharacterised proteins	Uncharacterised protein	1.3E+08	1.9E+08	0.5
Nmar_0589	0.03	Uncharacterised proteins	Uncharacterised protein	2.2E+09	2.8E+09	0.4
Nmar_0627	0.03	Uncharacterised proteins	Uncharacterised protein	2.3E+08	1.8E+08	-0.4
Nmar_0700	0.00	Uncharacterised proteins	Uncharacterised protein	1.1E+09	6.6E+08	-0.7
Nmar_0717	0.03	Uncharacterised proteins	Uncharacterised protein	1.4E+08	7.8E+07	-0.8
Nmar_0752	0.00	Uncharacterised proteins	Uncharacterised protein	4.0E+08	2.1E+08	-0.9
Nmar_1154	0.03	Uncharacterised proteins	Uncharacterised protein	1.9E+08	9.1E+07	-1.1
Nmar_1361	0.00	Uncharacterised proteins	Uncharacterised protein	1.0E+08	4.1E+07	-1.3
Nmar_1590	0.00	Uncharacterised proteins	Uncharacterised protein	6.3E+09	4.2E+07	-7.2
Nmar_1642	0.00	Uncharacterised proteins	Uncharacterised protein	1.3E+08	0.0E+00	Fe-limited only

Table A2.1 Proteins which change significantly in LFQ intensity between Fe treatments

Proteins which show a significant change in LFQ intensity (FDR adjusted *p* value/q-value < 0.05) between Fe treatments. Log_2 fold change (Fe-replete LFQ intensity /Fe-limited LFQ intensity) values in red indicate proteins that increase in intensity under Fe limitation and decrease in intensity under Fe replete treatments. Values in green indicate proteins which increase in intensity under Fe replete treatments and decrease in intensity under Fe limitation. Proteins which are only detected in Fe-limited treatments and Fe-replete treatments are denoted as 'Fe-limited only' or 'Fe-replete only'. Proteins are grouped by their biological function category.

Protein	GO Category	Gene ontology subcategory	Description	no. Fe-sites	LFQ intensity Fe-replete	LFQ intensity Fe-limited	Sig different?
Nmar_1502	Ammonia oxidation	Ammonia monooxygenase	Ammonia monooxygenase subunit C	3	9.4E+09	6.8E+09	N
Nmar_0238	Ammonia oxidation	Complex I and ferredoxins		3	2.4E+09	2.5E+09	N
Nmar_0239	Ammonia oxidation	Complex I and ferredoxins	4Fe-4S ferredoxin iron-sulphur binding domain protein	**3**	**1.3E+10**	**7.8E+09**	**Y**
Nmar_0281	Ammonia oxidation	Complex I and ferredoxins	4Fe-4S ferredoxin iron-sulphur binding domain protein	4	9.3E+07	1.2E+08	N
Nmar_0443	Ammonia oxidation	Complex I and ferredoxins	4Fe-4S ferredoxin iron-sulphur binding domain protein	4	5.3E+08	6.4E+08	N
Nmar_0965	Ammonia oxidation	Complex III	Rieske (2Fe-2S) domain protein	7	2.0E+08	1.9E+08	N
Nmar_1537	Ammonia oxidation	Complex I and ferredoxins	4Fe-4S ferredoxin iron-sulphur binding domain protein	**3**	**2.7E+10**	**6.9E+09**	**Y**
Nmar_1765	Ammonia oxidation	Complex I and ferredoxins	4Fe-4S ferredoxin iron-sulphur binding domain protein	**4**	**2.2E+09**	**8.3E+08**	**Y**
Nmar_1544	Ammonia oxidation	Complex III	Rieske (2Fe-2S) domain protein	2	8.7E+07	9.0E+07	N
Nmar_0184	Ammonia oxidation	Complex IV	Cytochrome c oxidase subunit I	1	1.2E+09	1.8E+09	N
Nmar_1543	Ammonia oxidation	Complex III	Cytochrome b/b6 domain	1	4.2E+08	6.2E+08	N
Nmar_0420	Biosynthesis (other)	Amino acid biosynthesis	3-isopropylmalate dehydratase large subunit	**4**	**4.5E+08**	**2.7E+08**	**Y**
Nmar_0422	Biosynthesis (other)	Amino acid biosynthesis	3-isopropylmalate dehydratase, large subunit	**10**	**1.5E+08**	**8.2E+07**	**Y**
Nmar_0678	Biosynthesis (other)	Amino acid biosynthesis	Thiamine thiazole synthase	**4**	**3.4E+08**	**5.5E+08**	**Y**
Nmar_0781	Biosynthesis (other)	Amino acid biosynthesis	Amidophosphoribosyltransferase	4	1.6E+08	1.9E+08	N
Nmar_0886	Biosynthesis (other)	Amino acid biosynthesis	Dihydroxy-acid dehydratase	19	4.3E+08	6.7E+08	N
Nmar_0037	Biosynthesis (other)	Other biosynthesis	7-carboxy-7-deazaguanine synthase	11	4.0E+07	4.3E+07	N
Nmar_0155	Biosynthesis (other)	Other biosynthesis	methylphosphonate synthase	2	1.7E+08	1.4E+08	N
Nmar_0554	Biosynthesis (other)	Co-factor biosynthesis	Cyclic dehypoxanthine futalosine synthase	3	2.7E+07	0.0E+00	N
Nmar_0592	Biosynthesis (other)	Co-factor biosynthesis	Radical SAM domain protein	11	2.4E+06	0.0E+00	N
Nmar_0742	Biosynthesis (other)	Co-factor biosynthesis	Radical SAM domain protein	5	3.1E+06	0.0E+00	N
Nmar_0821	Biosynthesis (other)	Co-factor biosynthesis	Biotin synthase	15	6.7E+06	0.0E+00	N
Nmar_1239	Biosynthesis (other)	Co-factor biosynthesis	Quinolinate synthase A	5	1.3E+08	0.0E+00	N
Nmar_1389	Biosynthesis (other)	Biosynthesis (other)	Oxidoreductase FAD/NAD(P)-binding domain protein	11	2.3E+08	2.6E+08	N
Nmar_0052	Genetic info. processing	Endonucleases	Endonuclease III	15	0.0E+00	8.3E+06	N
Nmar_0065	Genetic info. processing	DNA replication	DNA primase large subunit PriL	15	6.0E+07	5.4E+07	N

Nmar_1385	Genetic info. processing	Ribosome	Ribosomal RNA large subunit methyltransferase N	8	1.7E+07	1.5E+07	N
Nmar_0679	Metabolism (other)	Sulphur assimilation	Sulfite reductase (Ferredoxin)	**2**	**1.7E+09**	**2.4E+09**	**Y**
Nmar_1121	Metabolism (other)	Ferritin Dps protein	Ferritin Dps family protein	4	5.1E+08	4.5E+08	N
Nmar_1772	Metabolism (other)		Lysine 2,3-aminomutase related protein	3	4.0E+08	5.2E+08	N
Nmar_0261	TCA	Synthesis of succinate	Succinate dehydrogenase/fumarate reductase iron-sulphur	4	6.0E+07	6.6E+07	N
Nmar_0413	TCA	Electron transport chain	Pyruvate flavodoxin/ferredoxin oxidoreductase	2	3.3E+08	1.6E+08	Y
Nmar_0414	TCA	Electron transport chain	Pyruvate ferredoxin/flavodoxin oxidoreductase	0	2.3E+07	1.1E+08	N
Nmar_1482	TCA	Synthesis of alpha-ketoglutarate	Aconitate hydratase	**10**	**1.2E+09**	**7.4E+08**	**Y**
Nmar_1110	Carbon fixation	3-hydroxypropionate/4-hydroxybutyrate cycle	Iron-containing alcohol dehydrogenase	1	4.0E+09	4.2E+09	N

Table A2.2 Putative Fe-containing proteins and their corresponding LFQ intensity in *N. maritimus*

Proteins predicted to contain Fe and the putative number of Fe atoms bound to the protein based on analysis presented in Section 3.3.7. Proteins which change significantly in abundance between Fe treatments are highlighted in bold.

				Log$_2$ fold change		
				Proteins	Transcripts	
Protein/gene	**q-val**	**Category**	**Name**	**Fe-replete/ Fe-limited**	**Cu-limited/ Cu-replete**	**NH_4^+-replete/NH_4^+-starvation**
General limitation response						
Nmar_1765	0.03	Ammonia oxidation	4Fe-4S ferredoxin iron-sulphur binding domain protein	1.4	-4.13	1.33
Nmar_1691	0.03	Ammonia oxidation	V-type ATP synthase alpha chain	0.5	-3.43	0.27
Nmar_1528	0.04	Ammonia oxidation	ATPase	2	-3.39	0.43
Nmar_1690	0.03	Ammonia oxidation	V-type ATP synthase beta chain	0.4	-3.06	0.32
Nmar_1312	0.04	Ammonia oxidation	Glutamate dehydrogenase	0.6	-2.26	0.72
Nmar_0344	0.05	S-layer, cell wall and membrane	Hypothetical protein	0.6	-5.06	1.14
General metal limitation response						
Nmar_0717	0.03	Uncharacterised proteins	Uncharacterised protein	-0.8	2	n.d.
Nmar_1481	0.00	Cell sensing and signalling	Putative signal transduction protein with CBS domains	only Fe-limited	4.31	n.d.
Nmar_0239	0.03	Ammonia oxidation	Ferredoxin	0.7	-5.24	1.48
Nmar_1537	0.00	Ammonia oxidation	4Fe-4S ferredoxin iron-sulphur binding domain protein	1.9	-4.49	n.d.
Nmar_0279	0.03	Ammonia oxidation	NAD(P)H-quinone oxidoreductase	0.7	-1.97	n.d.
Nmar_0547	0.00	Biosynthesis	Chorismate synthase	0.6	-2.2	n.d.
Nmar_0265	0.04	Biosynthesis	Glutamyl-tRNA reductase	0.4	-1.96	n.d.
Nmar_0165	0.03	Biosynthesis	Glycosyltransferase	0.5	-1.9	n.d.
Nmar_1517	0.04	Biosynthesis	Pyridoxal-5-phosphate-dependent protein beta subunit	0.6	-1.82	n.d.
Nmar_1293	0.03	Biosynthesis	Pyruvate carboxyltransferase	0.6	-1.39	n.d.
Nmar_0164	0.01	Cell sensing and signalling	Putative signal transduction protein with CBS domains	-0.6	3.15	n.d.
Nmar_0010	0.00	Detoxification	Small heat shock protein	only Fe-replete	-1.99	n.d.
Nmar_1221	0.00	Genetic information processing	Zn-ribbon RNA-binding protein	only Fe-replete	-4.22	n.d.
Nmar_1490	0.04	Genetic information processing	Tryptophanyl-tRNA synthetase	0.6	-1.23	n.d.
Nmar_0141	0.04	Metabolism (other)	Long/very long chain acyl-CoA synthetase	-0.8	4.21	n.d.
Nmar_0496	0.04	Protein folding/Chaperone	FeS assembly protein (SufB)	0.6	-2.93	n.d.
Nmar_0495	0.04	Protein folding/Chaperone	FeS assembly protein (SufB)	0.6	-2.93	n.d.
Nmar_0516	0.04	Protein folding/Chaperone	FeS assembly ATPase (SufC)	0.7	-2.23	n.d.

Nmar_1795	0.04	S-layer, cell wall and membrane	Geranylgeranylglyceryl phosphate synthase	0.4	-1.24	n.d.
Nmar_0140	0.04	TCA/Glycolysis/Gluconeogenesis	4-hydroxy-2-oxovalerate aldolase	-1.2	2.91	n.d.
Nmar_1608	0.02	TCA/Glycolysis/Gluconeogenesis	Aldehyde dehydrogenase OS	0.6	-2.1	n.d.
Nmar_1482	0.02	TCA/Glycolysis/Gluconeogenesis	Aconitate hydratase	0.7	-1.87	n.d.
Nmar_1642	0.00	Uncharacterised proteins	Uncharacterised protein	-20	2.02	n.d.
Nmar_1361	0.00	Uncharacterised proteins	Uncharacterised protein	-1.3	2.85	n.d.
Nmar_0195	0.03	Uncharacterised proteins	Uncharacterised protein	0.8	-3.23	n.d.
Nmar_0196	0.02	Uncharacterised proteins	Uncharacterised protein	0.7	-3.23	n.d.
Nmar_0730	0.00	Uncharacterised proteins	Uncharacterised protein	only Fe-replete	-2.29	n.d.
Nmar_0589	0.03	Uncharacterised proteins	Uncharacterised protein	0.4	-1.75	n.d.
Cu-specific limitation response						
Nmar_1106	0.00	Biosynthesis	Pyridoxamine 5'-phosphate oxidase-related FMN-binding	only Fe-replete	2.29	n.d.
Nmar_1152	0.00	Genetic information processing	type I restriction-modification system, M subunit	0.3	2.53	n.d.
Nmar_1281	0.00	Genetic information processing	Transcriptional regulator, ArsR family	only Fe-replete	2.75	-0.11
Nmar_1159	0.00	Uncharacterised proteins	Uncharacterised protein	only Fe-replete	3.76	n.d.
Fe-specific limitation response (highly likely)						
Nmar_0875	0.00	ABC Transporters	phnD; phosphonate transport substrate-binding protein	-3.1	-3.97	0.87
Nmar_1500	0.02	Ammonia oxidation	Archaeal ammonia monooxygenase subunit A	-0.8	-3.26	0.86
Nmar_1627	0.03	Biosynthesis	ribonucleotide reductase	-0.7	-3.63	0.57
Nmar_0678	0.03	Biosynthesis	Thiazole biosynthesis enzyme	-0.7	-1.2	0.40
Nmar_1659	0.01	Detoxification	UspA domain protein OS	-1.7	-2.29	0.21
Fe-specific limitation response (highly likely)						
Nmar_0700	0.00	Uncharacterised proteins	Uncharacterised protein	-0.7	-4.32	n.d.
Nmar_0478	0.00	ABC Transporters	Hypothetical protein	-9.3	-2.46	n.d.
Nmar_1356	0.02	Ammonia oxidation	Flavodoxin	-1.2	-4	n.d.
Nmar_0815	0.00	Ammonia oxidation	Copper binding protein (plastocyanin/azurin family)	-2.4	-1.21	n.d.
Nmar_1478	0.03	Biosynthesis	Glutamine amidotransferase subunit PdxT	-0.6	-1.48	n.d.
Nmar_1549	0.02	Biosynthesis	Threonine synthase	-0.7	-1.11	n.d.
Nmar_0465	0.05	Cell sensing and signalling	chemotaxis protein	-1	-3.81	n.d.
Nmar_1386	0.00	Genetic information processing	DNA repair and recombination protein RadA	-0.9	-4.3	n.d.

Nmar_0033	0.00	Genetic information processing	Winged helix DNA-binding domain superfamily	only Fe-limited	-4.15	n.d.
Nmar_1628	0.04	Genetic information processing	Regulatory protein ArsR	-0.7	-1.52	n.d.
Nmar_0023	0.02	Metabolism (other)	Adenylylsulfate kinase	-1.2	-2.33	n.d.
Nmar_0679	0.04	Metabolism (other)	Sulfite reductase	-0.5	-1.78	n.d.
Nmar_1737	0.04	Oxidoreductases	NADH-dependent FMN reductase	-0.7	-1.6	n.d.
Nmar_1541	0.05	Uncharacterised proteins	Uncharacterised protein	-2.7	-2.15	n.d.
Nmar_1229	0.04	Uncharacterised proteins	Uncharacterised protein	-1.3	-1.47	n.d.
Nmar_1735	0.04	Uncharacterised proteins	Uncharacterised protein	only Fe-limited	-1.26	n.d.
Fe and NH_4^+ specific limitation response						
Nmar_0627	0.03	Uncharacterised proteins	Uncharacterised protein	-0.4	-2.23	n.d.

Table A2.3 Comparison of Cu, NH_4^+ and Fe limitation on protein abundances and gene expression

Differentially intense proteins in this study with differential gene expression in response to Cu/NH_4^+ limitation in **Qin et al. (2018)**. Proteins are categorised into those postulated to be a general limitation response, general metal limitation response, Cu-specific response, Fe-limitation response (highly likely), potential Fe-specific responses, and Fe and NH_4^+ response. All differential intensity/expression data is statistically significant at a significance level of 5%.

Tara sample number	Depth	Filter size (µm)	*phnD* (average copies cell^{-1})	*amoA* (average copies cell^{-1})	*phnD/amoA*
133	DCM	0.22-3	5.75E-06	1.42E-04	4.05E-02
58	DCM	0.22-3	8.41E-06	1.17E-04	7.20E-02
64	DCM	0.22-3	1.83E-05	1.78E-03	1.03E-02
122	DCM	0.22-0.45	2.60E-05	1.17E-04	2.22E-01
122	DCM	0.45-0.8	3.01E-05	5.45E-05	5.53E-01
128	DCM	0.22-3	3.05E-05	3.38E-04	9.00E-02
100	DCM	0.22-3	3.12E-05	5.67E-04	5.51E-02
36	DCM	0.22-1.6	4.25E-05	6.40E-05	6.64E-01
111	DCM	0.22-3	4.57E-05	7.53E-05	6.07E-01
72	DCM	0.22-3	5.05E-05	5.83E-04	8.67E-02
110	DCM	0.22-3	6.09E-05	2.04E-04	2.99E-01
65	DCM	0.22-3	6.16E-05	7.01E-04	8.79E-02
98	DCM	0.22-3	6.75E-05	8.91E-05	7.58E-01
112	DCM	0.22-3	7.30E-05	1.70E-05	4.29E+00
42	DCM	0.22-1.6	9.02E-05	1.15E-03	7.82E-02
18	DCM	0.22-1.6	9.40E-05	5.38E-05	1.75E+00
137	DCM	0.22-3	1.09E-04	5.86E-04	1.86E-01
7	DCM	0.22-1.6	1.58E-04	1.71E-04	9.22E-01
66	DCM	0.22-3	1.65E-04	1.06E-03	1.55E-01
68	DCM	0.22-0.45	1.65E-04	4.90E-03	3.37E-02
138	DCM	0.22-3	1.78E-04	1.95E-03	9.16E-02
76	DCM	0.22-3	1.87E-04	1.46E-03	1.28E-01
76	DCM	0.22-0.45	1.94E-04	5.56E-03	3.49E-02
150	DCM	0.22-3	2.21E-04	7.74E-04	2.85E-01
76	DCM	0.45-0.8	2.22E-04	1.91E-03	1.16E-01
100	DCM	0.22-3	2.29E-04	2.25E-03	1.02E-01
78	DCM	0.45-0.8	2.70E-04	1.86E-03	1.45E-01
122	DCM	0.22-3	2.88E-04	9.19E-05	3.14E+00
4	DCM	0.22-1.6	3.35E-04	6.28E-04	5.33E-01
132	DCM	0.22-3	3.52E-04	1.93E-03	1.82E-01
78	DCM	0.22-0.45	3.87E-04	4.54E-03	8.52E-02
122	DCM	0.1-0.22	3.97E-04	8.08E-04	4.91E-01
78	DCM	0.22-3	4.36E-04	3.64E-03	1.19E-01
68	DCM	0.45-0.8	4.50E-04	1.55E-03	2.91E-01
38	DCM	0.22-1.6	4.58E-04	1.06E-03	4.32E-01
68	DCM	0.22-3	4.97E-04	3.07E-03	1.62E-01
41	DCM	0.22-1.6	5.32E-04	1.42E-03	3.76E-01
151	DCM	0.22-3	8.80E-04	1.86E-03	4.73E-01
65	DCM	0.1-0.22	9.44E-04	2.28E-03	4.14E-01
23	DCM	0.22-1.6	1.23E-03	9.55E-04	1.29E+00
142	DCM	0.22-3	2.04E-03	7.80E-04	2.61E+00
9	DCM	0.22-1.6	2.93E-03	2.93E-03	9.98E-01
25	DCM	0.22-1.6	2.98E-03	2.83E-03	1.05E+00
34	DCM	0.22-1.6	7.72E-03	5.40E-03	1.43E+00
32	DCM	0.22-1.6	1.02E-02	5.01E-03	2.04E+00
39	MES	0.22-1.6	1.40E-04	3.39E-04	4.12E-01
39	MES	0.1-0.22	1.57E-04	1.03E-03	1.52E-01
38	MES	0.1-0.22	2.45E-04	1.09E-03	2.26E-01
38	MES	0.22-1.6	3.39E-04	1.21E-03	2.80E-01

78	MES	0.45-0.8	6.64E-04	1.79E-03	3.70E-01
68	MES	0.45-0.8	8.42E-04	2.74E-03	3.07E-01
110	MES	0.22-3	8.77E-04	4.19E-03	2.09E-01
109	MES	0.22-3	9.84E-04	6.21E-03	1.58E-01
122	MES	0.45-0.8	1.16E-03	1.79E-03	6.46E-01
37	MES	0.22-1.6	1.36E-03	2.29E-03	5.94E-01
111	MES	0.22-3	1.47E-03	6.98E-03	2.11E-01
138	MES	0.22-3	1.49E-03	3.83E-03	3.88E-01
137	MES	0.22-3	1.76E-03	4.42E-03	3.99E-01
98	MES	0.22-3	1.93E-03	7.91E-03	2.45E-01
68	MES	0.22-3	2.01E-03	6.61E-03	3.04E-01
148b	MES	0.22-3	2.02E-03	5.06E-03	3.99E-01
146	MES	0.22-3	2.38E-03	7.00E-03	3.40E-01
132	MES	0.22-3	2.45E-03	6.30E-03	3.89E-01
72	MES	0.22-3	2.63E-03	3.96E-03	6.64E-01
65	MES	0.22-3	2.65E-03	8.24E-03	3.21E-01
78	MES	0.22-3	2.78E-03	6.99E-03	3.97E-01
76	MES	0.45-0.8	2.84E-03	4.10E-03	6.93E-01
149	MES	0.22-3	3.10E-03	8.17E-03	3.79E-01
122	MES	0.22-3	3.27E-03	7.69E-03	4.25E-01
102	MES	0.22-3	3.71E-03	9.96E-03	3.72E-01
142	MES	0.22-3	3.73E-03	8.97E-03	4.16E-01
152	MES	0.22-3	4.06E-03	7.24E-03	5.61E-01
122	MES	0.1-0.22	4.13E-03	1.16E-02	3.57E-01
64	MES	0.22-3	4.14E-03	7.64E-03	5.42E-01
37	MES	0.1-0.22	4.32E-03	7.61E-03	5.67E-01
145	MES	0.22-3	4.64E-03	7.03E-03	6.60E-01
85	MES	0.22-3	4.87E-03	4.68E-03	1.04E+00
70	MES	0.45-0.8	4.99E-03	5.23E-03	9.54E-01
112	MES	0.22-3	5.44E-03	9.04E-03	6.02E-01
56	MES	0.22-3	6.09E-03	7.30E-03	8.35E-01
76	MES	0.22-3	6.24E-03	7.62E-03	8.18E-01
133	MES	0.22-3	6.32E-03	8.05E-03	7.86E-01
70	MES	0.22-3	6.92E-03	6.82E-03	1.01E+00
122	MES	0.22-0.45	8.03E-03	1.58E-02	5.07E-01
70	MES	0.22-0.45	1.31E-02	1.26E-02	1.04E+00
124	MIX	0.22-0.45	1.54E-05	1.05E-02	1.46E-03
124	MIX	0.22-3	2.00E-05	9.38E-03	2.13E-03
124	MIX	0.45-0.8	1.76E-04	6.50E-03	2.70E-02
123	MIX	0.22-0.45	2.44E-04	4.26E-03	5.72E-02
123	MIX	0.22-3	3.91E-04	6.30E-03	6.20E-02
125	MIX	0.22-3	4.47E-04	8.78E-03	5.09E-02
123	MIX	0.45-0.8	4.85E-04	7.17E-04	6.76E-01
152	MIX	0.22-3	5.13E-04	1.40E-03	3.66E-01
125	MIX	0.1-0.22	8.71E-04	1.03E-02	8.49E-02
123	MIX	0.1-0.22	8.96E-04	6.07E-03	1.48E-01
124	SRF	0.22-3	3.23E-06	1.59E-04	2.04E-02
30	SRF	0.22-1.6	4.38E-06	6.38E-06	6.87E-01
125	SRF	0.22-3	5.16E-06	9.42E-05	5.48E-02
84	SRF	0.22-3	5.69E-06	2.57E-05	2.21E-01
4	SRF	0.22-1.6	1.01E-05	3.07E-05	3.30E-01

76	SRF	0.45-0.8	1.06E-05	1.15E-04	9.15E-02
78	SRF	0.45-0.8	1.16E-05	1.70E-04	6.80E-02
70	SRF	0.22-3	1.75E-05	1.54E-04	1.14E-01
78	SRF	0.22-0.45	2.08E-05	7.41E-05	2.81E-01
78	SRF	0.22-3	2.37E-05	1.27E-04	1.87E-01
128	SRF	0.22-3	2.76E-05	2.62E-04	1.06E-01
64	SRF	0.22-3	2.98E-05	2.55E-04	1.17E-01
56	SRF	0.22-3	3.86E-05	8.45E-05	4.56E-01
125	SRF	0.22-0.45	4.38E-05	1.25E-02	3.51E-03
70	SRF	0.22-0.45	4.78E-05	2.63E-04	1.82E-01
25	SRF	0.22-1.6	5.65E-05	3.13E-05	1.81E+00
70	SRF	0.45-0.8	5.91E-05	1.82E-04	3.25E-01
7	SRF	0.22-1.6	6.04E-05	9.78E-05	6.18E-01
151	SRF	0.22-3	6.44E-05	1.12E-04	5.76E-01
57	SRF	0.22-3	8.15E-05	1.81E-04	4.49E-01
65	SRF	0.22-3	8.25E-05	6.43E-04	1.28E-01
68	SRF	0.22-0.45	8.97E-05	1.43E-03	6.28E-02
42	SRF	0.22-1.6	9.32E-05	6.35E-05	1.47E+00
66	SRF	0.22-3	1.01E-04	5.55E-04	1.81E-01
62	SRF	0.22-3	1.13E-04	1.00E-04	1.13E+00
67	SRF	0.45-0.8	1.29E-04	4.37E-04	2.95E-01
141	SRF	0.22-3	1.40E-04	2.45E-04	5.70E-01
67	SRF	0.22-3	1.49E-04	7.11E-04	2.09E-01
68	SRF	0.45-0.8	1.62E-04	9.61E-04	1.69E-01
67	SRF	0.22-0.45	1.84E-04	5.21E-04	3.54E-01
140	SRF	0.22-3	1.99E-04	3.75E-05	5.31E+00
150	SRF	0.22-3	2.53E-04	4.14E-04	6.11E-01
38	SRF	0.22-1.6	2.55E-04	4.55E-05	5.60E+00
68	SRF	0.22-3	2.80E-04	1.81E-03	1.55E-01
31	SRF	0.22-1.6	2.91E-04	1.97E-04	1.48E+00
152	SRF	0.22-3	3.03E-04	1.01E-03	2.99E-01
18	SRF	0.22-1.6	3.29E-04	2.39E-04	1.38E+00
32	SRF	0.22-1.6	3.63E-04	1.28E-04	2.83E+00
23	SRF	0.22-1.6	3.68E-04	2.86E-04	1.29E+00
125	SRF	0.45-0.8	5.81E-04	1.80E-03	3.24E-01
149	SRF	0.22-3	7.06E-04	1.65E-03	4.26E-01
33	SRF	0.22-1.6	1.10E-03	5.39E-04	2.04E+00
145	SRF	0.22-3	1.33E-03	2.41E-03	5.50E-01
142	SRF	0.22-3	1.54E-03	7.20E-04	2.14E+00
34	SRF	0.1-0.22	1.61E-03	1.35E-03	1.20E+00
34	SRF	0.22-1.6	1.64E-03	7.44E-04	2.20E+00
65	SRF	0.1-0.22	1.76E-03	3.32E-03	5.31E-01
146	SRF	0.22-3	2.16E-03	3.02E-03	7.16E-01
148	SRF	0.22-3	2.23E-03	1.57E-03	1.42E+00

Table A2.4 Analysis of *phnD* gene biogeography from *Tara* Oceans Gene Atlas

Abundances of *phnD* and *amoA* genes (average copies per cell) in *Tara* oceans database, in different filtered components. Corresponding *Tara* sample numbers are listed. DCM: dissolved chlorophyll maximum, SRF: surface layer, MIX: mixed layer, MESO: mesopelagic.

APPENDIX III

1 SUPPLEMENTARY METHODS

1.1 *N. maritimus* cultures

Polycarbonate culture vessels and culturing apparatus were acid cleaned in 10% (v/v) TraceMetal™ grade HCl (Fisher Scientific, Loughborough, UK) for 24 hours and UV-sterilised before use. Cultures of *N. maritimus* strain SCM1 were maintained as previously described (Amin et al. 2013; Shafiee et al. 2019 — Chapter two) for the purpose of intracellular Cu quota analysis. Basal salt medium and macronutrients were treated with Chelex 100 resin (BioRad, Watford, UK) to remove trace metal contaminants (Price et al. 1989) and passed through an acid-washed (10% HCl v/v) 0.1 µm polycarbonate filter to sterilise in a trace metal-free clean laboratory. The final pH of the media was 7.5 and was buffered with HEPES. Trace metals were added from filter-sterilised concentrated stocks made using > 99.999% trace metal basis salts (Sigma Aldrich, UK) and maintaining a constant concentration of 12 µmol L^{-1} EDTA. Previous studies have not found an inhibitory effect on *N. maritimus* growth with the addition of 12 µmol L^{-1} EDTA, relative to regular SCM media with 7.5 µmol L^{-1} EDTA. Fe′, Cu′ and cupric ion (Cu^{2+}) concentrations were calculated using Visual Minteq software (Gustafsson, 2010). Background Fe and Cu contamination of 7.3 and 12.5 nmol L^{-1}, respectively, from basal SCM medium was measured using inductively coupled plasma mass spectrometry (Zhang et al. 2018). We were interested in determining *N. maritimus*' Cu quota at the first instance that maximum growth (μ_{max}) is achieved in order to gain an indication of true metal requirement that is not influenced by internal trace metal storage or growth limitation. As such we acclimated *N. maritimus* to optimal Cu^{2+} concentrations determined using previous work (Amin et al. 2013) which showed that *N. maritimus* reaches μ_{max} at 1 pmol L^{-1} Cu^{2+}. Cultures were acclimated to 1 pmol L^{-1} Cu^{2+} by

consecutive transfer during late exponential growth phase into new media until growth rates did not vary with statistical significance (ANOVA, $p < 0.01$). Specific growth rate (d^{-1}) was calculated over the linear phase of semi-log plots of NO_2^- concentration over time, determined spectrophotometrically (Griess, 1879). Axenicity was tested by SEM imaging of cultures. *N. maritimus* cultures acclimated to 1 pmol L^{-1} Cu^{2+} were used to inoculate larger 2L triplicate cultures for trace metal quota analysis. Cultures were harvested during mid-exponential phase for trace metal analysis outlined below.

1.2 Intracellular trace metal quotas

Intracellular trace metal quotas were determined at the [Fe′] and [Cu^{2+}] that maximum growth, μ_{max}, is first achieved in order ensure that trace metal quotas are not elevated through storage under replete conditions but are not depleted due to limitation. The medium [Fe′] and [Cu^{2+}] in which to culture *N. oceani* for trace metal analysis were therefore informed by initial dose-response curves, with 5006 pmol L^{-1} Fe′ and 0.09 pmol L^{-1} Cu^{2+}/0.13 pmol L^{-1} Cu′ treatments deemed to represent the first instance of μ_{max}. We also maintained additional cultures of *N. oceani* at 828, 376 and 100 pmol L^{-1} Fe and 24.63 pmol L^{-1} Cu^{2+} for trace metal analysis. *N. maritimus* cultures were maintained at 1 pmol L^{-1} Cu^{2+} deemed to be optimal from previous work (Amin et al. 2013). All cultures were maintained in triplicate. We were unable to obtain enough biomass to perform trace metal analysis of *N. oceani* and *N. maritimus* Cu-limited cells. Due to the precipitation of Fe hydroxides from the medium, we were not able perform an experiment with high enough Fe′ to obtain trace metal quotas reflecting Fe storage in *N. oceani.* For ease of comparison with other marine microorganisms, in Figure 4.1 we present the minimum Cu and Fe quotas at μ_{max} normalised to cellular P. Quotas of Cu, Fe and P per cell at varying Fe′ and Cu^{2+} are shown in Figure A3.1 and Table 4.1

1.3 SEM imaging

Fe-limited (100 pmol L^{-1} Fe′) *N. oceani* cultures were harvested by centrifugation into a concentrated cell suspension and applied to poly-L-lysine coated glass coverslips which were then fixed with 2.5% glutaraldehyde and allowed to adhere for 5 min. Glass coverslips were rinsed 3 × with 0.1M phosphate buffer (pH 7.2) and then underwent secondary fixation with 1% OsO_4 for 45 min. Cells on coverslips were rinsed with water, dehydrated through a graded ethanol series to absolute ethanol, and then dried chemically with HDMS. Coverslips were mounted on carbon adhesive tape and splutter coated with 10 nm Au. Cells were examined using a GeminiSEM at an accelerating voltage of 3 kV and magnifications of × 5,000–100,000. Cell sizes were calculated using imageJ as described previously (Shafiee et al. 2019 — Chapter two) and are consistent with transmission electron micrographs obtained previously (Klotz et al. 2006).

1.4 FeDFB and ferrozine experiments

To examine whether *N. oceani* can utilise organically chelated Fe, *N. oceani* was cultured in medium with the addition of the siderophore desferrioxamine B mesylate (DFB; Merck), a fungal siderophore that has a greater stability constant ($\log K'_{FeL,\,Fe'}$ = 11.8) for Fe^{3+} compared with EDTA ($\log K'_{FeL,\,Fe'}$ = 8.6, pH 8) (Maldonado et al. 2005). *N. oceani* was cultured under replete total dissolved Fe, [dFe], (5006 pmol L^{-1} dFe) and low [dFe] (100 pmol L^{-1} dFe). A 1.3-fold excess of DFB was added over Fe, in order to reduce Fe′ to negligible concentrations (< 1×10^{-9} pmol L^{-1} Fe′) thereby making Fe bound to DFB the main Fe substrate. Fe′ in DFB-buffered media was calculated using the equation $[Fe'] = [FeDFB]/([DFB'] \times [K_{Fe'DFB}^{cond}])$ (Maldonado & Price, 2001). EDTA concentrations were kept constant at 12 µmol L^{-1} EDTA to buffer other trace metals. We used the ferrozine assay (Kranzler et al. 2011) to identify whether *N. oceani* adopts a reductive Fe-uptake pathway in Fe acquisition. *N. oceani* cultures acclimated to replete

and deplete Fe′ (5006 pmol L^{-1} Fe′ and 100 pmol L^{-1} Fe′) were then treated with 200 µmol L^{-1} ferrozine (FZ; 5,6-Diphenyl-3-(2-pyridyl)-1,2,4-triazine) at the beginning of experiments. As Fe^{2+}-FZ_3 complexes are unavailable for uptake across the plasma membrane, a reduction in growth rate suggests a reductive uptake pathway is present in Fe acquisition. All Fe-uptake experiments were performed in the dark to prevent the photoreduction of Fe^{3+} chelates.

1.5 Metal uptake transporters

AOA and AOB sequences from a wide range of environments were downloaded from UniProt and conserved domains were identified using NCBI conserved domains database (Marchler-Bauer et al. 2015). Only genome-encoded proteomes with a high genome completeness (as per UniProt BUSCO and CPD analysis) were used in the analysis. Orthologs of conserved trace metal transport domains (see Table A3.5 for full list) were BLAST searched against the AOA and AOB genomes (*E* value < 10^{-5}). Conserved domain annotations for the search were identified from reviewing published literature of trace metal uptake genes and by using the study of Hogle et al. (2016) as a framework. Our search focussed on genes involved in both periplasmic and inner membrane inorganic Fe^{2+} and Fe^{3+} uptake, Fe complex (siderophore) uptake, Fe siderophore biosynthesis, Cu uptake, Cu internal management and P-type ATPase Cu-efflux. All trace metal uptake systems and references are outlined in Table A3.5. We acknowledge that there may be as of yet unidentified systems which are unique to AOB and AOB which are revealed through deeper physiological and bioinformatic characterisation of existing and novel AOA/AOB isolates in the future. Due to the low number of available AOA and AOB marine genomes both coastal and open ocean marine species were used in the comparative analysis. Although we present data of the trace metal uptake complement of broader AOA and AOB species across all environments in Figure A3.6, its discussion is

beyond the scope of this study. However, we hope that it is a useful resource for future work exploring the trace metal niche separation of AOA and AOB in different environments.

1.6 Annotation of trace metal-binding sites in the genome-predicted proteome

The limited number of marine AOA and AOB pure isolates in culture precludes a robust analysis of the physiological trace metal requirements across the wider AOA/AOB community. To address this limitation, we adopted a bioinformatic approach to determine whether the intracellular trace metal quotas measured at μ_{max} in *N. oceani* strain C-107 and *N. maritimus* strain SCM1 are representative of phylogenetically diverse AOA and AOB. We annotated the hypothetical Cu- and Fe-binding sites in genome-predicted proteomes of marine AOA and AOB with the underlying assumption that a greater number of trace metal-binding sites will impart a greater intracellular quota at μ_{max}. Genome-predicted proteomes were only used in the analysis with a high genome completeness (> 96%). As full genomes of open ocean AOA and AOB are limited and in order to increase our sample size we tested whether number of trace metal-binding sites in genomes of coastal marine AOA and AOB vary with statistical significance from those of the open ocean. In AOB, we found that the values did not vary with statistical significance between coastal and open ocean species for either the number of Fe-binding sites (Figure A3.4; unpaired *T* test, two-tailed, $p = 0.95$), the relative number of Fe-binding sites per proteome (unpaired *T* test, two tailed, $p = 0.4$), the number of Cu-binding sites per proteome (unpaired *T* test, two tailed, $p = 0.41$), or the number of Cu-binding sites relative to proteome size (unpaired *T* test, two tailed, $p = 0.24$). As there is only one genome sequence for an open ocean AOA (*Ca.* N. brevis) we included genomes of coastal AOA in our analysis too — making the assumption that as shown in AOB, the mean number of Fe and Cu binding sites would not vary with statistical significance and that

any differences arising from the difference in habitat between coastal and open ocean AOA would show the same relative effect on both AOA and AOB (so would cancel out). Values were also normalised to total number of proteins per proteome to determine the proportion of the proteome dedicated to Cu or Fe use. Statistical significance in the number of trace metal-binding sites between AOA and AOB was examined using a Student's *T* test for parametric datasets (two tailed, $p < 0.01$) and Mann Whitney U for non-parametric datasets.

In order to confirm that the genome-expressed proteomic metal demand scales with expressed proteomic metal demand, we performed the same analysis as described above, using the limited available expressed AOA (Zorz et al. 2018; Pellitteri-Hahn et al. 2011; Jiang et al. 2015) and AOB proteome data (Santoro et al. 2015; Qin et al. 2018; Kerou et al. 2016; Shafiee et al. 2021b — Chapter three). To account for the varying methods by which protein abundances are calculated between studies, metal demands were calculated relative to total protein abundance: ((number of Fe/Cu-binding sites per protein × protein abundance)/total protein abundance). We found that expressed-proteome Cu and Fe demand is positively correlated with absolute genome-predicted proteome metal demand (Fe, $r^2 = 0.56$, $p < 0.01$; Cu, $r^2 = 0.42$, $p = 0.06$) and therefore the differences between AOA and AOB Fe/Cu demands based on predicted-proteomes as shown in Figure 4.3, hold true when compared based on expressed-proteomes (Figure A3.10; Figure A3.11).

1.7 Presence of Cu efflux genes in the *Tara* global metagenomes and metatranscriptomes

In order to examine for the potential for *in situ* AOB communities to be inhibited by high Cu^{2+} as suggested by our physiological results, we screened the Ocean Data Atlas, which mines data from the *Tara* Oceans metagenomes and metatranscriptomes for reads of known AOB (including *Nitrosococcus*, *Nitrosomonas* and *Nitrosospira*) Cu efflux

proteins — namely *copA* and *copB*. As AOA do not utilise Cu efflux proteins, it is not possible to perform a similar search in AOA. The significance level (*E*) was set as 1×10^{-10} and reads were returned as a percentage of total reads. Only reads ascribed to different AOB — either *Nitrosococcus*, *Nitrosospira* and *Nitrosomonas* were considered in subsequent analyses. The search returned numerous significant hits of AOB-ascribed reads homologous to AOB Cu efflux proteins — suggesting that these genes are widespread in the world's oceans (Figure A3.12). The *Tara* metatranscriptomic data are more limited than the metagenomic data, but many of the returned *Nitrosococcus* and *Nitrosomonas* hits are from metatranscriptomic samples (Figure A3.13) indicating that Cu efflux proteins are being actively expressed in the oceans. The fact that the search returned significant hits ascribed to the *Nitrosococcus*-genera is also support for the ubiquity of *Nitrosococcus* in the world's oceans and supports its use as a representative species in our study.

1.8 AOA and AOB niche separation

In order to place our results in the context of AOA and AOB niche separation, we explored the co-variance of key environmental parameters with AOA and AOB abundance profiles. Figure 4.5 in the main manuscript shows a schematic of the averaged published AOA and AOB *amoA* gene profiles (Full data available in Table A3.7 and Figure A3.9), dissolved total Fe (dFe) from GEOTRACES Intermediate Data Product 2017 and NH_4^+ depth profiles (Gruber, 2008).

1.9 *amoA* depth profiles

The presence of *amoA* genes in DNA extracted from environmental samples gives an indication of the organisms potentially capable of ammonia oxidation, while the presence of *amoA* transcripts indicates the presence of actively ammonia-oxidising microorganisms. It should be noted that while the physiological aspect of this work

examined the effect of trace metals on the growth of an AOB belonging to the recently updated Nitrosococcales order within the Gammaproteobacteria, the compiled AOB depth profile (shown in Figure 4.5) is primarily based on Betaproteobacteriales-AOB *amoA* sequences. This is due to the substantially fewer number of studies which have successfully detected and quantified Nitrosococcales *amoA* sequences and the historical bias towards the use of Nitrosospira *amoA* primers (discussed in Chapter 1). Therefore, it cannot be ruled out that the Nitrosococcales and the Betaproteobacteriales display distinct depth profiles and occupy different physicochemical niches in the water column – with our physiological data being more pertinent to the depth profile of Nitrosococcales. However, based on our comparative genomic analysis we predict that the physiological characteristics we observed in *Nitrosococcus oceani* (belonging to the Nitrosococcales) is likely reflective of wider AOB across both the Betaproteobacteriales and Nitrosococcales. By sharing similar physiological traits, we predict that both the Betaproteobacteriales and Nitrosococcales will occupy a similar environmental niche. However, additional data of the distribution of Nitrosococcales will be required to link the depth profiles of AOB more robustly with the physiological traits shown in this study.

Due to the wealth of AOA and AOB *amoA* gene distribution data, we were able to determine a robust pattern of abundance profiles (Figure A3.9). The fewer number of studies examining *amoA* transcripts precluded us from calculating a complementary *amoA* transcript depth profile. However, the few studies which have simultaneously examined gene copies and transcripts show that peak abundances/expression co-occur (Church et al. 2010; Jing et al. 2017). Further, studies measuring instantaneous AOA/AOB gene copies and transcripts (rather than depth profiles) typically co-vary such that when more cells are present the number of actively transcribing cells can be assumed to be greater (Abell et al. 2010; Tolar et al. 2016; Duff et al. 2017; Leininger et al. 2006)

although the ratio of gene copies to transcripts may vary depending on the environment. Based on the aforementioned discussion, we are confident that the *amoA* gene profiles provide an accurate picture of the abundance of microorganisms actively oxidising ammonia.

2 SUPPLEMENTARY RESULTS AND DISCUSSION

2.1 AOB Fe′ uptake proteins

In contrast to *Nitrosococcus* genomes which all encode the high-affinity FTR/Fet3p uptake system, only two genomes of the *Nitrosomonas* and *Nitrosospira* clade we examined contained FTR/Fet3p uptake genes —- none of which were marine species (Figure A3.6). We only found periplasmic Fbp or FutA1 Fe^{3+} transporters in marine *Nitrosomonas* and *Nitrosospira*. The FTR1/Fet3p used by *Nitrosococcus* and Fbp/FutA1 used by *Nitrosomonas* and *Nitrosospira* differ in their Fe substrate, using Fe^{2+} and Fe^{3+} respectively. Of the small proportion of dissolved Fe in the oceans which is unchelated, Fe primarily exists as Fe^{3+}. We hypothesise that the ability of *Nitrosomonas* and *Nitrosospira* to take up exogenous Fe^{3+} may provide them a competitive advantage relative to *Nitrosococcus* in terms of inorganic Fe acquisition. Yet Fe^{2+} accumulates to appreciable concentrations in some regions (Roy et al. 2008) and as such competition between *Nitrosococcus* and *Nitrosomonas* for unchelated Fe is likely to be spatially and temporally variable. As there are no marine *Nitrosomonas* pure isolates available, we are unable to demonstrate the physiological implication of this genetic difference. This will be an important avenue for future research as marine *Nitrosomonas* cultures become available. Nonetheless, the fact that all examined marine AOB all have Fe-specific (Fe′) uptake mechanisms, allows us to posit that AOB are conferred with a higher affinity for unchelated Fe′ in the oceans relative to the AOA — none of which have any specific Fe′ uptake transporters and must rely on generalist divalent cation transporters.

3 SUPPLEMENTARY FIGURES & TABLES

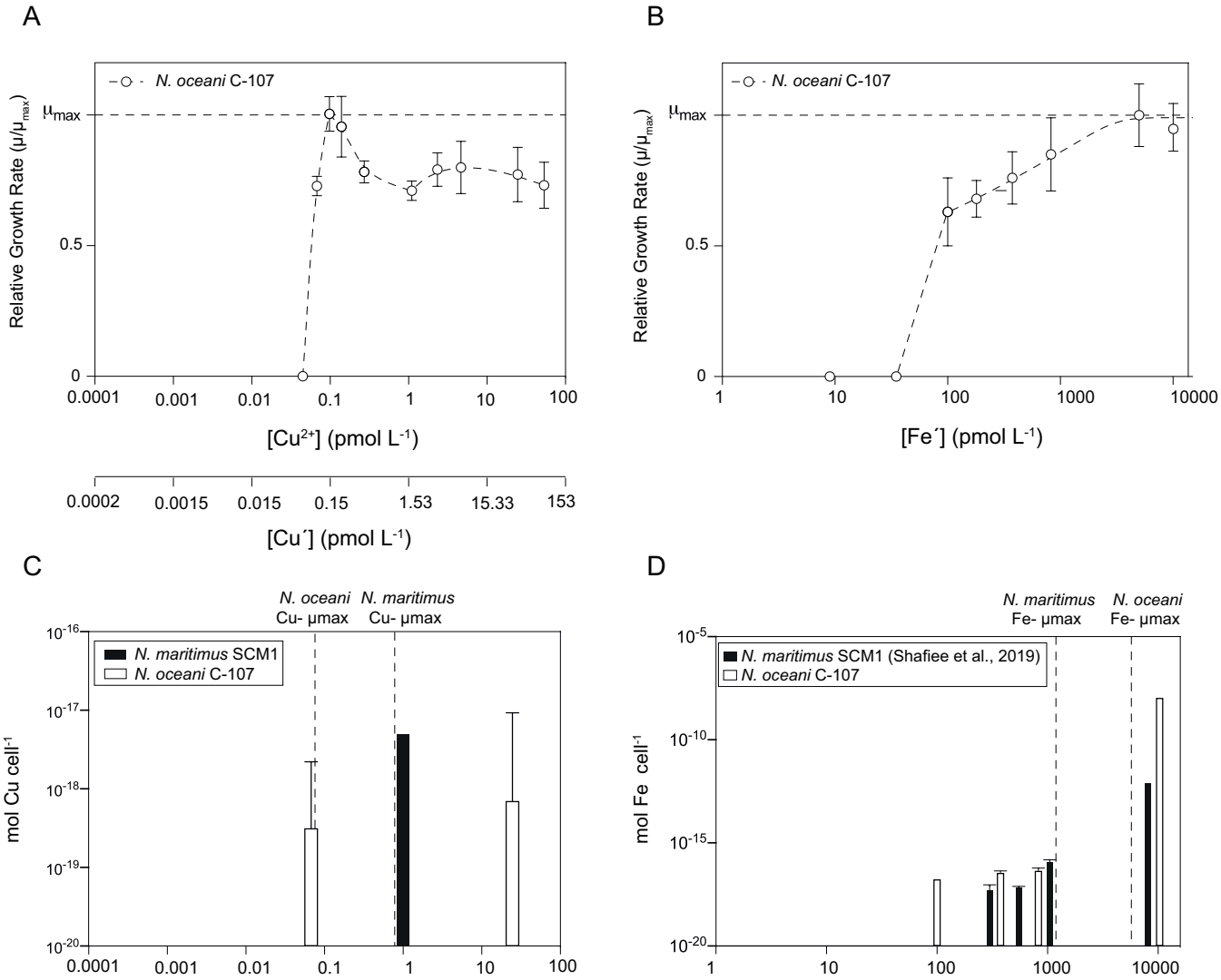

A
N. oceani C-107
μmax
Relative Growth Rate (μ/μmax)
0
0.5
0.0001
0.001
0.01
0.1
1
10
100
[Cu2+] (pmol L-1)
0.0002
0.0015
0.015
0.15
1.53
15.33
153
[Cu´] (pmol L-1)
B
N. oceani C-107
μmax
Relative Growth Rate (μ/μmax)
0
0.5
1
10
100
1000
10000
[Fe´] (pmol L-1)
C
N. oceani Cu- μmax
N. maritimus Cu- μmax
N. maritimus SCM1
N. oceani C-107
mol Cu cell-1
10-16
10-17
10-18
10-19
10-20
0.0001
0.001
0.01
0.1
1
10
100
D
N. maritimus Fe- μmax
N. oceani Fe- μmax
N. maritimus SCM1 (Shafiee et al., 2019)
N. oceani C-107
mol Fe cell-1
10-5
10-10
10-15
10-20
1
10
100
1000
10000

Figure A3.1 *N. oceani* Fe and Cu dose response curves and cellular trace metal quotas

N. oceani strain C-107 relative growth rate as a function of **A)** increasing Cu^{2+} (equivalent Cu′ is also shown for comparison) **B)** increasing Fe′. Cellular Cu **C)** and Fe **D)** quotas in mol $cell^{-1}$ at different [Cu^{2+}] and [Fe′]. Mol Fe $cell^{-1}$ in *N. maritimus* strain SCM1 is from a previously published dataset (Shafiee et al. 2019 — Chapter two). The [Fe′] and [Cu^{2+}] required to reach maximum relative growth rate (μ_{max}) is denoted by a dashed line – trace metal quotas under these [Fe′] and [Cu^{2+}] are those shown in the main text (Figure 4.1) Error bars denote standard deviation. n = 20 in A and B, n = 3 in C and D.

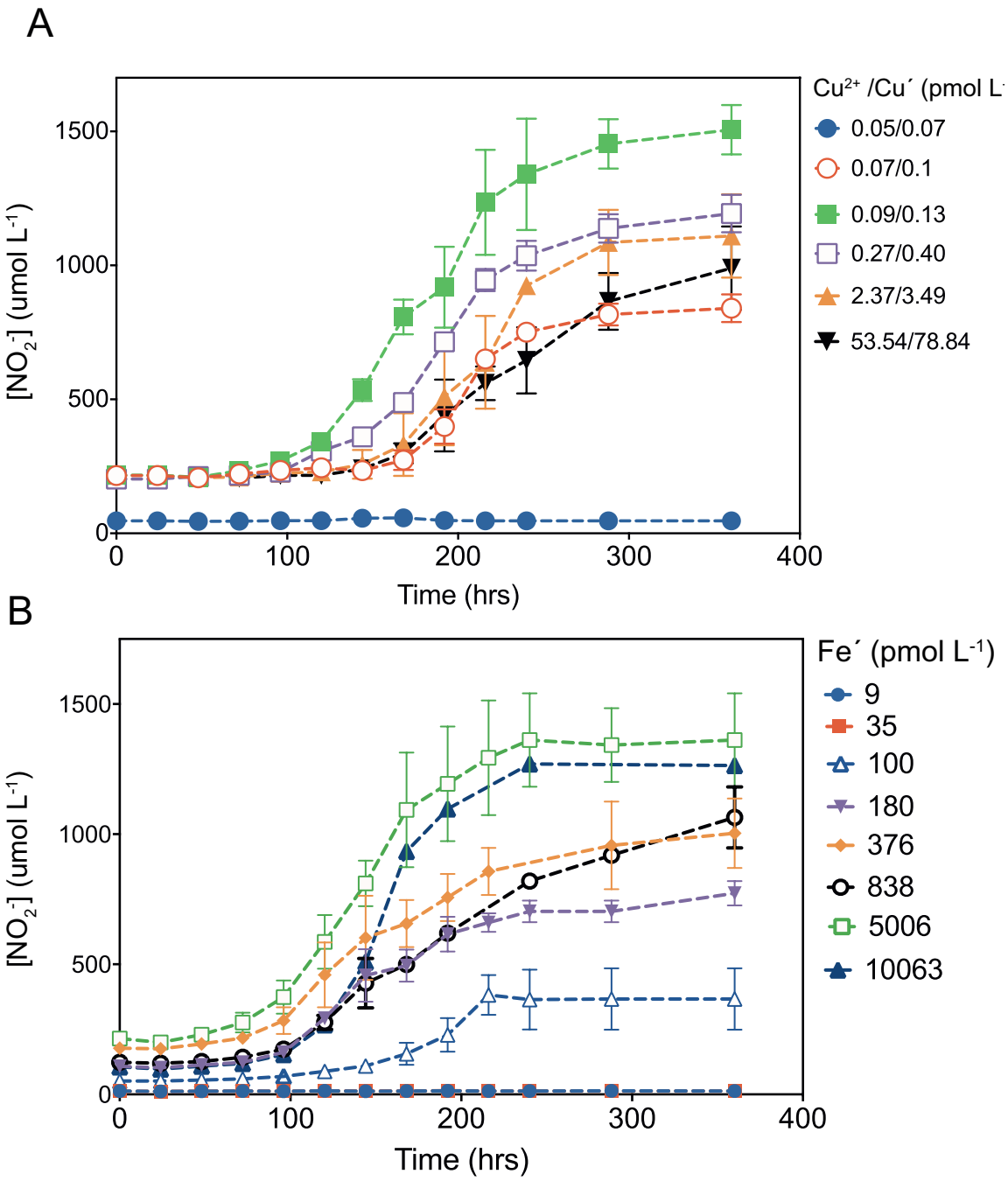


Figure A3.2 Effect of Fe´ and Cu´ on NO_2^- production in the marine AOB, *N. oceani*

Effect of cupric ion (Cu^{2+}) concentration (and corresponding unchelated Cu, Cu´) **A)** and unchelated Fe (Fe´) concentration **B)** on nitrite (NO_2^-) production in *N. oceani* cultures.

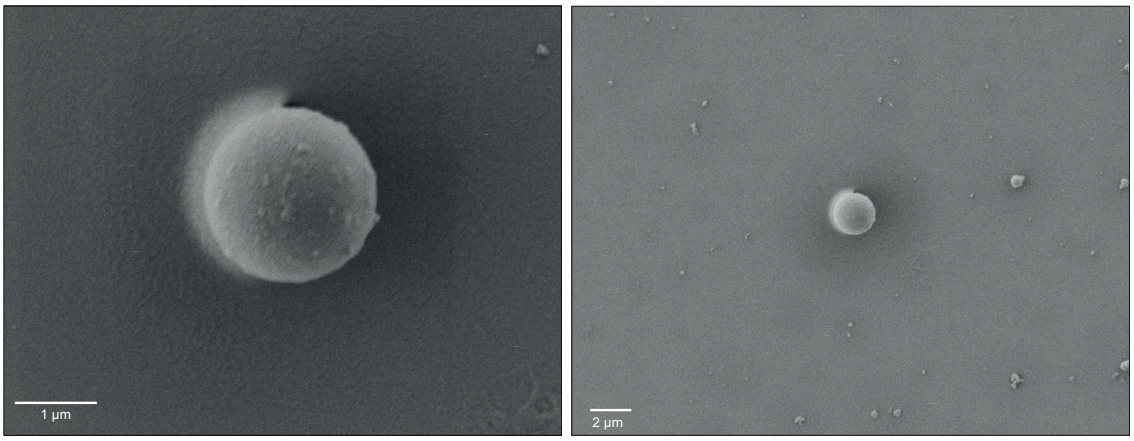


Figure A3.3 SEM images of *N. oceani* under Fe-limited and Fe-replete conditions

Scanning electron micrographs (SEM) of the marine AOB *N. oceani* (strain C-107) under Fe-limited (left) and Fe-replete (right) conditions. Scale bar represents 1 µm in the left image and 2 µm in the right image.

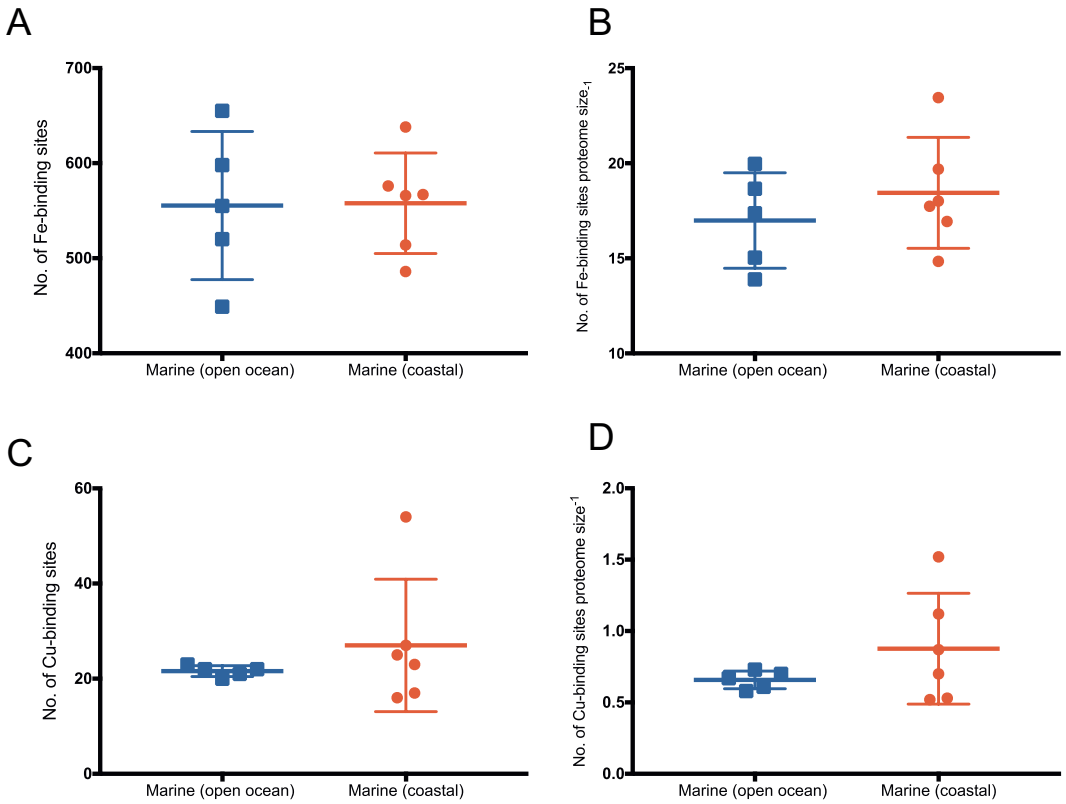


Figure A3.4 Fe and Cu binding proteome of marine open ocean and coastal AOA and AOB

Comparison of the absolute **A)** and relative (to proteome size) number of hypothetical Fe-binding sites **B)** absolute **C)** and relative (to proteome size) number of Cu-binding sites in genome-predicted proteomes of open ocean ammonia-oxidising bacteria (blue squares) and coastal ammonia-oxidising bacteria (red circles). Middle line represents the mean value, error bars represent standard deviation. Species-specific values are given in Table A3.3.

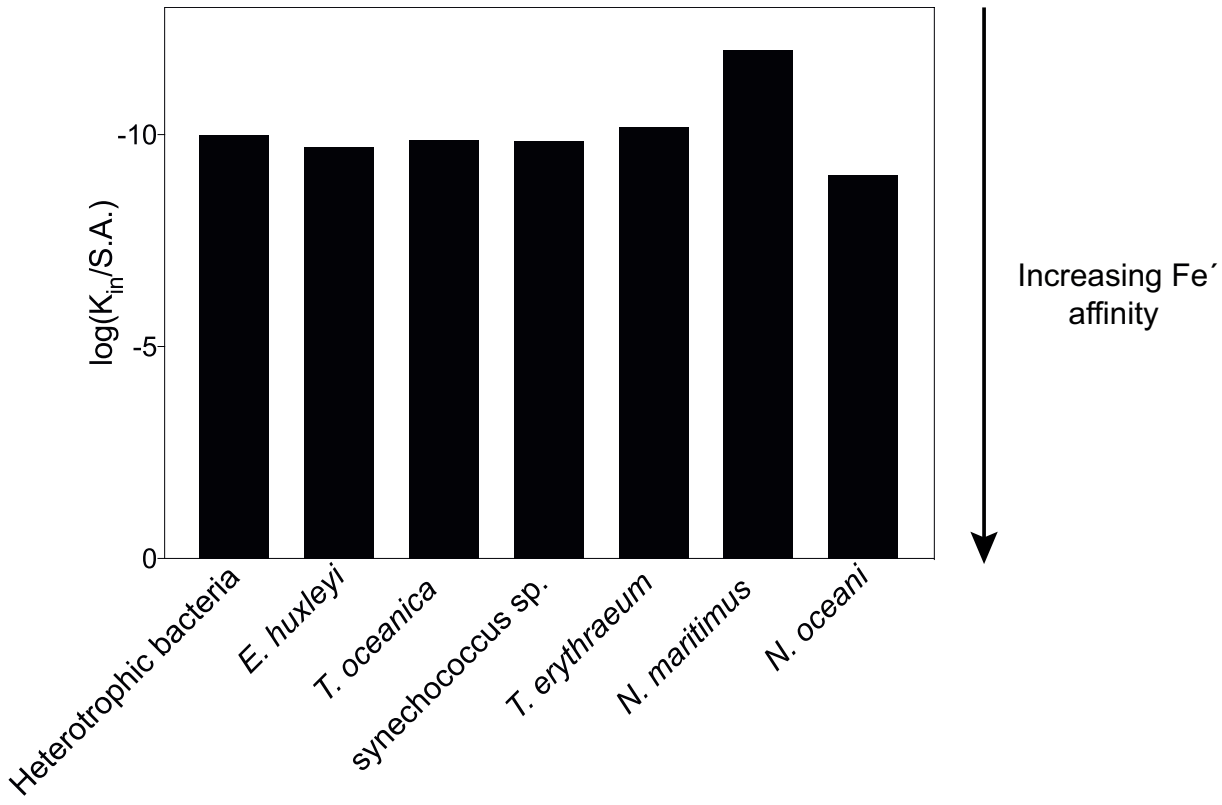


Figure A3.5 Fe affinities of marine AOA and AOB compared to cosmopolitan marine microorganisms

Log Fe´ steady-state uptake rate constant (k_{in}) normalised to cellular surface area (S.A.) in the marine AOB *N. oceani* (strain C-107) compared with previously published data of marine phytoplankton (Lis et al. 2015a), heterotrophic bacteria (Granger & Price, 1999) and *N. maritimus* strain SCM1 (Shafiee et al. 2019 — Chapter two), with greater values indicating a higher affinity for Fe´.


feoB
FTR/Fet3p
FTR
fbp
futA1
fecCD
hemS
fhuD
fiu
TonB
entE
entF
fepB
iucC
rbhC
CTR1
ctaA
copA
copB
cueO
cusCFBA
pcoE
copC
copD
copZ
ZIP
NRAMP
hupE/ureJ
nikABC
btuF
znuA
troA
cbtA
cbtB
corA
Fe2+
Fe3+
Feorg (uptake)
Feorg (biosynthesis)
Cu2+
Cu-efflux
Cu management
Fe2+/Zn2+ /Mn2+
other metals
AOA
Candidatus Nitrosopumilus sp. (NM25)
Candidatus Nitrosopumilus salaria (BD31)
Candidatus Nitrosotenuis uzonensis (N4)
Nitrososphaera gargensis (Ga9.2)
Candidatus Nitrosocaldus cavascurensis (SCU2)
Candidatus Nitrosopelagicus brevis (V2)
Nitrosopumilus adriaticus (NF5)
Nitrosopumilus maritimus (SCM1)
Nitrosopumilus piranensis (D3C)
Cenarchaeum symbiosum (A)
Candidatus Nitrosopumilus sediminis (AR2)
Nitrososphaera viennensis (EN76)
Candidatus Nitrososphaera evergladensis (SR1)
Candidatus Nitrosotalea sinensis
Candidatus Nitrosotalea devanaterra
Candidatus Nitrosotalea okcheonensis
AOB
Nitrosomonas nitrosa (Nm146)
Nitrosomonas sp. (Is79A3)
Nitrosomonas oligotropha (Nm 76)
Nitrosomonas marina (Nm 71)
Nitrosospira lacus (APG3)
Nitrosomonas stercoris (KYUHI-S)
Nitrosomonas eutropha (Nm 57)
Nitrosomonas halophila (SNm 1)
Nitrosococcus oceani (C-107)
Nitrosomonas sp. (Nm 51)
Nitrosomonas aestuarii (Nm 69)
Nitrosococcus halophilus (Nc 4)
Nitrosomonas mobilis
Nitrosomonas cryotolerans (ATCC 49181)
Nitrosococcus oceani (C-27)
Nitrosococcus wardiae (D1FHS)
Nitrosococcus watsoni (strain C-1
Nitrosomonas marina (Nm 22)
Nitrosospira multiformis (C -71)
Nitrosospira multiformis (Nl15)
Nitrosospira briensis (Nsp 8)
Nitrosospira sp. (Nsp 14)
Nitrosospira multiformis (Nsp 16)
Nitrosospira sp. (NpA
Nitrosospira sp. (Nsp 37)
Nitrosospira sp. (56-18)
Nitrosospira sp. (Nsp 22)
Nitrosomonas sp. Nm58
Nitrosomonas sp. (Nm 166)
Nitrosomonas sp. (Nm 33)
Nitrosomonas sp. (Nm 34)
Nitrosomonas europaea (strain ATCC 19718)
Nitrosomonas ureae (Nm 4)
Nitrosomonas ureae (Nm 9)
Nitrosomonas ureae (Nm 10)
Nitrosomonas ureae (Nm 15)
Nitrosomonas communis (Nm 1
Nitrosomonas sp. (APG5)
Nitrosomonas europaea (Nm 35)
Nitrosomonas sp. (Nm 120)
Nitrosomonas sp. (Nm 143)
Nitrosomonas sp.(Nm 132)
Nitrosomonas sp. (Nm 134)
Nitrosomonas sp. (Nm 141)
Brackish
Hotspring
Freshwater
Sewage
Soil
Marine
Unknown
0
Counts
18

Figure A3.6 Extended bioinformatic analysis of transporter families in AOA and AOB genomes

Heatmap of extended bioinformatic analysis of trace metal transporter families in AOA and AOB genomes. Colours describe the number of 'counts' or occurrences in genome of the given trace metal transporter. Description of uptake systems and further information on the genomes used in the analysis are given in Table A3.5.

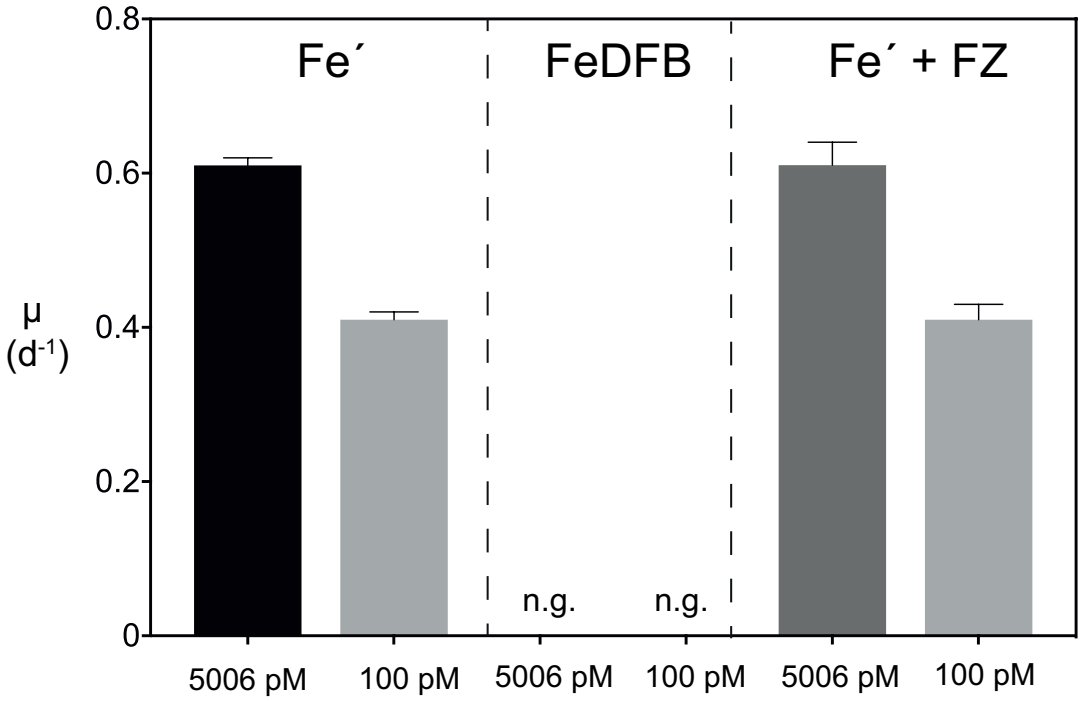


Figure A3.7 *N. oceani* growth rates under different Fe substrates and concentrations

N. oceani specific growth rates (d^{-1}) in **1)** EDTA-buffered medium with Fe´ ([Fe´] shown beneath) as the main Fe substrate (left panel) **2)** desferrioxamine B (DFB) buffered medium with FeDFB (organically-complexed Fe) as the main Fe substrate ([FeDBF]. n.g. indicates no growth observed (middle panel). **3)** EDTA-buffered medium with Fe´ ([Fe´] below bars) supplemented with Fe^{2+}-binding ferrozine (FZ) at the beginning of experiments (right panel). Error bars denote standard deviation, $n = 6$.

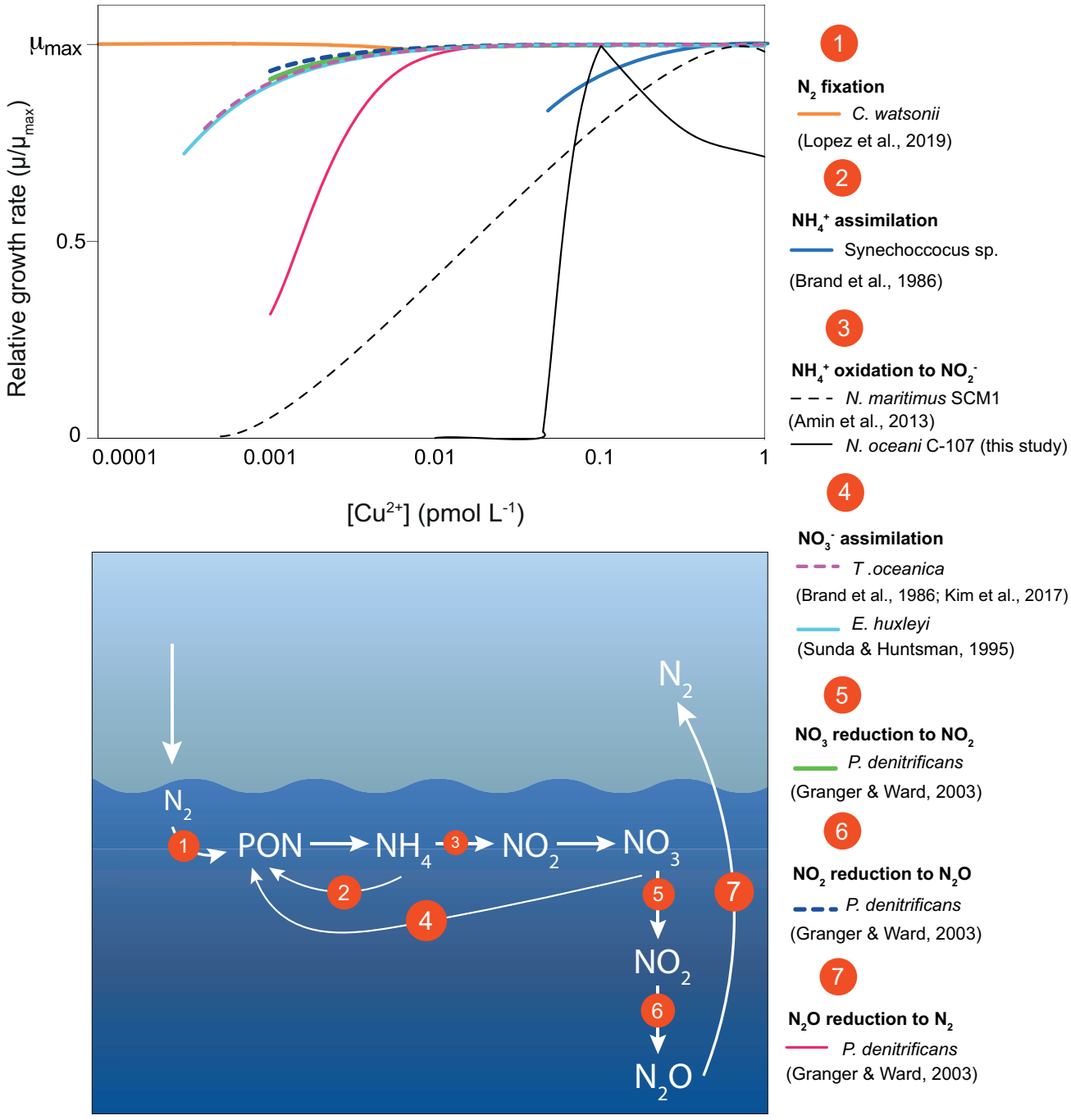


Figure A3.8 Cu requirements of different components of microbial N cycle

Effect of cupric ion concentration (Cu^{2+}) on the relative growth rate (μ/μ_{max}) of the AOB *N. oceani* compared with published data on AOA (*N. maritimus*) and other marine microorganisms mediating other components of the N cycle, with numbers corresponding to pathways shown on the bottom figure of the marine N cycle. All data available in Table A3.1.

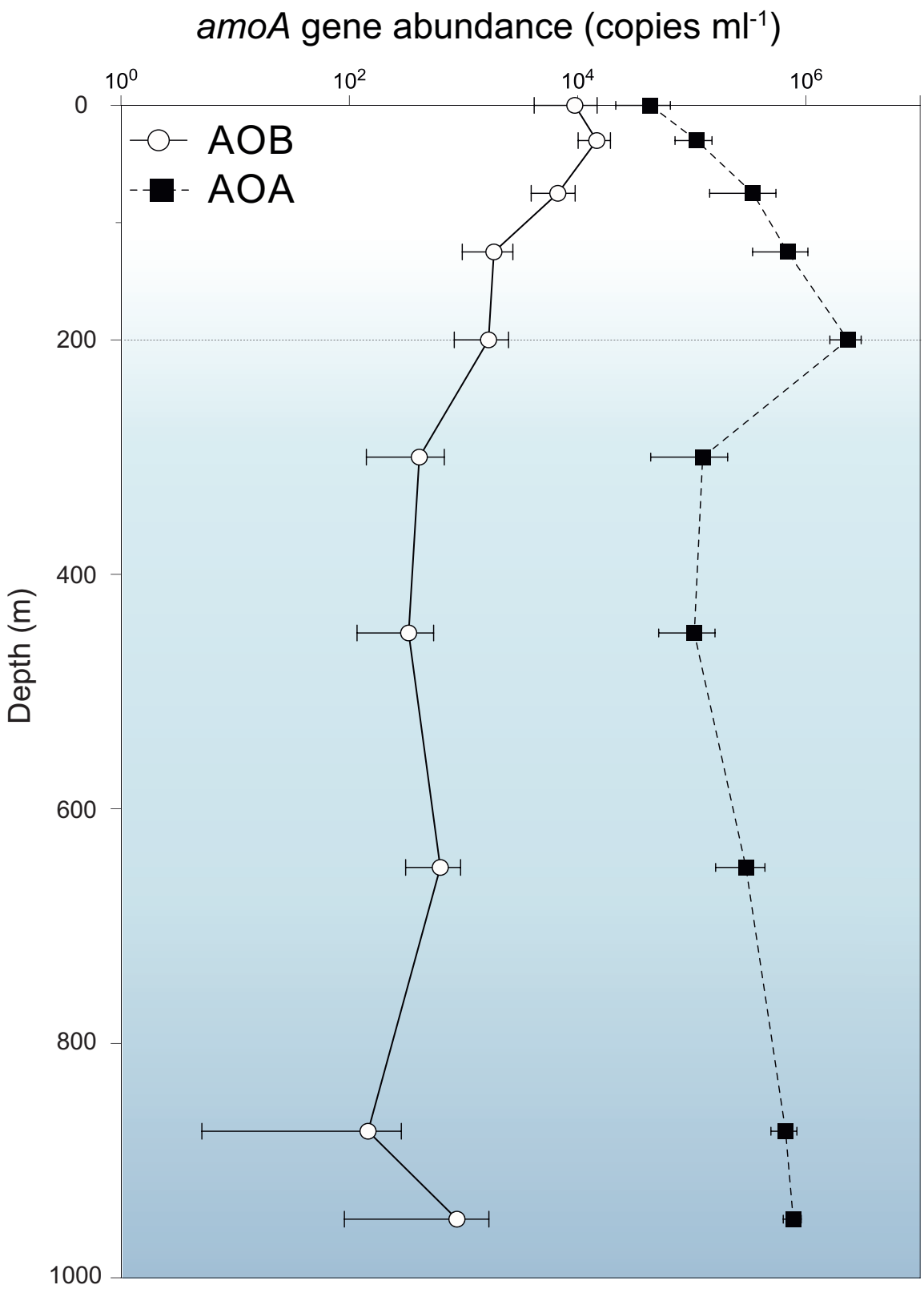


Figure A3.9 Mean AOA and AOB *amoA* gene abundances with depth

Mean AOB and AOA *amoA* gene abundances calculated in this study from compiled datasets – see Table A3.7 for full datasets. Error bars denote standard deviation.

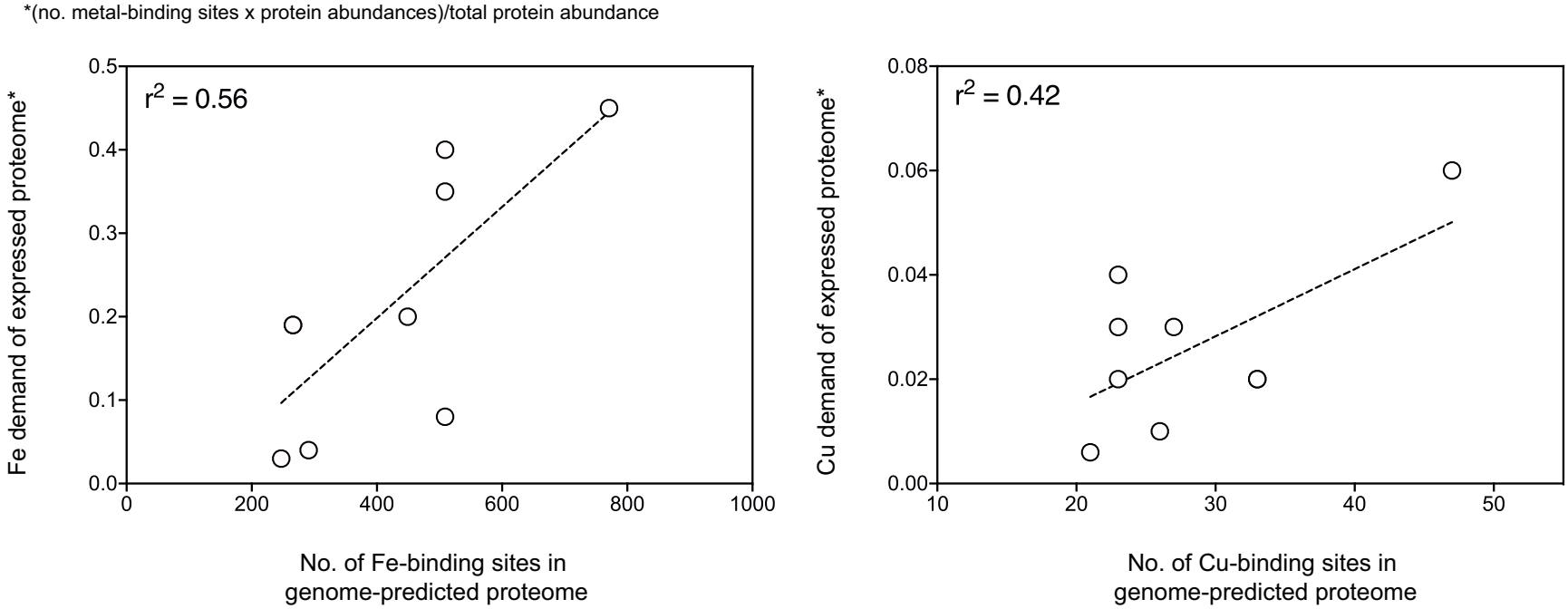


Figure A3.10 Relationship between genome-predicted proteome Cu/Fe demand expressed proteome demand

Comparison of the Fe and Cu demand calculated from the expressed proteome (calculated as (number of metal-binding sites × protein abundance)/total protein abundance) and equivalent Fe or Cu demand calculated from the genome-predicted proteome in marine AOA and AOB.

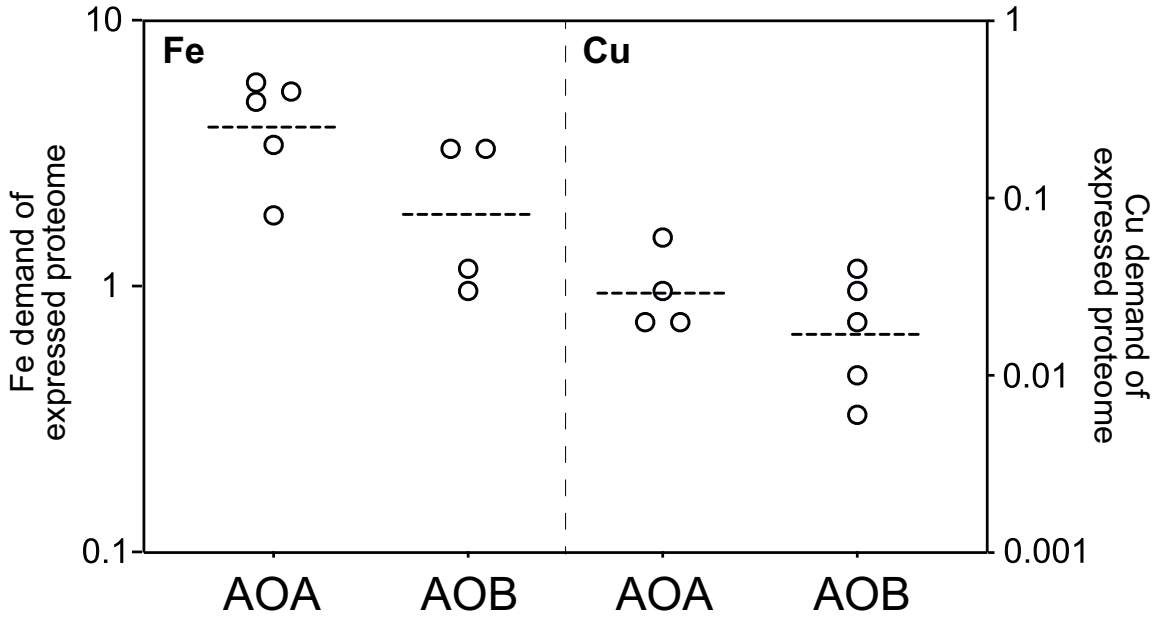


Figure A3.11 Expressed proteome trace metal demand of AOA and AOB

Comparison of the Fe and Cu demand calculated from the expressed proteome between AOA and AOB. Dashed line indicates the mean value.

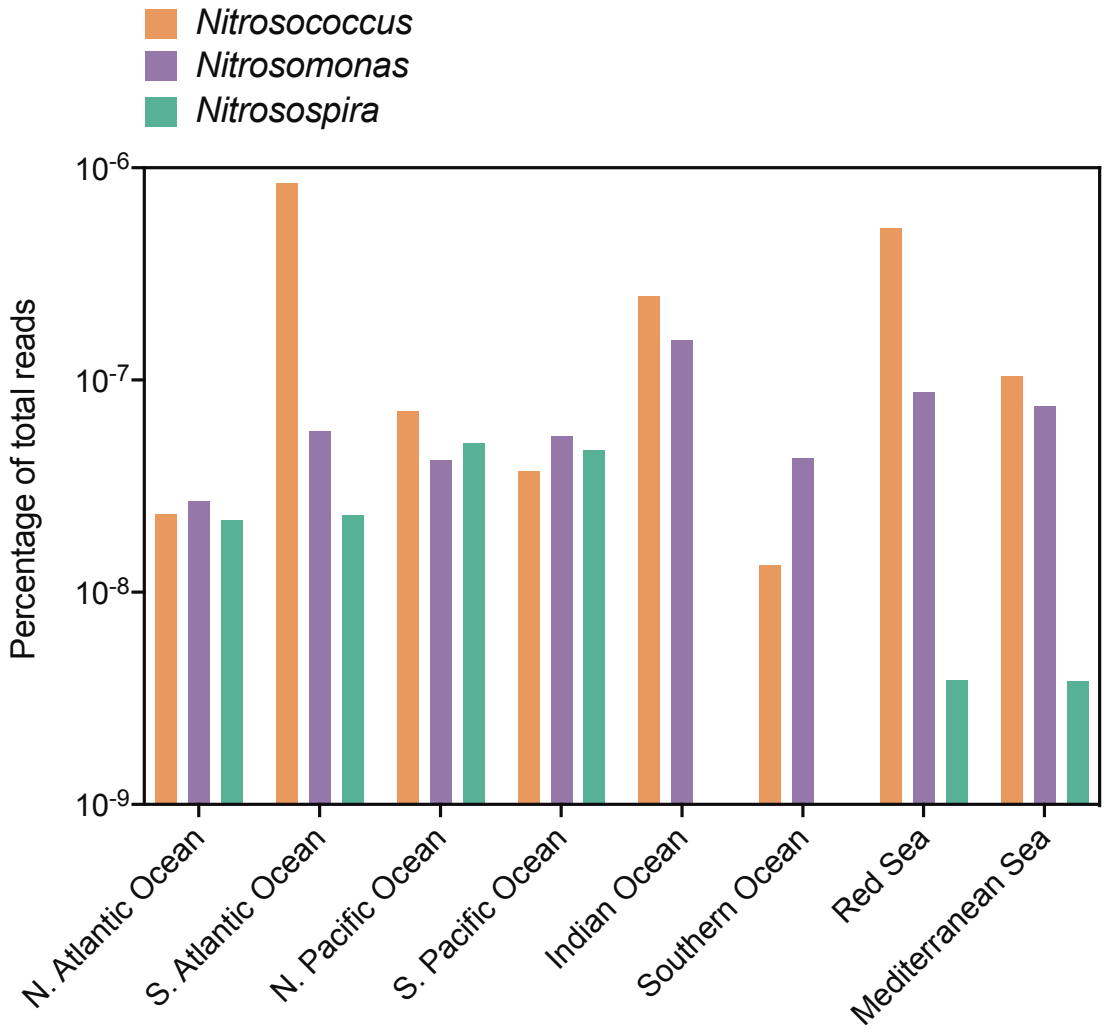


Figure A3.12 AOB detoxification genes in *Tara* oceans database

AOB-ascribed gene reads homologous to known AOB Cu detoxification genes (See Table A3.8 for data) as a percentage of total reads, grouped by genus and oceanic region from which *Tara* sample was obtained.

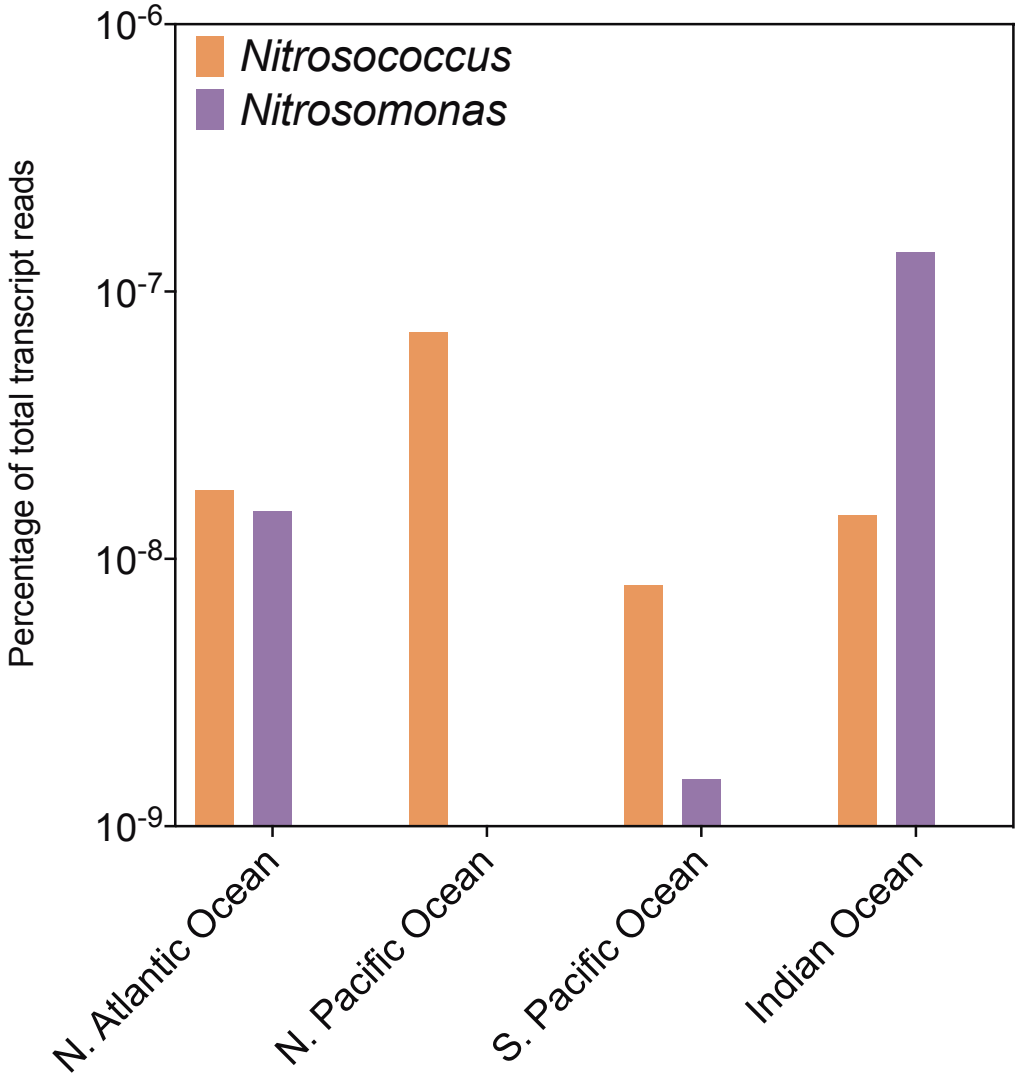


Figure A3.13 AOB detoxification transcripts in *Tara* oceans database

AOB-ascribed transcript reads homologous to known AOB Cu detoxification genes as a percentage of total reads (see Table A3.8 for data), grouped by genus and where reads were detected. No *Nitrosospira* homologues were detected in the *Tara* dataset.

Species	Cu^{2+} (pmol L^{-1})	μ (d^{-1})	μ/μ_{max}	Cu quota (mmol mol^{-1})
Brand et al. 1986				
E. huxleyi	0.13	1.27	0.97	
	1	1.31	1	
	12	1.24	0.95	
	23	1.27	0.97	
	48	1.21	0.92	
	131	1.07	0.82	
T. oceanica	0	1.81	0.90	
	0.13	1.89	0.94	
	1	1.90	0.95	
	12	1.94	0.97	
	23	2.01	1	
	48	1.87	0.93	
	131	0.99	0.49	
Synechococcus WH7808	0	1.40	0.93	
	0.13	1.50	1	
	1	1.33	0.89	
	12	0.95	0.63	
	23	n.g.	n.g.	
	48	n.g.	n.g.	
	131	n.g.	n.g.	
S. bacillaris	0	0.92	0.84	
	0.15	1.09	1.00	
	1	0.82	0.75	
	10	n.g.	n.g.	
	32		n.g.	
	117		n.g.	
	263		n.g.	
	707		n.g.	
Synechococcus WH7808	0	1.77		
	0.15	1.76	0.97	
	1	1.81	1	
	10	1.23	0.68	
	32	n.g.	n.g.	
	117	n.g.	n.g.	
	263			
	707			
Synechococcus WH6501	0	1.54		
	0.15	1.55	1	
	1	1.54	0.99	
	10	1.47	0.95	
	32	1.33	0.86	
	117	n.g.	n.g.	
	263			
	707			
Synechococcus WH8008	0	1.37		
	0.15	1.38	1	
	1	1.12	0.81	
	10	0.80	0.58	
	32	n.g.	n.g.	
	117	n.g.	n.g.	
	263			
	707			
Synechococcus WH8003	0	0.46	1	
	0.15	0.46	0.74	
	1	0.43	0.69	
	10	0.62	1	
	32	n.g.	n.g.	
	117			
	263			
	707			
Synechococcus WH7805	0	1.21		
	0.15	1.27	0.95	
	1	1.34	1	

	10	n.g.	n.g.	
	32			
	117			
	263			
	707			
Synechococcus WH8016	0	0.64		
	0.15	0.55	0.75	
	1	0.73	1	
	10	0.68	0.93	
	32	0.30	0.41	
	117			
	263			
Kim & Price (2017)				
T. oceanica	0.26	1.13	0.90	
	0.12	1.26	1	
	0.06	1.02	0.81	
	0.03	0.76	0.60	
	0.01	0.64	0.51	
Sunda & Huntsman (1995)				
T. oceanica	0.0007	1.53	0.94	
	0.001	1.54	0.94	
	0.003	1.53	0.94	0.14
	0.01	1.63	1	0.18
	0.03	1.60	0.98	0.32
	0.03	1.58	0.97	0.35
	0.03	1.60	0.98	0.41
	0.09	1.59	0.98	0.53
	0.3	1.63	1	0.63
	0.9	1.62	0.99	0.73
	3	1.62	0.99	0.88
	9	1.61	0.99	1.26
	30	1.62	0.99	2.20
E. huxleyi	0.0007	1.14	0.88	0.02
	0.001	1.20	0.92	0.10
	0.003	1.20	0.92	0.19
	0.009	1.30	1.00	0.21
	0.02	1.22	0.94	0.38
	0.02	0.98	0.75	0.30
	0.08	1.09	0.84	0.40
	0.2	1.15	0.88	0.50
	0.8	1.09	0.84	0.97
	2	0.98	0.75	1.46
	8	1.13	0.87	1.67
	28	0.94	0.72	11.56
T. pseudonana	0.0007	1.86	0.98	0.08
	0.0007	1.89	1	0.08
	0.01	1.87	0.99	0.38
	0.03	1.86	0.98	0.59
	0.09	1.86	0.98	0.63
	0.3	1.85	0.98	0.84
	0.3	1.86	0.98	0.84
	0.3	1.86	0.98	0.96
	0.9	1.85	0.98	1.19
	3	1.87	0.99	1.55
	9	1.74	0.92	2.54
Posacka et al. (2019)				
Heterotrophic Bacteria (Dokd-P16)	0.0001	0.17	1.63	0.06
	0.001	0.31	2.91	0.07
	0.005	0.70	6.64	0.08
	0.01	0.73	6.95	0.14
	0.02	1.00	9.46	0.12
Heterotrophic Bacteria (Palt-P26)	0.0001	0.82	5.10	0.06
	0.001	0.93	5.78	0.05
	0.005	0.78	4.87	0.06
	0.02	1.00	6.22	0.02
Heterotrophic Bacteria (Palt-P2)	0.001	0.75	10.05	0.03
	0.005	1.00	13.47	0.03

	0.01	1.09	12.32	0.03
Heterotrophic Bacteria (*R. pomeroyi)*	0.0001	0.82	16.32	0.05
	0.001	1.00	19.93	0.11
	0.005	1.00	19.87	0.14
	0.02	0.83	16.59	0.15
Lopez et al. (2019)				
C. watsonii WH0402	0.8	0.13	0.32	
	1	0.29	0.70	
	0.4	0.27	0.66	
	0.09	0.32	0.76	
	0.0001	0.42	1	
	0.02	0.40	0.97	
C. watsonii WH0005	2	0.05	0.12	
	0.6	0.02	0.05	
	1	0.11	0.26	
	0.2	0.10	0.22	
	0.09	0.28	0.66	
	0.01	0.28	0.65	
	0.00006	0.43	1	
C. watsonii WH0003	2	0.14	0.33	
	0.9	0.19	0.44	
	0.5	0.21	0.49	
	0.2	0.26	0.61	
	0.1	0.32	0.76	
	0.01	0.29	0.69	
	0.0001	0.43	1.00	
Granger & Ward (2003)				
P. denitrificans (NO_3^- to NO_2^-)	0.001	1.93	0.91	
	0.01	2.12	1	
P. denitrificans (NO_2^- to N_2O)	0.001	1.79	0.93	
	0.01	1.92	1	
P. denitrificans (N_2O to N_2)	0.001	0.09	0.17	
	0.01	0.52	1	
Amin et al. (2013)				
N. maritimus strain SCM1	0.0005	n.g.	n.g.	
	0.001	n.g.	n.g.	
	0.01	0.34	0.55	
	0.08	0.47	0.76	
	0.1	0.57	0.92	
	0.4	0.60	0.97	
	0.9	0.62	1	
	1.99	0.60	0.97	
	19	0.58	0.94	
	43	0.56	0.90	

Table A3.1 Cu requirements of marine microorganisms compiled from published literature.

SGR refers to specific growth rate (d^{-1}), RGR refers to relative growth rate (μ/μ_{max})

Species	**Fe´ (pmol L^{-1})**	**μ (d^{-1})**	**μ/μ_{max}**	**Fe quota (mmol mol^{-1})**
Sunda & Huntsman (1995)				
Emiliania huxleyi	3	0.70	0.63	
	5	0.88	0.78	0.39
	9	0.99	0.88	1.17
	24	1.10	0.98	1.41
	71	1.07	0.95	2.79
	253	1.04	0.92	3.52
	750	1.12	1	
Schulz et al. (2004)				
Emiliania huxleyi	0.1	0.36	0.22	
	0.9	0.66	0.41	

	2	1.20	0.75	
	4	1.33	0.82	
	138	1.62	1	
Sunda & Huntsman (1995)				
Thalassiosira oceanica	3	0.73	0.46	
	10	1.10	0.69	0.52
	28	1.36	0.86	0.75
	78	1.55	0.98	1.20
	253	1.55	0.98	3.64
	760	1.58	1	
Sunda & Huntsman (2015)				
Synechococcus bacillaris (CCMP 1333)	37	0.11	0.17	
	98	0.45	0.73	10.33
	328	0.52	0.84	12.01
	964	0.58	0.93	17.47
	3268	0.62	1	24.16
Berman-Frank et al. (2001)				
Trichodesmium erythraeum	16	0.04	0.34	
	32	0.05	0.38	
	128	0.06	0.49	
	386	0.09	0.71	
	15773	0.12	1	
Shi et al. (2012)				
Trichodesmium erythraeum	58	0.29	0.67	39.74
	530	0.40	0.93	211.75
	1411	0.43	1	367.74
Boatman et al. (2018)				
Trichodesmium erythraeum	584	0.18	0.51	
	584	0.21	0.58	
	417	0.28	0.77	
	706	0.26	0.73	
	3607	0.36	1	
	6174	0.32	0.88	
Tortell et al. (1996)				
Marine Heterotrophic bacteria	40000	8.08	0.75	
	40000	10.06	0.94	
	40000	10.70	1	
	40000	10.61	0.99	
	40000	6.82	0.64	
	25	7.87	0.74	
	25	6.69	0.63	
	25	4.10	0.38	
	25	3.38	0.32	
	25	3.87	0.36	
Granger & Price (1999)				
Marine Heterotrophic bacteria	2	6.74	0.52	
	2166	12.90	1	0.15
	2	1.21	0.28	
	2166	4.27	1.00	1.06
	2	2.18	0.30	
	2166	7.37	1	0.20
	2	9.95	0.63	
	2166	15.70	1.00	2.28
	2	5.79	0.49	
	2166	11.90	1	0.29
	2	5.55	0.27	
	2166	20.90	1	0.91

Table A3.2 Fe requirements of marine microorganism compiled from published literature

Environment	Group	Species	Strain	Proteome ID	no. proteins	no. Fe sites	% Fe sites	no. Cu sites	% Cu-sites
AOB									
Marine	γ-Proteobacteria	*Nitrosococcus halophilus*	Nc 4	UP000001844	3770	655	17.37%	22	0.58%
Marine	γ-Proteobacteria	*Nitrosococcus oceani*	ATCC 19707	UP000006838	2995	598	19.97%	22	0.73%
Marine	β-Proteobacteria	*Nitrosomonas aestuarii*	Nm 69	UP000199533	3744	520	13.89%	23	0.61%
Marine	β-Proteobacteria	*Nitrosomonas halophila*	Nm 1	UP000198640	2974	555	18.66%	20	0.67%
Marine	β-Proteobacteria	*Nitrosomonas* sp.	Nm 51	UP000198732	2986	449	15.04%	21	0.70%
Marine (coastal)	γ-Proteobacteria	*Nitrosococcus oceani*	C-27	UP000028839	3247	576	17.74%	17	0.52%
Marine (coastal)	γ-Proteobacteria	*Nitrosococcus wardiae*	D1FHS	UP000294325	3542	638	18.01%	54	1.52%
Marine (coastal)	γ-Proteobacteria	*Nitrosococcus watsoni*	C-113	UP000000393	2880	567	19.69%	25	0.87%
Marine (coastal)	β-Proteobacteria	*Nitrosomonas cryotolerans*	ATCC	UP000185062	2414	566	23.45%	27	1.12%
Marine (coastal)	β-Proteobacteria	*Nitrosomonas marina*	49181	UP000199459	3276	486	14.84%	23	0.70%
Marine (coastal)	β-Proteobacteria	*Nitrosomonas mobilis*	Nm 22	UP000198729	3034	514	16.94%	16	0.53%
AOA									
Marine	*Thaumarchaeota*	*Candidatus* Nitrosopelagicus brevis	V2	UP000030944	1444	291	20.15%	27	1.87%
Marine	*Thaumarchaeota*	*Nitrosopumilus maritimus*	SCM1	UP000000792	1795	266	14.82%	33	1.84%
Marine (coastal)	*Thaumarchaeota*	*Nitrosopumilus adriaticus*	nf5	UP000032408	2184	265	12.13%	30	1.37%
Marine (coastal)	*Thaumarchaeota*	*Nitrosopumilus piranensis*	D3C	UP000032027	2161	231	10.69%	24	1.11%
Marine (sediment)	*Thaumarchaeota*	*Candidatus* Nitrosopumilus sediminis	AR2	UP000006100	1974	181	9.17%	45	2.28%
Marine (sponge)	*Thaumarchaeota*	*Cenarchaeum symbiosum*	A	UP000000758	2022	239	11.82%	15	0.74%

Table A3.3 Analysis of Fe and Cu binding sites in AOB and AOB genome expressed proteomes

Results of Fe and Cu annotation of genome-predicted proteomes of marine AOA and AOB (downloaded from Uniprot), indicating the predicted number of Fe and Cu binding sites and the number of metal-binding sites relative to the size of the proteome.

				Genome-predicted proteome		Expressed proteome		
Species	**Strain**	**Proteome ID**	**# proteins**	**No. Fe binding sites**	**No. Cu binding sites**	**Fe-binding proteome**	**Cu-binding proteome**	**Expressed proteome reference**
AOB								
Nitrosomonas ureae	Nm10	UP000182882	3069	449	21	0.2	0.60%	Zorz et al. (2018)
Nitrosomonas europaea	ATCC 19718	UP000001416	2375	509	23	0.08	4.00%	Zorz et al. (2018)
Nitrosomonas europaea	ATCC 19718	UP000001416	2375	509	23	0.4	2.00%	Pellitteri-Hahn et al. (2011)
Nitrosomonas europaea	ATCC 19718	UP000001416	2375	509	23	0.35	0.03	Jiang et al. (2015)
Nitrosospira multiformis	ATCC 25196	UP000002718	2732	771	26	0.45	0.01	Zorz et al. (2018)
AOA								
Candidatus Nitrosopelagicus brevis	V2	UP000030944	1444	291	27	0.04	0.03	Santoro et al. (2015)
Nitrosopumilus maritimus	SCM1	UP000000792	1795	266	33	0.19	2.00%	Qin et al. (2018)
Nitrososphaera viennensis	EN76	UP000027093	3117	247	47	0.03	6.00%	Kerou et al. (2016)
Nitrosopumilus maritimus	SCM1	UP000000792	1795	266	33	0.19	2.00%	Shafiee et al. (2021b – Chapter three)

Table A3.4 Percentage of AOA and AOB Fe/Cu-binding expressed proteomes

Comparison of the metal annotation analysis of genome-predicted proteome (Table A3.3) with that of available expressed proteomes.

Substrate	Gene name	Function	Reference
Fe (II)'	*feoB*	Fe (II) inner membrane permease	Velayudhan et al. (2000)
	FTR/Fet3p	Fe (II) inner membrane permease	Eide (1997)
Fe (III)'	*fbpB*	Fe (III) periplasmic binding protein	Adhikari et al. (1996)
	FutA1	Fe (III) periplasmic binding protein	Katoh et al. (2001)
	fecCD	Fe-citrate periplasmic binding protein	Braun & Herrmann (2007)
Fe(org)-complex uptake	*hemS*	Haem, cytoplasmic chaperone	Schneider et al. (2006)
	fhuD	Ferric siderophore solute binding protein	Coulton et al. (1987)
	Fiu	Iron-catecholate outer membrane transporter	Grinter & Lithgow (2019)
	TonB	TonB-dependent outer membrane Fe-siderophore transporters	Moeck & Coulton (1998)
Siderophore biosynthesis	*entE*	Enterobactin siderophore biosynthesis	Gehring et al. (1998)
	entF	Enterobactin siderophore biosynthesis	Gehring et al. (1998)
	fepB	Enterobactin transport protein	Sprencel et al. (2000)
	iucA/iucC	Aerobactin biosynthesis	de Lorenzo & Neilands (1986)
	Rbhc	Siderophore biosynthesis	Hogle et al. (2016)
Copper Importers	CTR1	Cu(I), high-affinity permease	Kuo et al. (2001)
	ctaA	Cu-transporting ATPases	Vulpe & Packman (1995)
	copA/pacS	Cu(I) efflux, P-type ATPaseCu-transporting ATPases: transports Cu intracellularly	Brown et al. (1995)
Copper efflux	*copB*	Cu(II) efflux, P-type ATPase	Silver & Phung (2005); Solioz & Stoyanov (2003)
	cueO	Cu efflux	Singh et al. (2004)
	cusCFBA	Cu efflux	Yu (2011); Franke et al. (2003)
	pcoE	Cu-efflux	Andrews (2002)
Copper chaperones	*copC/pcoC**	Cu chaperone *PcoC is a homologue of CopC	Lawton et al. (2016)
	*copD/pcoD**	Cu chaperone *PcoD is a homologue of CopD	Zhang et al. (2006)
	copZ	Cu-binding chaperone delivers Cu to CopA	Solioz & Stoyanov (2003)
General M^{2+} transporters	ZIP	Fe (II), Zn (II) inner membrane permease	Eide (1997)
	NRAMP	Fe(II), Mn (II) Inner membrane permease	Eide (1997)
	hupE/ureJ	Ni(II) transport associated with hydrogenase/urease	Rodionov et al. (2006)
	nikABC	Ni(II), solute binding protein	Rodionov et al. (2006)
	btuCDF	Co(II) as vitamin B12	Korkhov et al. (2012)
Other metal transporters	*znuA*	Zn (II)	Eide (1997)
	TroA	Zn (II), Mn(II)	Zheng et al. (2011)
	cbtA	Co (II), inner membrane channel	Kiefer et al. (2009)
	cbtB	Co (II), inner membrane channel	Kiefer et al. (2009)
	corA	Co(II), Ni(II), Mg	Niegowski & Eshaghi (2007)

Table A3.5 Known microbial trace metal transport systems

Reference	Depth (m)	pCu (-log $[Cu^{2+}]_{10}$)
Coale & Bruland (1988)	11	13.30
	27	13.41
	34	13.21
	57	13.70
	80	13.48
	123	13.40
	152	12.87
	203	11.44
	250	11.38
	298	11.00
	401	11.06
	509	11.38
	1011	11.38
	1406	11.56
Coale & Bruland (1990)	20	13.94
	38	14.06
	57	14.00
	77	13.94
	97	14.20
	146	13.81
	198	12.04
	298	11.26
	497	10.98
	21	13.88
	41	13.72
	63	13.90
	83	13.75
	101	14.94
	151	13.13
	204	11.42
	301	11.02
	501	10.91
	8	13.91
	23	13.90
	40	13.26
	63	13.01
	82	13.40
	105	11.62
	153	11.36
	203	10.92
	306	10.85
	500	10.45
	8	13.43
	22	13.64
	40	13.31
	62	13.11
	82	12.90
	100	11.25
	147	10.86
	302	10.86
	502	10.83
Moffett & Dupont (2007)	36	13.18
	36	13.34
	105	13.54
	143	12.94
	487	13.23
	1507	12.38
	2996	12.65
	24	
	43	13.58
	89	13.83
	153	13.21
	502	13.64
	1005	13.25

	1510	12.35
Whitby et al. (2018)	10	15.70
	25	14.70
	50	15.40
	75	14.90
	100	15.30
	200	15.30
	400	14.60
	600	14.70
	800	14.80
	1000	14.90
	1200	14.60
	10	14.10
	25	14.80
	50	14.70
	75	14.50
	100	14.90
	200	14.90
	400	14.90
	800	14.90
	1000	14.70
	1200	14.30
	1400	14.40
Heller & Croot (2015)	23	13.36
	48	13.58
	96	12.96
	201	13.12
	404	13.24
	1012	13.25
	24	13.42
	75	13.20
	119	13.27
	250	13.19
	504	13.20
	2843	12.96
	24	13.44
	59	13.37
	101	13.68
	202	13.34
	505	13.31
	3048	13.20
Buckley & van den Berg (1986)	1	12.70
	500	12.15
Semeniuk et al. (2016)	10	14.90
	20	14.70
	40	14.70
	10	14.60
	37	14.60
	10	15.10
	35	14.90
Thompson & Ellwood (2014)	0	13.51
	43	13.37
	43	13.65
	130	13.58
	174	13.33
	217	13.61
	290	13.68
	507	13.60
	754	13.17
	1014	13.27
	1522	12.48
	2014	12.33
	2536	10.81
	3000	12.22
	20	13.76
	38	13.22
	48	13.07

68	12.95	
88	12.83	
111	13.47	
141	13.27	
182	13.37	
304	13.28	
497	12.99	
752	13.09	
998	13.22	

Table A3.6 Oceanic dissolved Cu^{2+} measurements compiled from published literature

Reference		*amoA* copies ml^{-1}	
	Depth (m)	AOA	AOB
Santoro et al. (2013)	20	5.4E+01	
	33	2.6E+02	
	41	1.4E+03	
	56	1.4E+04	
	20		1.8E+01
	33		1.6E+01
	41		1.8E+02
	56		6.1E+02
	150		3.0E+00
	128		6.7E+00
	116		8.6E+00
	100		
	51	2.1E+02	
	115	2.3E+03	
	131	9.5E+03	
	152	6.3E+03	
Horak et al. (2013)	2	1.4E+03	
	13	2.2E+05	
	18	3.1E+05	
	23	6.0E+05	
	32	6.2E+05	
	42	6.8E+05	
	52	1.3E+06	
	72	7.5E+05	
	93	9.1E+05	
	117	1.4E+06	
	3		2.9E+04
	6		2.4E+04
	11		5.6E+04
	13		2.6E+04
	16		2.8E+04
	22		3.0E+04
	31		3.3E+04
	42		3.4E+04
	51		4.0E+04
	72		2.7E+04
	90		1.9E+04
	116		2.1E+04
Newell et al. (2013)	8	0.0E+00	
	38	0.0E+00	
	68	0.0E+00	
	96	1.4E+05	
	129	3.1E+04	
	159	6.9E+02	
	7		0.0E+00
	38		0.0E+00
	66		0.0E+00
	109		4.8E+03
	141		0.0E+00

	169		7.6E+03
Martens-Habbena et al. (2015)			
	4	5.0E+02	
	17	2.0E+03	
	50	8.3E+03	
	58	1.4E+04	
	68	1.2E+04	
	77	1.4E+04	
	99	1.3E+04	
	124	1.4E+04	
	148	1.4E+04	
	297	1.3E+04	
	4		4.5E+03
	17		6.5E+03
	50		6.7E+03
	58		7.6E+03
	68		5.6E+03
	77		6.4E+03
	99		5.7E+03
	124		5.6E+03
	148		3.1E+03
	297		1.5E+03
Peng et al. (2016)	0	8.7E+01	
	27	1.9E+01	
	48	1.1E+01	
	62	5.1E+02	
	72	1.1E+04	
	78	1.8E+04	
	90	1.0E+04	
	105	1.3E+04	
	106	2.4E+03	
	128	2.4E+03	
	150	7.8E+02	
	256	4.5E+02	
	508	9.4E+02	
	562	6.0E+03	
	562	1.3E+02	
	0		1.3E+02
	29		1.3E+02
	51		1.4E+02
	63		4.0E+02
	106		1.0E+02
	154		1.6E+02
	503		1.2E+02
	559		1.6E+02
Santoro et al. (2017)	91	0.0E+00	
	109	9.3E+04	
	111	2.6E+05	
	130	4.3E+05	
	140	3.0E+06	
	188	3.0E+05	
	191	4.6E+04	
	286	0.0E+00	
	384	0.0E+00	
	477	0.0E+00	
	570	0.0E+00	
	62	7.1E+06	
	75	6.1E+05	
	94	8.3E+05	
	115	5.3E+05	
	148	0.0E+00	
	202	0.0E+00	
	256	0.0E+00	
	301	0.0E+00	

	405	0.0E+00	
Jing et al. (2017)	0	4.3E+04	
	0	1.5E+05	
	0	2.3E+05	
	200	2.3E+07	
	200	2.4E+06	
	200	8.4E+05	
	1000	5.1E+04	
	1000	9.2E+04	
	1000	1.5E+05	
	3000	8.9E+04	
	3000	1.5E+05	
	3000	9.6E+05	
Agogué et al. (2008)	2071	2.4E+03	2.2E+02
	1633	5.0E+02	7.2E+01
	1014	2.4E+03	6.3E+01
	498	4.7E+03	1.8E+02
	99	7.1E+03	2.0E+02
	2500	3.5E+02	2.0E+01
	1897	4.5E+02	1.0E+01
	1147	1.4E+02	
	450	3.6E+03	1.6E+01
	149	2.2E+04	2.0E+01
	3878	8.5E+01	5.9E+02
	2999	1.4E+02	8.9E+00
	1897	8.0E+01	3.0E+00
	597	5.5E+03	
	146	9.5E+03	9.8E+02
	2750	7.8E+01	1.3E+02
	800	8.0E+01	5.2E-02
	499	1.4E+02	
	249	7.5E+02	
	99	2.5E+03	8.9E-02
	4001	2.0E+02	6.6E-01
	2748	1.5E+01	6.0E-02
	899	7.7E+01	9.7E-01
	501	1.6E+03	9.3E-01
	249	4.7E+03	2.3E+00
	100	2.3E+04	5.9E+01
	3999	1.0E+01	1.4E+00
	2751	3.4E+01	2.6E+00
	900	3.8E+01	1.3E+01
	499	1.9E+02	5.3E+01
	250	2.6E+03	1.1E+02
	100	2.5E+04	1.9E+01
	4001	3.8E+00	
	2751	6.1E+00	4.3E-02
	900	1.8E+01	
	500	1.4E+01	
	251	8.2E+02	
	100	3.3E+04	
	2501	5.5E+01	1.5E-01
	1799	6.5E+00	
	901	1.5E+01	1.3E-01
	498	1.7E+02	4.4E-02
	252	2.4E+03	2.3E-01
	100	1.2E+04	4.3E-01
	2502	6.5E+01	
	1800	3.5E+01	
	749	1.3E+04	4.0E-02
	498	1.4E+02	3.9E-02
	250	2.7E+03	9.8E-02
	99	2.5E+04	3.2E-02
	2500	6.7E+00	1.6E-01

	1798	6.8E+00	
	901	1.7E+00	2.0E-01
	499	5.3E+02	1.8E-01
	249	3.2E+02	1.2E-01
Mincer et al. (2007)	0	0.0E+00	0.0E+00
	108	0.0E+00	0.0E+00
	194	1.1E+02	1.1E+02
	279	1.2E+02	1.2E+02
	358	1.3E+02	2.3E+02
	461	1.7E+03	9.3E+02
	544	1.3E+04	3.0E+03
	635	5.9E+03	1.5E+03
	728	6.8E+03	1.2E+03
	811	2.9E+03	5.7E+02
	909	3.0E+03	2.8E+02
	1000	1.8E+04	3.2E+03
Church et al. (2010)		2.6E+05	
	248	5.7E+04	
	492	3.8E+05	
	697	4.4E+05	
	846	1.1E+06	
	897	1.1E+06	
	920	1.1E+06	
	949	1.0E+06	
	980	1.1E+06	
	35	3.6E+05	
	278	7.2E+05	
	527	3.2E+05	
	714	1.3E+06	
	870	1.3E+06	
	896	1.3E+06	
	905	1.3E+06	
	961	1.3E+06	
	988	1.3E+06	
	0	4.4E+05	
	247	4.3E+05	
	492	3.9E+05	
	693	6.2E+05	
	837	1.1E+06	
	868	1.1E+06	
	891	1.1E+06	
	927	1.1E+06	
	953	1.1E+06	
	980	1.1E+06	
	8	1.2E+05	
	38	2.0E+05	
	72	2.6E+05	
	98	1.7E+05	
	154	8.8E+05	
	126	5.3E+05	
	299	9.5E+05	
	499	9.7E+05	
	744	8.5E+05	
	995	8.4E+05	
Wuchter et al. (2006)	100	4.4E+04	1.4E+03
	1016	1.2E+04	5.3E+01
	100	1.9E+04	8.4E+02
	150	3.6E+04	8.5E+02
	100	4.3E+04	1.5E+03
	400	5.0E+03	6.7E+00
	150	1.9E+04	3.6E+02
	400	8.0E+03	1.7E+01
	100	1.0E+04	2.2E+02
	600	3.0E+04	2.0E+02

	148	3.1E+04	1.2E+03
	150	3.6E+04	1.7E+02
	95	2.4E+04	1.7E+00
	95	9.0E+03	2.5E+00
	99	3.7E+04	9.8E+02
	100	2.0E+04	5.6E+02
	243	1.6E+04	1.4E+02
	100	3.2E+04	3.9E+02
	266	1.0E+04	2.3E+02
	103	5.5E+04	1.7E+03
Sintes et al. (2013)	0	9.3E-01	
	0	4.3E+00	
	0	5.9E+00	
	0	9.3E+00	
	0	1.3E+01	
	0	3.6E+01	
	13	1.8E+01	
	52	3.7E+00	
	51	1.7E+01	
	51	2.6E+01	
	51	4.6E+01	
	51	8.6E+01	
	50	1.6E+02	
	49	2.3E+02	
	49	6.6E+02	
	98	8.5E+02	
	197	2.9E+03	
	269	3.6E+03	
	269	5.3E+03	
	270	2.4E+04	
	296	1.5E+04	
	298	3.9E+03	
Peng et al. (2015)	0	1.0E+02	
	27	2.1E+01	
	49	1.2E+01	
	58	4.9E+02	
	67	9.7E+03	
	74	2.0E+04	
	89	9.7E+03	
	100	1.4E+04	
	102	2.2E+03	
	127	2.7E+03	
	151	8.2E+02	
	250	4.9E+02	
	500	9.5E+02	
	0		1.4E+02
	27		1.3E+02
	48		1.5E+02
	59		3.8E+02
	100		1.1E+02
	105		1.1E+02
	153		1.5E+02
	498		1.1E+02
Shiozaki et al. (2016)	0	1.0E+04	0.0E+00
	50	1.0E+05	0.0E+00
	100	1.0E+06	1.0E-02
	150	3.2E+06	1.0E+01
	200	1.0E+06	0.0E+00
	0	1.0E+03	0.0E+00
	50	1.0E+03	0.0E+00
	100	1.0E+04	0.0E+00
	150	3.2E+06	0.0E+00
	200	1.0E+06	0.0E+00
	0	1.0E+03	0.0E+00
	50	1.0E+04	0.0E+00

100	1.0E+05	0.0E+00
150	3.2E+06	0.0E+00
200	1.0E+06	0.0E+00
0	1.0E+03	0.0E+00
50	1.0E+03	0.0E+00
100	1.0E+04	0.0E+00
150	3.2E+06	0.0E+00
200	1.0E+06	0.0E+00
0	1.0E+01	0.0E+00
50	1.0E+01	0.0E+00
100	1.0E+04	0.0E+00
150	1.0E+06	0.0E+00
200	1.0E+06	0.0E+00
0	1.0E+01	0.0E+00
50	1.0E+01	0.0E+00
100	1.0E+04	1.0E+02
150	3.2E+06	0.0E+00
200	3.2E+06	0.0E+00
0	1.0E+01	0.0E+00
50	1.0E+03	0.0E+00
100	1.0E+07	1.0E+03
150	1.0E+07	1.0E+02
200	1.0E+07	1.0E+02
0	1.0E+01	1.0E+02
50	1.0E+03	1.0E+02
100	1.0E+07	1.0E+03
150	1.0E+07	1.0E+04
200	1.0E+07	1.0E+04

Table A3.7 Marine archaeal and bacterial *amoA* gene abundances compiled from published literature

Genes	***Nitrosococcus***	***Nitrosomonas***	***Nitrosospira***
South Pacific Ocean	2.49E-07	1.55E-07	3.83E-09
Mediterranean Sea	1.04E-07	7.52E-08	0.00E+00
North Atlantic Ocean	2.33E-08	2.69E-08	2.19E-08
North Pacific Ocean	7.14E-08	4.21E-08	5.04E-08
Red Sea	5.19E-07	8.81E-08	3.85E-09
South Atlantic Ocean	8.48E-07	5.73E-08	2.31E-08
Southern Ocean	1.34E-08	4.30E-08	0.00E+00
Transcripts	***Nitrosococcus***	***Nitrosomonas***	***Nitrosospira***
North Atlantic Ocean	1.81E-08	1.51E-08	0.00E+00
North Pacific Ocean	7.01E-08	0.00E+00	0.00E+00
South Pacific Ocean	7.99E-09	1.50E-09	0.00E+00
Indian Ocean	1.45E-08	1.40E-07	0.00E+00

Table A3.8 Biogeography of AOB Cu efflux genes and transcripts

Presence of genes and transcripts homologous to AOB Cu efflux genes in *Tara* Oceans Gene Atlas, full analysis outlined in Appendix III, section 1.7.